



Dipl.-Ing. Michael Martin

Systematic method for quantifying measures to decrease the CO₂ emissions of a vehicle fleet

Systematische Methodik zur Quantifizierung von Maßnahmen für die Reduktion der CO₂ Emissionen einer Fahrzeugflotte

Doctoral Thesis

to achieve the university degree of
Doktor der technischen Wissenschaften

submitted to

Graz University of Technology

Supervisors:

Assoc. Prof. Dipl.-Ing. Dr. techn. Arno Eichberger
Institute of Automotive Engineering, Graz University of Technology
Member of [FSI]

Ao. Univ.-Prof. Dipl.-Ing. Dr. techn. Eranda Dragoti-Cela
Institute of Discrete Mathematics, Graz University of Technology

Graz, October 2017

Acknowledgement

This thesis was created during my work at the Energy Management and Drivability department at Magna Steyr Engineering AG & Co KG. I would like to thank Robert Premstaller, the former head of the department, for giving me the opportunity to work on this thesis and for his support as an advisor. There are many peoples without whom this work would not be possible. Of my colleagues at Magna Steyr, I would like to thank Michael Mandl, my group leader, Michael Kalunder, head of the Energy Management and Drivability department, my colleagues from the the Energy Management and Drivability department, my colleagues from the Research Cooperations and Funding department, my colleagues from the Advanced Development department, and finally my graduate students.

In particular, I would like to thank my thesis advisor, Assoc. Prof. Arno Eichberger of the Institute of Automotive Engineering at Graz University of Technology, for his continuous support of my doctoral thesis.

I would also like to acknowledge the second reader of this thesis, Ao. Univ.-Prof. Eranda Dragoti-Cela of the Institute of Discrete Mathematics at Graz University of Technology, for her very valuable comments on this thesis.

For the funding of my doctoral thesis, I would like to thank the Austrian BMVIF and the FFG, as this thesis was part of the funding program “Talents” and “Mobility of the future”.

Finally, I must express my deepest gratitude to my parents for their unfailing support and continuous encouragement throughout my years of study and through the process of researching and writing this thesis.

Thank you all for your support!

Michael Martin, Graz, October 2017

Statutory Declaration

I declare that I have authored this thesis independently, that I have not used other than the declared sources / resources, and that I have explicitly marked all material which has been quoted either literally or by content from the sources used. The text document uploaded to TUGRAZonline is identical to the present doctoral thesis.

.....
(date) (signature)

Abstract

Driven by global warming and the related strict regulations, the reduction of the fleet-average CO₂ emissions is one of the biggest challenges in the automotive industry. New technologies for vehicles must be developed and implemented. Thus, for new vehicles to be developed, a combination of technical measures has to be devised to achieve the given targets. Up to several millions of combinations are possible, depending on the number of vehicles and measures considered. For competitiveness of the manufacturers, the costs associated with the implementation of new measures needs to be minimized.

This thesis deals with the development of a method to quantify measures for the achievement of the fleet-average CO₂ emissions targets for a defined selection of vehicles. Interactions between measures, vehicles and vehicle targets are taken into consideration to identify the optimum and cost-effective selection of measures. The method to achieve this optimization is divided into two parts: the simulation for the evaluation of measures and the optimization to determine the optimum combination. Simulation techniques are deployed to determine the influences of a variety of measures on CO₂ emissions and driving performance. A simulation model, validated by measurements from a real vehicle, is adapted to include the different measures. The simulation environment is automated to ensure an efficient handling of the large number of simulation runs. Out of the results, a multi-step optimization approach based on meta-heuristics selects the cost-optimum group of measures while taking into account constraints and interactions related to targets for both the vehicle and the fleet-average.

The applicability of the approach is tested on a fictional vehicle fleet and several scenarios. The results show that the optimum selection of measures depends quite strongly on the relevant boundary constraints, such as vehicle targets, vehicles and markets. The results clearly demonstrate the need for a holistic approach in order to ensure an optimum achievement of CO₂ emissions targets.

Kurzfassung

Aufgrund der globalen Erderwärmung und daraus resultierender gesetzlicher Regulierungen ist die Reduktion von CO₂-Emissionen eine der wichtigsten Entwicklungsschwerpunkte in der Automobilindustrie. Um die Zielwerte zu erreichen, müssen neue Technologien entwickelt und implementiert, sowie schlussendlich daraus eine Kombination von Maßnahmen für neu zu entwickelnde Fahrzeuge definiert werden. Abhängig von der Anzahl der betrachteten Fahrzeuge und Maßnahmen gibt es Millionen von Kombinationsmöglichkeiten. Des Weiteren ist die Implementierung von Maßnahmen mit zusätzlichen Kosten für den Hersteller verbunden. Mit Hinblick auf die Wettbewerbsfähigkeit gilt diese Kosten minimal zu halten.

Die vorliegende Dissertation befasst sich mit der Erstellung einer Methodik, um gezielt Maßnahmenkombinationen für eine Auswahl an Fahrzeugen zu definieren. Bei der Suche nach der geeignetsten Kombination muss auf Wechselwirkungen zwischen verschiedenen Technologien, Fahrzeugen und anderen Gesamtfahrzeug-Zielwerten, sowie auf ein Kostenminimum, geachtet werden. Die Methodik ist in zwei Hauptbestandteile untergliedert: die Simulation zur Bewertung von Maßnahmen und die Optimierung zur Selektion von Maßnahmenpaketen. Die Einflüsse von verschiedenen Technologien und Maßnahmen auf CO₂-Emissionen und Fahrleistungen werden durch ein Simulationsmodell ermittelt. Das Simulationsmodell wird mit Fahrzeugmessungen validiert und erweitert, um die verschiedenen Maßnahmen abzubilden. Die Simulationsumgebung ist automatisiert, damit eine hohe Varianten-Zahl an Simulationsläufen effizient abgearbeitet werden kann. Die Ergebnisse der Simulationsschleifen werden mittels eines mehrstufigen Optimierungsalgorithmus analysiert, um eine kostenoptimale Selektion von Maßnahmen zu erhalten. Der Algorithmus beruht auf Meta-Heuristiken, berücksichtigt Wechselwirkungen und Nebenbedingungen von Maßnahmen und ist in der Lage auf individuelle Fahrzeugzielwerte als auch auf Flotten-Durchschnittszielwerte hin zu optimieren.

Die Funktionalität des Algorithmus wird an einer fiktiven Fahrzeugflotte und verschiedenen Szenarien überprüft. Die Ergebnisse zeigen, dass abhängig von den zu betrachtenden Nebenbedingungen, wie zum Beispiel Fahrzeugziele, Fahrzeuge und Märkte, unterschiedliche Maßnahmenpakete kostenoptimal sind. Sie verdeutlichen damit auch die Notwendigkeit eines solchen Optimierungsansatzes, um die Zielwerte bestmöglich abzusichern.

Contents

Acknowledgement	i
Statutory Declaration	iii
Abstract	v
Kurzfassung	vii
Contents	xii
Abbreviations	xiii
Symbols	xvii
1. Introduction	1
1.1. Pressure on the automotive industry to reduce CO ₂ emissions	1
1.2. Problems of alternative power-trains and energy sources	2
1.3. Motivation	3
2. State-of-the-art	7
3. Background	13
3.1. Introduction	13
3.2. Legal regulations	13
3.2.1. Overview	13
3.2.2. Europe (EU-28)	14
3.2.3. Republic of China	17
3.2.4. USA and California	20
3.3. Vehicle technologies	23
3.3.1. Introduction	23
3.3.2. Energy flow of a vehicle	23
3.3.3. Internal combustion engine	24
3.3.4. Auxiliaries	27
3.3.5. Transmission	30
3.3.6. Vehicle	31
3.3.7. Hybrid power-train	35
4. Modeling and Simulation	39
4.1. Introduction	39
4.2. Requirements for the simulation environment	39
4.3. Simulation environment	42
4.4. Model adaptation	45
4.4.1. Sub-model partitioning	45

4.4.2.	Driver model	47
4.4.3.	Internal combustion engine model	48
4.4.4.	Auxiliaries model	50
4.4.5.	Power-train model	51
4.4.6.	Vehicle model	52
4.4.7.	Thermal model	54
4.4.8.	Mild-hybrid model	56
4.5.	Model validation	59
4.6.	Automated simulation	64
4.6.1.	Scripting	64
4.6.2.	Definition of vehicles and components	67
4.6.3.	Simulation and analysis of driving cycles	69
4.6.4.	Energy flow analysis	74
5.	Optimization	77
5.1.	Introduction and problem statement	77
5.2.	General terms	78
5.3.	Abstraction of the fleet optimization problem	78
5.3.1.	Introduction	78
5.3.2.	Parameter vector	79
5.3.3.	Objective function (costs)	80
5.3.4.	Inequality constraint (vehicle targets)	81
5.4.	Discussion of optimization methods	83
5.4.1.	General optimization algorithms	83
5.4.2.	Multi-criteria optimization	86
5.4.3.	Multi-level optimization	86
5.4.4.	Automotive applications of optimization algorithms	86
5.4.5.	Specific aspects of the investigated optimization methods	88
5.5.	Interface between simulation and optimization	88
5.5.1.	General approach	88
5.5.2.	Meta-model	90
5.5.3.	Analysis of interactions	90
5.5.4.	Final approach	95
5.6.	Multi-step approach	96
5.6.1.	Introduction	96
5.6.2.	Cycle-based optimization (CBO)	97
5.6.3.	Vehicle-based optimization (VBO)	109
5.6.4.	Fleet-based optimization (FBO)	120
5.6.5.	Overview of the optimization steps	126
6.	Results	127
6.1.	Definition of the considered vehicles, platform and fleet	127
6.2.	Example: Optimization of a vehicle	131
6.2.1.	Cycle-based optimization on NEDC	131
6.2.2.	Sensitivity analysis	132
6.2.3.	Effect of NEDC-optimal selection on other cycles	135
6.2.4.	Vehicle-based optimization	137
6.2.5.	Influence of target setting	138
6.2.6.	Discussion of the results	140
6.3.	Example: Optimization of a platform	140

6.3.1.	Transition from vehicle to platform level	140
6.3.2.	Influence on the optimal solution for NEDC vs WLTC	144
6.3.3.	Influence of new technologies	146
6.3.4.	Influence of sales volume by year	147
6.3.5.	Discussion of the results	148
6.4.	Example: Optimization of a fleet	148
6.4.1.	Interactions due to different segments	149
6.4.2.	Interactions due to different markets	150
6.4.3.	Discussion of the results	151
7.	Discussion	153
8.	Summary	157
	List of Figures	I
	List of Tables	V
	Listings	VII
	Bibliography	IX
A.	Appendix: Legal fundamentals	XVII
A.1.	Europe	XVII
A.1.1.	Super-credits	XVII
A.1.2.	Phase-in period	XVII
A.1.3.	ECO innovations	XVIII
A.1.4.	Definition of the test weight classes	XVIII
A.1.5.	ECE-R 101 test sequence for hybrid vehicles	XIX
A.1.6.	WLTP gear-shifting for manual transmission	XX
A.1.7.	WLTP monitoring electric power supply	XXI
A.1.8.	WLTP test sequence for hybrid vehicles	XXI
A.2.	China	XXII
A.2.1.	Fuel consumption limits	XXII
A.2.2.	Credits for new energy vehicles	XXII
A.3.	USA	XXV
A.3.1.	Fuel economy and greenhouse gas limits for passenger cars	XXV
A.3.2.	Credits for alternative vehicles	XXVI
A.3.3.	Off-cycle credits	XXVI
A.3.4.	Definition of the test weight classes	XXVI
A.3.5.	Test sequence for hybrid vehicles	XXVIII
B.	Appendix: Vehicle fundamentals	XXIX
B.1.	Internal combustion engine	XXIX
B.1.1.	Description of technologies	XXIX
B.1.2.	Overview of technologies and their expected benefits	XXXII
B.2.	Auxiliaries	XXXVIII
B.3.	Transmission	XLI
B.4.	Vehicle	XLIII
B.4.1.	Vehicle weight	XLIII
B.4.2.	Aerodynamic drag	XLIV

B.4.3. Rolling resistance and traction	XLVI
B.5. Hybrid	XLVII
B.5.1. Start-stop and generator control	XLVII
B.5.2. Mild-hybrid (48 V)	XLIX
C. Appendix: Simulation	LI
C.1. Control Logic	LI
C.1.1. Engine start-stop	LI
C.1.2. Generator control	LI
C.1.3. Cylinder deactivation	LII
C.2. Validation of the baseline simulation model	LIV
C.3. Automation	LX
C.3.1. Definitions of components	LX
C.3.2. Definitions of measures	LXIII
D. Appendix: Fleet definition	LXVII
D.1. Vehicle definition	LXVII
D.2. Measure definition	LXXV
E. Appendix: Optimization	LXXIX
E.1. Utility analysis	LXXIX
E.2. Vehicle-based optimization	LXXIX
E.3. Optimization of a platform	LXXXIV

Abbreviations

0D	Simulation with time dimension
1D	Simulation with time and one position-dependent dimension
3R	Vehicles with three or more rows of seats
4WD	Four-wheel drive
AC	Air conditioning
ACEA	Association Constructeurs Européens d'Automobiles
AGS	Active grill shutter
AMT	Automated manual transmission
AT	Automatic transmission or transmissions with automated gear-shifting in general
AWD	All-wheel drive
BEV	Battery-electric vehicle
BiW	Body in white
BMEP	Brake mean effective pressure
BMWi	German Federal Ministry for Economic Affairs and Energy
BSFC	Brake specific fuel consumption
CAFE	Corporate-average fuel economy
CAFC	Corporate-average fuel consumption
CARB	California Air Resources Board
CATARC	China Automotive Technology and Research Center
CBO	Cycle-based optimization
CH ₄	Methane
CN	China
CNG	Compressed natural gas
CO	Carbon monoxide
CO ₂	Carbon dioxide
CoG	Center of gravity
CoP	Conformity of production
CFR	Code of federal regulation
CVS	Constant volume sampler
CVT	Continuously variable transmission
CVW	Curb vehicle weight
D	Diesel (engine)
DC	Direct current
DCT	Double clutch transmission
E5	Petrol with 5% ethanol
EC	European Community
ECE-R	Economic Commission for Europe Regulation
ECO	Economic
ECU	Electronic control unit
EGR	Exhaust gas recirculation
EHPS	Electric-hydraulic power steering

EM	Electric motor
EPA	Environmental Protection Agency
EPA2	Combined driving cycle of FTP75 and HWFET
EPCA	Energy Policy Conservation Act
EPS	Electric power steering
ESS	Engine start-stop
EU	European Union
F0	Coast-down parameter (constant value)
F1	Coast-down parameter (linear value)
F2	Coast-down parameter (square value)
FC	Fuel consumption
FE	Fuel economy
FBO	Fleet-based optimization
FCV	Fuel cell vehicle
FTP	Federal test procedure
FWD	Front-wheel drive
G	Gasoline (engine)
GA	Genetic algorithm
GB	Mandatory Chinese National Standard (chin.: Guobiao)
GHG	Greenhouse gas
GN	Gauss-Newton method
GPS	Global positioning system
GVW	Gross vehicle weight
H ₂	Hydrogen
HCU	Hybrid control unit
HEV	Hybrid-electric vehicle
HPS	Hydraulic power steering
HSLA	High-strength low-alloy steel
HWFET	Highway fuel economy test
HV	High voltage
HVAC	Heating, ventilation and air conditioning
I4	In-line engine with four cylinders
I6	In-line engine with six cylinders
ICE	Internal combustion engine
IEC	International electrotechnical commission
ISO	International organization for standardization
JAC	Jacob-seeking method
LDT	Light-duty truck
LED	Light-emitting diode
MC	Monte-Carlo method
MOSFET	Metal-oxide semiconductor field-effect transistor
MPV	Multi purpose vehicle
MRF	Magnetorheological fluid
MT	Manual transmission
MVEG-B	Motor vehicle emission group cycle version B
NEDC	New European driving cycle
NHTSA	National Highway Traffic Safety Administration
NiMH	Nickel metal hydride
NO _x	Nitrogen oxides

O ₂	Oxygen
P0	Parallel hybrid architecture with the electric motor installed on the belt drive
P1	Parallel hybrid architecture with the electric motor installed on the crankshaft
P2	Parallel hybrid architecture with the electric motor installed on the transmission input-shaft
P3	Parallel hybrid architecture with the electric motor installed on the transmission output-shaft
PC	Passenger car
PHEV	Plug-in hybrid-electric vehicle
PSO	Particle swarm optimization
PT1	First order lag element
PVW	Performance vehicle weight
PWM	Pulse width modulation
RIM	Reaction injection moulding
RWD	Rear-wheel drive
SA	Simulated annealing
SAE	Society of Automotive Engineers
seg.	Segment
SMC	Sheet moulding compound
SOC	State-of-charge
SPX	Simplex method
SULEV	Super ultra-low emission vehicle
SUV	Sport utility vehicle
TCS	Traction control system
TCU	Transmission control unit
THC	Total hydrocarbon
TRR	Tire rolling resistance
TS	Tabu search
US	United States
USA	United States of America
VBO	Vehicle-based optimization
V6	V-engine with six cylinders
V8	V-engine with eight cylinders
VL	Vehicle-specific limitation
VVL	Variable valve lift
VVLT	Variable valve lift and timing
VVT	Variable valve timing
WLTC	Worldwide harmonized light vehicles test cycle
WLTP	Worldwide harmonized light vehicles test procedure
WR	Weight reduction

Symbols

Parameters, constants and variables

a	acceleration in m/s^2
a	gradient of CO ₂ fleet emissions regulation in $\text{gCO}_2/\text{km} \cdot 1/\text{kg}$
A_x	frontal area in m^2
b_{mep}	brake mean effective pressure in bar
c	costs
c_d	aerodynamic drag coefficient
cr	cost ratio
crd	credits for fleet-average CO ₂ emissions and fuel consumption
d	(driven) distance in m
d	difference
dir	optimization direction of a cycle
dw	weighted difference
E	energy in Wh
EC	electric energy consumption in Wh/km
EM	CO ₂ emissions in gCO_2/km
er	equality rating between cycle-specific parameter vectors
F	force in N
F_0	coast-down parameter (constant value) in N
F_1	coast-down parameter (linear value) in N / km/h
F_2	coast-down parameter (square value) in N / $(\text{km/h})^2$
f_a	auxiliary function
f_r	rolling resistance coefficient
FC	fuel consumption in l/100km
FE	fuel economy in mpg
fp	foot print of a vehicle in ft^2
FP	total monetary fleet penalty
fpi	phase-in factor
FS	fleet-average status
FT	fleet-average target
g	gravitational acceleration in m/s^2
g	inequality constraint
h	equality constraint
I	current in A
i	counter
j	counter for inequality constraints
k	counter for equality constraints
K_{fuel}	correction factor for fuel consumption in l/100km per Ah
m	mass in kg
m	measure state of the measure vector

M	torque in Nm
n	total number
n	engine speed in 1/min
ndv	ratio of engine speed to vehicle speed
ng	number of forward gears
p	parameter of the parameter vector
P	monetary penalty
P	power in W
pv	production volume of a vehicle
Q	capacity (charge balance) of a battery in Ah
\dot{Q}	heat flow in W
s	wheel slip
s	status of a cycle or of a measure
s_m	status of a parameter vector of a cycle
$Scafc$	actual status for corporate average fuel consumption in l/100km
SOC	battery state-of-charge
$Svfc$	actual status of vehicle fuel consumption in l/100km
$svol$	sales volume of a vehicle
T	temperature in °C
t	target of a cycle
t	time in s
$Tcafc$	target for corporate-average fuel consumption in l/100km
$Tcafe$	target for corporate-average fuel economy in mpg
$Tghg$	target for corporate-average greenhouse gases in gCO ₂ /mi
TM	test mass in kg
$Tvfc$	target for vehicle-specific fuel consumption in l/100km
$Tvfe$	target for vehicle-specific fuel economy in mpg
$Tvghg$	target for vehicle-specific greenhouse gases in gCO ₂ /mi
U	voltage in V
v	vehicle speed in m/s
VT	vehicle target
w	weighting factor
ΔT	difference of fleet target setting
η	efficiency factor
μ	adhesion coefficient
ρ_{air}	air density in kg/m ³
ω	angular speed in rad/s

Vectors and matrices

$\mathbf{0}$	vector with zeros
\mathbf{c}	costs of measures (without sub-variants)
\mathbf{cr}	cost ratio of measures
\mathbf{cw}	cycle-weighting factor
\mathbf{g}	vector for inequality constraint
\mathbf{h}	vector for equality constraint
\mathbf{m}	parameter vector for measures
\mathbf{M}_c	cost of measures and sub-variants

M_{Δ}	influences of measures in driving cycles
m_{Δ}	influences of measures in driving cycles (without sub-variants)
M_{svar}	matrix describing the sub-variants of the measures
M_{used}	definition in which vehicle - cycle combination a measure is used
mw	measure-weighting factor
n_{svar}	vector including the number of sub-variants of all measures
p	parameter vector in general
P	valid design space
S_{bl}	status matrix for baseline results (multiple vehicles)
s_{bl}	status vector for baseline results (one vehicle)
S_{m}	actual status matrix for a given solution (parameter matrix)
$svol$	sales volume of vehicles or measures
t_v	vector describing the targets of a vehicle
tl	vector tabu list
T_{vc}	matrix describing the targets of each vehicle - cycle combination
T_{Δ}	matrix describing the difference between the target and the status
t_{dir}	vector for optimization direction of targets (cycles)
T_{of}	matrix describing the target overfulfillment

Indices

0	reference
<i>ags</i>	active grill shutter
<i>Aux</i>	auxiliaries
<i>avail</i>	available
<i>avg</i>	average
<i>Batt</i>	battery
<i>bl</i>	baseline
<i>c</i>	(driving) cycle
<i>child</i>	children
<i>comb</i>	combination
<i>Cl</i>	clutch
<i>Cool</i>	coolant
<i>Cs</i>	crankshaft
<i>cv</i>	considered vehicles
<i>cvw</i>	curb vehicle weight
<i>di</i>	direct injection
<i>e</i>	engine
<i>ess</i>	engine start-stop system
<i>f</i>	fleet
<i>g</i>	inequality constraint
<i>Gen</i>	generator / alternator
<i>h</i>	equality constraint
<i>ICE</i>	internal combustion engine
<i>i</i>	numbering
<i>idle</i>	idle operation
<i>init</i>	initial
<i>j</i>	equivalent (mass) including rotary inertia

<i>loss, s</i>	losses due to slip
<i>m</i>	measure
<i>mkt</i>	market
<i>max</i>	maximum
<i>max, 95</i>	95% of the maximum
<i>min</i>	minimum
<i>min, drive</i>	minimum for driving operation
<i>nom</i>	nominal
<i>P</i>	parameter
<i>p</i>	(theoretical) potential
<i>par</i>	parent
<i>pf</i>	platform
<i>pl</i>	payload
<i>of</i>	(target) overfulfillment
<i>opt</i>	optimal
<i>rated</i>	rated maximum
<i>reess</i>	rechargeable energy storage system
<i>ref</i>	reference
<i>req</i>	required
<i>rmf</i>	remaining fleet
<i>S</i>	solution
<i>s</i>	selected measure
<i>spec</i>	specific
<i>svar</i>	sub-variant of a measures
<i>t</i>	test (mass)
<i>Tr</i>	transmission
<i>trc</i>	traction (force)
<i>trr</i>	tire rolling resistance
<i>twc</i>	test weight class
<i>t_0_100</i>	time from 0 to 100 kph
<i>t_80_120</i>	time from 80 to 120 kph
<i>u</i>	unused measures
<i>w</i>	wheel
<i>wot</i>	wide-open throttle
<i>wr</i>	weight reduction
<i>v</i>	vehicle
<i>vmax</i>	maximum speed
<i>y</i>	year
<i>x</i>	x-direction
<i>z</i>	z-direction
Δ	improvement of a measures (delta compared to baseline)

1. Introduction

1.1. Pressure on the automotive industry to reduce CO₂ emissions

The global average temperature has increased by about 0.6°C since the beginning of the 20th century, the fastest rate in the last 1000 years [1]. One reason discussed by scientists is the greenhouse effect, whereby 5 to 40% of the greenhouse gases are related to CO₂ emissions [2]. Worldwide CO₂ emissions rose by around 50% from 1990 to 2007 [3], with a further increase of 41% expected from 2007 to 2030 [4]. One reason for this increase is the burning of fossil resources, such as coal, oil or gas. Therefore, in 1997 the Kyoto Protocol was adopted in order to reduce the greenhouse gases by around 5% in comparison to the value of 1990 from 2008 to 2012 [1].

There are various sources of CO₂ emissions. Figure 1.1 shows the distribution of anthropogenic CO₂ emissions from a study presented in [5]. This study identified that 12% of the CO₂ emissions are caused by passenger car traffic. Other literature has confirmed this distribution, with a range between 11.5% to 14% for passenger cars [2] [6] [7]. Thus, the automotive industry has a responsibility to contribute to the reduction of emissions by passenger cars.

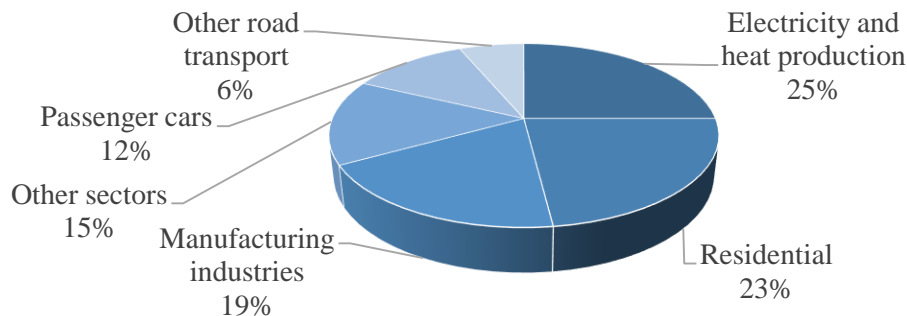


Figure 1.1.: Distribution of global anthropogenic CO₂ emissions (based on [5])

The reduction of CO₂ emissions from passenger car traffic can be divided into seven overarching topics: [3] [8] [9]

- Promoting vehicles with small size and weight
- Reducing the annual traveled distances for each car owner
- Encouraging efficient driving behavior
- Improving traffic stream
- Increasing content of fuel produced from biological sources or reducing carbon content in the fuel
- Increasing market share of vehicles with alternative power-trains and energy sources (e.g. hydrogen, electricity)

- Improving power-train efficiency and reducing vehicle energy demand

Finally, many parties, including politicians, consumers, and the automotive industry itself, must contribute to this improvement. In the case of the automotive industry, the tasks are to develop cars with alternative power-trains and to improve vehicle energy efficiency. To encourage this, politicians have introduced legal regulations to limit the CO₂ emissions of new passenger cars in standardized test cycles. In addition to the CO₂ emissions regulations, other trends will influence future vehicle development [7], such as urbanization, the limited availability of fossil fuels, increasing fuel prices and changing customer behavior. An outlook on the trend for fuel prices in the EU is provided in [7], which predicts an increase of around 150% by 2020 and around 250% by 2030, in comparison to the average fuel prices in 2012. In conclusion, vehicle development faces two key challenges: meeting requirements for individual mobility that are evolving due to demographic changes, and improving vehicle fuel consumption and CO₂ emissions that are evolving due to legal regulations and increasing fuel prices. This thesis addresses the latter challenge.

1.2. Problems of alternative power-trains and energy sources

“Wir wollen bis 2020, dass eine Million Elektroautos auf unseren Straßen fahren. Bis dahin haben wir noch einen weiten Weg zu gehen.” (By 2020, we would like to see one million electric automobiles on our streets. To reach this goal, we still have a long way to go.)

German Federal Chancellor Angela Merkel while the formation of the “Nationalen Plattform Elektromobilität”, May 1st 2010 .

One potential method for reducing vehicle CO₂ emissions that has received much attention is the development and integration of alternative power-trains in combination with other energy sources, such as electricity or hydrogen. Current worldwide regulations for measuring CO₂ emissions capture only the CO₂ emissions from tank to wheel. CO₂ emissions caused by the production of the fuel and electricity (i.e. well to tank) are not included. This means that vehicles powered by electricity or hydrogen drive are considered to have “zero emissions”. In accordance with the legal regulations (see Chapter 3.2), the vehicles sold and their CO₂ emissions are combined to determine one fleet-average CO₂ emission value, which is weighted by the sales volume. Thus, vehicles with very low CO₂ emissions can greatly reduce the fleet-average CO₂ emissions. However, despite this advantage for CO₂ emissions, alternative power-trains still have a number of disadvantages for the customer, including:

- Limited driving range and long charging time for battery-electric vehicles
- Battery lifetime [10]
- Infrastructure for electric charging and hydrogen stations
- Higher costs and weight [11]

In addition to technical discussions and the afore mentioned advantages and disadvantages, customers also have a significant influence on CO₂ emissions because they decide what type of car they want to purchase. The study in [6] provides predictions for the future market shares of different power-train technologies in the EU-15 states. Based on this paper, Figure 1.2 summarizes the development of the market share assuming a moderate or slight increase in alternative power-trains. The comparison shows that, regardless of the rate of alternative power-train increase, conventional Diesel and gasoline-driven vehicles will continue to play a significant

role for mobility in the near future. Thus, to ensure the short and mid-term reduction of CO₂ emissions, the improvement of conventional vehicles is of considerable importance.

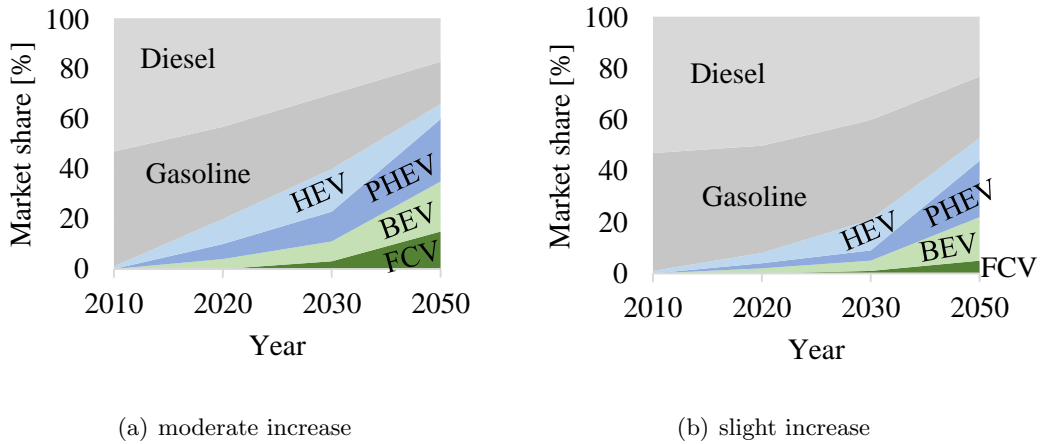


Figure 1.2.: Study on the market share of power-train types with a moderate and slight increase of alternative power-trains (based on [6])

1.3. Motivation

Scope of this work

Conventional vehicles with Diesel or gasoline engines will continue to have a high market share at least in the short- and mid-term perspective. Therefore, this thesis focuses on improving conventional vehicles. Due to the high sales volume, they will have a significant influence on the calculation for the fleet-average CO₂ emissions. To this end, there are several existing technologies (hereinafter called “measures”) designed to achieve given vehicle and fleet-average CO₂ emissions targets. All of these measures are coupled with costs and other boundary constraints. The question, therefore, is which of the available measures have to be selected and implemented into the considered vehicles in order to achieve these targets? In this context, the optimization should be focused on minimizing total fleet costs. In summary, Figure 1.3 outlines, the scope of the present work. Three inputs are given:

- Input 1: the targets of the market-specific fleet-average CO₂ emissions based on the legal regulations, but also targets for other vehicle attributes, such as driving performance
- Input 2: the vehicle matrix, defined by the engines, transmissions, tires, bodies, etc.
- Input 3: the available measures and technologies to improve CO₂ emissions, described by simulation parameters, costs and availability

The output of this work should be a list of selected measures to be implemented for every vehicle in the vehicle matrix and the expected cost. To obtain the information required for the expected output, a methodology should be derived. This methodology, shown in the middle of the figure, is the major content and innovation of the thesis and is divided into two parts. First, using a simulation environment, the influence of each measure is evaluated for every vehicle and every driving cycle. Based on these results, an optimization algorithm should be developed that is capable of determining the cost-optimal selection of measures to achieve all defined targets.

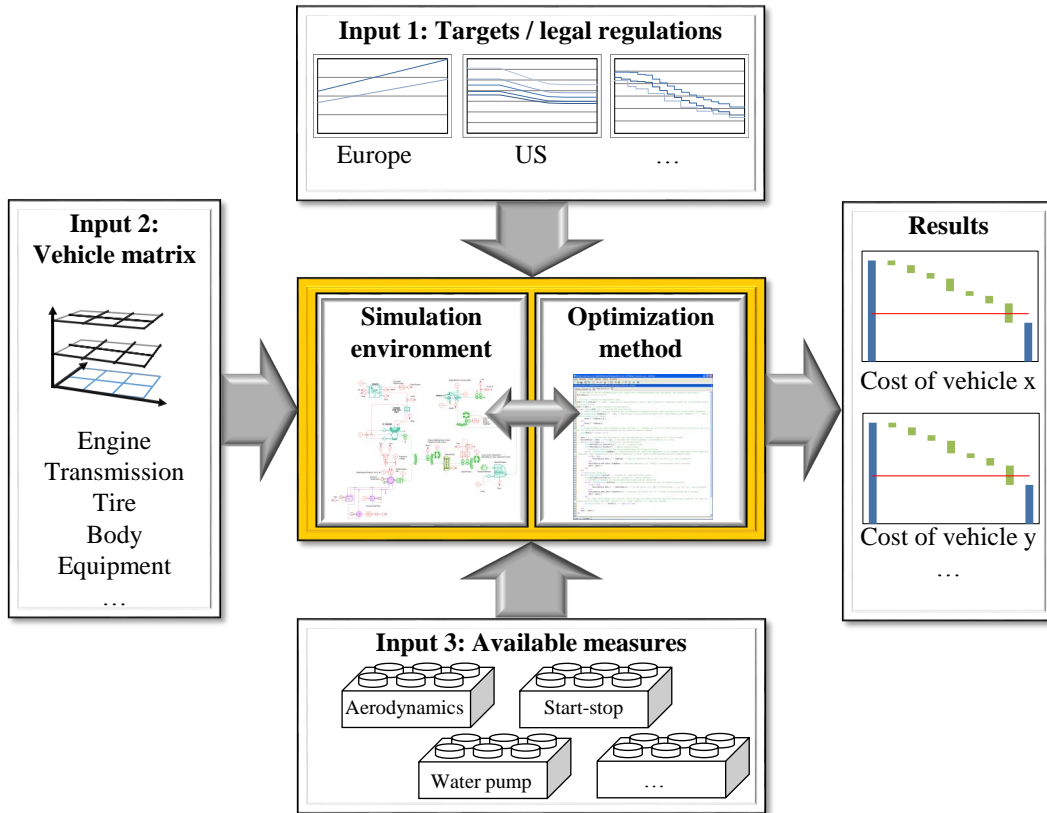


Figure 1.3.: Overview and content of the doctoral thesis

Challenges

In the context of the reduction of CO₂ emissions some challenges for the simulation and optimization have to be considered and met within this thesis. These challenges increase the complexity of the methodology:

- *Possible measures and their interactions* - Reducing CO₂ emissions is a task for the complete-vehicle development. A set of components and technologies for the reduction of CO₂ emissions have to be considered, including body¹, tires, power-train, power-net and engine. In addition, interactions and secondary effects between different components and technologies are becoming more and more important. Technologies have to be considered in complete-vehicle context and not only individually.
- *Driving performance and drivability* - Some measures that have a positive effect on CO₂ emissions may have a negative effect on driving performance and drivability. Boundary constraints in the form of acceleration times or maximum speed are related to driving performance. Drivability, which captures characteristics such as load response, load alternation, and acceleration reserves, evaluates if transitions between operating states are harmonic and jerk-free [14] [15].
- *Different markets* - Across the world, there are different regulatory frameworks in different markets. The regulations differ in the amount of CO₂ emissions limitations and in the definition of the test procedure for evaluating CO₂ emissions. For this reason, the required reduction of CO₂ emissions differs, as do the influences of measures.

¹The body describes the design of the vehicle body (e.g. sedan, hatchback) [12] [13].

- *Costs of technologies* - The implementation of CO₂ emission-reducing measures will effect costs. The cost-optimal combination of measures has to be determined.
- *Consideration of modular assemblies* - The increasing number of carry-over parts between different vehicles and vehicle platforms² leads to interactions of the selection process of measures between vehicles. Improving a component of one vehicle may also influence the CO₂ emissions of another vehicle in the case of carry-over parts.
- *Number of vehicle variants* - Due to customer desires for individualism and manufacturers' search for new business cases, the number of possible vehicle variants and configurations (vehicle matrix) has increased in recent years [18]. This must be considered when calculating the average CO₂ fleet emissions and increased the vehicle matrix.
- *Role of virtual development* - To save cost for prototype vehicles and to reduce development times, the role of virtual development is becoming more and more important. Figure 1.4 explains the degree of freedom for a vehicle across the development process and shows that, for the most part, only simulation is available in the early development phase. The intention should be to use simulation to analyze and decide on required measures as early as possible in the vehicle development. However, the simulation must be validated in order to get accurate results already in early development phases.

Structure of this work

To derive this optimization method, this thesis is divided into five further chapters:

Chapter 2 analyzes other publications and the state-of-the-art. The focus is on investigating general topics related to CO₂ fleet emissions, their reduction, and simulation-based optimization. Based on these studies, the current state-of-the-art regarding optimization approaches for reducing CO₂ fleet emissions is evaluated.

Chapter 3 includes the background on the calculation and target setting of the fleet-average CO₂ emissions based on market-specific regulations. The second part of Chapter 3 describes the background of common and available technologies for reducing the CO₂ emissions of conventional vehicles.

Chapter 4 covers the simulation. Sub-chapters define the requirements for the simulation and the adaptation of the simulation model. In addition, the automated simulation environment for an automated execution of simulation loops is described.

Chapter 5 derives the optimization approach itself, beginning with a general discussion about optimization algorithms and the analysis of typical applications of optimization on other automotive examples. The interaction between optimization and simulation, as well as the final implemented algorithm are described.

Chapter 6 covers the application of the optimization method using examples to show the functionality and need for such a method for practical purposes. The examples are based on fictional virtual vehicles.

Assumptions and boundaries for this work

Because the optimization of the fleet-average CO₂ emissions is a wide field of research with many influences, the following constraints are set for the thesis:

²A vehicle platform describes the sharing of a technical basis for several car models, such as front floor, underfloor, suspension, steering, braking system, electronics, wiring and engine-transmission matrix [16] [17].

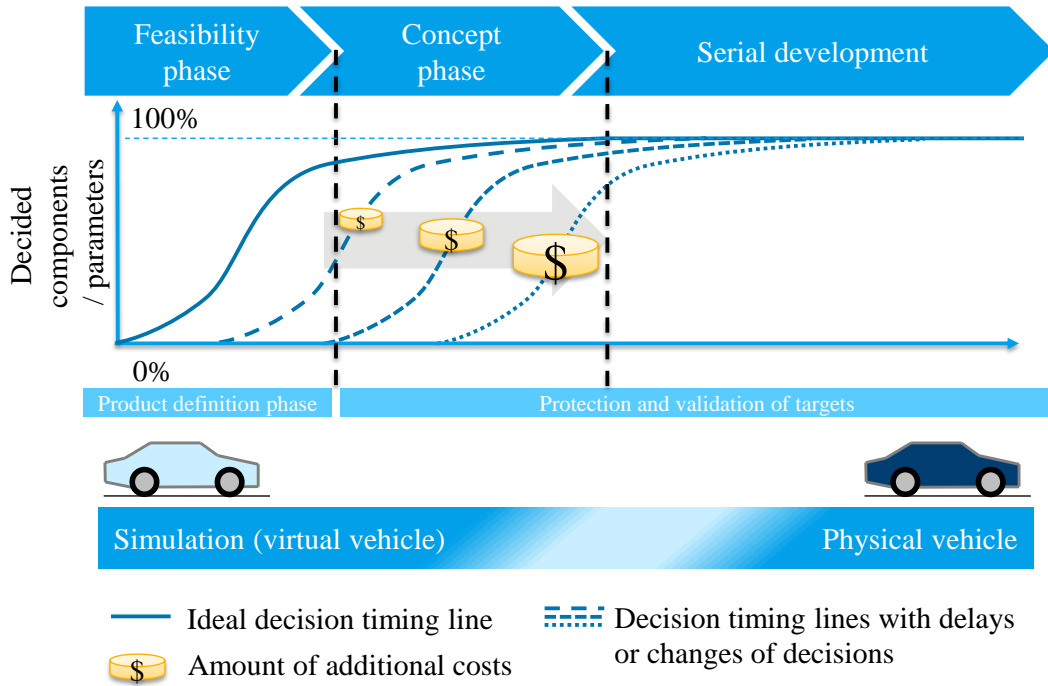


Figure 1.4.: Role of virtual methods in vehicle development

This figure explains the degree of freedom for the vehicle across the development process. The majority of decisions for components and parameters are made during the feasibility phase. Only few parameters are still variable during the concept phase, which are finally fixed during the serial development phase. The intention is to define the required measures for reducing CO₂ emissions and to ensure the targets during the feasibility phase (solid line). Although measures can also be selected in a later phase (dashed lines), this leads to higher development cost due to the need to retroactively alter components that were previously selected and fixed. One problem is that physical vehicles are first made available in later development phases. Decisions have to be made using results from simulations.

- Presetting fixed selling numbers - The present methodology does not seek to take into account changing sales numbers (e.g. due to the promotion of battery-electric vehicles to reach CO₂ emissions fleet targets).
- No final statement and rating of technologies - This thesis focuses on the method for rating measures, rather than the final ratings of individual technologies, as these can differ depending on input data and fleet definition.
- No changes of vehicle architecture - Only conventionally powered vehicles (gasoline, Diesel) are considered for the optimization and change of the vehicle architecture to reduce CO₂ emissions, for example using full-hybrid or plug-in-hybrid power-train technologies, are not considered.
- The three markets with the highest sales volume, EU, USA and China, are considered in order to compare the influence of different legal targets, different driving cycles and the composition of the market-specific fleet.
- For boundary constraints regarding driving performance, only acceleration times and maximum speed are considered for the development of the optimization approach, while drivability aspects are excluded.
- The examples for the application of the method are based on a fictional fleet and vehicles.

2. State-of-the-art

The task of this thesis - a holistic consideration and optimization of CO₂ fleet emissions - combines five key features. The starting point for the development of the optimization method is an analysis of the state-of-the-art to provide an inventory of these features, as described in this chapter. The key features are:

- Legal fleet standards for CO₂ emissions
- Possibilities and technologies for reducing CO₂ emissions
- Simulation environment for CO₂ emissions and driving performance
- Balancing targets of individual vehicles
- Optimization algorithms

The major inputs for the method to be developed are the legal fleet standards for CO₂ emissions, fuel economy and fuel consumption. The regulations, which are official documents, will be described in greater detail in Chapter 3.2.

A variety of publications address general considerations for the reduction of the CO₂ emissions of a fleet. In [8], an overall reduction of greenhouse gases for real driving is described, as was shown above in Chapter 1.1. In summary, only the item related to improving vehicle technologies can be addressed by the manufacturers themselves. The other items (e.g. traveled distances, carbon content of fuel) are primarily driven by the politics, markets and customer behavior. Furthermore, the article mentions that alternative power-trains have only a long-term potential for reducing CO₂ emissions. As conventional vehicles will hold a high market share in the short- and medium-term, technologies and improvements for conventional vehicles will have a high impact on the holistic fleet improvement to reduce CO₂ emissions. A comparable statement also appears in [9]. This article describes various vehicle technologies for reducing CO₂ emissions, such as engine downsizing or weight reduction, but focuses only on the US market. This restriction to a single market is an undesirable limitation. For example, weight reduction is one typical measure that can have a highly different effect depending on the market. While weight reduction has a high effect in the US test procedure, the effect in the EU is limited because the legal fleet-average target is coupled to the weight. A reduction of weight also leads to a decreased CO₂ emissions target in the EU. Furthermore, the article argues that technologies such as gasoline-turbo engines or Diesel engines have a high potential in the US. This is not the case in the EU, where such engines are already the state-of-the-art. This means that both the starting point and the available measures depend on the market. Thus, the optimization and selection of technologies within different markets will be quite different. Two important assumptions for this paper are that vehicles will be in production for four to five years, and that the vehicle development process will need some years before the start of production. In conclusion, anticipating the legal regulations by the end of the vehicle production time will become very important for the selection of technologies.

A more detailed example regarding CO₂ emissions fleet targets is explained in [19]. The potentials for reducing the fleet consumption were evaluated on six exemplary vehicles that represent

a fleet. The six example vehicles were chosen to represent typical European passenger cars: three with gasoline engines and three with Diesel engines. Measures were analyzed in terms of the complete vehicle, including weight, aerodynamics, tire and engine efficiency. Interactions between these various measures are listed and discussed. The goal was to show that in the EU, the fleet target of 130 gCO₂/km can be achieved by improving conventional vehicles only. One factor to reduce CO₂ emissions is the increased market share of Diesel vehicles. The weakness of this publication is that it fails to address other important measures, such as auxiliary improvements, thermal management or micro hybridization, and there is no discussion of the related costs. No statement is made regarding an optimal selection of measures. However, one additional interesting discussion in this paper is about reducing fleet consumption by using ECO or off-cycle innovations. Although a reduction of up to 7 g/km would be possible in the EU, a discussion about the cost trade-offs between vehicle and off-cycle technologies would be necessary in this context as well.

Another study is presented in [11] with a fleet status of 169 gCO₂/km in 2000 as starting point, and considering different vehicles separately. This report mentions that hybrid systems will provide a huge benefit, but with significant disadvantages in cost and geometrical size. Thus, cheaper and less complex technologies are needed to reduce the CO₂ fleet emissions. The further improvement of conventional vehicles will make a significant contribution, as discussed in the introduction of this thesis. Several engine and power-train technologies (e.g. engine start-stop, downsizing) are mentioned, and interactions are considered as well. However, this paper does not investigate of technologies on the complete-vehicle level (e.g. aerodynamics)..

A suitable method to analyze the influence of technologies on a vehicle is a complete-vehicle simulation model. Simulation models for driving performance and CO₂ emissions have already been well discussed, and the physics behind them are well known. Therefore, dozens of commercial applications are available on the market. For example, C. Haupt explains a multi-physical simulation-model in his doctoral thesis [20]. His state-of-the-art analysis discusses a wide range of other publications and software solutions. In contrast to this approach, the complexity within this work moves from the simulation of one vehicle to the handling of the simulation of a whole vehicle fleet with different components and architectures, for example. This requires an efficient automation and post-processing of simulation runs, as well as data documentation. Such an automation for the simulation of fuel consumption is presented in [21]. Here, the automated simulation environment is used to evaluate the influences of CO₂ emission-improving technologies and their influence on other vehicle attributes, such as driving performance. The measures are evaluated only for a set of reference vehicles and are then extrapolated to the whole fleet. Since the cost factor is not mentioned, the publication makes no claims about rating technologies. The following requirements are mentioned for such a simulation environment:

- Integration and consideration of all vehicles from a manufacturer, including different transmission types, engine types, and power-train configurations as well as future vehicle concepts, such as electric, hybrid or hydrogen vehicles
- Low effort for the maintenance and adaptation of models
- Modular structure of models with flexible interfaces
- Simplified models for low computation time; characteristic map-based models are preferred
- Models focused on the evaluation of energy and power flow in driving cycles
- Sub-model partitioning: engine, transmission, power-train, vehicle and driving resistance, auxiliaries, control units, driver model and hybrid components; components should be deactivated if they are not used by a certain vehicle model, in order to improve computation

time.

In addition, public authorities, such as the Environmental Protection Agency (EPA), the National Highway Traffic Safety Administration (NHTSA) and the German Federal Ministry for Economic Affairs and Energy (BMWi), have conducted many studies on improving fuel economy and CO₂ emissions. The documents [7] and [22] summarize the results related to the influence of technologies and cost expectations. However, the technologies are only described at a high level, and not in terms of specific vehicle examples.

In a second step, beyond the evaluation of CO₂ emission-improving measures, it is important to address the interactions between technologies as well as the conflicts between various vehicle targets. An outlook for such interactions between technologies is given in [7], which is summarized in Figure 2.1. This figure describes in matrix form the correlation of two measures in each case. For example, heat recovery has negative correlations with engine technologies because the improvement of the engine efficiency leads to less heat loss and therefore to less potential for technologies based on recovering this heat. D. Tscharnuter addressed the interactions which occur due to various vehicle targets in his doctoral thesis [23], including the influence on fuel consumption, driving performance and driving comfort for different vehicle layouts. The variables analyzed are the torque converter characteristic, transmission and final drive ratios. An optimization algorithm is used to determine the best parameter setting for one defined cycle. In this case, just one cycle is considered with no additional boundary constraints for other cycles. For the other cycles, only the effect is shown and discussed, but it is not included in the optimization algorithm. The thesis does also not cover the handling of different targets or a discussion about costs.

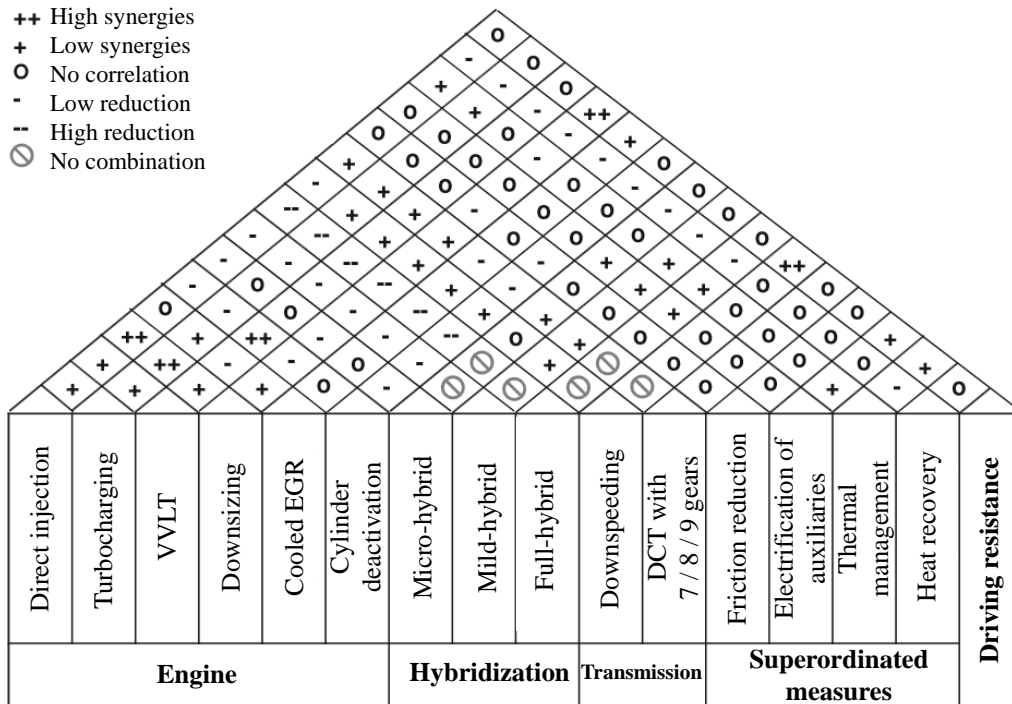


Figure 2.1.: Overview of interactions between technologies [7]

To achieve the CO₂ emissions target, it is necessary to choose from a set of available measures. In [24], an overview is given regarding which facts must be known about the measures in order to implement them into a vehicle:

- Influence on CO₂ emissions
- Influences on other vehicle attributes
- Interactions and compatibility between measures
- Costs
- Date of availability

In summary, the lessons learned from the described excerpts of the available publications and the differentiation of this thesis are as follows:

- The physics behind a complete-vehicle simulation is already known and discussed.
⇒ *The focus in this thesis regarding the simulation is on describing the specification and adaptation of models and variables and the development of an automated simulation environment.*
- A vehicle platform is typically in production for four to five years. This leads to two important inputs. First, the legal regulations and their limits have to be met within this production time, so a forecast of the targets is needed. Second, it is expected that it is not possible to change the CO₂ emissions of vehicles during the production period. Additional technologies to meet the legal standards can only be implemented with a model change or a facelift¹. To achieve the targets, each vehicle has to be considered in relation to the given time frame. The publications mentioned above offer either a general discussion about the whole fleet or detailed analysis of individual vehicles. A combination of both points of view was not found.
⇒ *This thesis deals with the question of which technologies have to be implemented in which vehicles to achieve a given CO₂ emissions fleet target for a defined time frame. The intention is to combine the analysis of several specific vehicles while considering the achievement of fleet-average targets.*
- Technologies and measures for reducing CO₂ emissions are already known and are taken as input for this thesis. The evaluation of technologies is discussed either on a high fleet level in general or on one defined specific vehicle in detail. In addition, interactions between technologies can occur. Such interactions are often mentioned, but not included in the analyses. Furthermore, target conflicts between various vehicle targets (e.g. driving performance) can influence the optimization of an specific vehicle. Such conflicts are often only considered as boundary constraints for detailed investigations of individual vehicles and are not mentioned if technologies are discussed in general on a high fleet level.
⇒ *When focusing on a specific vehicle development project, a general discussion of technologies on a high fleet level is not possible. Technologies have to be discussed on vehicle level. The selection process of measures will be influenced by interactions between technologies and can have a negative impact on other vehicle attributes. In addition, technologies must be analyzed on vehicle level because the influence of CO₂ emissions can vary depending on vehicle and driving cycle. The intention of this thesis is to use simulation to evaluate the influence of measures on CO₂ emissions for each vehicle individually. This step provides the best input for the optimization.*
- Diesel engines and downsized gasoline engines are mentioned as having high potential in the US market to reduce CO₂ emissions. Such technologies are already state-of-the-art in Europe and will lead to different strategies in the markets. Such influences need to be

¹A facelift is an update of the vehicle during the production time, including e.g. small styling updates, new options, new power-train configurations.

considered for a manufacturer that sells vehicles in various markets.

⇒ *The algorithm in this thesis should be able to determine the best selection of measures for each market individually, depending on the starting point, available measures and defined targets.*

- Costs of technologies are often mentioned, but not included in the analysis.
⇒ *The defined optimization task is not to find the minimum possible CO₂ emissions of a vehicle or a fleet. Rather, the task is to ensure a given CO₂ emissions target based on a fleet-average target, which goes hand-in-hand with the balancing of other vehicle targets. As a target for optimization, the cost involved in implementing the measures should be minimized.*
- Optimization methods focused on reducing CO₂ emissions are only found by considering one vehicle.
⇒ *In the publications, no optimization approach was found for optimizing CO₂ emissions and selecting technologies based on costs and focusing on the selection of measures for more than one vehicle. Since no basis is given for this, a discussion of different mathematical optimization algorithms is needed within this thesis. The intention is to develop an optimization approach which is able to consider more than one vehicle and to show its application and benefits based on examples.*
- The achievement of the fleet-average CO₂ emissions targets was generally discussed in the literature only on a high fleet level. In a vehicle development project, the fleet-average target must be broken down to individual vehicle targets. Such an approach was not found in the literature.
⇒ *The method developed here should be able to derive the CO₂ emissions target for each vehicle considered based on the given fleet-average target focusing on minimum overall costs.*

3. Background

3.1. Introduction

As highlighted in figure 1.3, beyond the considered vehicles themselves, the optimization problem requires that two additional inputs be considered: the legal regulations that define the CO₂ fleet emissions targets and technologies for improving them.

The first sub-chapter below describes the legal regulations for the three regions with the highest market shares - the EU, USA and China. This information is needed to determine the average CO₂ emissions target for a defined fleet depending on year and market, as well as for the target breakdown from the fleet-average target to vehicle-specific targets. In addition, information regarding additional benefits and credits will influence the target setting. Finally, the driving cycles evaluating of CO₂ emissions will be described.

The second sub-chapter addresses the vehicle technologies (hereinafter called “measures”) which can improve CO₂ emissions and describes the underlying physics, variables, costs and general impacts of these measures. This analysis will provide the basis for the adaptation of the simulation model.

3.2. Legal regulations

3.2.1. Overview

All important automotive markets have adopted regulations to reduce CO₂ emissions or improve the fuel economy of newly produced or newly registered passenger cars. Figure 3.1 shows regions where regulations for CO₂ emissions or fuel economy exist [25].

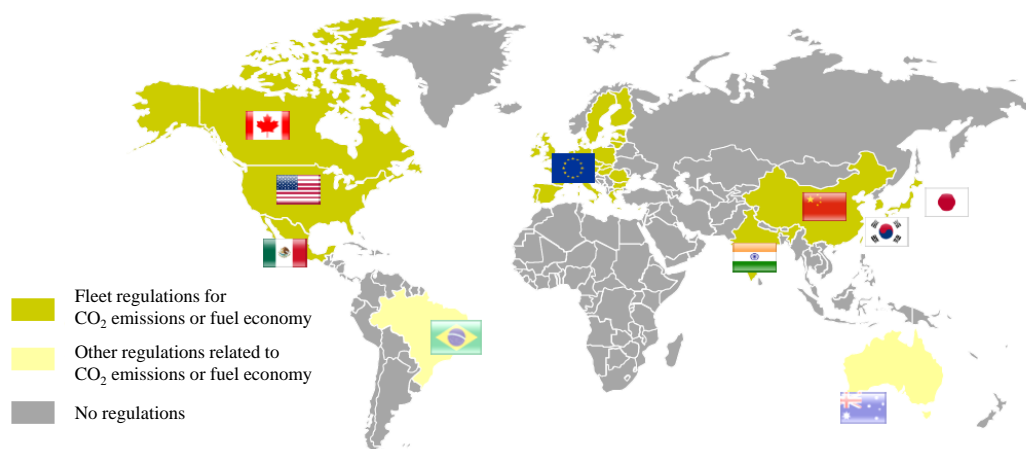


Figure 3.1.: Overview of existing CO₂ emissions or fuel economy regulations [25]

A driving cycle driven on a roller test bench to achieve for reproducible test conditions is used to evaluate CO₂ emissions and fuel consumption. The layout of such a roller test bench is described in [26], for example. The driving cycles and test conditions depend on the market. These values must be evaluated for each vehicle configuration of the fleet and are then combined to one fleet-average value for each market. Because the legal regulation limits the average CO₂ emissions of a fleet, the average CO₂ emissions, rather than the vehicle-specific CO₂ emissions, must be ensured. Thus, balancing between vehicles is possible.

Depending on the specific market involved, exceeding the targets results in monetary penalties or prohibition of vehicle selling. To avoid this, the limiting values contained in the different market-specific regulations are the major inputs for the optimization method. The following sections describe the regulations and driving cycles for the markets in the EU, China and the USA.

3.2.2. Europe (EU-28)

3.2.2.1. CO₂ emissions fleet limits

In discussions about climate change, the automotive sector makes an essential contribution to human-sourced CO₂ emissions. The Association Constructeurs Européens d'Automobiles (ACEA) was founded in 1991 and consists of the 16 biggest European automotive manufacturers and suppliers. One issue they addressed was reducing the sourced CO₂ emissions during the vehicle use phase, but also during manufacturing, logistics and transport. Based on the outcome of the Kyoto protocol in 1997, the European Union agreed to reduce the greenhouse gas emissions from 2008 to 2012 by around 8% in comparison to the reference value of 1990. Thus, the first voluntary agreement between the European Commission and the ACEA was made in 1998 to reduce the CO₂ emissions of new passenger cars to 140 gCO₂/km in 2008. As a next step, a reduction to 120 gCO₂/km was planned for 2012, but this value was increased to 130 gCO₂/km in the year 2007. However, because the voluntary intermediate goal of 140 gCO₂/km was not met in 2008, a legal binding agreement was concluded. The final regulation, *EC No. 443/2009* [27], was adopted in 2009 to take effect as of 2012. The extension is defined in *EC No. 333/2014* [28] to take effect as of 2020. [7] [29]

The CO₂ fleet emissions regulations *EC No. 443/2009* [27] and *EC No. 333/2014* [28] contain the following important facts:

- Super credits for vehicles with less than 50 gCO₂/km

Vehicles emitting less than 50 gCO₂/km receive extra credits. They will be counted multiple times in the statistics, which leads to a further reduction of the fleet-average status. The amount of credits is shown in Table A.1 in Appendix A.1.1.

- Calculation of the CO₂ fleet emissions target

The calculation for the manufacturer-specific fleet target is a linear characteristic depending on the average fleet weight. Each year, only the newly registered vehicles are considered. The equation for calculating the reference target VT_i in gCO₂/km for an individual vehicle i reads

$$VT_i = EM_0 + a \cdot (m_i - m_0) , \quad (3.1)$$

where EM_0 describes reference CO₂ emissions, a the gradient between the weight and the CO₂ emissions, m_i the curb vehicle weight (CVW) of the vehicle i , and m_0 a defined reference mass. The parameters are given in Table 3.1 based on the year. The reference weight will be adjusted every three years by monitoring the current average weight of the newly registered vehicles. Figure 3.2 shows the dependence of the target on the weight.

Table 3.1.: Parameters for calculating the vehicle target, based on year [27] [28]

Parameter	EM_0	a	m_0
Unit	gCO ₂ /km	gCO ₂ /(km·kg)	kg
2012-2015	130	0.0457	1372
2016-2019	130	0.0457	1392.4
from 2020	95	0.0333	to be defined

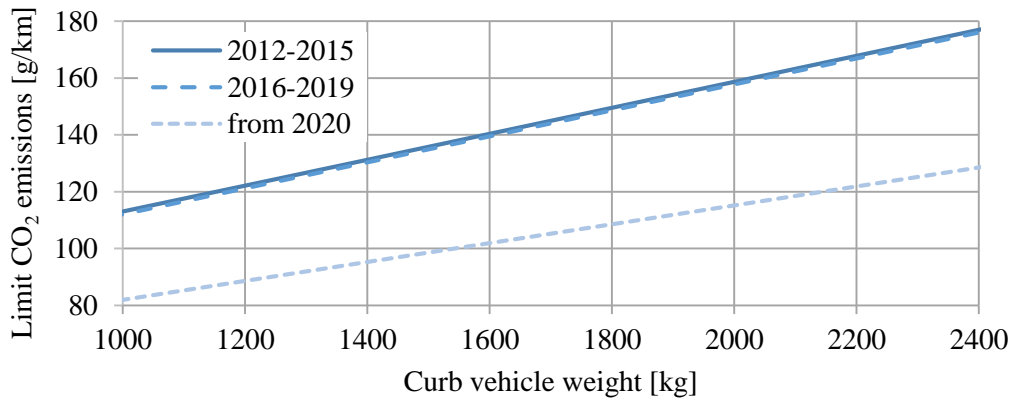


Figure 3.2.: Fleet target in the EU, based on year and curb vehicle weight [27] [28]

The calculation for the fleet-average target FT_y for a defined year y is an average value of all vehicle targets VT_i . These values are weighted by the sales volume $svol_{i,y}$ and the super-credit factor $crd_{i,y}$ depending of the vehicle i and year y . Equation (3.2) shows this correlation. [30]

$$FT_y = \frac{1}{\sum_i svol_{i,y} \cdot crd_{i,y}} \cdot \sum_i svol_{i,y} \cdot crd_{i,y} \cdot VT_{i,y} \quad (3.2)$$

The actual status of the fleet FS_y can be calculated by using Equation (3.3) considering the measured CO₂ emissions EM_i of each vehicle i in gCO₂/km [30].

$$FS_y = \frac{1}{\sum_i svol_{i,y} \cdot crd_{i,y}} \cdot \sum_i svol_{i,y} \cdot crd_{i,y} \cdot EM_i \quad (3.3)$$

- Monetary penalty for exceeding the targets

If a manufacturer exceeds its individual fleet-average target, a monetary penalty must be paid. The penalty amount P_y is shown in Table 3.2 and depends on the gap and the year y . The gap is defined as the difference between the fleet status FS and the fleet target FT . The final penalty for the whole fleet FP_y is multiplied by the fleet sales volume $\sum svol$ and described by Equation (3.4).

$$FP_y = P_y (\max \{0; FS_y - FT_y\}) \cdot \sum_i svol_{i,y} \quad (3.4)$$

Table 3.2.: Monetary penalty $P_y(gap)$ for exceeding the fleet target based on year and gap

Gap / Year y	for the 1 st gCO ₂ /km	for the 2 nd gCO ₂ /km	for the 3 rd gCO ₂ /km	for the 4 th gCO ₂ /km	for the x th ($x \geq 5$) gCO ₂ /km
until 2018	5 €	+15 €	+25 €	+95 €	+95 €
from 2019	95 €	+95 €	+95 €	+95 €	+95 €

- Phase-in periods

As a buffer for the step-wise reduction of the fleet target, a phase-in has been defined. Only a fixed percentage of newly registered vehicles of the fleet are considered. The percentages are summarized in Table A.2 in Appendix A.1.2.

- Approval of ECO innovation

The term “ECO innovations” is applied to technologies whose benefits for CO₂ emissions are not measurable in the legal standardized test cycle (see Chapter 3.2.2.2), but which will have a benefit on real driving. Thereby, the CO₂ emissions of a vehicle can be reduced up to 7 gCO₂/km by integrating such technologies. An overview of approved technologies is given in Appendix A.1.3.

- Implementation of predefined technologies

As a compensation for the increase from 120 to 130 gCO₂/km fleet-average target in 2007, additional technologies can be implemented. These technologies are highly efficient air conditioning, tire pressure control system, tires with low rolling resistance, gear shift indicator and bio fuel [7] [31] [32]. Here, 5 g are related to the use of bio fuels, and the other 5 g are related to the other technologies listed [33].

3.2.2.2. Legal test driving cycle - NEDC and WLTC

To ensure reproducible and comparable measurements, the CO₂ emissions EM_i for a vehicle are evaluated via standardized test cycles and test procedures on a roller test bench. The test cycle and test procedure in Europe is defined by the regulation *ECE-R 83* [34] for conventional vehicles and *ECE-R 101* [35] for electric and hybrid-electric vehicles. Since 2000, the New European Driving Cycle (NEDC) (also called Motor Vehicle Emission Group Cycle Version B (MVEG-B)) has been used as a test cycle. The speed profile is indicated with the black line in Figure 3.3.

In addition to the test cycle, the regulation describes the test procedure. For the NEDC, the following facts are important for the testing and for the simulation of vehicles:

- Preconditioning with a temperature between 20 and 30°C to perform a cold-start¹
- Payload of 100 kg, representing one driver and baggage

¹Additional losses occur during the warm-up of the engine due to higher friction and additional cold-start enrichment if the engine and transmission do not operate at their operating temperatures.

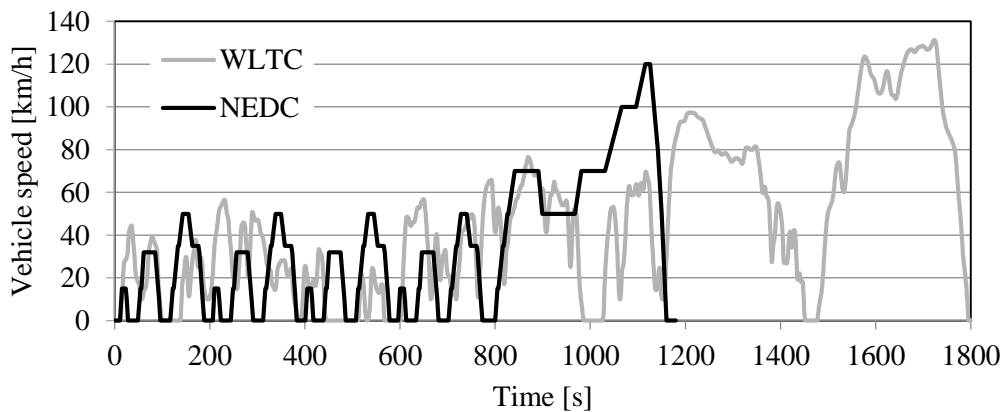


Figure 3.3.: Speed profile of NEDC and WLTC

- The inertia (accelerated mass) is divided into discrete test weight steps, with a step size around 110 kg (see Appendix A.1.4)
- A fixed gear profile over time for vehicles with manual transmission
- Activation of minimal auxiliaries (e.g. no headlights, radio or air conditioning)
- No balancing of a discharged low-voltage battery
- Special test sequences for hybrid vehicles (see Appendix A.1.5)

In 2021, the Worldwide Harmonized Light Vehicles Test Cycle (WLTC) will finally replace the NEDC [36] [37]. The test procedure is described by the Worldwide Harmonized Light Vehicles Test Procedure (WLTP). The WLTP is still being defined, but the draft version [38] describes the current status. The speed profile is indicated with the gray line in Figure 3.3. This new cycle features the following characteristics:

- Preconditioning with a temperature between $23 \pm 3^{\circ}\text{C}$ to perform a cold-start
- Payload of 100 kg plus 15% of the remaining payload, representing one driver and baggage
- No inertia classes; inertia weight is equal to the test weight
- An customized, pre-calculated gear profile for every vehicle with manual transmission (see Appendix A.1.6)
- Activation of minimal auxiliaries (e.g. no headlights, radio or air conditioning)
- Balancing calculation of the discharged low-voltage battery (see Appendix A.1.7); No battery recharge while the precondition phase is allowed
- Special test sequences for hybrid vehicles (see Appendix A.1.8).

3.2.3. Republic of China

3.2.3.1. Fuel consumption limits

In contrast to Europe, the Chinese regulation was not inspired by the greenhouse gas effect and the CO₂ emissions. The high growth of the Chinese automotive market has led to a

higher demand for oil. For this reason, the China Automotive Technology and Research Center (CATARC) launched a study on the feasibility of a Chinese fuel consumption standard in 2001. The first standard *GB 19578-2004* [39] was finalized in 2004 and is divided into two stages which took effect in 2006 (GB Stage I) and 2008 (GB Stage II). Both stages include a weight-dependent fuel consumption limit for every vehicle. Exceeding the limits leads to a prohibition on selling the vehicle. The limits depend on the vehicle curb weight in order to encourage the sale of small vehicles. Because regulations in the USA, Europe and Japan became more stringent and the cost of oil and the need for oil imports increased, the standard was extended in 2008. Stage III, described in the standard *GB 27999-2011* [40], was finalized in 2010 to take effect in 2012. Stage III was now based on an average fleet target to allow the manufacturers to balance the fuel consumption gaps between vehicles. Stage IV, which was finalized in 2014 to take effect in 2016, is described by the standards *GB 19578-2014* [41] and *GB 27999-2014* [42]. This regulation now also includes credits for special vehicles to encourage the sale of alternative vehicles (e.g. BEV or PHEV). [43] [44]

The fuel consumption targets are characterized by the following important facts:

- Individual vehicle limits and corporate-average fuel consumption targets

Since Stage III, two limits have had to be considered - the vehicle-specific limit and the fleet-average limit. Primarily, the vehicles have to meet an vehicle-specific limit. In addition, the complete fleet has to meet a corporate-average fuel consumption target. The regulations describing the limits are summarized in Table A.4 in Appendix A.2.1. The targets for the vehicles depend on the vehicle curb weight, the power-train type (MT² or AT³) and the vehicle type⁴, as shown in Figure 3.4. The concrete values are summarized in Appendix A.2.1 in Table A.5.

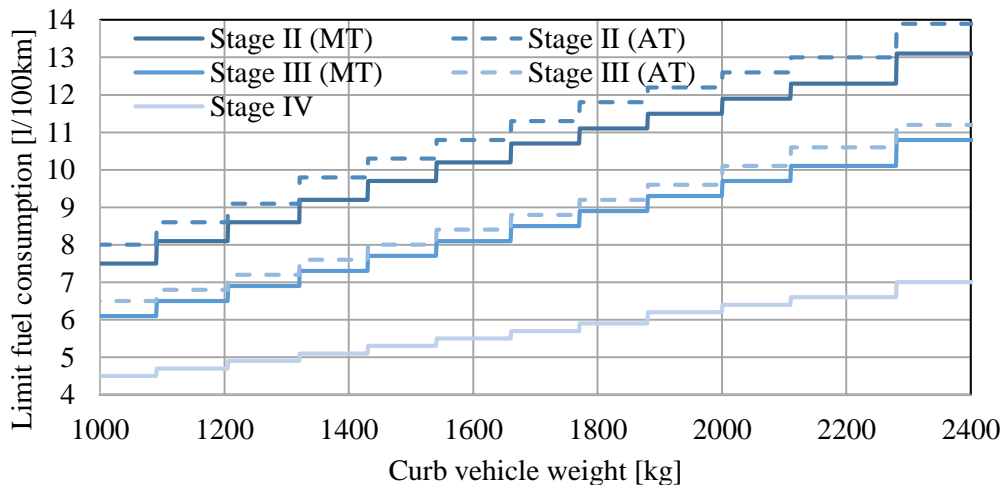


Figure 3.4.: Fleet targets in China, based on curb vehicle weight, stage and power-train type [39] [40] [41] [42]

- Phase-in periods

As shown in Figure 3.4, the change of the fleet targets between the stages has been erratic. A

²Vehicles with manual transmission

³Vehicles with automated gear-shifting (e.g. automatic transmission, automated manual transmission, double clutch transmission)

⁴Vehicles with three or more rows of seats (3R) have another target.

phase-in is defined to buffer the step-wise reduction. The target value of a year y is multiplied by a factor fpi_y . Table 3.3 shows the factors for Stage III and Stage IV.

Table 3.3.: Phase-in factors for fleet targets [39] [40] [41] [42]

Year y	Phase-in factor fpi_y
until 2011	no fleet target
2012 (Stage III)	1.09
2013 (Stage III)	1.06
2014 (Stage III)	1.03
2015 (Stage III)	1.00
2016 (Stage IV)	1.32
2017 (Stage IV)	1.28
2018 (Stage IV)	1.20
2019 (Stage IV)	1.10
from 2020 (Stage IV)	1.00

- Credits for new energy and ultra-low-fuel-consumption vehicles

New energy vehicles (battery-electric vehicles (BEV), fuel cell vehicles (FCV), plug-in hybrid-electric vehicles (PHEV)) with an electric driving range of at least 50 km as well as ultra-low-fuel-consumption vehicles with a fuel consumption less than or equal to 2.8 l/100km have been granted extra benefits since Stage IV. The amount of the credits is shown in Table A.6 in Appendix A.2.2. Such vehicles are counted multiple times by a factor crd_y depending on the year y .

- Credits for innovative real-world fuel-saving technologies

Within Stage IV, up to 0.5 l/100km are chargeable to the fleet-average status for innovative technologies that reduce fuel consumption for real-world driving but are not measurable within the official test procedure. Such technologies can include a tire pressure monitoring, high-efficiency air conditioning, start-stop system and gear shift indicator.

- Calculation of the corporate-average fleet target and status value

The calculation of the individual manufacturer's fleet target $Tcafc_y$ for a year y is based on the reference target $Tvfc_{i,y}$ and the sales volume $svol_{i,y}$ of each vehicle i , as well as the phase-in factor fpi_y . Each year, only the newly registered vehicles are considered. The equation to calculate this target is given in (3.5).

$$Tcafc_y = \frac{\sum_i Tvfc_{i,y} \cdot svol_{i,y}}{\sum_i svol_{i,y}} \cdot fpi_y \quad (3.5)$$

The calculation for the current status fleet value $Scafc_y$ of an individual vehicle i reads

$$Scafc_y = \frac{\sum_i Svc_i \cdot svol_{i,y}}{\sum_i svol_{i,y} \cdot crd_{i,y}}, \quad (3.6)$$

where Svc_i is the fuel consumption status of a vehicle i and crd the credit factor.

3.2.3.2. Legal test driving cycle - NEDC

The test procedure and test cycle (NEDC) currently used in China is similar to those in Europe. The procedures are defined in *GB 19233-2008* [45] for conventional vehicles and *GB 19753-2013* [46] for hybrid and electric vehicles.

3.2.4. USA and California

3.2.4.1. Fuel economy and greenhouse gas targets

The oil crisis in 1973 led to a discussion about limiting the fuel consumption of vehicles to reduce the need to import foreign oil. With the Energy Policy Conservation Act (EPCA), the U.S. congress adopted a fuel economy standard in the form of a corporate-average fuel economy (CAFE) from the model year 1978 for passenger cars (PC)⁵ and from the model year 1975 for light-duty trucks (LDT)⁶. The standard is administered by the NHTSA. For passenger cars, a minimum fuel economy of 18.0 mpg was set in 1978, with a steady increase to 27.5 mpg in 1990. Since 1991 the standard has remained constant. The fleet-average fuel economy is weighted by the sales volume of the vehicles. If the fleet does not meet the minimum fuel economy, a monetary penalty of \$5.5 per 0.1 mpg is imposed. This first fuel economy target was independent of the vehicle size, but the NHTSA adapted the regulation to a footprint⁷-based target in 2006. [7] [32] [47] [48]

In addition to the federal law, every state is allowed to limit emissions itself. Due to the unfavorable geographic basin location of California and the high air pollution [30], the California Air Resources Board (CARB) passed a law to reduce greenhouse gas (GHG) emissions of vehicles in 2007. The California regulation is based on GHG emissions and exists parallel to the federal fuel economy limitation. If a fleet does not meet the GHG fleet target, vehicle models that cause the fleet to exceed the limit are prohibited from being sold in the California market. In addition, special credits are available for vehicles that feature very high fuel economy, optimized air conditioning and the usage of bio fuels. [7]

Based on the CARB regulation for GHG emissions, the EPA also adopted a national GHG emissions standard, which took effect in 2012. The targets of the NHTSA's CAFE standard and the EPA's GHG standard have been harmonized. In 2012, the regulations for the phase from 2017 until 2025 were defined. [22]

The regulations in the USA are characterized by the following facts:

- Corporate-average fuel economy standards

Two regulations and limits exist - one for fuel economy (NHTSA) and one for greenhouse gas emissions (EPA). Both regulations are based on a fleet-average target based on the vehicle footprint and described as an annual reduction of the limits. The targets for fuel economy are shown in Figure 3.5, and the targets for CO₂ emissions are shown in Figure 3.6. The detailed calculation of the curves is described in Appendix A.3.1. Because the limit for GHG is more stringent than that for fuel economy, only the GHG fleet target will be considered as an input for the optimization approach in this thesis.

⁵Passenger cars are defined as four-wheeled vehicles not designed for off-road use which transport fewer than 10 people [32].

⁶Light-duty trucks are defined as four-wheeled vehicles designed for off-road or vehicles between 6000 and 8500 lbs gross vehicle weight (GVW) [32].

⁷The footprint is the area defined by the wheelbase and the wheel track.

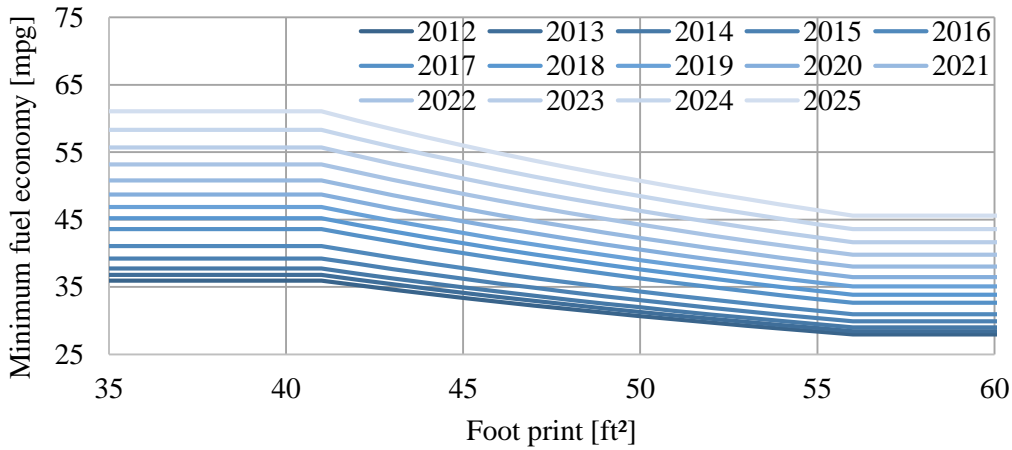


Figure 3.5.: Fuel economy fleet targets for passenger cars according to NHTSA, based on year and footprint [22]

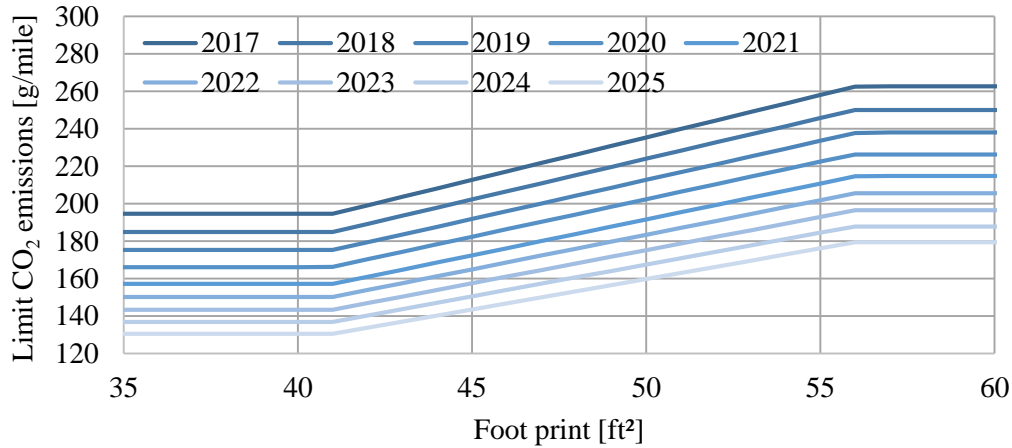


Figure 3.6.: Greenhouse gas emissions fleet targets for passenger cars according to EPA, based on year and footprint [22]

- Benefits for alternative vehicles

Alternative vehicles have two advantages related to the fleet-average calculation. First, the electric consumption will not be considered in the CO₂ emissions balance until 2025. As of 2025, the electric energy consumption is planned to convert to 0.574 gGHG/Wh. Second, alternative vehicles will count multiple times until 2021. The multipliers are listed in Table A.9 in Appendix A.3.2. From 2022 to 2025, only the first benefit will be available. [22]

- Calculation of the corporate-average fleet target

The calculation for the manufacturer-specific fuel economy fleet target $Tcafe_y$ for a year y is based on the reference target $Tvfe_{i,y}$ and the production volume $pv_{i,y}$ of each vehicle i . The equation is given in (3.7). For simplification, the production volume pv and the sales volume sv will be assumed to be the same in the following equation.

$$Tcafe_y = \frac{\sum_i pv_{i,y}}{\sum_i Tve_{i,y}} \quad (3.7)$$

- Off-cycle technologies

It is possible to get extra credits for technologies which cannot be measured by the standardized test procedure (Federal Test Procedure (FTP), Highway Fuel Economy Test (HWFET)). These technologies are called “off-cycle credits”. One part involves the improvement of the A/C system. The related technologies are listed in Table A.10 in Appendix A.3.3. Up to 5.0 gCO₂/mile can be considered for extra credits. In addition, other technologies, which are comparable to the European ECO innovations, are possible, which are listed in Table A.11 in Appendix A.3.3. Therefore, the EPA set a default value for the credits. If a manufacturer expects a higher improvement with their technology, they can apply for a greater credit. In addition, the technologies have to be implemented in a defined minimum percentage of the vehicles produced. [22]

3.2.4.2. Legal test driving cycle - FTP75/HWFET

The test cycle and test procedure for the evaluation for the CAFE or the GHG emissions in the USA is based on the 2-cycle test described in *40 CFR 600* [49]. This test consists of two cycles: the FTP75, which represents city driving, and the HWFET, which represents highway driving. The speed profile of both driving cycles is shown in Figure 3.7. In addition, the test procedure for hybrid vehicles is described in *SAE J 1711* [50].

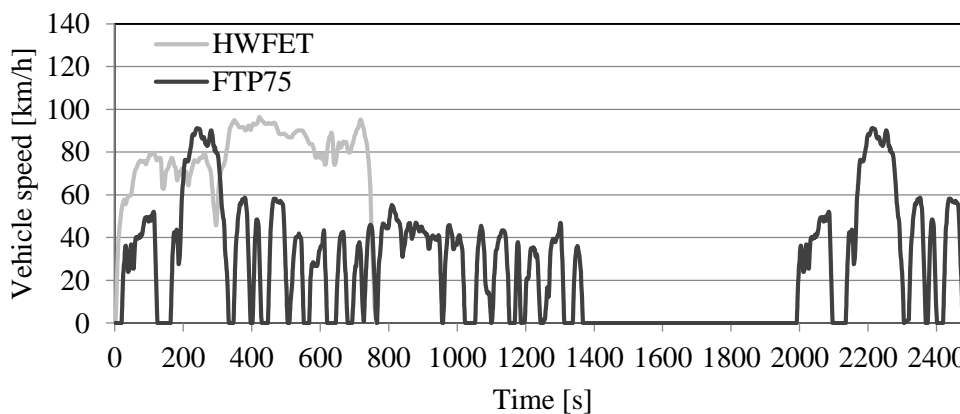


Figure 3.7.: Speed profiles of FTP75 and HWFET

For the 2-cycle test, the following facts are important:

- FTP75: Preconditioning with a temperature between 20 and 30°C to perform a cold-start
- HWFET: Preconditioning with a temperature between 20 and 30°C, but before the officially measured test, a precondition cycle is driven to perform a warm-start
- The final fuel economy is calculated based on both cycles. The FTP75 counts 55% and the HWFET 45%, according to Equation (3.8).
- Payload of 136 kg, representing one driver, package and a portion of options

- The inertia (accelerated mass) is divided into discrete test weight steps with a step size of around 55 kg (see Appendix A.3.4).
- A fixed-gear profile over time for vehicles with manual transmission
- Activation of minimal auxiliaries (e.g. no headlights, radio or air conditioning)
- No balancing of a discharged low-voltage battery
- Special test sequences for hybrid vehicles (see Appendix A.3.5)

$$FE_{\text{comb}} = \frac{1}{\frac{0.55}{FE_{\text{FTP75}}} + \frac{0.45}{FE_{\text{HWFET}}}} \quad (3.8)$$

3.3. Vehicle technologies

3.3.1. Introduction

To achieve a CO₂ emissions target, vehicle technologies that influence CO₂ emissions have to be improved. To this end, a view of the complete vehicle is needed. The vehicle can be divided into different sub-systems. The following sub-sections describe the energy flow through a vehicle and provide a basic overview of common technologies for improving CO₂ emissions. Based on literature research, a more detailed and summarized overview of technologies for every sub-system, their effects on CO₂ emissions and their expected costs can be found in Appendix B.

3.3.2. Energy flow of a vehicle

Based on various sub-components, Figure 3.8 illustrates the energy flow through a vehicle from tank to wheel. Depending on the driving cycle speed profile, the internal combustion engine is controlled by the driver via the accelerator pedal. The combustion engine burns and converts the fuel into mechanical energy via a thermodynamic process. One important influence thereby is the warm-up of the engine, which decreases the efficiency until the engine is warm. In addition, the engine has to support mechanical and electrical auxiliaries. Via the transmission and the drive-train, also including losses, the mechanical energy is transferred to the wheels. On the wheel, the energy is divided into the loss due to the driving resistance (aerodynamic drag and rolling resistance) and the kinetic energy of the vehicle mass and the rotary inertia to accelerate the vehicle. During braking phases, the kinetic energy is reduced by deploying the mechanical brake and converted into thermal energy. The driver uses the brake pedal to control the brake pressure. Based on this energy flow, Figure 3.9 shows a typical distribution of the energy losses of an exemplary vehicle based on a simulation. The simulation model used and the energy flow in the simulation model will be explained in more detail in Chapter 4. For conventional vehicles, the most significant loss occurs in the engine itself due to the thermodynamic process. However, the other components also have an appreciable amount of loss and therefore affect the fuel consumption. This example highlights that both the complete vehicle and several individual technologies have to be considered in the process of reducing fuel consumption and CO₂ emissions.

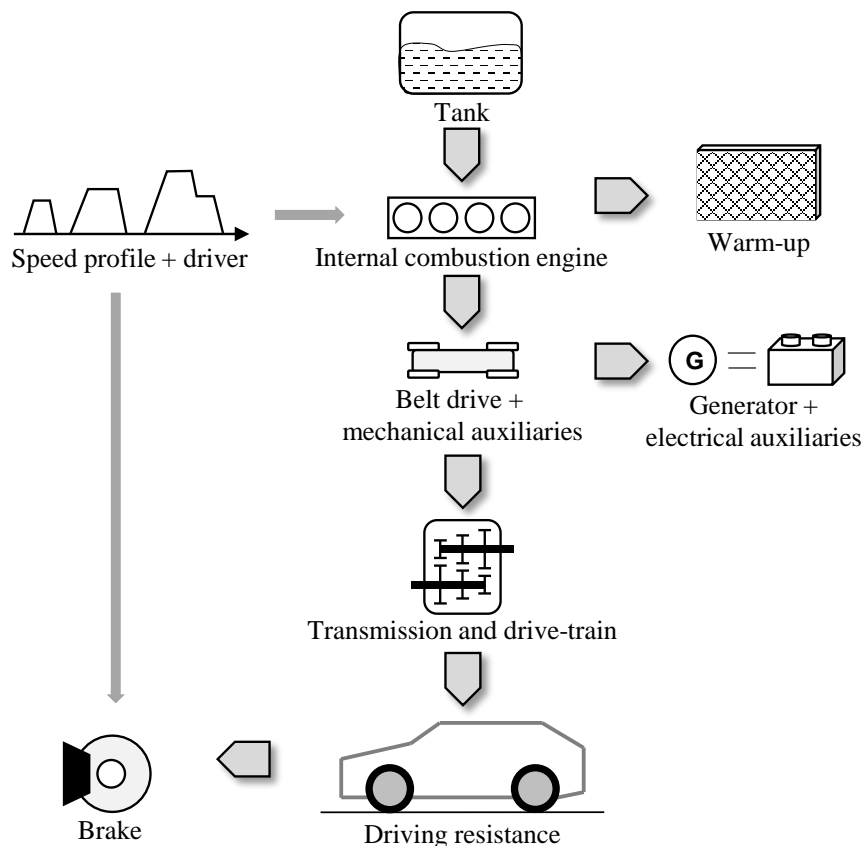


Figure 3.8.: Simplified energy flow and sinks in a vehicle

3.3.3. Internal combustion engine

3.3.3.1. Efficiency of gasoline engines

The efficiency of an internal combustion engine (ICE) is defined by the efficiency of the ideal Otto cycle and the efficiency of the real motor cycle. The efficiency of the real engine is reduced by:

- The non-ideal Otto cycle; due to the limited time, the combustion is not based on the ideal constant volume, so not all fuel is burned at the highest possible pressure [51] [52].
- Real combustion; imperfect combustion due to the non-ideal chemical equilibrium [51]
- Thermal heat losses to the cylinder wall, coolant and exhaust [51] [52]
- Pumping losses; gas exchange losses due to expansion, compression throttling and flow loss [51] [52]
- Mechanical losses (e.g. piston, crankshaft, valves), whereby friction is more dependent on engine speed than on engine torque [51] [52].
- Aerodynamic and pressure losses (e.g. air cleaner, intake and exhaust manifold, valves, silencer, catalyst), whereby the losses depend on the air flow rates [51] [52].
- Leakage due to piston ring (leads to loss of pressure) [51]

In general, engine efficiency and thus fuel consumption can be improved by:

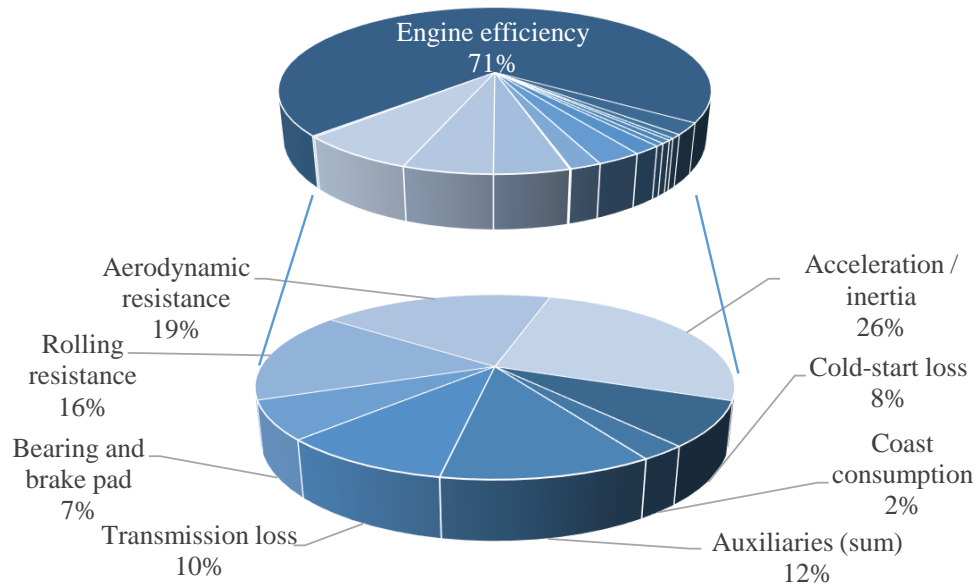


Figure 3.9.: Example of the energy loss distribution in a vehicle (NEDC) based on simulation

- Increasing the efficiency of the thermodynamic cycle [53]
- Reducing pumping and throttling losses [53]
- Reducing internal friction [53]
- Recovering heat losses to coolant and exhaust

Figure 3.10 shows a simple illustration of a specific fuel consumption map. For typical technologies that improve fuel consumption, the indicated map regions show where the major benefit of the technology is expected.

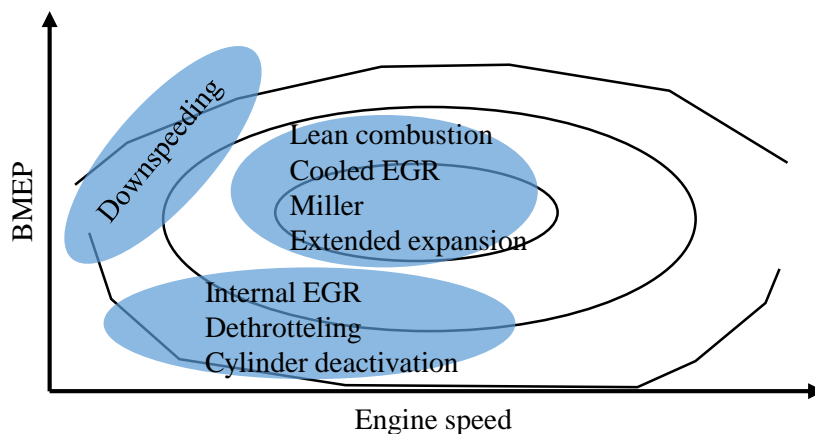


Figure 3.10.: Illustration of a specific fuel consumption map with typical technologies for improving fuel efficiency and their map regions where the improvement is expected (based on [54])

To improve the efficiency of the engine, the following typical technologies are already in use or are under development:

- Miller and Atkinson cycle
- Direct injection
- Variable valve train (VVT)
- Cylinder deactivation
- Turbo charging and downsizing
- Variable compression
- Exhaust gas recirculation (EGR)

A more detailed description of these technologies is provided in Appendix B.1.1.

3.3.3.2. Efficiency of Diesel engines

Due to their physical principle, Diesel engines have a higher efficiency than gasoline engines. This is due to the higher compression ratio (16 to 24) and the resulting higher thermodynamic efficiency. Due to direct injection and lean burning, there are no pump and throttle losses [22] [52]. Furthermore, Diesel engines have less potential for further improvement because turbo charging and inter-cooling are already state-of-the-art [52]. Further potentials can be only tapped by improving existing technologies, such as injection pressure, optimization of geometries, exhaust gas recirculation, and variable turbocharger geometry [55]. The major priority for Diesel engine development is to reduce nitrogen oxide (NO_x) emissions and sooty particles [52].

3.3.3.3. Engine friction

One factor affecting engine efficiency is mechanical losses. The friction sources of an engine can be divided into the following categories [52] [56] [53]:

- Piston and piston rings (depending on speed, oil temperature, engine load)
- Valve train
- Bearing (depending on oil temperature, speed and geometry)
- Oil pump
- Ventilation of crankshaft
- Fuel pump

To improve the friction, the following measures are possible:

- Friction-optimized surface coating [7] [22] [52] [53]
- Lubricants and oil with low viscosity [7] [22] [52] [53]
- Improved design of the piston rings or reduced number of rings [22] [47] [52]
- Improved tolerances between bore and piston [52] [53]
- Weight reduction of moving parts (e.g. valves, piston) [52]
- Use of roller cams [22] [52]
- Improving oil pump, reducing pressure losses in the oil circuit, implementing a variable oil pump [52] [57]

3.3.3.4. Thermal management

Most legal test cycles (NEDC, FTP75, ...) are driven after a precondition time. The engine is typically started at 23°C. In contrast the operating temperature of the engine is around 90°C. For this reason, the cold-start involves additional losses. The main influencing factor is the increased friction at lower temperature [58]. Another influence is the engine control. The adaptation of the ignition angle to ensure the operation and drivability of the cold engine and the support of the warm-up of the catalyst conflict with a control logic for the optimum engine efficiency. [58] [59]

Improving the additional cold-start consumption primarily involves improving the oil or coolant warm-up:

- Minimize oil volume to be warmed-up, e.g. by a two-chamber system [60] [61]
- Intelligent thermal management by using separate cooling circuits (for engine block and head), radiator shutter and controllable water pump [7] [61]
- Preserve thermal energy from previous driving, e.g. by a fluid heat storage [61] [62]
- Warm-up support by an electric heater [61]
- Warm-up of the transmission oil [61]

3.3.3.5. Engine heat recovery

Based on the analysis of the energy loss (e.g. in Figure 3.9), the biggest portion of the losses is related to the engine efficiency. The chemical energy is converted to thermal energy in the engine block, the coolant, the oil (26 to 32% [7]) and the exhaust (20 to 32% [7]). In general, this thermal energy is lost. One way to increase the system efficiency is to recover this thermal energy. Because the temperature level of the coolant and oil is too low (below 100°C), no practical system is currently available for automotive application. The focus of heat recovery systems is on the exhaust gas, which features temperature above 250°C. [52]

In this context, the following methods are being developed:

- Thermo-electric generator / Seebeck-effect [7] [30] [52] [63]
- Thermo-mechanical by using the ranking cycle (steam engine) [7] [30] [52]
- Turbo-compounding by using the exhaust pressure to generate additional torque via a turbine on the crankshaft (although the pressure in passenger cars is too low) [52] [64]
- Exhaust turbo charging (see Section 3.3.3.1) [52]

3.3.4. Auxiliaries

3.3.4.1. Overview

To operate the vehicle and ensure all functions at the required operation points, a set of mechanical and electrical auxiliaries are needed in the vehicle [2]. Components can be separated into the following main functions:

- Operation of the engine itself: fuel pump, supply with lubricants, cooling and vacuum

- Electrical power supply: generator
- Ensure comfort and safety-relevant functions: steering, air conditioning

The problem with mechanical systems is that they are directly coupled to the engine (e.g. via the belt drive), and the operation is proportional to the engine speed. To ensure the functionality of all systems, they have to work during engine-idle operation, at full load and on maximum engine speed. This often leads to an over-sizing of the system / components and results in additional drag loss and less efficiency. Since the normal operation is in partial load, it is not the optimal design point. In addition, auxiliary components are often carry-over parts from modular assemblies and therefore are not optimized for each specific engine and vehicle. [2]

Two principle approaches exist to reduce the loss caused by auxiliaries [2]:

- Improve the efficiency
- Reduce the energy demand

The following sub-chapters describe different components in greater detail.

3.3.4.2. Engine cooling circuit components

The cooling system is designed for extreme operating points and is oversized in most driving phases. The temperature of the engine is regulated by a thermostat, which divides the flow to a short circuit or to the radiator. A mechanical cooling pump runs continuously independent of the real cooling demand, but depending on engine speed. [65]

Possible measures for reducing the power demand of cooling components or improving the operation of the combustion engine are:

- Electrically actuated thermostat to control the temperature, e.g. increase the temperature of the combustion engine at partial load [2] [65]
- Controlled fan with Pulse Width Modulation (PWM) (which is already state-of-the-art in passenger cars) [2] [65]
- A switchable or electrical water pump to adapt the demand-actuated power [2] [65]; in addition, no coolant flow during the engine warm-up will support the process [2].
- Reduce pressure losses in the cooling circuit to reduce the necessary hydraulic power of the pump [66]

3.3.4.3. Compressor for air conditioning

The drag torque caused by an air conditioning (AC) compressor can be improved by engaging or disengaging the compressor with a magnetic clutch or by using a compressor with a variable displacement volume. Because legal test cycles are based on the activation of minimal auxiliaries (e.g. deactivated heating, ventilation and air conditioning (HVAC)), the target should be focused on minimal drag torque of the compressor. For real-life driving, an operating HVAC requires additional electrical energy demand for cabin blower and fan, in addition to the mechanical compressor work, which also influences fuel consumption. [2]

3.3.4.4. Power steering

Power steering can also be optimized via on-demand actuated power requests. Three typical systems exist: [2] [67]:

- Hydraulic Power Steering (HPS): A hydraulic pump connected to the engine supplies a constant oil volume flow. The pump also functions during idle operation. To improve this base system, two methods are possible. The first method is to use a variable HPS where a variable-displacement pump improves the volume flow. The second concept involves combining a coupled HPS and EHPS system. [2] [53]
- Electric-Hydraulic Power Steering (EHPS): With this improvement, an electric motor is connected to the hydraulic steering pump instead of the direct connection to the crankshaft, which provides pressure only when needed.
- Electric Power Steering (EPS): Here, an electric motor is connected to the steering, which eliminates the hydraulic system and its losses. Power is required only in case of steering operation, and unlike an EHPS, no efficiency is lost due to the intermediate transformation to hydraulic energy.

3.3.4.5. Vacuum pump for brake booster

Vehicles with Diesel engines or gasoline engines with direct injection need an additional vacuum pump to ensure the required low-pressure for the brake booster [2]. This pump is often mechanically coupled to the crankshaft. A benefit is expected with the use of an electric vacuum pump due to demand-actuated control.

3.3.4.6. Alternator

The alternator is typically a claw pole generator with a PWM-controlled excitation field supplied by a collector ring [68]. The efficiency is around 65% on average [2] [69]. The efficiency can be improved by using Metal-Oxide Semiconductor Field-Effect Transistors (MOSFET) instead of diodes for current rectification (~10% efficiency), optimized stator winding to reduce the resistance (~12% efficiency), or using permanent magnets instead of a collector ring (~15% efficiency) [2].

3.3.4.7. Electrical System

The energy demand of the additional electrical auxiliaries can be improved by an intelligent energy management control. For example, during braking phases, the electrical energy is produced without use of fuel and is therefore free. Auxiliaries can be controlled to increase their operation during such periods and to reduce the operation afterwards to save fuel. An electric heater can heat the oil or coolant water with such free energy to improve the engine warm-up and reduce losses related to cold-start [7] [70] [71]. Another possibility is to reduce the energy demand, for example by replacing halogen head lights with light-emitting diodes (LED) light or improving the energy demand with PWM control (e.g. a PWM-controlled fuel pump [7]). Table B.4 in Appendix B.2 provides an overview of the electric power demand of consumers.

3.3.5. Transmission

The transmission / power-train has five tasks in the vehicle: [51] [72]

- Transfer the torque from the engine to the wheel
- Function as a starting element (torque converter, clutch) because an engine has a minimal speed (idle speed) and so a vehicle launch from zero is not possible without a starting element.
- For driving backwards, the rotary direction must be reversed because a combustion engine in the automotive industry is designed to operate in one rotary direction only.
- Increase the operating range of the engine with several gears for the compromise between high wheel torque at low vehicle speed and a defined maximum vehicle speed
- Influence the engine operating point via gear selection and select an operating point with the best fuel efficiency.

Figure 3.11 shows the components of the power-train. In this context, the losses in the power-train relate to the following effects:

- Losses due to slipping operation of the starting element
- Transmission losses due to windage, oil churning, slide friction and rolling friction losses of the gears [73] [74]
- Drag of the oil pump in an automatic transmission [75]
- Drive-train losses due to joints of the prop-shaft and side-shafts, as well as due to oil seals, bearings and the brake pad drag [52]
- Controlling the transmission and the starting element via a control unit; An operating strategy defines the slip operation phase of the starting element and the gear selection of the transmission. The gear selection influences the engine operating point and therefore the fuel efficiency of the engine.

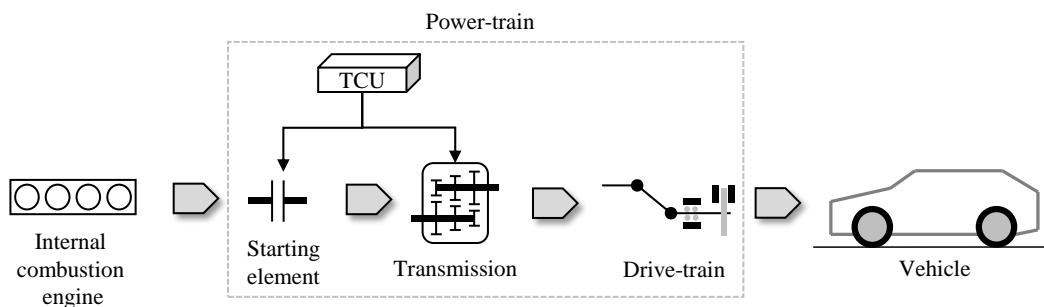


Figure 3.11.: Components of the power-train sub-system

Improving the fuel consumption by the adaptation of the power-train components is focused on the following actions:

- Reduce the losses
- Optimizing the gear ratio and the shifting strategy for optimal engine operation points; A lower engine speed and higher engine torque will reduce throttling and friction losses, which leads to better fuel efficiency [52].

Various approaches exist to reduce the losses caused by the transmission and drive-train:

- Reduction of transmission losses with low-friction oil to reduce oil churning losses [76]. However, except the improvement of actuators, no radical improvements are currently anticipated due to the mechanical limitations [72].
- Implementation of a lockup clutch for a torque converter in automatic transmission; Based on the physical principle, a torque converter never operates without slip and therefore always results in losses. However, a lockup clutch bypasses the torque and equalizes the input-shaft and output-shaft to the same speed [52] [53] [76].
- Improve the torque converter efficiency by redesigning the impeller blades to improve the oil flow [52]
- Eliminating the torque converter by replacing it with a clutch (use of a double clutch or an automated manual transmission instead an automatic transmission) [47]
- Using a variable oil pump to prevent the correlation between flow rate and engine speed; At higher speeds, excessive flow is available, which results in greater loss. This can be reduced by using a variable-displacement oil pump [74].
- Changing the power-train architecture (e.g. rear-wheel drive to front-wheel drive or from front-longitudinal to front-transverse engine/transmission integration) to eliminate losses caused by the prop-shaft and the rear differential [47] [77]
- Improve warm-up of the oil to reduce temperature-dependent losses
- Improve the seals and bearings in the transmission [22]
- Reduce losses by using low-tension oil seals, low-viscosity lubricants, optimizing bearing dimensioning and preload, and using rigid calipers to reduce contact with the brake disc [22] [52].

In addition, the following methods will help ensure that the engine functions at better operation points, which is also a task of the power-train:

- Fuel-consumption-optimized shifting strategy, for example with a so-called “ECO” mode [22] [52] [53] [76]
- Replace the manual transmission with an automated manual transmission to use optimized gear selection by a control unit instead of a fixed-gear selection defined for manual transmission according to the legal test procedure [53]
- Adapting the gear ratio selection and increasing the spread between the first and last gear [52] [76] as well as downspeeding⁸ [7]
- Increasing number of gears up to a continuous variable transmission [22] [52] [53]

3.3.6. Vehicle

3.3.6.1. Overview

As shown in Equation (3.9), a vehicle has three factors that influence the energy demand for the vehicle driving resistance. The equation for the traction force F_{trc} on the wheels required

⁸Downspeeding is the reduction of the gear ratios to allow lower engine speeds. Lower engine speeds results in lower fuel consumption. Downspeeding is often used as secondary measure for engine downsizing or weight reduction.

for driving and accelerating the vehicle on a flat road reads

$$F_{\text{trc}}(v, a) = m_t \cdot f_r(v) \cdot g + \frac{1}{2} \cdot \rho_{\text{air}} \cdot c_d \cdot A_x \cdot v^2 + (m_{\text{twc}} + m_j) \cdot a . \quad (3.9)$$

The influencing variables can be separated into the following sub-groups:

- **Vehicle Weight:** The test weight m_t , defined as the curb vehicle weight plus a cycle-specific payload, influences the rolling resistance and the acceleration inertia. For the acceleration, a test weight class m_{twc} can be defined by the legal regulation. The resulting acceleration force depends on the acceleration a . Depending on the cycle specification, this mass can be equal to the test weight or, especially in the NEDC and FTP cycles, test weight classes for the inertia weight are defined (e.g. see Appendix A.1.4).
- **Tire rolling resistance:** The rolling resistance is defined by a rolling resistance coefficient $f_r(v)$ based on the vehicle speed v . This coefficient is defined by the selected tire. The absolute rolling resistance force also depends on the test weight m_t and the gravitational acceleration g .
- **Vehicle aerodynamics:** The aerodynamic resistance is described by a drag coefficient c_d and the vehicle frontal area A_x . It depends on the air density ρ_{air} and the square of the vehicle speed v . For this reason, the effect the aerodynamic resistance increases at higher speed.
- **Rotary inertia:** Besides the vehicle mass m_{twc} , the equivalent mass of the rotary inertia m_j also influences the traction force. The rotary inertia includes all rotary parts, such as wheels, gear wheel and miscellaneous shafts.

Figure 3.9 already showed an energy flow analysis of an exemplary vehicle in the NEDC. In this case, it can be seen that all three parts (rolling resistance, aerodynamics, acceleration of inertia and mass) have considerable influence.

3.3.6.2. Vehicle weight

The increasing demand for comfort functions (e.g. electric seats, mirrors, air conditioning) as well as safety aspects (e.g. air bags, active and passive safety measures) are steadily increasing the vehicle weight [47]. Higher weight has a negative effect on both fuel economy and driving performance. Measures have to be defined to reduce the weight in general and to compensate for the weight increase caused by new comfort- and safety-related functions and components.

For weight reduction, four possible primary practices exist:

- Changing materials (e.g. replace steel with aluminum or fiber-reinforced plastic); This method results in much higher cost due to more expensive materials and altered manufacturing process. [7] [47] [53]
- Changing design (e.g. reduce wall thickness, tailored blank and function integration into components and improved package); This requires no change in material. By saving material, it is possible to reduce costs. [7] [53]
- Using a self-supporting body (already state-of-the-art in passenger cars) [53]
- Reducing of rotary inertia

One important factor for weight reduction is the consideration of secondary effects. On the one hand, secondary effects can lead to further weight reduction. In the case of a weight reduction based on the listed primary methods, a lower complete-vehicle weight may lead to a smaller suspension or brake system, as well as safety measures [9]. On the other hand, weight reduction always benefits driving performance. A typical additional secondary measure is downspeeding of the gear ratios to get a similar performance to the baseline vehicle, but with better fuel efficiency. For example, according to [78], up to 3.5 gCO₂/km improvement can be achieved by reducing the weight by only 100 kg. An additional 5.0 gCO₂/km reduction can be achieved by adapting the gear ratio.

3.3.6.3. Aerodynamic drag

The movement of an object results in counteracting forces caused by the air. The complete resistance can be separated into two sub-effects: pressure resistance due to deviation of the ideal flow, and the friction resistance due to the surface [77]. This aerodynamic drag depends on various factors:

- Pressure drag due to the stagnation pressure in front of the vehicle and the resistance force on the tearing edge [30] [79] [80]
- Frictional resistance on the surface [30] [79] [80]
- Induced resistance due to turbulence caused by vehicle movement and pressure difference between vehicle top and bottom sides [30] [79]
- Internal resistance due to perfusion through cooling-related components (engine, brakes) and climate control of the cabin (Whereby a vehicle is never completely closed.) [30] [79] [80] [81]

Overall, the aerodynamic drag in driving direction x is described with a unit-less coefficient value c_d and the vehicle frontal area A_x

As shown in Figure 3.12, the contribution of the aerodynamic drag can be separated into four essential areas. To improve the aerodynamic resistance, three measures exist: adapting the vehicle design, optimal selection of parts and the integrating additional parts:

- Vehicle design: flow-optimized design of underbody parts, optimized A and C pillar, optimized mirrors (or replacing them with cameras), optimized windshield wipers, optimized door handles [7] [47] [77]
- Improvements of the wheel: wheel cover, thinner tires, remove mud flaps, tire selection [7] [77] [82]
- Improvements around the wheels: wheel spoiler, improve fairing for lateral circulation around the wheels, rear body, height of the luggage compartment, smooth rear diffuser [77]
- Reduce ground clearance (e.g. depending on speed) [7] [52] [77] [82]
- Engine compartment: add radiator shutter, efficient cooling air flow [7] [47] [77] [82]
- Additional parts: front air dam, side skirts, rear spoiler (adaptive), underbody cover [77] [83]

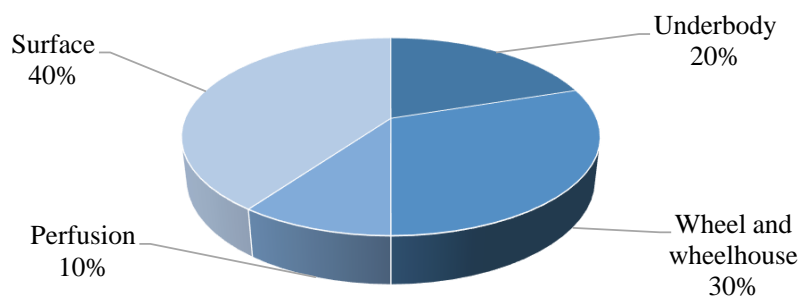


Figure 3.12.: Contribution of various vehicle components to the aerodynamic drag c_d [84]

3.3.6.4. Rolling resistance and traction

Three tire-related factors are important for driving performance and fuel consumptions:

- Rolling resistance coefficient f_r , which effects the required rolling resistance force
- Slip, which limits the maximum transmitted traction force and additionally acts as a power loss
- Acceleration resistance due to the inertia of the wheel

The rolling resistance itself is caused by various influences:

- Flexing resistance caused by internal friction of the rubber elements due to the elasticity and reversible deformation of the tire; A tire represents an analogous spring damper model and is coupled to losses. The flexing resistance accounts for around 80 to 95% of the complete rolling resistance. [30] [79] [85]
- Frictional resistance due to the friction and relative movement at the road-tire contact; This results in additional abrasion resistance. The slip angle is also an influencing factor, but it is insignificant when focusing on longitudinal dynamics [30] [79].
- Aerodynamic resistance due to flow loss of the rotating tire caused by air circulation; This vehicle-specific effect is already considered in the aerodynamic resistance and is not included in the rolling resistance coefficient. [30] [79]
- Resistance due to deformation of the road (e.g. on a gravel road); this effect is nearly zero on tests related to fuel consumption and driving performance (due to the use of special test tracks and test benches). [79]

In addition, the rolling resistance coefficient depends on the wheel load, tire pressure, run duration, temperature and vehicle speed [79]. Based on the physical background, different methods exist to improve the rolling resistance:

- Tire selection in general; The rolling resistance depends on size, aspect ratio, width and speed rating [53], as well as design and compound.
- Increase tire diameter to reduce deformation [53] [86]
- Increase tire pressure to reduce the contact area [86]
- Flat labeling and optimized design of the tread, shoulder and sidewall to reduce air swirls [52] [53] [86]

- Rubber composite and materials to reduce deformation energy [52] [53] [86]
- Reduce volume and weight [86]
- Stiffness of tire pattern to reduce deformation [52] [86]

Nevertheless, besides the rolling resistance, the traction between wheel and road and its physical limitations must also be considered in the driving performance analysis. The traction is described by the adhesion coefficient μ depending on the slip s . The adhesion coefficient also depends on the road condition and the tire. The longitudinal slip characteristic of a tire is discussed in more detail in [79]. The slip influences the actual transferable traction force F_{trc} of the tire, depending on the slip-depended adhesion coefficient μ and the vertical wheel load $F_{z,w}$, and reads

$$F_{\text{trc}} = \mu(s) \cdot F_{z,w} . \quad (3.10)$$

The balance of forces between the wheel and the counteracting force on the road are equal. The slip influences the balance of the speeds, as shown in Equation (3.11). Here v_w is the peripheral speed of the wheel and v_v the vehicle speed. The term $s \cdot v_w$ defines the portion of the loss. The power is the product of the force and the speed. Due to the speed difference, the slip directly relates to the power loss $P_{\text{loss}, s}$, as defined by Equation (3.12). This power loss also has to be considered in the energy flow analysis and the evaluation of CO₂ emissions.

$$v_v = (1 - s) \cdot v_w = v_w - s \cdot v_w \quad (3.11)$$

$$P_{\text{loss}, s} = s \cdot P_w = s \cdot v_w \cdot F_{\text{trc}} \quad (3.12)$$

3.3.7. Hybrid power-train

3.3.7.1. Classification of hybridization levels

Hybrid vehicles can be classified based on their functionality and the power range of the electric motor (EM). In principle, four categories exist. Table 3.4 provides an overview of the classification based on [33]. This thesis considers the micro and mild hybridization levels, which are explained in greater detail in the following chapters.

3.3.7.2. Start-stop system and generator control (micro hybridization)

The entry-level hybridization, the micro-hybrid, is based on the conventional 12-V-electrical system. In this first step, the electric machine is still used only as a generator. An operating strategy controls the generator to improve fuel consumption. This improvement is achieved via the following functions:

- Engine start-stop: Stopping the engine while vehicle standstill phases eliminates the idle operation and minimizes idle consumption.

Table 3.4.: Classification of hybridization levels based on functionality and power range [33]

Hybrid level	Functionality	Power range EM
Micro-hybrid	- Start-stop - Recuperation	2 - 3 kW
Mild-hybrid	in addition to micro-hybrid: - Boost - Load point shifting - Electric driving at low vehicle speed	10 - 15 kW
Full-hybrid	in addition to mild-hybrid: - Electric driving for short distances	> 15 kW
Plug-in-hybrid	in addition to full-hybrid: - Electric driving for longer distances - External charging	> 15 kW

- Extended engine start-stop: Stopping the engine during coasting⁹ and braking as well, when no propulsion torque is needed from the engine.
- Generator control: Increasing the generator load during braking phases to use the kinetic energy of the deceleration to generate electrical energy. The braking energy is stored in the battery. Afterwards, during normal driving, the battery supplies the electrical system as far as possible and unloads the generator to save fuel.

3.3.7.3. Mild hybridization

Hybrid-electric vehicles have two energy sources: the conventional combustion engine and an additional electric traction motor and battery. The difference between micro and mild hybridization is that in a mild-hybrid the electric motor can be used for propulsion (electric driving or boosting). The fuel consumption and driving performance are improved due to the following functions, in addition to the functions listed above for micro hybridization: [51] [76]

- Boost (engine and electric motor provide torque in parallel) for better system peak torque and power and also to provide better load response time in case of turbo lags
- Shifting load points by changing operating points of the engine and charging or discharging the battery with the electric motor for a better overall system efficiency
- Better motor / inverter technology of hybrid motors: The efficiency of electric motors used in mild-hybrids is around 90%, compared to around 65% for a 12 V alternator. Thus, the power supply for the on-board electronics is also more efficient.

⁹Coasting is the driving state when both pedals, the brake and the accelerator pedal, are released and the engine is connected to the wheel (no neutral gear). The vehicle is decelerated due to the driving resistance, drive-train and engine friction.

- Partly electric driving in phases with low driver-requested torque and an inefficient engine operating point

In addition to the classification based on power and functionality, hybrid vehicles can be further divided based on their principle power-train architecture (serial, parallel, power-split) and their voltage level ($< 60\text{ V}$, $> 60\text{ V}$). In the present thesis, the hybridization is limited to 48 V hybridization technologies with parallel architecture. Full-hybrid and plug-in-hybrid vehicles are not considered in this approach. A parallel architecture means that the electric motor works in parallel to the power flow of the combustion engine. Figure 3.13 shows the typical layout of a hybrid power-train, consisting of the conventional 12-V -electrical system, which is supplied by a DC/DC converter that replaces the alternator. The second voltage level is connected with the DC/DC converter, a battery and typically one electric motor. There are different locations possible for the parallel architecture to connect the motor with the power-train. For 48 V hybridization, the following locations are typical: P0, which features a connection of the electric motor to the belt drive; P1, with a connection directly to the crankshaft of the engine; and P2, with a connection to the transmission input-shaft. Due to this positioning of the P2 architecture, a clutch is added between the electric motor and the combustion engine. Using a P2 enables disengaging of the ICE and pure electric driving. This topology allows for a higher recuperation rate because the drag torque of the engine is eliminated in a disengaged state.

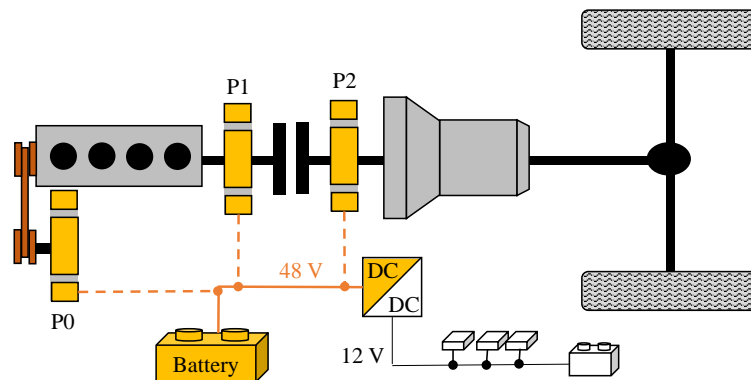


Figure 3.13.: Hybrid power-train with different parallel architectures

The limitation to 48 V is related to the European Regulation *ECE-R 100* [87], which requires a protection against contact for voltage levels above 60 V . An over-voltage protection and logging of voltage and current errors is needed above 54 V . Compared to a high-voltage hybrid system (typically around 400 V), a 48 V system can be implemented with less effort [88]. When comparing the different electric motor topologies, additional advantages and disadvantages have to be balanced. A belt-driven starter/generator (P0) is often limited to 10 kW and brings additional disadvantages due to the efficiency of the belt-drive. However, such a system can be implemented with less effort. Instead of an integrated starter/generator on the crankshaft, (P1) can typically deliver up to 15 kW with better efficiency, but the integration effort is higher. An electric motor on the transmission input-shaft (P2), which provides the greatest recuperation potential, requires an alteration of the transmission design and a more complex operating strategy. [89]

4. Modeling and Simulation

4.1. Introduction

In Chapter 1.3, Figure 1.3 illustrated the approach of this thesis and highlighted the two main parts. The first part, the simulation methodology, will be described in this chapter. The simulation is used to analyze the baseline values for fuel consumption and driving performance, as well as to evaluate the influences of measures in the various driving cycles for each vehicle. This information is the input for the second part - the optimization.

This chapter is divided into five sub-chapters. The requirements for the simulation will be described first, followed by an overview of the simulation environment used. The next two sub-chapters describe the simulation model, the necessary adaptations of the simulation model based on the considered vehicle technologies, and a validation of the simulation model. Finally, the automated simulation environment using scripts is described to improve the efficiency of the simulation process.

4.2. Requirements for the simulation environment

As shown in Figure 1.3, the three influences and inputs for the optimization task are targets based on driving cycles, vehicle configurations and measures. The task of the simulation is to evaluate the influence and improvement yielded by each defined measure for each defined driving cycle and vehicle configuration. These results will ultimately provide the input for the optimization in the next step.

In order to prepare the input with the greatest degree of detail as possible to ensure an exact optimization result, the influences of given measures must be evaluated for each vehicle individually. The reason for this effort will be explained using two examples - engine start-stop and aerodynamic improvement. Figure 4.1 summarizes the potentials of an engine start-stop system based on literature research (see references in Table B.9 in Appendix B.5) in the gray bars. The influence of start-stop ranges between 3% and 5%. The differences are due to the fact that the benefit of an engine start-stop system depends on the transmission (type, energy demand during idle operation), engine efficiency (idle consumption) and the baseline fuel consumption as relative reference. In comparison to the literature values, the range of simulation results is also shown in the black bar. To generate these results, the vehicles of a fictional fleet (see Appendix D.1) were simulated both with and without a start-stop system. Here, the range is broader, from 2% to around 5% improvement. Since the relative influence is different for each vehicle, an individual evaluation of this potential is needed to yield an exact input. Using the literature values as input for the optimization could lead to an error. The magnitude of this error and the final effect on penalties related to CO₂ fleet emissions regulations can be explained with the following example, using the European regulation and penalties (see Chapter 3.2.2). Based on the tolerance of $4 \pm 1\%$ from the literature applied on a fictional vehicle with 150 gCO₂/km, the influence can be calculated to 6 ± 1.5 gCO₂/km. This tolerance is multiplied by the monetary

penalty of €95 per gCO₂/km. In the worst case, the deviation means a penalty of €142.5, due to the lack of a detailed evaluation of the engine start-stop influence. In order to minimize this risk, we consider the impact of each measure on each vehicle in terms of simulations.

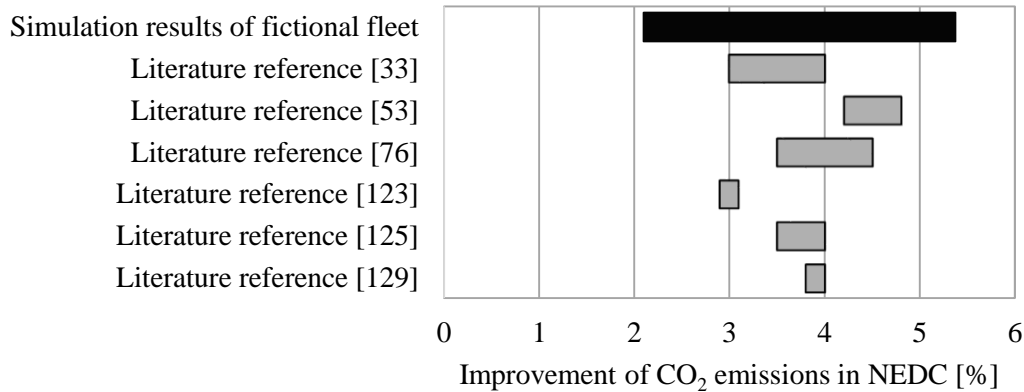


Figure 4.1.: Range of the influence of an engine start-stop system, based on various literature sources and simulation results

Results from another study based on simulations are depicted in Figure 4.2. This figure shows the improvement of an aerodynamic drag c_d reduction by 30 points¹. These influences were also evaluated for a fictional fleet (see Appendix D.1), as used in the previous example of the engine start-stop system. In this example, the different driving cycles, NEDC, EPA2² and WLTC, of the various markets are also analyzed. It can be seen that the influence differs for driving cycle and vehicle segment³, but also for the vehicle configurations within one segment. The result of this example is that the improvement of aerodynamics has to be evaluated for every vehicle individually in order to get an accurate input for the optimization.

Based on this information, the simulation of driving performance and CO₂ emissions provides an important input for the optimization and measures selection. Because the input for the optimization is a three-dimensional simulation matrix indexed by driving cycles, vehicles and measures, several hundred up to thousands of simulation runs can occur. To handle this high number of simulations, an efficient and flexible simulation model and environment is needed. Therefore, and in reference to the state-of-the-art analysis in Chapter 2, the following requirements are defined:

- Focusing on 0D / 1D simulation⁴ to save computation time
- Focusing on longitudinal vehicle dynamics and closed-loop simulation (with driver model) to include driving dynamics
- Vehicle modeled as one mass point, but with dynamic axle-load distribution, simplified tire slip and traction control system (TCS) model
- Evaluation of the CO₂ emission-improving technologies described in Chapter 3.3

¹Differences in the aerodynamic drag c_d are described with points. A value of 30 points correlates to a difference of $\Delta c_d = 0.03$.

²EPA2 is the combined fuel economy for the US GHG and CAFE regulation weighted with 55% FTP75 and 45% HWFET, see Equation (3.8).

³A segment describes the classification of cars [90] [91].

⁴The dimension describes the dependence on variables. 0D / 1D simulation uses the time dimension (0D) and one additional position-dependent dimension (1D).

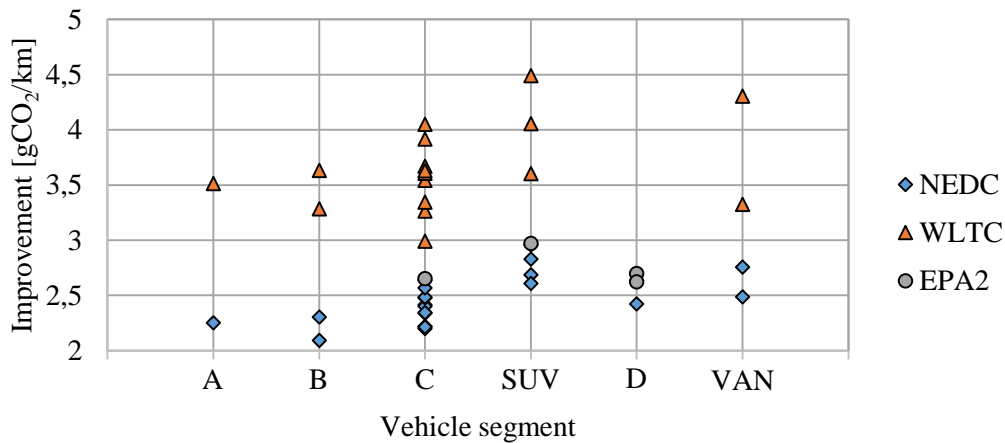


Figure 4.2.: Influence on CO₂ emissions of an aerodynamic drag reduction c_d by 30 points by vehicle segment and driving cycle based on simulation of fictional vehicles

- Modularity and standardized interfaces to exchange sub-components with different levels of detail. The selection of models and components is a compromise between available input data, computation time and expected results quality. Modularity also means standardized external interfaces of the sub-components to the overall simulation model.
- Limited number of simulation models to reduce the maintenance effort: one simulation model for all conventional power-train configurations, and one simulation for mild-hybrid power-trains
- Ability to calculate the energy flow, power flows and loss analysis
- Simulation of different driving cycles (CO₂ emissions, driving performance) and different preconditioning (cold-start, warm-start)
- Multi-physical environment to handle mechanical (vehicle, power-train), electrical (auxiliaries, hybrid power-train) and thermal (cooling circuit, warm-up) interactions
- Ability to integrate control units and signal flow logics
- Standardized data management to allow for the use of the same models and parametrization type for all customer projects and their input data and to enable the use of similar data structure for the parametrization for the exchange of sub-components (e.g. for different transmission models)
- Automated environment, coupling with script-based pre-processing, execution of simulation and post-processing
- Different gear control setting depending on transmission type and test maneuver: automatic transmission with shifting map (fuel consumption and driving performance), manual transmission with gear-shifting profile depending on time (fuel consumption), manual transmission with gear-shifting depending on engine speed (driving performance) and driving with locked gear (passing acceleration)

4.3. Simulation environment

Based on the requirements listed in Chapter 4.2, the developed simulation environment is built on three modules: the simulation model, a script-based environment for automation and the database. The interactions between the three modules are shown in Figure 4.3.

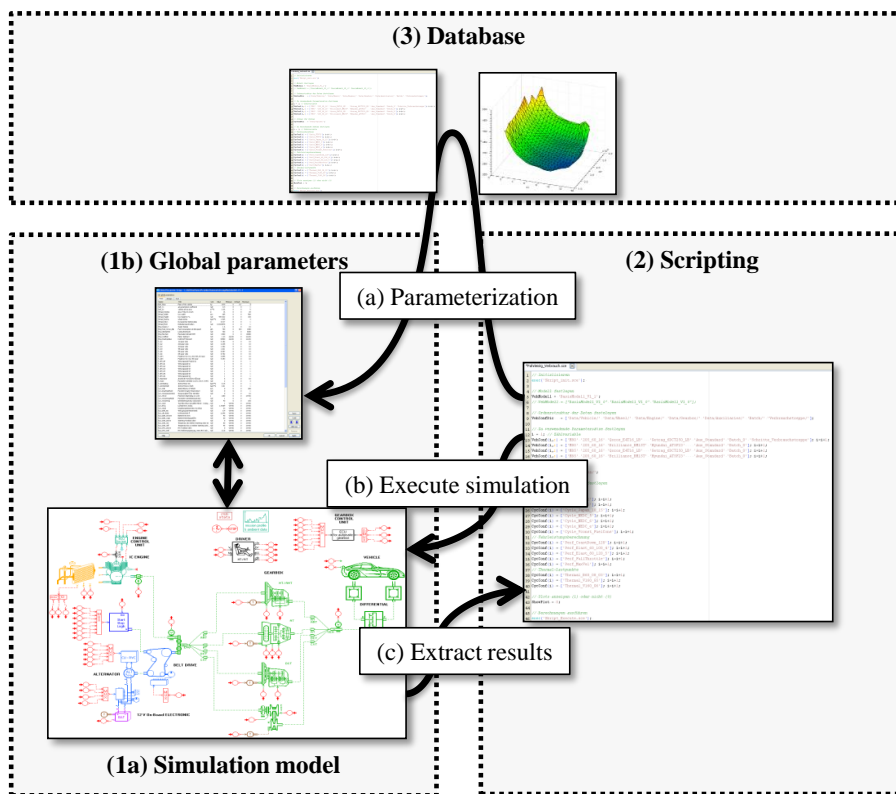


Figure 4.3.: Interactions and workflow between simulation model (1), scripting (2) and database (3)

For the simulation model itself, see module (1a) in Figure 4.3, the related physics are state-of-the-art and will not be discussed in this thesis. Several commercial softwares for longitudinal vehicle dynamics are currently available on the market. Simulation tools for analyzing system behaviors are based on either causal modeling or non-causal modeling. A causal, or signal-oriented, modeling rests upon cause and effect. The calculation of the output is a function of the input. Thus, a definition of input and output signals is required. An alternative method of modeling is non-causal, also called object-oriented modeling. Here, a system is described based on physical principles using constitutive or conservation equations. It is not necessary to define the definition of input and output, and equations are automatically transformed based on the connection to other components. [92] [93] [94] [95]

In this thesis, the software tool *LMS Imagine.Lab AMESim* from Siemens Industry Software GmbH [96] is used. AMESim is a simulation tool that uses causal modeling. This tool provides a multi-physic modeling environment with libraries, for example for thermal, mechanical, electrical and signal flow components. The available libraries are focused on automotive usage. Due to the multi-physic linkages between different components, an interdisciplinary simulation model is enabled. Figure 4.4 illustrates the multi-physic for an electric motor, for example. This model has four interfaces: a rotatory mechanical interface for the connection to the power-train, an

electrical interface for the connection to a battery model, a thermal interface for the connection to a thermal mass for the temperature calculation, and a signal interface to a control unit. For example, a desired torque is sent from a control unit as a signal to the motor. Based on the physics within the electric motor model, a torque is sent to the power-train and a current load to the battery. Depending on the efficiency factor, a heat loss is given to the thermal models. In order to meet the requirement of creating new models and adapting existing models, the used software also provides a sub-tool called *AMESet*, which allow for the creation and adaptation of a model based on programming code. Such a feature is needed to adapt the existing base simulation models according to the required level of detail of the existing input data and to create new control units.

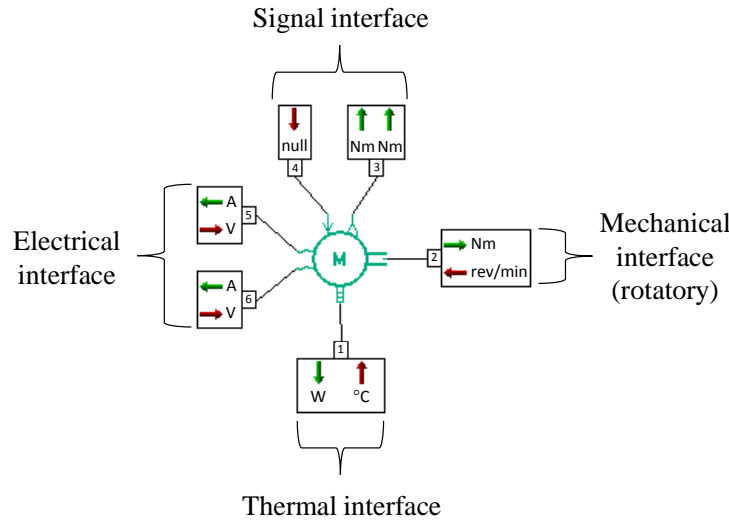


Figure 4.4.: Multi-physics interfaces of an electric motor model (based on [97])

Figure 4.5 shows the principle signal flow of the simulation model used. Within the electrical sub-system, the battery provides a voltage U_{Batt} , which depends on the internal resistance, the open circuit voltage of the battery model and the current I_{Batt} , calculated from the sum of the electric auxiliaries I_{Aux} and the load of the generator I_{Gen} . The second sub-system is the thermal system. The engine model provides a thermal output $\dot{Q}_{\text{ICE,Cool}}$ to the coolant. Based on the thermal mass and the heat balance, a coolant temperature T_{Cool} is defined. The third and largest sub-system is the mechanical part. The torque from the engine M_{ICE} and the drag torque from the mechanical auxiliaries M_{Aux} and the generator M_{Gen} are summed and transferred to the first rotational inertia model. This inertia combines the crankshaft of the engine and the input-shaft of the clutch. Within the first inertia model, the torque balance from the connector M_{Cs} and the clutch M_{Cl} leads to a change of the rotatory speed of the inertia. The engine can be disconnected from the wheel and the transmission input-shaft using the clutch model. The engine speed ω_{Cs} can be different from the input-shaft speed of the transmission ω_{Tr} . Based on the clutch position and speed difference, a transmitted torque is defined. The torque is forwarded via the transmission, including the gear ratios, to the inertia of the wheel. In the simplest case, the transmission model itself handles only the ratio of the selected gear and the torque loss. Between the transmission and the wheel, the second rotational inertia model is located, which calculates the wheel speed ω_{w} depending on the torque balance between the transmission's output torque M_{Tr} and the wheel torque M_{w} . The second inertia combines the output-shaft of the clutch, the input-shaft and the output-shaft of the transmission, the side-shafts and the wheels. Due to the gears of the transmission and the differential, the ratios between the shafts

have to be considered for the calculation of one equivalent rotational inertia. The wheel itself has a similar characteristic to a clutch model. The current grip and the wheel load define the traction force F_{trc} , which can be transmitted via the wheel to the road according to Equation (3.10). Depending on the traction force, the rolling resistance, the aerodynamic drag and the vehicle inertia, an acceleration occurs based on Equation (3.9), which leads to a calculation of the actual vehicle speed v_v .

Finally, the used simulation model itself is more complex and has still more interfaces and connections, which are omitted in this illustration and explanation in order to provide a better overview. For example, the thermal system has a connection to the electrical and mechanical auxiliaries. The radiator fan and the water pump can be activated depending on the coolant temperature, which results in an additional electrical or mechanical power request. Besides the mechanical interfaces, signal interfaces have to be considered in the simulation. Signal interfaces are used for electronic control units (ECU). For example, the transmission control unit (TCU) reads the engine speed, transmission output speed and the accelerator pedal position to control the clutch and the gear selection.

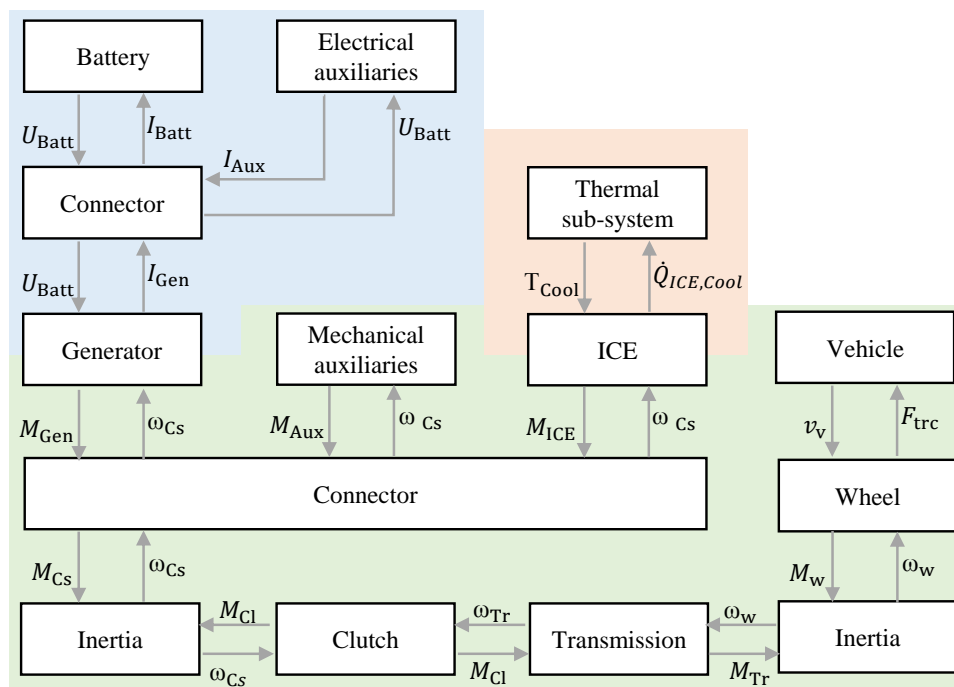


Figure 4.5.: Principle signal flow of the simulation model used

In addition to the signal flow and models, the parametrization of the models is important. The sub-models are parametrized individually. For the whole simulation model, a list of global parameters exist, see (1b) in Figure 4.3 and in more detail in Figure 4.6. In this list, all variable parameters are defined (e.g. vehicle mass, engine maps).

The second module is the software interface to a script-based tool, such as *Matlab* from the MathWorks Inc. [98] or *Scilab* from Scilab Enterprises S.A.S [99] for the automation of the simulation. Within this thesis, *Scilab* is used as scripting tool. The optimization algorithm will be implemented in Scilab as well, so the execution and analysis of simulation runs can go hand-in-hand with the optimization in one program. The simulation results can be used directly as input for the optimization with no further data export required. The setup and adaptation of the scripting environment will be described in more detail in Chapter 4.6. The scripting

Name	Title	Value	Unit
▲ Cycle			
Cyc_Vinit	Initial Velocity of Vehicle	0	km/h
Cyc_EngSpdInit	Initial Speed of Engine	680	rev/min
Cyc_FixedGear	Gangvorgabe fuer Getriebe	0	
Cyc_Tfinal	Final time depending on cycle	1180	s
Cyc_Drv	Typ Fahrzyklus manueller Fahrer: 1 Gangvorgabe / 2 Schaltlogik / 3 AMT	1	
Cyc_Type	Zyklus Type, 0 = standard, 1 = performance	0	
Cyc_RhoL	Luftdichte im Zyklus	1.1918873782423	kg/m**3
Cyc_Tamb	Umgebungstemperatur im Zyklus	23	degC
Cyc_RoadStiction	Road stiction coefficient	1	null
Cyc_VelFile	file for velocity vs time (driving cycle)	C:/AMESim/Databas...	
Cyc_GearFile	file for gear demand vs speed (driving cycle)	L:/GRZ/14-E/16-E/0...	
Cyc_Slope	slope in %	0	
▲ Vehicle			
▲ Mass			
Veh_Mass	Mass of the vehicle	1300	kg
Veh_UseIWC	Use IWC instead of normal weight for acceleration (1 yes)	1	
Veh_IWC	Vehicle Inertia Weight Class	1250	kg
▲ Aerodynamic			
Veh_Cx	air penetration coefficient	0.235	null
Veh_Ax	vehicle active area	2.2	m**2
▲ RollerTestBench			
Veh_UseRoadParam	Use Road parameter (1) / Use Roller test bench parameter (0)	1	
Veh_Roll_Const	Constant Parameter for Roller test bench	190	N
Veh_Roll_Linear	Linear Parameter for Roller test bench	6	N/(km/h)
Veh_Roll_Quadrat	Quadratic Parameter for Roller test bench	0.3	N/(km/h)^2
▲ Geometry			
Veh_DistFrntRr	Distance FrontAxle to RearAxle	2.685	m
Veh_DistFrntCoG	Distance FrontAxle to Center of Gravity	1.074	m
Veh_HghtCoG	Height of Center of Gravity	0.5	m
▲ BrakeBearing			
BB_Loss_Frnt_Map	Brakpad and Bearing Loss front wheel dep on speed	Data/Wb&Brake/Br...	
BB_Loss_Rr_Map	Brakpad and Bearing Loss rear wheel dep on speed	Data/Wb&Brake/Br...	
▶ Engine			
▶ Transmission			
▶ Auxiliaries			
▶ Wheel			
▶ Brake			
▶ Cooling			
▶ Hybrid			

Figure 4.6.: Excerpt from the global parameter list in the AMESim simulation model

environment, (2) in Figure 4.3, is needed to automate the simulation by using *Scilab*. The high number of simulations resulting from the different existing vehicles, cycles and measures, the handling of the simulation result, and need to reduce human-sourced input-data errors demand such an approach. The scripting has the tasks of (a) parametrizing the simulation model based on the vehicle and cycle definition by accessing the standardized database, (b) executing the simulation and (c) extracting the results and signals needed for post-processing.

The final module is the database, see (3) in Figure 4.3. Hereby, the challenge is to standardize the simulation input data in the context of the required data format of the simulation model parameters. The intention of the standardization is to use similar simulation model components and parameters to reduce the effort required for adaptations if the method and simulation are used for other future projects.

4.4. Model adaptation

4.4.1. Sub-model partitioning

Figure 4.7 shows the initial simulation model which was taken as the starting point for the thesis. The model consists of components selected from the available libraries and includes a driver

for manual transmission, an engine, a warm-up curve for the engine, a manual transmission, a one-mass-point vehicle model and an alternator with a constant load and brake light. It was used to evaluate the status of fuel consumption and driving performance. In addition, simplified sensitivity analyses of parameters (e.g. variation of gear ratio, aerodynamic drag, vehicle mass) were performed to evaluate their influence on fuel consumption and driving performance. Depending on the type of transmission (manual transmission, automatic transmission), several simulation models exist. In this case, Figure 4.7 shows a model with a manual transmission. The gear selection is performed by the driver model.

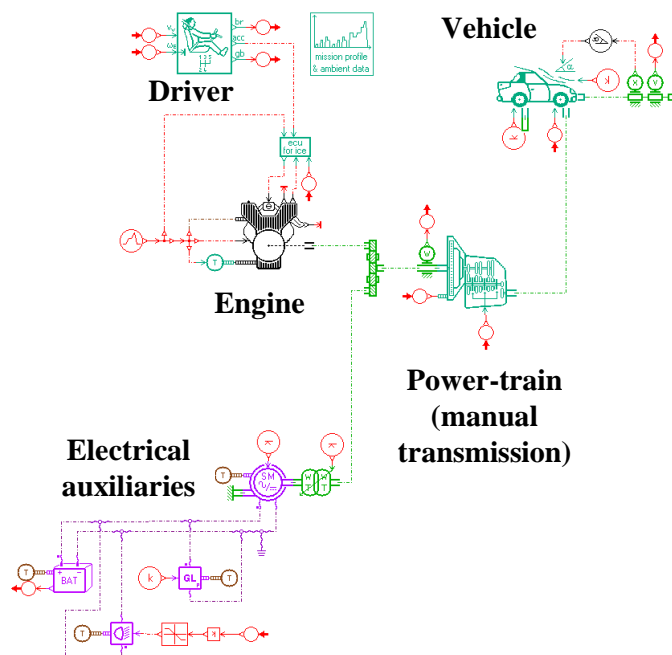


Figure 4.7.: Initial simulation model for a vehicle with manual transmission

Due to the variation of engine / transmission configurations (vehicle matrix) and the various available technologies for improving CO₂ emissions, it was necessary to adapt this initial simulation model. This means creating a defined and flexible structure, sub-model partitioning, adapting existing models and creating new components to fulfill the requirements outlined in Chapter 4.2. The adapted simulation model is shown in Figure 4.8. The model is divided into six different sections:

- Driver
- Engine
- Thermal circuits
- Auxiliaries
- Power-train
- Vehicle.

The adaptations of the listed sub-models will be explained in detail in the following sub-chapters.

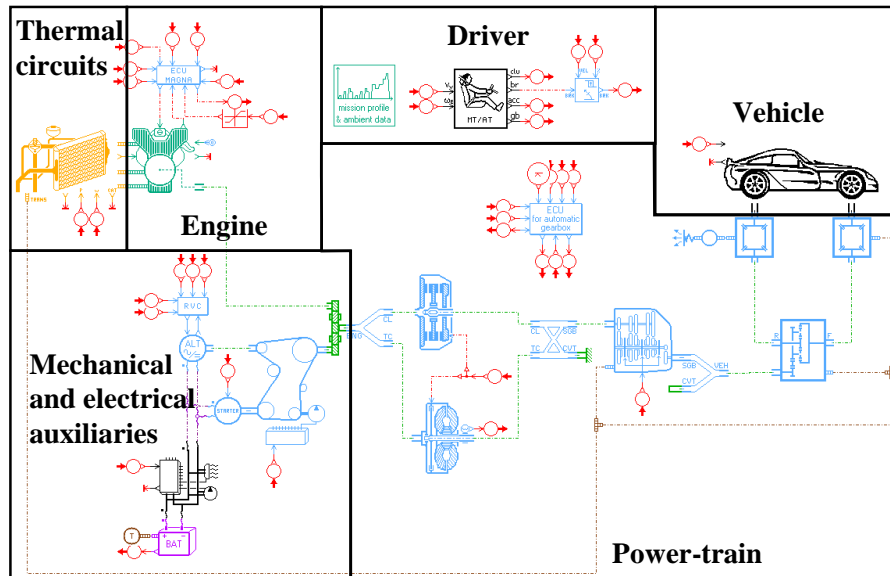


Figure 4.8.: Adapted simulation model

4.4.2. Driver model

The simulation model is built up as a closed-loop model to take into account dynamic effects during acceleration and deceleration. This means a driver model controls the accelerator and the brake pedal by taking into account the difference between a time-dependent speed profile and the actual vehicle speed. The brake pedal is connected to the brake and results in a brake torque. The accelerator pedal is connected to the engine and, depending on the pedal position and the engine characteristic, provides a torque to the wheel via the power-train. Depending on the resistance forces acting on the vehicle, the brake and the engine torque, an acceleration or deceleration results. In each iteration step, the driver model compares the desired and the actual vehicle speed and adapts the pedal positions via a controller.

The driver model controls the accelerator pedal and brake pedal and should be capable of covering different engine and transmission types within one simulation model. Two blocks are defined for the driver model, which are shown in Figure 4.9. The first block is the driver model (1) itself. In the case of a manual transmission, an additional control for the manual gear box is required, which is defined by two additional outputs for the clutch pedal and the gear lever. The control logic for gear selection is based on two different control strategies: one for a time-dependent gear selection, as defined in legal test cycles for CO₂ emissions, and one for an engine-speed-dependent gear selection used for acceleration tests. In order to enable the use of a single overall driver model for the simulation of the whole vehicle fleet with different power-train types and test cycles, all three driver models must be integrated. Therefore, the driver model is composed of three sub-models: a driver for automatic transmissions (1c), a driver for manual transmission and time-dependent gear selection (1a) for driving cycles related to CO₂ emissions, and a driver for manual transmission and engine-speed-dependent gear selection (1b) for test cycles related to driving performance. The three driver models are configurable and can be activated or deactivated depending on the cycle definition and transmission type. In principle, all driver models are based on two PID controllers, one for the accelerator pedal and one for the brake pedal. In the closed-loop simulation, the driver has the task of following the speed profile. Therefore, each test for CO₂ emissions and for driving performance has to be

described with such a speed profile, which will be referred to as a “(driving) cycle” below. The cycles for the evaluation of CO₂ emissions are defined by the legal regulation. Examples can be found in Figure 3.3 for the NEDC and WLTC. In addition, in the case of driving performance tests, a driving cycle has to be defined. For example, for a full-throttle acceleration, the driving cycle is defined as a constant speed value higher than the maximum vehicle speed. Since the driver model attempts to follow the desired speed (e.g. maximum speed), the controller does a full-throttle acceleration from vehicle standstill to achieve the target speed.

The second block is a hill-hold function (2). If the vehicle is on a slope, this block holds the brake pedal position a defined time after releasing the brake pedal to allow the driver to build up propulsion torque and to prevent backwards rolling. This block is needed for the investigation of gradeability test maneuvers. Gradeability targets will not yet be considered as a constraint, but can be added in a future stage of expanding the tool.

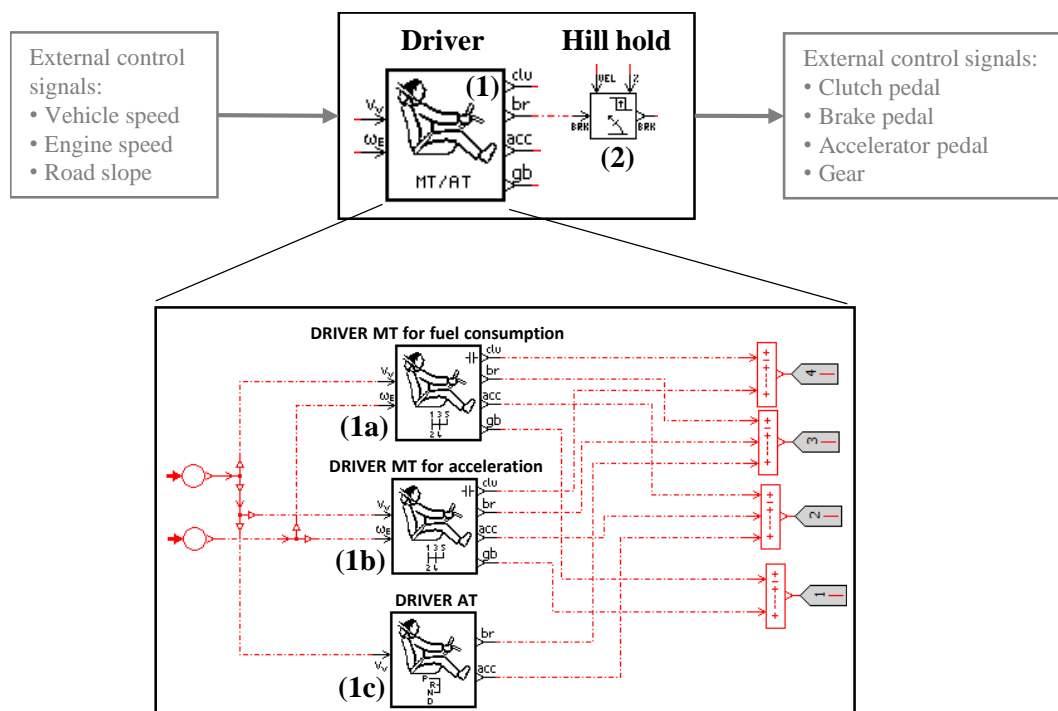


Figure 4.9.: Sub-system driver including driver model and hill-hold control

4.4.3. Internal combustion engine model

Figure 4.10 shows the models used for the internal combustion engine (2) and its ECU (1).

The base ECU has the following tasks:

- Forward accelerator pedal signal to the engine model
- Idle speed control
- Maximum speed limitation.

Due to the requirements for evaluating measures for the improvement of CO₂ emissions, the base ECU was extended with the following functions:

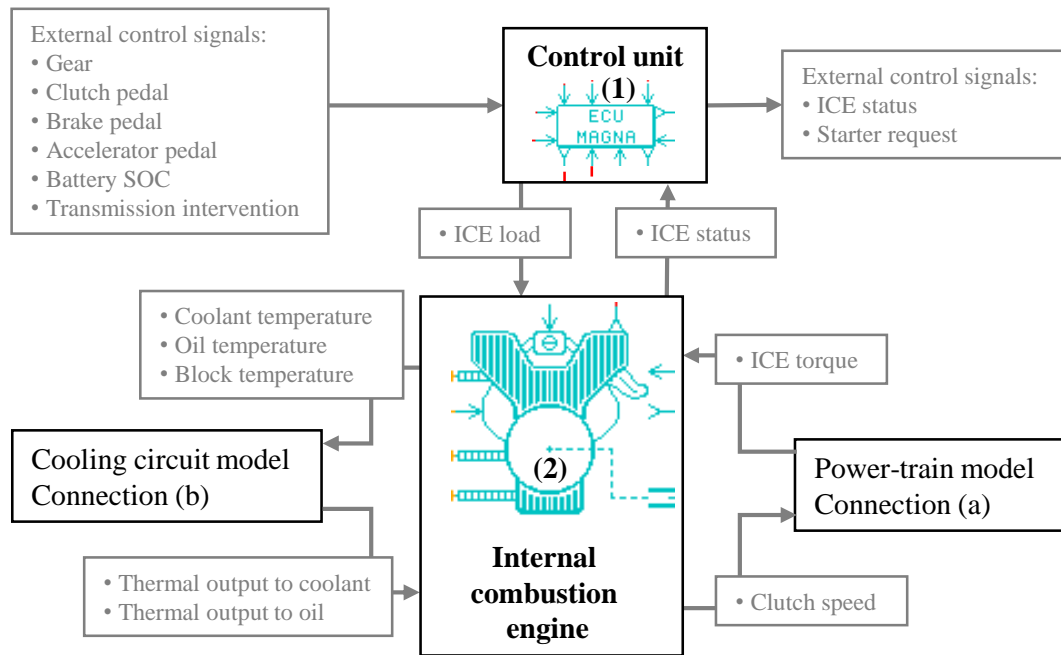


Figure 4.10.: Sub-system internal combustion engine including engine control unit

- Fuel cut-off function⁵; depending on engine temperature and gear
- Engine start-stop function; depending on engine temperature, battery SOC, brake pedal position and transmission state. In addition, a variable vehicle speed threshold is included to handle engine start-stop at vehicle standstill (standard engine start-stop), but also as an extended engine start-stop while driving (extended start-stop or sailing). As an additional output, a connection to a starter motor model was added. The control logic is described in detail in Appendix C.1.1.
- Cylinder deactivation; depending on predicted engine operating point, engine temperature and time limitations. The control logic is described in detail in Appendix C.1.3.
- Overboost function⁶; depending on engine speed and time limitations
- An optional accelerator pedal map; The accelerator pedal is either directly transferred to the engine or adjusted by an accelerator pedal map.

The second component is the engine model (2). This model has to handle three tasks:

- Convert the requested engine load into torque to the power-train
- Calculation of fuel consumption by considering the influencing factors (e.g. influence of cold-start or cylinder deactivation)
- Calculation of the heat losses into the oil and the engine block

The engine model is based on characteristic curves and maps, such as a map for fuel consumption and a curve to describe the maximum torque. The static torque of the engine is calculated from the actual maximum torque and the requested engine load from the ECU (1). Thus, the base engine model is adapted by the overboost function. Two torque characteristic curves are integrated in the engine model and selected according to the ECU logic. In the case of turbo

⁵This function disables the fuel supply while coasting.

⁶An overboost function is a temporary increase of the boost pressure to improve the maximum available torque.

engines, the dynamic output torque is calculated based on the predicted static torque and a calibratable dynamic time constant with a PT1 characteristic to take into account the dynamic effects of the turbocharger. The mechanical output of the engine is connected to the clutch model of the power-train sub-model. The clutch model contains the inertia of the engine.

The fuel consumption is calculated by a map based on engine speed and torque. In addition, the fuel consumption is influenced by an oil-temperature-dependent friction torque, an temperature-dependent cold-start enrichment and an additional consumption due to catalyst heating. Two fuel consumption maps are integrated in the engine model, one for normal operation and a second in case of cylinder deactivation. Based on the fuel consumption, the CO₂ emissions are calculated using a conversion factor that depends on the fuel type, for example, around $23.5 \frac{g_{CO_2}}{km}$ per $\frac{l}{100km}$ for gasoline. If CO₂ emission-improving engine technologies are to be analyzed (e.g. turbocharging, direct injection), a new engine map has to be parametrized. In the actual simulation process, the maps have to be prepared via pre-processing. Finally, the heat inputs are calculated based on the friction torque for the oil and a heat input map for the engine block. The engine sub-model is connected to the power-train (a) via the auxiliary sub-system and to the thermal sub-system (b). In addition, signal inputs and outputs are present for control.

4.4.4. Auxiliaries model

The baseline simulation model already takes auxiliaries into account, but the modeling was limited to the alternator and an average electrical load. The adapted part of the auxiliaries can be seen in Figure 4.11. The auxiliary sub-system is located between the engine model (connection a) and power-train model (connection b). The activation of auxiliaries leads to a drag torque on the belt drive, either directly from mechanical auxiliaries or via the alternator load in case of electrical auxiliaries. This torque is subtracted from the engine torque and reduces the torque transferred to the power-train input.

In accordance with the model requirements, the simulation model is extended with the following components:

- A belt drive (1) for operating the mechanical auxiliaries, including an efficiency factor
- Mechanical auxiliaries (1) (water pump, vacuum pump, oil pump, steering pump, AC compressor) defined by a drag torque
- Starter motor (2) to restart the engine after an engine start-stop phase
- Intelligent alternator control (3), which discharges the battery during driving and vehicle standstill and charges the battery during braking phases. The control logic is described in detail in Appendix C.1.2.
- More detailed electrical auxiliaries (4); Several auxiliaries (e.g. water pump, brake light) can be activated or deactivated in general, based on time or control logics.

Because auxiliaries do not operate continuously over the whole cycle, a dynamic activation or PWM control has to be implemented. Both the dynamic demand of the auxiliaries (e.g. fan or pumps) and the control of the alternator request signal information from other sub-systems. These connections have to be considered (e.g. brake light activation based on brake pedal position). Because the electrification of auxiliaries is one key point for reducing of CO₂ emissions, all mechanical auxiliaries (water pump, vacuum pump, oil pump, steering pump) exist as mechanical and electrical components. For example, depending on the parametrization,

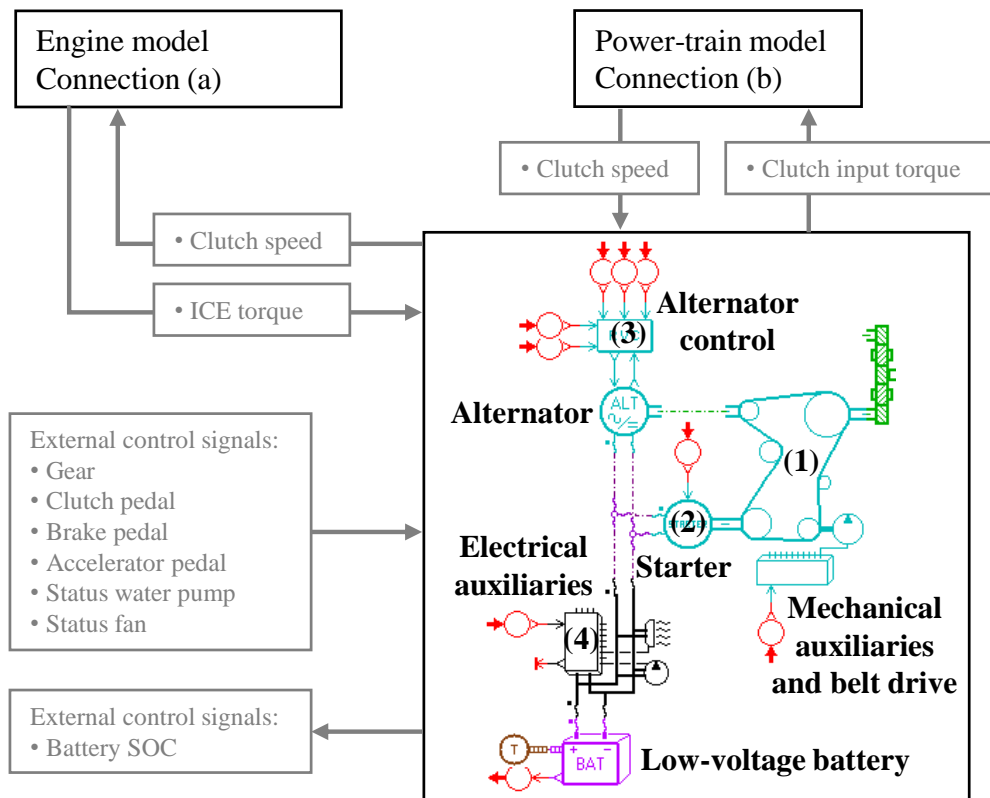


Figure 4.11.: Sub-system auxiliaries

either a mechanical or electrical water pump can be simulated. In addition, an interaction with the thermal circuit exists. For example, based on the coolant temperature, the coolant pump or the fan is activated, which results in an electric load request. This load results in a current depending on the current voltage. The mechanical auxiliaries are modeled with a defined drag torque based on the rotary speed. Additional ratios for the components and the efficiency factor of the belt drive must be defined.

4.4.5. Power-train model

Because a vehicle fleet consists of various vehicles, different power-train types (e.g. manual transmission, automatic transmission) have to be considered in the simulation. To reduce the effort required to maintain several complete-vehicle simulation models, all relevant power-train types and their relevant component models are implemented in one simulation model. With this modeling approach, the power-train model has the following three flexible features based on the component selection and the powerflow determined by the vehicle configuration:

- Starting element: clutch or torque converter
- Transmission type: manual transmission (MT), automated transmission (AMT), automatic transmission (AT), double clutch transmission (DCT) or continuously variable transmission (CVT)
- Driven axle: front, rear or all-wheel drive

For the simulation of a certain vehicle and its power-train, the signal flow through the power-train from the engine to the wheel has to be defined. To this end, so-called “switch elements” are included in the power-train to control the signal flow. In addition, the component models in the power-train are activated, and unused components are deactivated.

Figure 4.12 shows the sub-system of the power-train and two potential power flows. The green solid line shows the power flow of manual, automated manual and double clutch transmissions using a clutch model (1) as the starting element and a gearbox (3). The blue dashed line shows the power flow of an automatic transmission using a torque converter (2) as the starting element and a gearbox. The power flow is set by configurable switching elements (7) based on the power-train definition. In addition, a placeholder for continuous variable transmission is included, although it is not considered within this thesis. The third flexible feature is the power flow via the transfer case (4) to the vehicle. Either front-wheel drive (FWD), rear-wheel drive (RWD) or all-wheel drive (AWD) can be selected. If AWD is not selected, the transfer case works only as a dummy, and the unused differential (5) is deactivated. Since this thesis only considers front-wheel-driven vehicles, the transfer case is only set as a dummy in this model.

Since the transmission control unit (6) is used to control the clutch, torque converter and gearbox, it must be able to handle different transmission configurations. The base control unit only considers the shifting strategy as a map based on vehicle speed and accelerator pedal position and a torque converter lockup clutch control based on the impeller speed. Therefore, the transmission control unit is adapted with the following functions:

- Clutch control at low engine speed; open the clutch depending on the current idle speed
- Transmission torque intervention to the engine; during shifting, the torque can be limited by the transmission
- Shifting procedure for automated manual transmission, including traction interruption and opening and closing the clutch based on a defined time sequence
- Control to engage the neutral gear in automatic transmission at vehicle standstill to reduce the load on the torque converter
- Adaptation of the torque converter lockup clutch control with a slip-controlled mode

The control unit is influenced by the transmission type. In the case of a manual transmission, the control unit is deactivated, and the gear and clutch information from the driver model is used instead.

The transmission and differential losses are based on efficiency maps and are also dependent on the temperature. A coupling with the thermal system is added, to transfer the transmission power loss to the thermal system and the oil temperature back to the transmission model.

4.4.6. Vehicle model

The vehicle model is shown in Figure 4.13. The baseline vehicle model was based on one mass point and considered the driving resistance, which consists of aerodynamic (3), rolling (2) and slope (1) resistance. The model is extended with the following functions:

- Consideration of additional losses due to brake pad and bearing (4)
- Partition into front and rear axle for the torque input
- Integration of a tire model with slip and traction limitation based on a dynamic axle load distribution (5), as well as a simplified TCS model

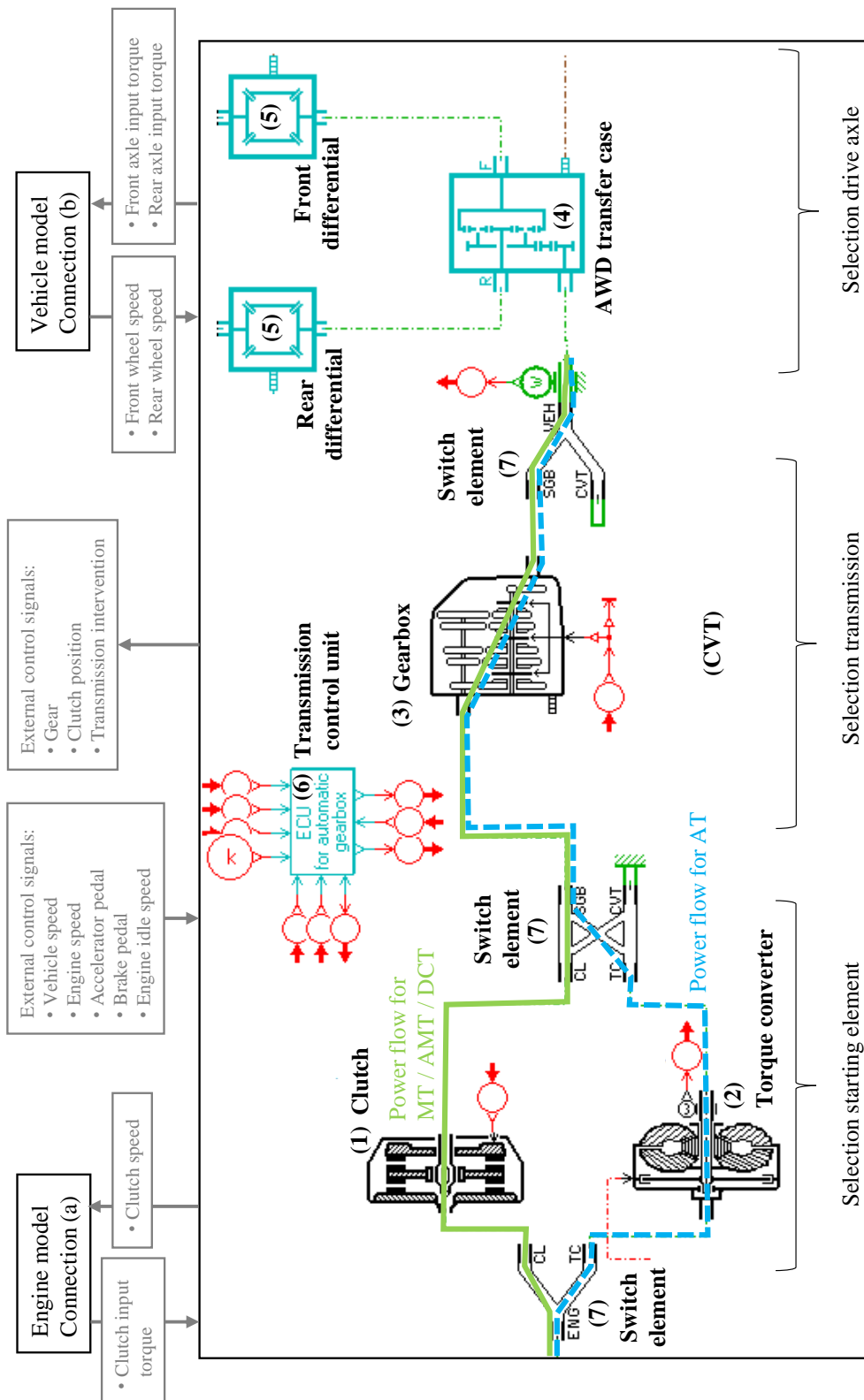


Figure 4.12.: Sub-system power-train and the visualization of potential power flows

- Ability to select vehicle parameters or coast-down parameters (6) as a basis for the parametrization of the driving resistance
- Ability to select between using test mass or test weight class (7)

Two major changes are required according to the requirements described for the simulation model. The initial mass-point vehicle model featured only one common torque input for the front and rear axles. This model was extended with separate torque inputs for the front and rear axles, a center of gravity (CoG) and a dynamic axle load distribution. The dynamic axle load distribution results from accelerating or decelerating the vehicle with a CoG located above the road. A simplified linear wheel slip model is added to take into account traction limitations for full-throttle acceleration and hill launch tests. The simplified TCS model controls the brakes and sends a torque intervention to the engine control unit in the case of wheel slippage in order to reduce the transmitted torque to the wheel. In addition, the wheel slip is an energy sink, which increases the CO₂ emissions according to Equation (3.12).

A second change is required due to the two different test cycles types: test cycles for CO₂ emissions on a roller test bench and test cycles for driving performance / drivability on real roads. For tests on real roads, the test mass and the road resistance, which consists of aerodynamic and rolling resistance, are used. For tests on the test bench, the test weight class is used for acceleration inertia. In addition, either the vehicle parameters or the coast-down curve can be used to parametrize the driving resistance. The vehicle parameters for describing the driving resistance can be found in Equation (3.9). The coast-down curve is a measured driving resistance of a vehicle, described by three parameters, F0, F1 and F2, and the testing procedure is defined by the related regulation, such as in the *ECE-R 83* [34]. The selection of the test mass and the type for the driving resistance should be configurable depending on cycle definition and data availability. In early development phases, primarily the vehicle parameters are used to simulate the driving resistance. The coast-down coefficients are normally used if measurement data from vehicles are available.

4.4.7. Thermal model

In the initial simulation model, shown in Figure 4.7, the warm-up behavior of the engine and the coolant temperature was given as a fixed curve based on time. For a more detailed simulation, the cooling circuit must also be modeled because measures for improving CO₂ emissions can also influence the warm-up behavior, which ultimately influences the additional cold-start consumption. In addition, the mechanical and electrical work of the coolant pump and the fan have to be considered in the energy balance. The thermal system has to model the heat flow, which yields the coolant and oil temperatures. This is important for CO₂ emission-related driving cycles, where the influence of the warm-up and additional fuel consumption due to cold-start enrichment and higher friction due to cold oil should be considered. Detailed models and different possible levels of detail of the thermal systems are explained in [20], [55], [62], [65], [100] or [101], for example. In accordance with [101], the thermal model in this thesis uses a simplified model to reduce computation time. To analyze the influences of thermal components in detail, a more complex thermal system can be included in this simulation model, if necessary. This is possible due to the modular layout of the overall simulation model. Since two thermal circuits are considered, the coolant and the oil temperature, two heat sources are required. The heat input to the oil is calculated from the engine friction power. The heat input to the coolant is calculated from the engine efficiency, either by a measured heat input map or simplified by a constant percentage value of the chemical energy of the fuel.

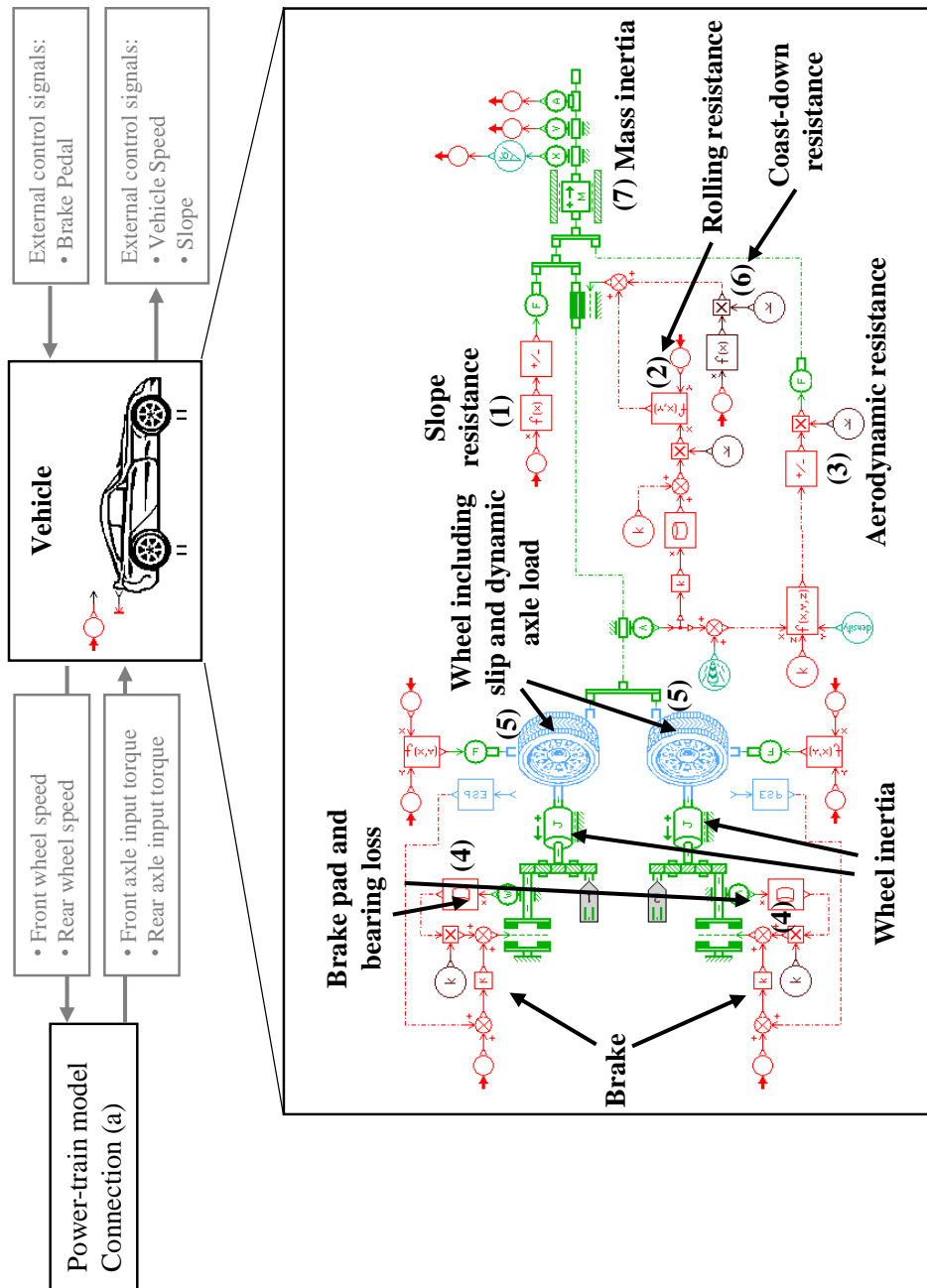


Figure 4.13.: Vehicle sub-system

The thermal model can be seen in Figure 4.14. The heat input from the combustion is connected to a thermal mass (1) representing the engine block and is transferred via a heat transfer model (2) to the coolant. The pump (3) supplies a volume flow for the coolant. Depending on the thermal output and the volume flow, a coolant temperature is generated. The thermostat (4) distributes the volume flow through a radiator (5) or to the by-pass, depending on the temperature. The friction heat flow is connected to a thermal mass representing the engine mass. Via a heat transfer model (7), the heat is transferred to the oil, which is also represented as a thermal mass (8). This simplified model does not consider a detailed oil circuit with volume flow. In addition, an oil coolant heat exchanger (9) can be included.

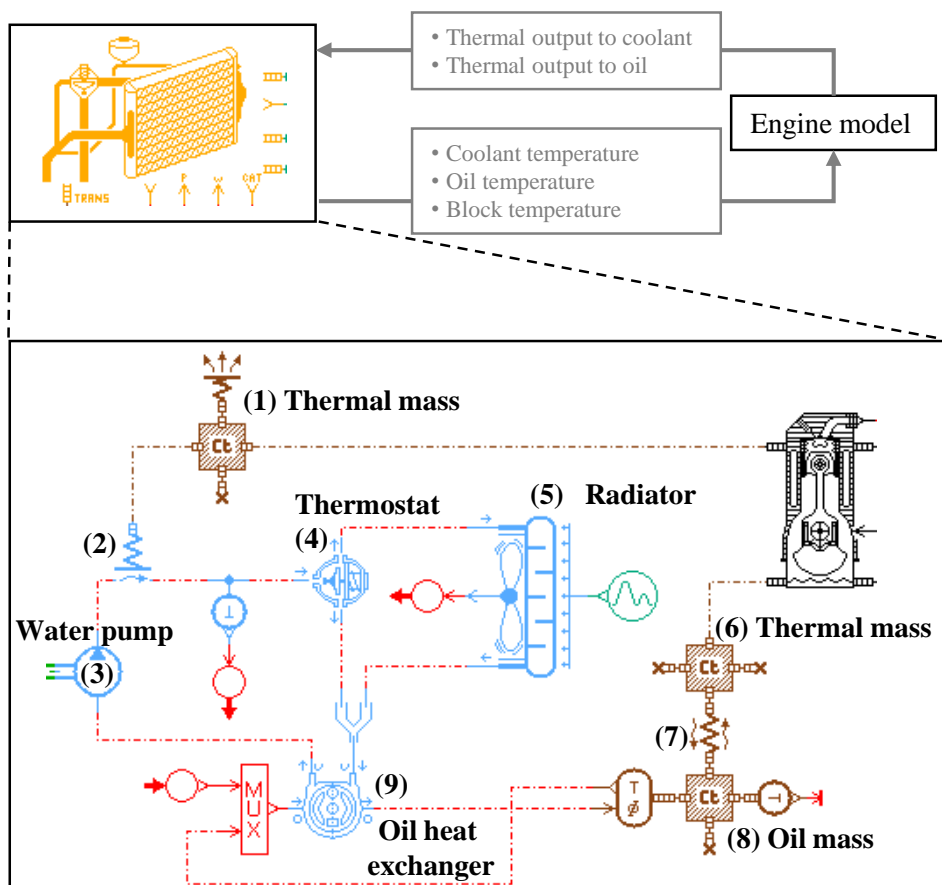


Figure 4.14.: Sub-system cooling circuit

4.4.8. Mild-hybrid model

This thesis also includes the technology of 48-V-mild-hybrid as a measure in the analysis. Therefore, a second simulation model is created with a hybrid power-train. The flexible and modular layout of the simulation model is important, as it reduces the model maintenance effort. The adapted sub-systems are highlighted in Figure 4.15 and contain the component changes listed below. The vehicle, driver and engine sub-systems remain the same. Only the auxiliary and power-train sub-systems are adapted with the following components:

- Traction battery (1) with 48 V or higher voltage

- Replace the alternator with a DC/DC converter (2) for the power-supply of the 12-V-electrical system
- Electric motor and inverter (3)
- Additional clutch (4) to handle a P2-hybrid architecture
- Switching element (5) to define the location of the electric motor
- Hybrid control unit (HCU) for the actuation of the clutches, ICE and electric motor

To handle the different parallel hybrid architectures, a switching element for the electric motor is included. This element defines the power flow of the electric motor. In the case of a P0-hybrid, the orange solid power flow is used. The mechanical connection of the electric motor is on the belt drive, which is the location of the alternator in conventional vehicles. A P1-hybrid uses the orange dashed power flow, connected to the crankshaft. The difference between the location of P0 and P1 is an additional belt drive ratio and the belt drive efficiency factor considered for the P0 architecture. The P2-hybrid is connected to the transmission input using the dashed-dotted orange flow. Since an additional clutch model is included, the P2 motor can be used in vehicle standstill with the ICE in idle mode when the normal clutch or torque converter is opened. Otherwise, if the second clutch (4) is opened, the ICE can be deactivated, and only the electric motor is used for driving. Electric driving and recuperation without engine drag torque are possible. The last power flow via the orange dotted line is a P3 architecture connected to the transmission output via an additional gear ratio.

In principle, this simulation model for the hybrid power-train can also be used for full-hybrid and plug-in-hybrid vehicles with parallel architectures. The difference between the mild-hybrid, full-hybrid and plug-in-hybrid is only the parametrization of the electric motors, the traction battery and the operating strategy in the HCU.

Since two energy sources are now used, an additional control unit is required. The so-called HCU has to distribute the torque between the electric motor and the engine, depending on the desired driver-requested wheel torque. The following hybrid functions are included in the control logic:

- Recuperation (regenerative braking) - If the driver requests a deceleration (negative torque), then the electric motor operates as a generator and charges the battery, depending on the electric motor and battery capabilities and the driver request. In the case of a P2-hybrid, the second clutch is opened to increase the charging power by eliminating the engine drag torque.
- Charging - If the state-of-charge (SOC) of the traction battery is too low, then the torque request of the ICE is increased to charge the battery via the electric motor. The electric motor operates in the generator mode. The requested charge power is a function depending on the SOC of the traction battery.
- Boost - In the case of full-throttle acceleration, both the ICE and the electric motor work at maximum torque to improve driving performance. This logic also includes the component capability, i.e. transmission input torque, motor and battery capabilities.
- Electric driving (only with a P2 or P3 architecture) - A torque threshold is defined based on the battery SOC and electric motor capability, including a hysteresis. If the driver torque request is above this threshold, the vehicle drives with the ICE. If the torque request is below the threshold, the second clutch is opened, the ICE is deactivated, and the vehicle drives only with the electric motor. Because 48-V-mild-hybrids have limited electrical

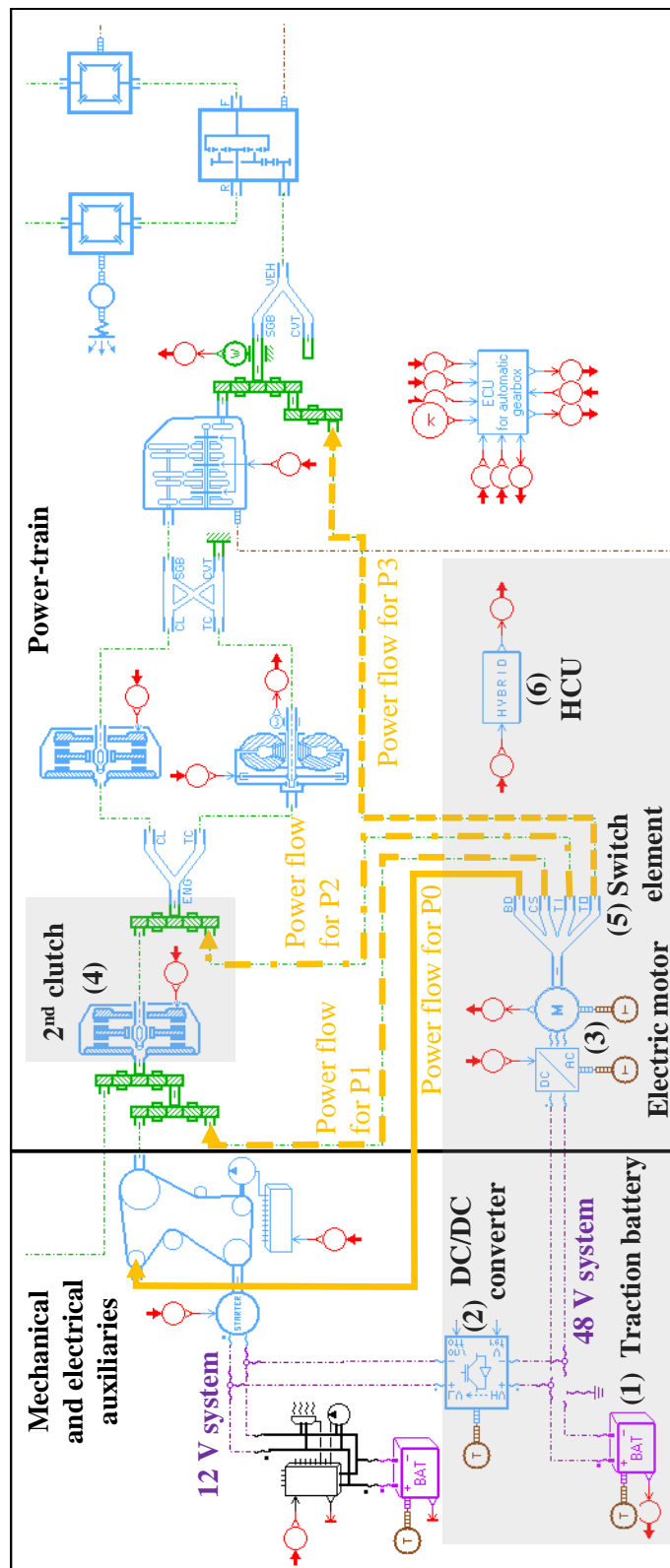


Figure 4.15.: Adapted sub-systems for auxiliaries and power-train due to hybridization

power, this function is primarily used for smooth acceleration and constant speed driving at low vehicle speed only.

- Overlying deactivation logic of the ICE - Overlying the listed functions, the ICE deactivation allowance is considered. This means, for example, that the engine has to run until warm condition is achieved before the first deactivation is allowed. In addition, time hysteresis is included for drivability reasons to prevent too frequent activation / deactivation.

4.5. Model validation

The proposed optimization approach will only work with a verified simulation model that provides accurate simulation results. Chapter 3.2 described the legal regulations. Failure to meet the fleet target can result in either penalties or sales prohibitions. For example, in the EU, a penalty of €95 has to be paid for every vehicle sold and every gram CO₂ exceeding the limit. On the other hand, implementing too many measures and bringing the fleet status far below the target would involve an over-investment. Accurate simulation results are needed to minimize the risk of target overfulfillment or exceeding the limits. Either problem will lead to unnecessary increase in the vehicle total cost of vehicle ownership and thereby limit customer acceptance. To guarantee the accuracy of the simulation model, a validation of the simulation represents an important starting point. This includes the validation of the baseline vehicle, as well as also the validation of the technologies for improving CO₂ emissions that are under consideration.

C. Haupt built a multi-physic complete-vehicle simulation model in his doctoral thesis [20]. He mentions that both components and their combinations in a complete-vehicle model have to be validated. In this thesis, the input data for the components are provided by suppliers. They are based either on simulation or test bench measurement. It is assumed that this input data are valid. Therefore, this chapter focuses on the validation of the described complete-vehicle simulation model.

The starting point for validating of a model is defining the area of application. A simulation model should be validated for all of the maneuvers for which it will be deployed [102]. In this case, the complete-vehicle simulation model should be valid for legal CO₂ emissions test cycles and driving performance. These two scenarios have different foci. For the legal test cycles, the energy balance (losses and efficiencies) is important, while the focus for the driving performance is the power balance (dynamic). Both scenarios have to be validated.

In [102], different approaches for model validation are listed: conceptual model validation, specification verification, implementation verification and operational validation. While the first three approaches refer to the modeling of the simulation itself, the focus in this chapter is the operational validation of the model, which will determine if the output behavior has an acceptable accuracy with respect to the intended use of the model. This publication also mentions several validation techniques. Of these techniques, the following two are relevant for this thesis:

- Event validity - Checking if events occur at similar moments in time in the simulation and the measurement
- Sensitivity analysis - Changing inputs and parameters

In this work, the simulation model was validated on a real vehicle with the following data:

- Vehicle: sedan (C-segment)
- Engine: 1.6 l gasoline engine (with VVT and turbocharger, 115 kW and 210 Nm)

- Transmission: 6-gear DCT
- Test weight: 1470 kg (NEDC), 1550 kg (WLTC), 1590 kg (driving performance)

The experimental setup up of the vehicle is described in more detail in Appendix C.2.

The validation is split into two parts: the determination of CO₂ emissions and driving performance. The simulation model is parametrized with the available input data and adapted to one driving cycle. The input data of the vehicle were provided by Magna Steyr, the manufacturer and the component suppliers and are restricted by a nondisclosure. The input data consist of component test rig measurement results (e.g. efficiency map for the transmission, fuel consumption map for the engine), calibration data (e.g. transmission gear-shifting map) and measurements of the complete vehicle (e.g. coast-down curve, generator load). First, the general behavior (e.g. gear-shifting, behavior of variables) of the simulation is checked and compared to the measurement. Since all relevant input parameters are not available, it is necessary to identify the values of unknown parameters, such as the thermal mass and the heat transfer characteristic for the thermal circuits. A parameter variation was performed to enter values to these parameters in order to achieve a defined behavior of an output signal. In the case of the thermal mass and the heat transfer, the coolant temperature is defined as an output signal because this signal will influence the additional cold-start consumption of the engine. The values of these parameters are varied until the average difference between the simulation and measurement of the coolant temperature is below a defined value of 1°C (see third graph in Figure 4.16).

To check the validity of the existing and assumed input parameters, additional cycles were executed. These tests checked if valid results were generated without further adaptations of the input data. In the case of CO₂ emissions, first the NEDC cycle simulation at 23°C was compared to the measurement. In the second step, the simulation was compared to a WLTC measurement at 23°C as a sensitivity analysis. The only difference between the NEDC and WLTC tests is the speed profile and the vehicle inertia weight on the test bench. The model validation is intended to compare the cycle-representing value, that is, the total CO₂ emissions for the legal test cycle and the acceleration time for driving performance tests. In a third step, the general behavior of the signals during the simulation is important.

Figure 4.16 shows the validation of an NEDC, including the comparison of the vehicle speed, the accumulated CO₂ emissions and coolant and oil temperature between the simulation and two measurements. It is evident, that the difference between the two measurements is around 2%. Two measurement were done to show the repeatability of the measurement. Both the general behavior of the CO₂ emissions and the temperature match the measurements signals. To evaluate the difference between simulation and measurement, the difference of the CO₂ emissions is investigated in more detail. The difference between the accumulated CO₂ emissions of the simulation and the average accumulated CO₂ emissions of the two measurements is calculated. The tolerance range is calculated from a defined percentage value of the total CO₂ emissions. By adapting simulation parameters (thermal masses, heat transfer and average engine efficiency), it was possible to validate the simulation model within a 1% tolerance range, which is lower than the repeatability of the measurement itself. As additional validation of the simulation model, a second driving cycle (the WLTC) was considered. No parameters were changed in comparison to the NEDC. Instead, the inertia weight was adapted from 1475 kg to 1550 kg, in accordance with the WLTP. The result can be seen in Figure C.7 in Appendix C.2. The delta on the accumulated CO₂ emissions is calculated and falls within a tolerance range of 2%. This difference is still acceptable compared to the measurement tolerance evaluated with the two NEDC measurements.

The same kind of comparison was performed for the validation of the driving performance. The

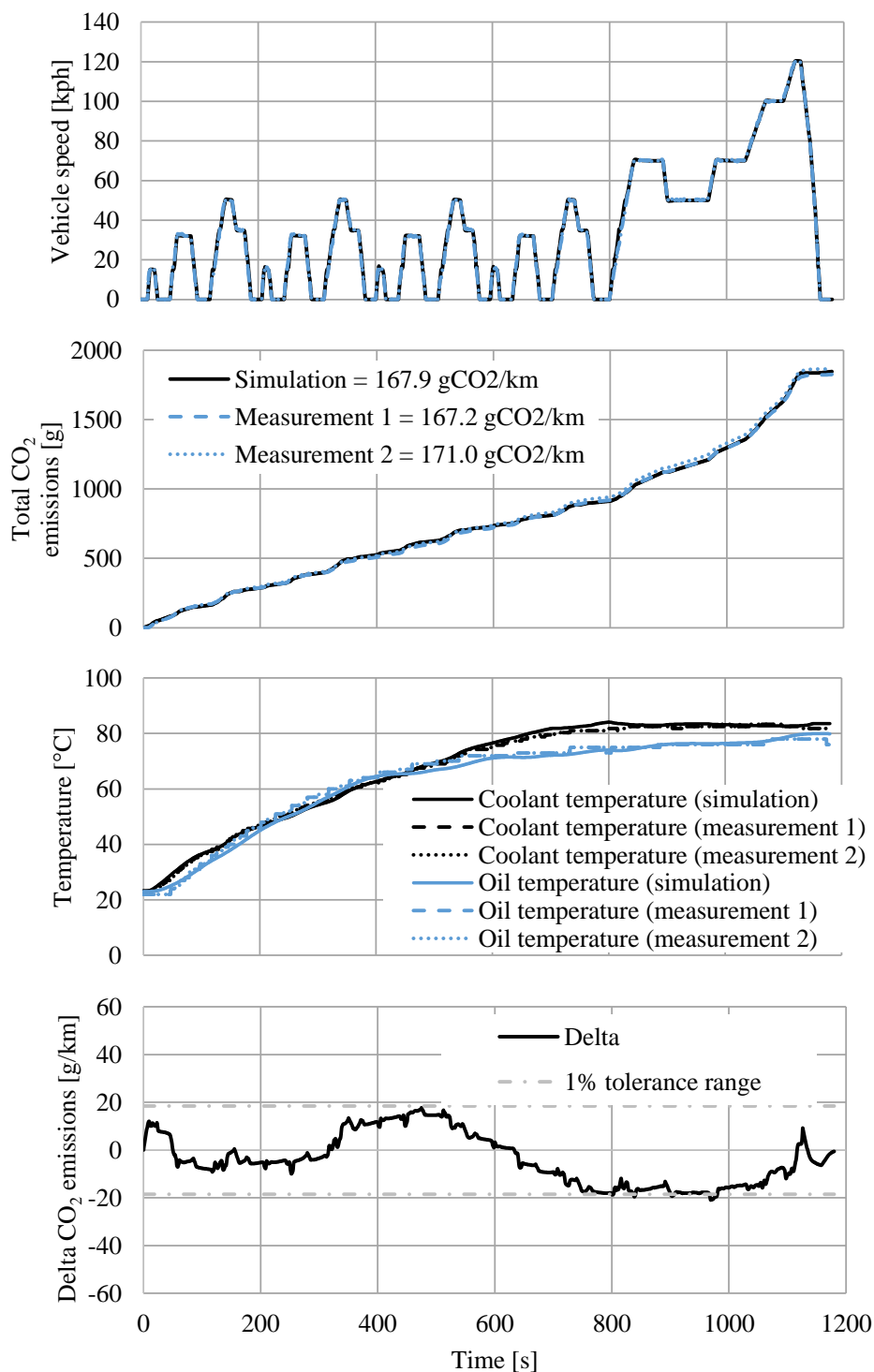


Figure 4.16.: Comparison of simulation and measurement, maneuver: NEDC

unknown parameters for the validation are the dynamic of the engine model and the shifting strategy (e.g. shift time, torque intervention during shifting). In the simulation model, the dynamic of the engine turbocharger is modeled by a PT1 time delay. To evaluate this value, a full-throttle acceleration with tip-in and fixed 4th gear from 50 to 100 kph was measured on the test track. The gear was fixed to avoid influences in engine torque caused by the gear-shifting. The time constant was adapted with a parameter variation until a similar behavior of the generated torque was reached. This comparison is shown in Figure 4.17. To analyze the accuracy of the acceleration, the difference in the acceleration time was analyzed. The difference in the time between the same vehicle speed in the simulation and the measurement is calculated. Here again, the difference is within a tolerance range of 1%. In the next step, the maneuver from 60 to 100 kph without fixed gear was considered. This maneuver includes a back-shift from the 5th to the 3rd gear. The third maneuver to show the reproducibility of the simulation is a full-throttle acceleration from 0 to 100 kph. Both validation results can be found in Figures C.8 and C.9 in Appendix C.2. The vehicle parameters remain the same in all simulations. Only the event and system behavior of the control unit were adapted according to the measurement, which means the point of time for a back-shift or up-shift process of the transmission gear ratio and the amount of the torque limitation during the shifting process. For both maneuvers, the difference in acceleration time between measurement and simulation was also evaluated. Both maneuvers also fall within a 1% tolerance range. Some deviations in this difference in the acceleration time occur during the gear shift. However, as long as the total acceleration time remains valid, such differences are acceptable because the highest influence on acceleration time is the torque transmitted to the wheel. Thus, the length of the shifting time and the torque reduction during shifting have more influence on the acceleration time than the starting point of the shifting event.

In the next step, the implementation of functions such as an engine start-stop system or intelligent generator control must also be validated. In this case, the focus is on the comparison of the events (e.g. engine on - engine off). The plan was to validate these two functions on a vehicle, but the vehicles and equipment were not available in time.

The summary of these examples shows that the presented physics and logic of modeling of the complete-vehicle simulation matches the real vehicle within a defined tolerance range of the cycle-representing value. Finally, in a development project, the success and accuracy of the simulation model strongly depend on the available input data. In addition, the ability to validate and verify the simulation results of the next-generation vehicles with measurements from the current model generation should be the starting point for further analysis and optimization. Because the vehicle input data used are subjected to a non-disclosure, it was decided to define fictional vehicles for the further investigation in this thesis. If this work is used for development projects in the future, the validation of the vehicles used is an important step for the success to the optimization method.

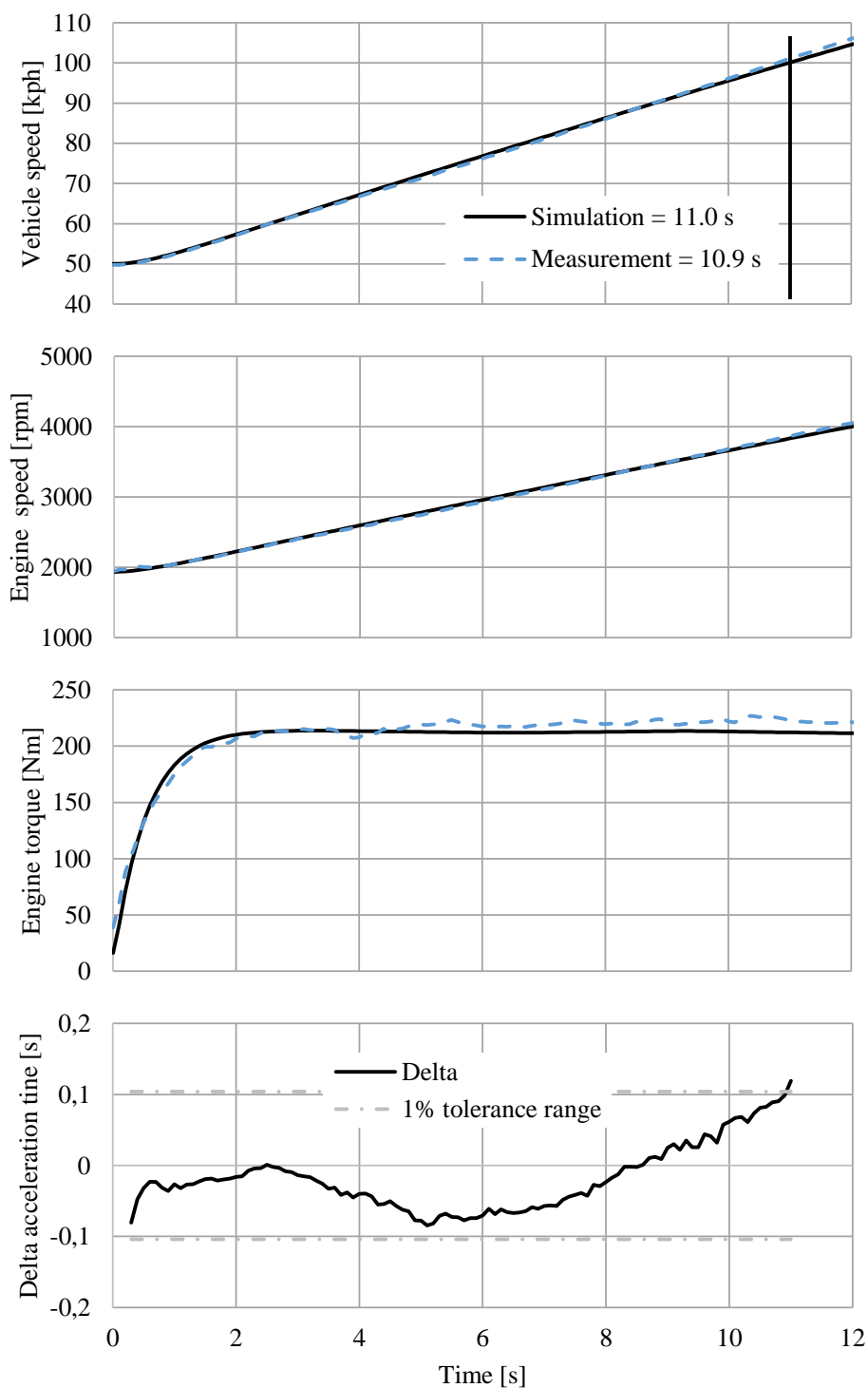


Figure 4.17.: Comparison of simulation and measurement, maneuver: Full-throttle acceleration from 50 to 100 kph with locked 4th gear

4.6. Automated simulation

4.6.1. Scripting

The principle interaction between the simulation model and the scripting was shown in Figure 4.3. The scripting has to handle the selection of the simulation model, the input data and parametrization, and the analysis of the simulation results.

The flow chart for the execution of the script-based simulation is shown in Figure 4.18. The whole script is divided into several sub-scripts to provide a better overview. The sub-scripts and steps are sequentially executed within the main script. First, the system variables and the links to the simulation models and the database have to be defined for initialization. In this thesis, two simulation models are defined - one for conventional vehicles and one for a 48-V-mild-hybrid vehicle. In the next step, the vehicles and the considered cycles have to be defined. Samples of these scripts are shown in Listings 4.2 and 4.3 and will be described in more detail in the next chapter. After this initialization, the simulation loop is executed, and the simulation results are stored. The execution of the simulation runs is shown in Figure 4.19 and consists of two cascaded loops and two counters: i_v for counting the vehicles, and i_c for counting the cycles. First, i_v is initialized with the first vehicle. An “*if*” statement decides whether this vehicle should be considered in the current loop or not. In the next step, the simulation model is selected, and the vehicle parameters (e.g. engine, transmission) are loaded into the workspace. Thereafter, the second sub-ordinary loop for the driving cycles occurs. Here as well, the counter i_c is initialized. It is checked if the current cycle should be considered for the current vehicle. Various driving cycles can be defined for each vehicle, such as NEDC or FTP/HWFET. For example, for an European vehicle, only the NEDC (and no FTP/HWFET) should be considered. The cycles, which are also described by scripts in more detail, are executed. The counter of the cycle i_c is then increased, and this iteration is repeated until the maximum number n_c of available cycles is reached. Once all defined cycles for a vehicle have been evaluated, the counter of the vehicle i_v is increased, and the iteration of the cycles starts again with the next vehicle until all n_v vehicles are completed.

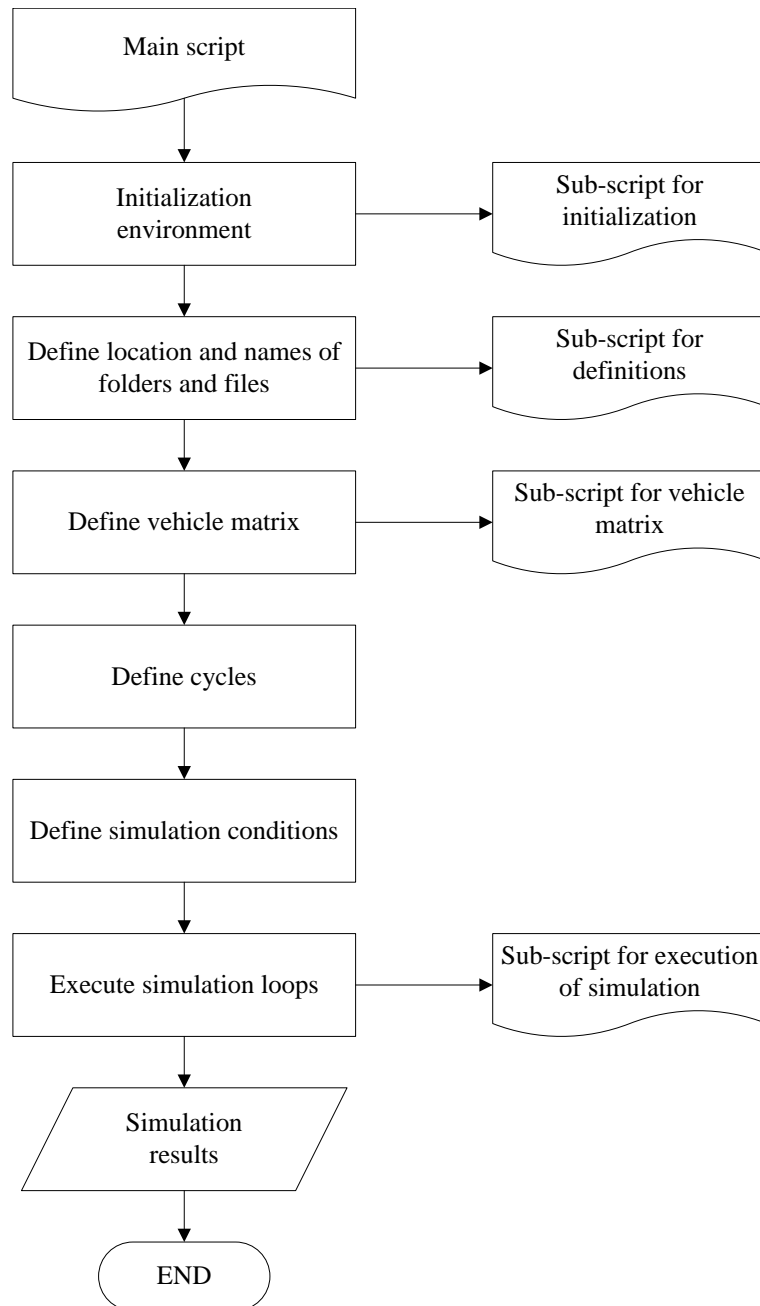


Figure 4.18.: Script-based execution of simulation loops including the setting of variables

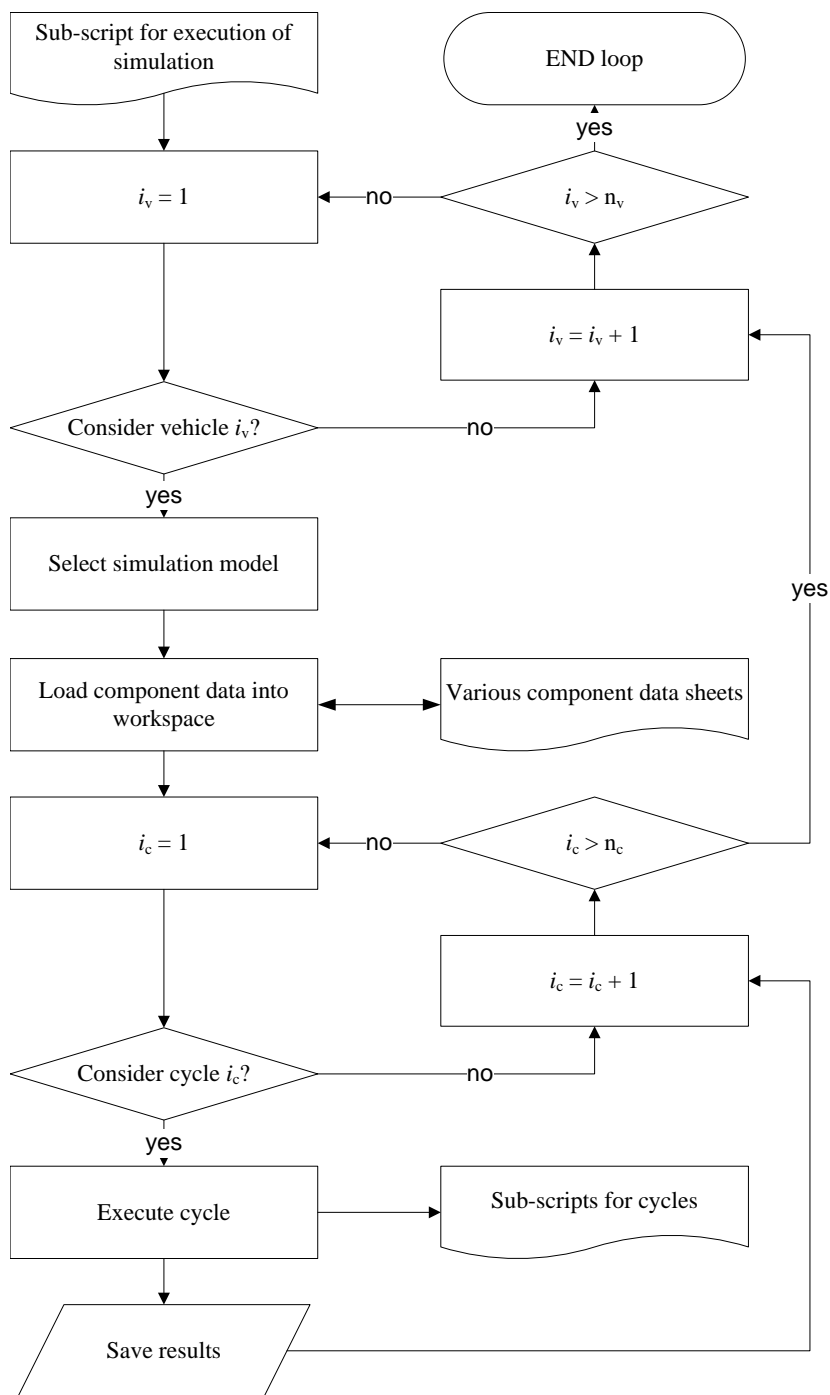


Figure 4.19.: Execution of a simulation loop for vehicles and cycles

4.6.2. Definition of vehicles and components

Within the script, the definition of the vehicles and the vehicle matrix is required. Thereby, the important characteristics of a vehicle are the market, the sales volume, the reference simulation model, components and the complete-vehicle targets. For example, the script used for the definition is shown in Listing 4.1. The sales volume can be one value or a vector based on several years. In addition, a reference simulation model has to be defined, for example whether a conventional or hybrid power-train should be considered. Finally, the targets for the driving cycles have to be set. A value of zero means that this specific target / test cycle is not considered for the vehicle. These target values represent the reference targets as input for the optimization algorithm. Furthermore, the definition of the components used in the vehicle are considered.

Listing 4.1: Exemplary source code to describe vehicle #1

```
VehConfName(1) = 'EU_A_Hatch_G060_MT'; // vehicle configuration name
VehConfMarket(1) = 1; // sales market 1 = EU, 2 = US, 3 = CN
VehConfSales(1,:) = [22000]; // sales volume forecast
VehConfModel(1) = 1; // reference simulation model, 1 = basis conventional model,
    2 = basis mild hybrid model

VehConfVeh(1) = 'Body_Segment_A'; // complete-vehicle data (aerodynamic, mass,
    geometry)
VehConfTire(1) = '185_65_R15'; // tire data
VehConfEng(1) = 'Gas_1_0_1'; // engine data
VehConfTrans(1) = 'MT_6'; // transmission data
VehConfHybrid(1) = 'noHybrid'; // hybrid operating strategy (for hybrid) > not
    considered for this vehicle
VehConfBatt(1) = 0; // battery data (for hybrid) > not considered for this vehicle
VehConfDCDC(1) = 0; // DC/DC data (for hybrid) > not considered for this vehicle
VehConfEMot(1) = 0; // electric motor data (for hybrid) > not considered for this
    vehicle
VehConfAux(1) = 'Aux_Sedan'; // auxiliaries data
VehConfCool(1) = 'Cool_Standard'; // cooling data

VehConfTarget(1,1) = 5.3; // target NEDC [l/100km]
VehConfTarget(1,2) = 0; // target US FTP/HWFET [l/100km] > not considered for this
    vehicle
VehConfTarget(1,3) = 6; // target WLTC [l/100km]
VehConfTarget(1,4) = 12.5; // target acceleration 0...100 [sec.]
VehConfTarget(1,5) = 12; // target acceleration 80...120 [sec.]
VehConfTarget(1,6) = 175; // target max speed [km/h]
```

In this case, the vehicle is defined by the vehicle body, engine, transmission, tire, auxiliaries and cooling system. In the special case of hybridized vehicles, the information about the traction battery, DC/DC converter, electric motor and the hybrid operating strategy is also required. Listing 4.2 provides an example of the definition of the vehicle body in more detail. Such a definition exists for each vehicle body of the fleet. The vehicle body is described by the mass, aerodynamics, geometry, coast-down parameter and friction loss. Various parts of weight information can be defined depending on the driving cycle (e.g. a special weight for driving performance tests). In the case of legal driving cycles, the required inertia weight class is calculated automatically based on the curb vehicle weight. The geometry is required for the calculation of the dynamic axle load distribution for accelerations. In addition, this information is needed to calculate the footprint for the reference of the US GHG regulation. The driving resistance of the vehicle can be described either by the measured coast-down parameter (F0, F1, F2) or by the complete-vehicle parameters (aerodynamics, drive-train friction and rolling

resistance). Here, the rolling resistance is defined in the tire component and not in the body. The parameter “*Veh_UseRoadParam*” is used to set the type of driving resistance, using either the coast-down or the complete-vehicle parameter. Depending on this setting, the simulation model automatically selects the required resistance calculation.

In principle, a vehicle is defined by the segment (e.g. C-segment vehicle) with additional configurations as sub-variants, for example engine / transmission configuration as a sedan with gasoline 100 kW engine and manual transmission. Thus, the vehicle body parameters (e.g. mass or aerodynamics) can be different for each vehicle within a segment. Several sub-variants for a vehicle body can exist. The data sheet in Listing 4.2 describes the parameters for one vehicle body of one segment. To improve the data handling, sub-variants of the vehicle body can be defined within a single data sheet for the same vehicle segment. The variation of different variants (e.g. changes in weight of other engine / transmission configurations) is described by such a sub-variant. An example of the weight adaptation of a second C-segment variant is shown in the bottom part of this listing below. Therefore, it is not necessary to create a separate data sheet for each vehicle. With this approach, all C-segment vehicles with their body-specific parameters can be defined in a single sheet. A similar structure is used for the other components as well. A further overview of the remaining component definitions is given in Appendix C.3.1. Parameters can be defined as a value or as a path to a characteristic map (e.g. in the case of the friction-loss map).

Listing 4.2: Exemplary source code for vehicle body data

```
// vehicle: C-segment vehicle

// vehicle weights
Veh_CVW = 1320; // curb vehicle weight [kg]
Veh_GVW = Veh_CVW + 540; // gross vehicle weight [kg]
Veh_PVW = Veh_CVW + (Veh_GVW - Veh_CVW) / 2; // vehicle weight for driving
           performance

// geometry
Veh_DistFrntRr = 2.660; // wheel base [m]
Veh_DistFrntCoG = Veh_DistFrntRr * (1 - 0.5); // distance front axle to CoG (
           center of gravity) [m]
Veh_WideTrack = 1.530; // track width [m]
Veh_HghtCoG = 0.590; // height CoG [m]

// aerodynamics
Veh_Cd = 0.3; // aerodynamic drag coefficient cd [-]
Veh_Ax = 2.29; // frontal area [m2]

// friction loss due to brakepad, bearing, side-shaft
FriLoss_Frnt_Map = 'Data/FrictionLoss_Front.data'; // loss data map [Nm] on front
           wheel
FriLoss_Rr_Map = 'Data/FrictionLoss_Rear.data'; // loss data map [Nm] on rear
           wheel

// coast-down parameter
Veh_UseRoadParam = 1; // 0 = use coast-down parameter (F0, F1, F2) / 1 = use road
           parameter (cd, Ax, rrc, ...)
Veh_F0 = 190; // coast-down parameter constant value [N]
Veh_F1 = 6; // coast-down parameter linear value [N/(km/h)]
Veh_F2 = 0.3; // coast-down parameter square value [N/(km/h)2]

// sub-variants of vehicle
if VehConfVehSub(i_v) == 2 then // sub-variant #2 > change weight information
```

```

    Veh_CVW = 1415;
    Veh_GVW = Veh_CVW + 540;
    Veh_PVW = Veh_CVW + (Veh_GVW - Veh_CVW) / 2;
end

```

4.6.3. Simulation and analysis of driving cycles

The detailed routine for the execution and analysis of the cycles is shown in Figure 4.20. In the first step, each cycle is defined by various parameters. An overview of the parameters is given with the source code in Listing 4.3.

Listing 4.3: Exemplary source code to describe a cycle

```

Cyc_VelFile = 'Data/Cycles/NEDC/cyc.data'; // map of time-dependent speed profile
[m/s]
Cyc_GearFile = 'Data/Cycles/NEDC/gear_6.data'; // map of time-dependent gear
profile
Cyc_TransmissionGear = 0; // fixed a gear (0 - use gear profile)
Cyc_Tfinal = 1180; // simulation time [s]
Cyc_Vinit = 0; // initial vehicle speed [m/s]
Cyc_Slope = 0; //slope [%]
Cyc_Type = 1; // type of driver in case of manual transmission: 1 time-deepening
gear profile for CO2 emission driving cycle / 2 shifting strategy for
performance cycles
Cyc_Tamb = 23; // ambient temperature [°C]
Cyc_RhoL = 101325 / (287.058 * (273.15 + Cyc_Tamb)); // calculation air density
depending on ambient temperature

// cycle-specific adaption of vehicle parameters
Cyc_CoolSoll = 'cold'; // precondition cooling: 'cold' = cold-start, 'warm' = warm
-start
Cyc_AuxSoll = 'min'; // activation of auxiliaries: 'min' = minimal activation of
auxiliaries
Cyc_Mass = 'NEDC'; // reference vehicle mass: 'CVW', 'GVW', 'PVW', 'NEDC', 'WLTC', 'FTP
,
Cyc_Payload = 100; // payload

```

The driving cycle is described by a speed profile, simulation time, road slope and the ambient temperature. One interesting point is the definition of the shifting strategy. In the case of a manual transmission, the time-dependent gear profile is given for CO₂ emission-related cycles. For driving performance, the driver has to shift depending on the engine speed. Vehicles with automatic transmission generally use a shifting strategy from the TCU. A special case is the passing time from 80 to 120 kph in fixed 5th gear. Here, the gear has to be fixed without any shifting strategy. The second point is the preconditioning and the adjustment of the vehicle. There must be a differentiation between cold-start and warm-start. Based on this setting, different calibrations of the cooling model are defined. In the case of a warm-start, the cooling model will be omitted and replaced by a constant warm setting. In the case of a cold-start, the cooling model includes the warm-up of the engine. Furthermore, the setting of the auxiliaries is important. In this consideration of CO₂ emissions and driving performance cycles, minimal auxiliaries are always used. This means only the auxiliaries required for driving, but no radio or HVAC will be activated, for example. The fourth point is the setting of the vehicle test mass. In the case of a driving performance test, the setting “PVW” is used. This means that the performance weight is used, which is defined in the vehicle configuration (see Listing 4.2). Special cases are the CO₂ emission-related cycles. A separation into test mass and inertia weight class

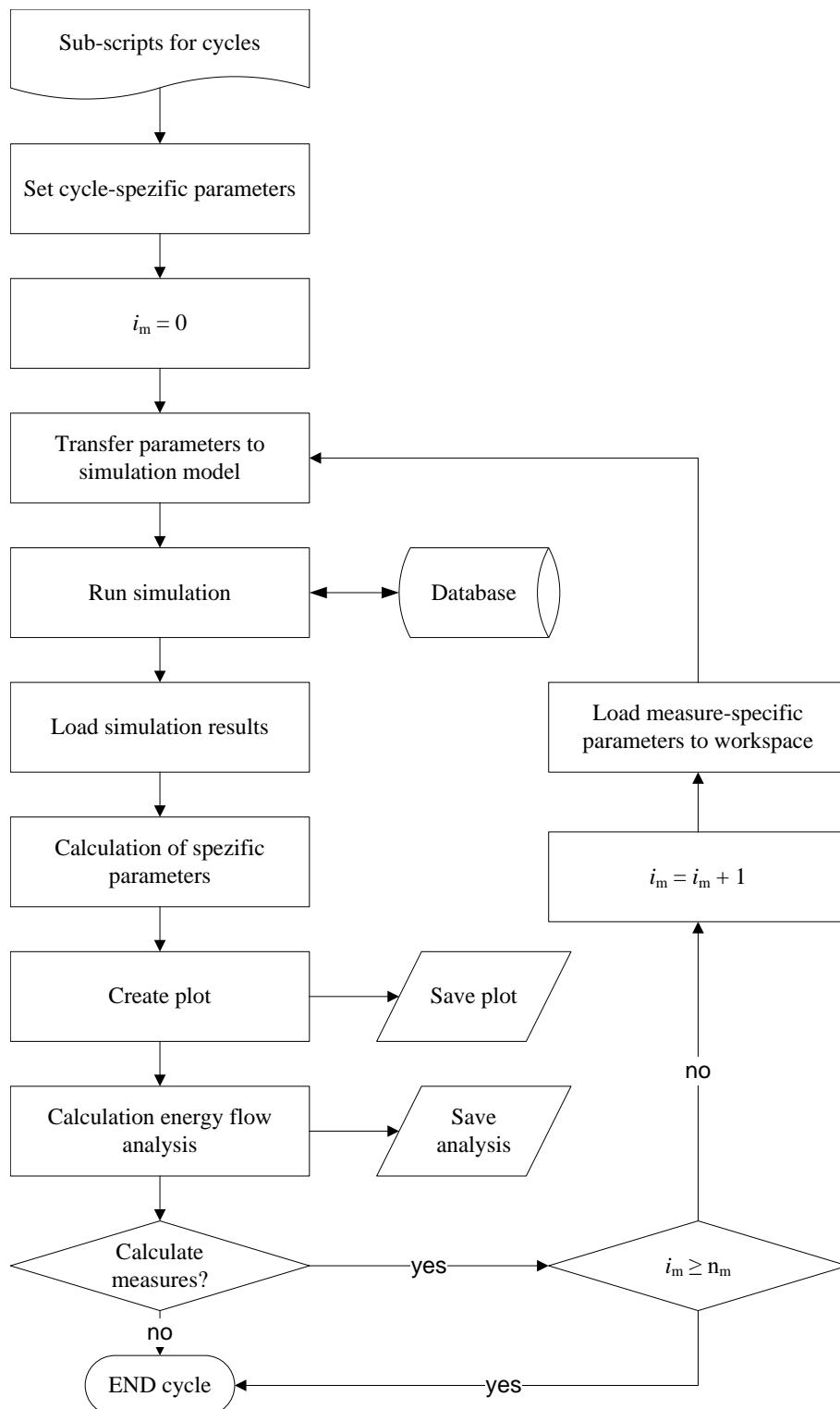


Figure 4.20.: Interaction of simulation and scripting during the execution of a driving cycle simulation loop

is needed. The test mass m_t is thereby connected to the rolling resistance, and the test weight class m_{twc} is connected to the accelerated mass, which is described in Equation (3.9) in Chapter 3.3.6. The definition of the test weight class depends on the curb vehicle weight and can be seen in Appendix A.1.4, in the case of the NEDC test cycle. The test mass m_t reads

$$m_t = m_{CVW} + m_{pl} , \quad (4.1)$$

where m_{CVW} is the curb vehicle weight (CVW) and m_{pl} a defined payload depending on the test procedure. In the case of the NEDC and the *ECE-R 83* [34], the payload is 100 kg. This definition of the test weight and test weight class depends on the legal driving cycle and the test procedure. Different pre-processing scripts for each driving cycle (NEDC, FTP/HWFET, WLTC) have to be taken into account. In addition, in the case of the WLTC, the gear-selection profile for vehicles with manual transmission has to be calculated in advance. This gear-shifting sequence is different for every vehicle and depends on the engine characteristic, gear ratio and driving resistance. A rough overview of the calculation is given in Appendix A.1.6.

After setting the cycle-specific parameters to the workspace, a counter for measures i_m is defined. The script starts the third iteration loop for the evaluation of various defined measures for the improvement of CO₂ emissions. With the initialization $i_m = 0$, the baseline vehicle without any measures is simulated. In the next step, the script transfers the parameters for the simulation from the workspace to the global parameter list of the simulation model and executes the simulation. If a parameter is linked to a datasheet, the simulation model accesses the link in the database, where characteristic maps and curves are stored. After finishing the simulation run, the simulation results and important variables are loaded to the workspace for post-processing. In the context, the following signals are relevant:

- Total fuel consumption [l]
- Distance traveled [km]
- Energy balance of the low-voltage battery [Ah]
- Vehicle speed [km/h]

Based on the cycle-specific post-processing, the simulation results are calculated. Each driving cycle has one characteristic resulting value, such as fuel consumption [l/100km] for the NEDC or acceleration time [s] for driving performance cycles. One aspect to be considered is the energy balance of the low-voltage battery. Current European and US regulations do not require such consideration. However, the WLTP will consider this balance in the future. A negative battery energy balance, which means a battery discharge, decreases fuel consumption. In this case, the load on the generator is partly reduced in the driving cycle, which leads to less torque request on the ICE and therefore to less fuel consumption (see Appendix A.1.7 for a more detailed description). In addition, the handling of the fuel consumption of hybridized vehicles is more complex. Unlike for conventional vehicles, more than one driving cycle have to be simulated and analyzed. A more detailed overview is given in Appendices A.1.5, A.1.8 and A.3.5. After the post-processing of the characteristic parameters, the simulation results can be plotted. An example of a Scilab-plot for the NEDC and acceleration time simulation is shown in Figure 4.21.

This first simulation run represents the baseline simulation of a vehicle and a cycle. No special measures are considered yet. This baseline values are saved in the baseline result matrix $S_{bl}(i_v, i_c)$. In the next step, this simulation procedure is repeated for the measures. A list of measures for improving CO₂ emissions is given. Each measure will be simulated individually until the whole list of n_m measures is processed. If a certain measure is not important for the

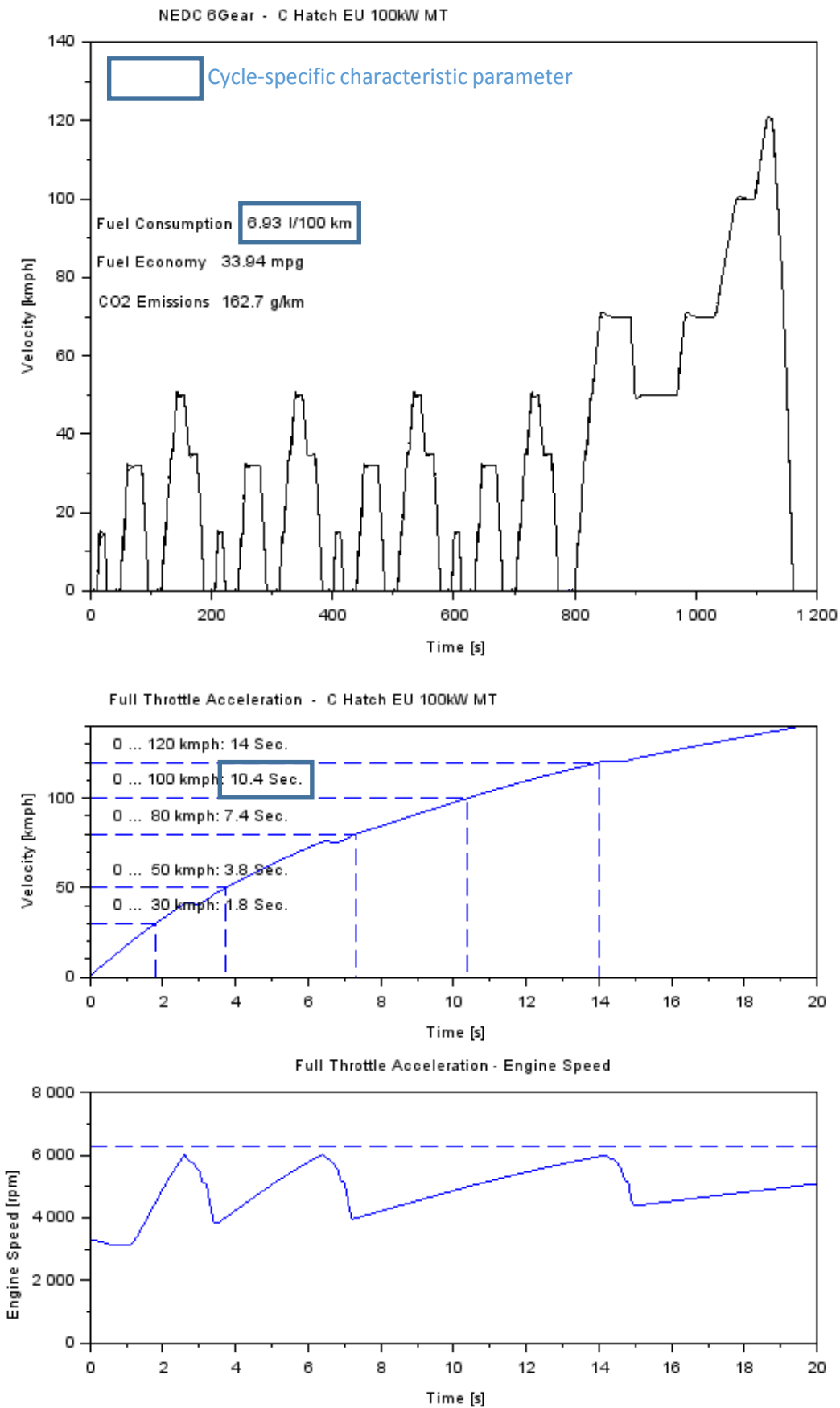


Figure 4.21.: Sample Scilab-plot for an NEDC and a full-throttle acceleration simulation

selected vehicle and cycle, than the algorithm jumps directly to the next measure. Each measure has to be described. Listing 4.4 shows an example of such a description. First, a definition of the simulation parameters, which can be changed, is required. This is shown in the upper lines. Both individual parameters (e.g. an activation of a start-top system or change of an aerodynamic parameter) and complete datasheets of components (e.g. another engine or transmission) can be changed. A measure itself is defined by various parameters. First, “*M_Type*” describes the type of a measure. Three options are possible for the type:

- 1 = simulation result - The simulation is used to analyze the influence of a measure. The required parameters will be set to the simulation model, and the simulation will be executed. The difference between the baseline simulation and the simulation including a measure is the influence of the measure.
- 2 = relative value - Without using simulation, a relative influence can be defined, for example x% improvement compared to the baseline value.
- 3 = absolute value - Without using simulation, an absolute influence can be defined, for example 0.x l/100km improvement. This point can be used, for example, for ECO innovations or off-cycle credits, which will be added in addition to the fleet-average value or to include monetary penalties, such as in the EU regulation.

This differentiation into the three definitions provides the advantage that an input for the algorithm can also be defined without a simulation. Therefore, all influences on the measures can be defined directly by values, and the optimization approach is able to function without a simulation. This improves the flexibility of the whole method.

By using the parameter “*M_global*”, the measures can be defined as so-called “global” or “local” measures. Local measures can be selected for each measure individually, while global measures have to be selected for all vehicles. The difference will be explained in Chapter 5.6.4.4 in more detail. In addition, boundary constraints can be defined for a measure. A measure can be restricted to certain markets, vehicles, engines, transmissions and cycles. So, for example, a measure can be used for every vehicle or only for a C-segment vehicle with a manual transmission in the European market and the NEDC cycle. For each measure, several sub-variants can be defined, which are in “or” relation among themselves. This means either the measure is not selected, sub-variant 1 is selected, or sub-variant 2 is selected. The measures are defined by four parameters. The parameter “*M_Result*” includes the delta values if the measure is defined as a relative or an absolute measure. “*M_Model*” selects the simulation model for the sub-variant. In general, the reference model of the basis vehicle “*VehConfModel*” is used. But in special cases, for example for the measure of the mild hybridization, another simulation model can be selected. The last two parameters, “*M_Cost*” and “*M_Value*”, include the cost of the sub-variants and the parameters. The simulation parameters to be changed are defined in the second column in “*M_Value*”. This number is coupled with the parameter of the variable “*M_VarList*”, for example “6” for the aerodynamic drag. Listing 4.4 shows this parameter setting in the case of an aerodynamic measure. Further examples are shown in Appendix C.3.2.

Listing 4.4: Exemplary source code to describe a measure

```
// list of variable parameters
M_VarList(1) = 'Engine'; // change engine-file
M_VarList(2) = 'Trans'; // change transmission-file
M_VarList(4) = 'StartStop_Active'; // start-stop [0/1]
M_VarList(6) = 'Veh-Cd'; // aerodynamic cd [-] -> DELTA value
M_VarList(x) = ...
```

```

// ...
// ...
// — measure ID 27: aero underbody —
i=27;
M_Type(i) = 1; // type: 1 = simulation, 2 = relative, 3 = absolute
M_global(i) = 0; // type of measure: 0 = local, vehicle specific / 1 = global

// boundary constraints
M_Market(i,:) = [1 1 1]; // in which market it should considered: 1=EU, 2=US, 3=
    CN > here all markets considered
M_ConsVeh(i,:) = [1]; // considered vehicles > only vehicle #1 considered
M_ConsEng(i,:) = [0]; // considered engines > no restriction
M_ConsTrans(i,:) = [0]; // considered transmission > no restriction
M_ConsCyc(i,:) = [1 1 1 1 1 1 1]; // considered cycles > all cycles considered

// sub-variant 1: 'aero underbody front'
M_Result(i,1) = 0; // only in case of relative or absolute type
M_Model(i,1) = 0; // used simulation model, 0 = reference model from base vehicle
M_Cost(i,1) = 20; // additional cost of measure [Euro]
M_Value(i,6,1) = -0.01; // delta Cd

// sub-variante 2: 'aero underbody complete'
M_Result(i,2) = 0;
M_Model(i,2) = 0;
M_Cost(i,2) = 70;
M_Value(i,6,2) = -0.03;

M_VarNum(i) = 2; // number of all sub-variants for measure i

```

Finally, all simulation results of the three cascaded loops (vehicles, cycles, measures) are saved in a list. Three major results are important: the matrix for the baseline results $\mathbf{S}_{bl}(i_v, i_c)$, the influences of the measure-variants $\mathbf{M}_{\Delta}(i_v, i_c, i_m, i_{svar})$ and the cost matrix $\mathbf{M}_c(i_m, i_{svar})$. In addition, based on the boundary constraints, an additional matrix is created, which describes which measure is used for which vehicle: $\mathbf{M}_{used}(i_v, i_c, i_m)$. These four result-matrices are used as input for the optimization. The definition of these matrices will be explained in Chapter 5.3 in more detail.

4.6.4. Energy flow analysis

An additional step of the cycle execution loop shown in Figure 4.20 is the analysis of the energy flow of a driving cycle. Such a result was already shown in Figure 3.9 in Chapter 3.3.2. The energy flow analysis will be used later in Chapter 5.5.3 for the optimization. For the calculation, three vehicle states have to be considered with the definition given in Lookup table 4.1.

Table 4.1.: Lookup table for vehicle states

State	Transmission force closure	Engine load
<i>Driving</i>	yes	> 0
<i>Coasting</i>	yes	= 0
<i>Idle operation</i>	no	/

Of these three conditions, only the conditions *driving* and *idle operation* are used for the energy

flow analysis. The condition *coasting* is only used for the calculation of the coast consumption because the engine is not used actively to operate the vehicle or auxiliaries in this driving condition.

For the detailed calculation of the energy flow, additional measurement points and signals are needed. Hereby, the power signals are measured and integrated into an energy value based on the vehicle state. In general, the signals are only integrated when the vehicle is in the *driving* or in the *idle operation* state. In the *coasting* state, only the actual fuel consumption is integrated into the total coast consumption. An overview of these signals and the location where they are measured in the simulation model are shown in Figure 4.22 for the engine, power-train and the auxiliary models, and in Figure 4.23 for the vehicle sub-model.

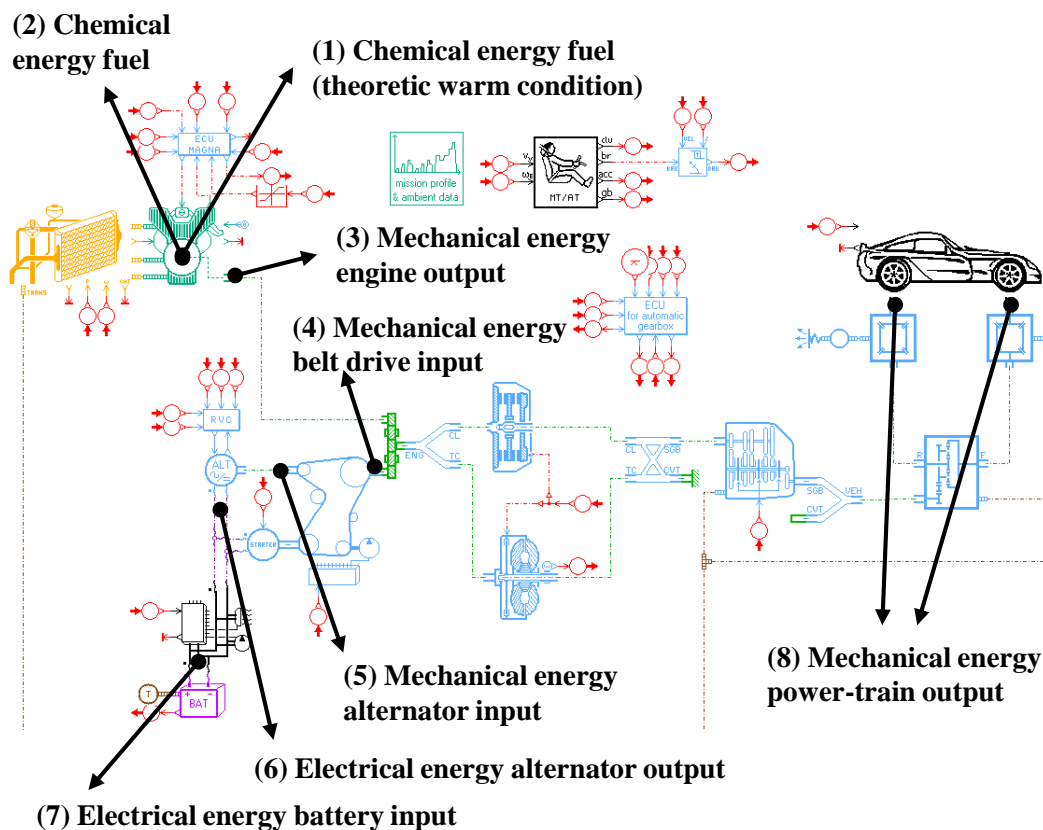


Figure 4.22.: Measurement points for energy flow analysis (engine, auxiliaries, power-train)

The result of a sample vehicle with conventional power-train in the NEDC and the calculation of the energy based on the measurement points is shown in Table 4.2. The table also provides the calculation based on the measurement points for each sink.

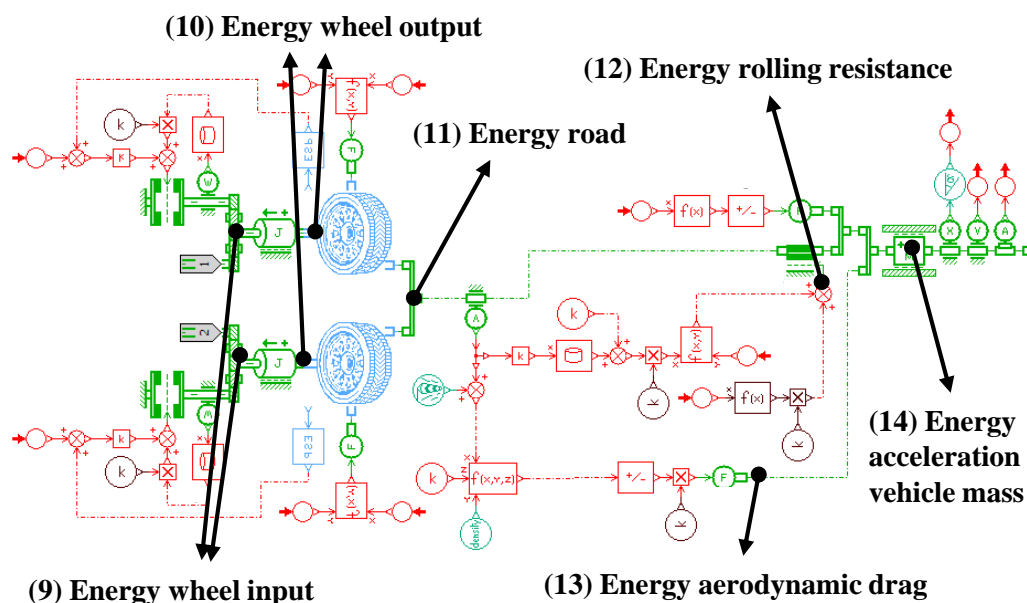


Figure 4.23.: Measurement points for energy flow analysis (vehicle)

Table 4.2.: Energy sinks of a sample vehicle in an NEDC simulation

Energy sink	Energy loss [kWh]	Calculation and measurement point
<i>Total</i>		
Fuel	7.05	(2)
<i>Engine</i>		
Cold-start loss	0.16	(2) - (1)
Coast consumption	0.05	(1)
Engine loss (incl. idle operation)	5.02	(1) - (3)
<i>Auxiliaries</i>		
Belt drive loss	0.03	(4)
Mechanical auxiliaries	0.04	(4) - (5)
Alternator loss	0.04	(5) - (6)
Electrical auxiliaries	0.12	(6) - (7)
Battery balance	0	(7)
<i>Power-train</i>		
Transmission loss	0.19	(3) - (4) - (8)
Bearing and brake pad loss	0.14	(8) - (9)
<i>Vehicle</i>		
Wheel slip	0.01	(10) - (11)
Rolling resistance	0.32	(12)
Aerodynamic resistance	0.39	(13)
Acceleration vehicle	0.51	(14)
Acceleration inertia	0.02	(9) - (10)

5. Optimization

5.1. Introduction and problem statement

The task of the optimization algorithm is to find an optimal solution to achieve all pre-defined targets based on simulation results. Thereby, a solution describes a set of selected measures. The following chapters describe the derivation of an algorithm for this purpose. Primarily, the algorithm has to solve the following three tasks:

- Find a solution where all targets are achieved
- Optimize the solution with a focus on minimizing costs
- Consideration of boundary constraints, such as driving performance targets or interactions between measures

In a first simplified step, the statement of the task can be described as follows: a set of vehicles n_v and a set of targets (cycles) n_c are defined. Since the number of targets is the same for each vehicle, overall n_v times n_c targets have to be considered. In addition, a set of measures n_m exists for each vehicle - cycle configuration. The measures are technologies which can be implemented into the vehicles that will improve or worsen a cycle result. The state of each measure can be varied between two states: “selected” and “not-selected”. Each measure can be combined with any other measure. So overall, $n_{\text{comb}} = 2^{n_m}$ combinations and solutions exist in principle to define the solution space. As described in Chapter 3.3, several tens of measures exist to reduce CO₂ emissions, when taking the complete vehicle into account. In the case of 20 measures, already over one million combinations already exist. The issue is to find one combination out of the whole solution space which meets all targets with minimum costs. This can be achieved with two mathematical methods:

1. Calculate all possible combinations with an iterative loop in terms of a complete enumeration algorithm: This approach can find the global optimum, but requires significant computation time, which increases prohibitively with the number of measures, cycles and vehicles.
2. Using a partial enumeration or a heuristic algorithm: Depending on the complexity of the optimization problem, this approach cannot guarantee that global optimum will be found. As a disadvantage, optimization algorithms carry the risk of ending in local optima. However, the benefit consists in much lower required computation time because only a few combinations are analyzed, depending on the algorithm.

In the chapters below, the derivation of the optimization algorithm is structured as follows. First, general mathematical terms related to optimization will be explained. The next chapter describes the simplified statements mentioned above in more detail. After the discussion of the abstraction of the problem, general optimization methods, including a state-of-the-art analysis, will be described. Finally, the last two chapters include the description of the interface between the simulation environment and the optimization algorithm and finally the derivation of the algorithm itself.

5.2. General terms

For an optimization problem, a parameter set \mathbf{p} of variable parameters p_i exists which influences the result of a function f . The parameter vector is defined as:

$$\mathbf{p} = (p_1, \dots, p_i, \dots, p_{n_p}) \quad p_i \in \mathbb{R} . \quad (5.1)$$

Due to the combination of the different states of each parameter, many possible parameter sets exist. The intention is to find a parameter set \mathbf{p}^* which leads to a minimum of the function f . Thereby, the parameter set \mathbf{p}^* is defined as the optimal solution, and the function reads

$$f(\mathbf{p}^*) = \min(f(\mathbf{p})) \quad \mathbf{p} \in \mathbf{P} , \quad (5.2)$$

where \mathbf{P} is the set of all possible values of the parameter.

In addition, a parameter set \mathbf{p} is limited with parameter constraints. A variation of a parameter p_i is limited by its value range $p_i^{\min} \dots p_i^{\max}$, as in (5.3). The value range limits the valid area for one parameter.

$$p_i^{\min} \leq p_i \leq p_i^{\max} \quad (5.3)$$

A parameter set \mathbf{p} always consists of several parameters p_i , which are generally interdependent. Such boundary constraints are defined as inequality constraints $g(\mathbf{p})$, according to Equation (5.4), and equality constraints $h(\mathbf{p})$, according to Equation (5.5). Let n_g be the number of inequality constraints and n_h the number of equality constraints.

$$g_j(\mathbf{p}) \leq 0 \quad j = 1 \dots n_g \quad (5.4)$$

$$h_k(\mathbf{p}) = 0 \quad k = 1 \dots n_h \quad (5.5)$$

The final optimization task reads

$$f^*(\mathbf{p}^*) = \min \{f(\mathbf{p}) \mid \mathbf{p} \in P\} \quad P = \{\mathbf{p} \in \mathbb{R} \mid \mathbf{g}(\mathbf{p}) \leq 0, \mathbf{h}(\mathbf{p}) = 0\} , \quad (5.6)$$

where P is the valid design space depending on the value range and the constraints, including the ranges given in Equation (5.3). [103] [104]

5.3. Abstraction of the fleet optimization problem

5.3.1. Introduction

Chapter 5.1 described the simplified optimization task. The goal is to find a combination of measures which results in the minimum total costs while achieving all targets. Related to this

task, the principle optimization terms were shown in Chapter 5.2. Based on this, the detailed optimization task is defined using the definitions described within this chapter.

5.3.2. Parameter vector

The variable parameters of this optimization problem are the possible measures. Measures are technologies to improve CO₂ emissions or driving performance, which can be implemented into the vehicles. When using n_m measures, the parameter vector \mathbf{m}^1 reads

$$\mathbf{m} = (m_1, \dots, m_i, \dots, m_{n_m}) \quad m_i \in \mathbb{N}_0 . \quad (5.7)$$

The various items m_i of the parameter vector are described by natural numbers, which represent the state of the measures. For a better illustration, Equation 5.8 shows an example of this:

$$\mathbf{m}^* = \begin{pmatrix} s_{\text{ess}} \\ s_{\text{ags}} \\ s_{\text{wr}} \\ s_{\text{trr}} \\ \dots \end{pmatrix} = \begin{pmatrix} 0 \\ 1 \\ 3 \\ 2 \\ \dots \end{pmatrix} \quad (5.8)$$

The item states of the measures can be defined with “0” or a number equal to or higher than “1”. The value “0” means that the measure is not implemented. A number equal to or greater than “1” means that this measure is implemented. In the case of the sample parameter vector \mathbf{m}^* , an active grill shutter (ags) is implemented (=1), and an engine start-stop system (ess) is not implemented (= 0). Thus, for these two measures, there is a “yes” or “no” decision. In addition, other measures can have several sub-variants for the implementation. In the case of weight reduction (wr), various reduction steps are possible, such as 20 kg reduction, 40 kg reduction or 60 kg reduction. Here, the weight reduction step 3 is selected. In addition, the tire rolling resistance (trr) can be defined with different sub-variants describing the selected tire. The sub-variants have an “or” relation among themselves. That means either sub-variant 1, sub-variant 2, or sub-variant i_{svar} can be implemented. These measures, with their various sub-variant implementation steps, are defined in an additional matrix. The measure-sub-variant-matrix \mathbf{M}_{svar} describes the sub-variants of each measure, where the rows correspond to the measures and the columns to their sub-variant, respectively. For a better understanding, Equation 5.9 shows the simplified design of this matrix of the different steps. For the coupling to the simulation, a more detailed list of parameters and data is required. A detailed description of the format was shown in Chapter 4.6 in Listing 4.4 using the variables “*M_Value*” and “*M_VarList*”.

$$\mathbf{M}_{\text{svar}}(i_m, i_{\text{svar}}) = \begin{pmatrix} 0 = \text{no} & 1 = \text{yes} & - & - \\ 0 = \text{no} & 1 = \text{yes} & - & - \\ 0 = \text{no} & 1 = 20 \text{ kg} & 2 = 40 \text{ kg} & 3 = x \text{ kg} \\ 0 = \text{no} & 1 = f_r - 0.1\% & 2 = f_r - 0.2\% & - \\ \dots & \dots & \dots & \dots \end{pmatrix} \quad (5.9)$$

¹In Chapter 5.2, the parameter vector was defined with a “p”. For better conformity to the indices, the letter is changed to “m”, which is associated with masures.

The number of sub-variants $n_{\text{svar}_{i_m}}$ for each measure i_m is different. An additional vector \mathbf{n}_{svar} is defined to specify the maximum numbers of steps for each measure, which reads

$$\mathbf{n}_{\text{svar}} = (n_{\text{svar}_1}, \dots, n_{\text{svar}_{i_m}}, \dots, n_{\text{svar}_{n_m}}) \quad n_{\text{svar}_{i_m}} \in \mathbb{N}_0 . \quad (5.10)$$

The definition of this vector is described by “*M_VarNum*” in Chapter 4.6 in Listing 4.4. The value $n_{\text{svar}_{i_m}}$ describes the maximum number of the sub-variants for a measure i_m .

In this case, for the sample vector \mathbf{m}^* (see Equation (5.8) and Equation (5.9)), the vector for the maximum numbers of sub-variants results as follows:

$$\mathbf{n}_{\text{svar}}^* = \begin{pmatrix} 2 \\ 2 \\ 4 \\ 3 \\ \dots \end{pmatrix} . \quad (5.11)$$

In contrast to the simplified assumption described in Chapter 5.1, the maximum number of possible combinations n_{comb} increases due to the higher number of sub-variants.

$$n_{\text{comb}} = \prod_{i_m=1}^{n_m} n_{\text{svar}_{i_m}} \quad (5.12)$$

5.3.3. Objective function (costs)

According to Equation (5.13), the objective function to be minimized is defined as the cost function $c(\mathbf{m})$.

$$c(\mathbf{m}) \longrightarrow \min \quad (5.13)$$

The total cost value c results from the selected measures of a parameter vector \mathbf{m} and combines the costs of the selected measures. To describe the costs of each measure and each sub-variant, an additional cost matrix \mathbf{M}_c has to be defined, see Equation (5.14). This matrix is comparable to “*M_cost*” in Listing 4.4 in Chapter 4.6. The variable $c_{i_m, i_{\text{svar}}}$ is the cost value for each measure i_m and sub-variant i_{svar} . The costs in the first column for $i_{\text{svar}} = 1$ is always 0 because these values represent the states if the measures are not selected.

$$\mathbf{M}_c(i_m, i_{\text{svar}}) = \begin{pmatrix} 0 & c_{1,2} & \dots & c_{1, \mathbf{n}_{\text{svar}}(1)} \\ 0 & c_{2,2} & \dots & c_{2, \mathbf{n}_{\text{svar}}(2)} \\ 0 & \dots & \dots & \dots \\ 0 & c_{n_m,2} & \dots & c_{n_m, \mathbf{n}_{\text{svar}}(n_m)} \end{pmatrix} \quad c_{i_m, i_{\text{svar}}} \in \mathbb{R} \quad (5.14)$$

The definition of the costs is flexible. Different costs can arise in the vehicle development and production. There are manufacturing costs, part costs and investment costs for research and

development and tooling [22] [24] [53]. In general, there is a fixed and a variable part of the component costs. Variable costs can be material, labor and administration costs. The fixed part consists of tooling, facilities, marketing and engineering [24] [53]. For the development of an optimization approach, only a fixed cost value is assumed in his thesis. The definition of costs are finally based on the user definition, but should be the same basis for each measure.

The cost value c of the parameter vector \mathbf{m} is defined as the sum of the costs of each selected measure sub-variant. The cost reads

$$c(\mathbf{m}) = \sum_{i_m=1}^{n_m} M_c \{i_m, \mathbf{m}(i_m)\} \quad c \in \mathbb{R}, \quad (5.15)$$

where $\mathbf{m}(i_m)$ defines the selected sub-variant of i_m .

In the third level of the optimization, the whole fleet with an average fleet target for CO₂ emissions will be analyzed. Not every measure will be available for every vehicle. The sales volume of the measures among themselves will differ. For this reason, the sales volume $svol_m$ of the measure i_m must be considered in the costs as well, if the total costs should be calculated for the whole fleet. Therefore, the cost reads

$$c(\mathbf{m}) = \sum_{i_m=1}^{n_m} M_c(i_m, \mathbf{m}(i_m)) \cdot svol_m(i_m) \quad c \in \mathbb{R}. \quad (5.16)$$

5.3.4. Inequality constraint (vehicle targets)

Besides the optimal costs, the issue of the optimization is to ensure vehicle targets for CO₂ emissions as well as driving performance targets. Achieving these targets is defined as a constraint. This requires an undershoot and not the exact achievement of the targets, which means the final result of a cycle can be lower than or equal to the given target t . The target vector \mathbf{t}_v for one vehicle reads

$$\mathbf{t}_v = (t_1, \dots, t_i, \dots, t_{n_c}) \quad t_i \in \mathbb{R}. \quad (5.17)$$

This target vector is comparable with the variable “*VehConfTarget*” in Chapter 4.6 in Listing 4.1. For example, the vector can be filled with the following targets and reads

$$\mathbf{t}_v^* = \begin{pmatrix} t_{\text{NEDC}} \\ t_{\text{EPA2}} \\ t_{\text{t.0_100}} \\ t_{\text{t.80_120}} \\ t_{\text{vmax}} \end{pmatrix}. \quad (5.18)$$

In a fleet, a set of vehicles are considered, and the targets are defined for each vehicle individually. The vehicle-target vector is extended to a vehicle-target matrix \mathbf{T}_{vc} , which is described by the rows corresponding to the various vehicles i_v and the columns to the cycles i_c and reads

$$\mathbf{T}_{vc}(i_v, i_c) = \begin{pmatrix} t_{v_1, c_1} & \cdots & t_{v_1, c_{nc}} \\ t_{v_2, c_1} & \cdots & t_{v_2, c_{nc}} \\ \cdots & \cdots & \cdots \\ t_{v_{nv}, c_1} & \cdots & t_{v_{nv}, c_{nc}} \end{pmatrix} \quad (5.19)$$

The aim of the optimization is to reach all defined targets. Depending on the parameter vector \mathbf{m} and its selection of measures, a status value s_m is calculated for each cycle. The status value is calculated from the baseline status $\mathbf{S}_{bl}(i_v, i_c)$ (initial status without implemented measures) and the evaluated influences of the selected measures $\mathbf{M}_{\Delta}(i_v, i_c, i_m, i_{svar})$. This calculation leads to a status forecast \mathbf{S}_m depending on a given parameter vector \mathbf{m} and reads

$$\mathbf{S}_m(i_v, i_c) = \mathbf{S}_{bl}(i_v, i_c) - \sum_{i_m=1}^{n_m} \mathbf{M}_{\Delta}(i_v, i_c, i_m, \mathbf{m}(i_m)) , \quad (5.20)$$

where $\mathbf{m}(i_m)$ describes the selected sub-variant of a measure i_m . The goal of the constraint is to compare the status of the cycles \mathbf{S}_m depending on the parameter vector \mathbf{m} and the target matrix \mathbf{T}_{vc} . The result \mathbf{T}_{Δ} defines the deviation between status and target, see Equation (5.21). The result should be less than or equal to 0, which means that a target is achieved or undershot.

$$\mathbf{T}_{\Delta} = (\mathbf{S}_m - \mathbf{T}_{vc}) \leq 0 \quad (5.21)$$

For a better explanation, later in the case study (Chapter 6) five driving cycles and targets will be considered for each vehicle. The status of the driving cycles for CO₂ emissions and driving performance should be minimized. A lower value is better than a higher value. The only exception is the target for the maximum speed, which should be maximized. A higher final speed is better than a lower speed. This maximization of the target for the maximum speed remains in conflict with the constraint definition of Equation (5.21). This means the optimization direction of the maximum speed is inverse. An additional vector \mathbf{t}_{dir} is defined to describe the optimization direction, which reads

$$\mathbf{t}_{dir} = (dir_{c_1}, \dots, dir_{c_i}, \dots, dir_{c_{nc}}) \quad dir_{c_i} \in (-1, 1) . \quad (5.22)$$

Applied to the five defined cycles (see Equation 5.18), the directions of the cycles are defined in \mathbf{t}_{dir}^* in this thesis, which reads

$$\mathbf{t}_{dir}^* = (1, 1, 1, 1, -1) . \quad (5.23)$$

The final constraint function, see Equation (5.21), is now updated with this direction vector and reads

$$\mathbf{T}_{\Delta} = (\mathbf{S}_m - \mathbf{T}_{vc}) \cdot \mathbf{t}_{dir} \leq 0 . \quad (5.24)$$

5.4. Discussion of optimization methods

5.4.1. General optimization algorithms

As described with the parameter vector \mathbf{m} , the issue is to find the optimal combination of measures, whereby, according to Equation (5.7), the state of a measure is $i_m \in \mathbb{N}_0$. Thus, a discrete optimization problem arises. In addition, the objective function and the constraints cannot be described with linear systems of equations. Therefore, a non-linear optimization algorithm has to be used. For the solution of non-linear problems, several mathematical approaches exist. The main categories are shown in Figure 5.1, and the principle characteristics will be explained in the following sections.

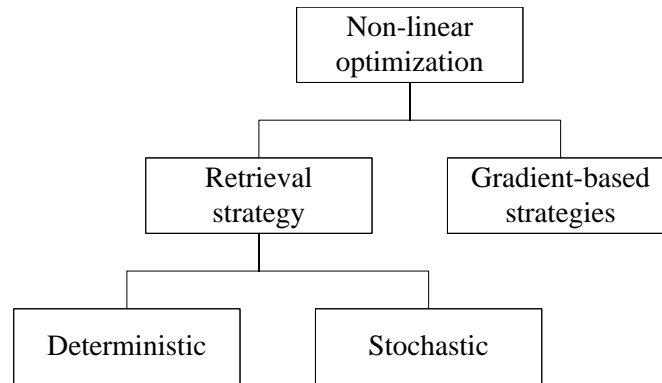


Figure 5.1.: Overview of non-linear optimization algorithms, based on [103]

A typical example of the gradient-based strategies is the *Gauss-Newton method* (GN). Using iterative steps, the search direction is evaluated with approximations. [23] [103] In principle, gradient-based strategies are used for continuous problems. Since the optimization problem in this thesis is a discrete problem, such algorithms are not applicable.

The *Jacob-seeking method* (JAC), the *Simplex method* (SPX) and the *Monte-Carlo method* (MC) are examples of deterministic retrieval strategies. Such deterministic methods use multiple sampling points as a basis for interpolation. The aim is to evaluate the search direction based on the solutions of the sampling points. For example, the JAC interpolates a linear objective function. The minimum of this objective function is the initial solution for the next iteration step. Compared to the gradient-based strategies, these methods can compensate for discontinuities in the solution space, but a general convergence of the solution space is assumed. [103]

Figure 5.2 shows a principle solution. The status for fuel consumption s_m and the costs c are calculated based on a parameter vector \mathbf{m} . The upper diagram shows the status of fuel consumption (blue points) compared to a given target (red solid line) as a boundary constraint. Only solutions where the fuel consumption is below the target are in the valid solution space. The lower diagram shows the costs of a parameter vector. The green points are solutions in the valid solution space, and the red dashes are solutions out of the valid solution range, where the fuel consumption target is not met. The parameter vectors are sorted by their binary coding in ascending order. The illustration shows that not every solution fulfills the constraint of the fuel consumption target, and the costs also show no continuously increasing or decreasing trend. The correlations between the solutions and the costs lead to many local minima and maxima. Therefore, the objective function has no continuous behavior and convergence. Although the cost for each parameter vector can be calculated, the problem is that not every vector leads

to a solution. The definition of the valid solution space is not possible using a gradient-based or deterministic method [103]. Due to the high number of local minima, a global-oriented optimization and robust approach is required [23].

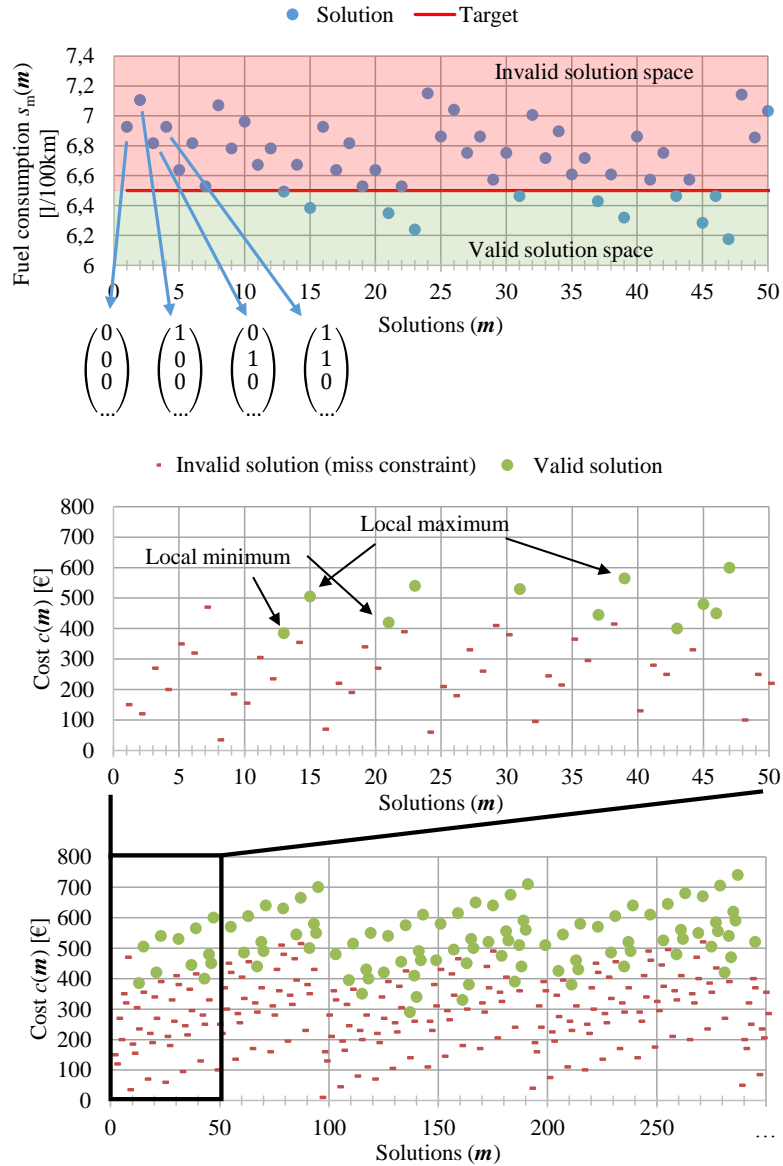


Figure 5.2.: Example of fuel consumption and costs depending on parameter vectors

In principle, this figure shows in the upper diagram the actual fuel consumption status depending on parameter vectors and a given fuel consumption target. In addition, a discontinuity of the function can be seen because not every solution is in the valid solution space (meets the fuel consumption target). The two lower diagrams show the resulting costs of the parameter vector. The green points are valid solutions, and the red dashes are invalid solutions where the fuel consumption target is not met. This illustration highlights the challenge for the optimization method.

As previously described, the deterministic optimization uses sampling points as a basis for determining the initial solution for the next iteration step. The algorithm is always searching for a better solution. It is a so-called iterative improvement algorithm. The investigated solution space is reduced step by step. Since the whole solution space is not considered, the optimization

algorithm can end in a local minimum. In comparison, stochastic algorithms use additional random functions. This helps the algorithm to leave the current investigated solution space. With this approach, the whole solution space is always available in the background, which helps to leave local minima. Typical examples of stochastic strategies are the *Particle Swarm Optimization* (PSO), *Genetic Algorithm* (GA), *Simulated Annealing* (SA) and *Tabu Search* (TS). In principle, a set of initial solutions is defined as a starting point. Depending on the selected algorithm and a random influence, the variables of the parameter vector are changed until a minimum is reached [103] [104] [105]. Such stochastic methods, which seem to be the most suitable for the described optimization problem, will be explained in more detail in Chapter 5.6. Because a search within the whole parameter space is required to find the global optimum, such methods have the disadvantage of the convergence speed [23].

This decision regarding the pre-selection of an applicable optimization algorithm for the optimization problem in this thesis can also be proven by comparing of the characteristics of the various optimization methods. An overview of such a comparison is presented in [103]. Table 5.1 shows an excerpt of [103] and summarizes the advantages and disadvantages of different optimization algorithms and methods. The following characteristics are compared:

- Smoothness, which describes the properties of the objective function (e.g. discontinuity)
- Number of parameters n_p
- Convergence, influencing the computation time.

The characteristics are rated according to their suitability for the algorithms. The suitability concerning smoothness and convergence are rated with “-”, “o” and “+”. For example, the GN is unsuitable for discontinuous functions (“-”), but it is recommended if a fast convergence (“+”) is required. On the other hand, a GA or SA are suitable for a high number of parameters, where “high” is defined as more than 31 parameters, according to [103].

In this example, a gradient-based strategy, the *Gauss-Newton method*, is also included for comparison. Based on a utility analysis, it can be seen that the stochastic methods (*Genetic Algorithm* and *Simulated Annealing*) are most suitable for the required characteristics. This means they can handle non-smooth objective functions, as shown in Figure 5.2, and the large number of parameters required to consider various measures, cycles and vehicles. Of course, these advantages remain in contrast to the inferior convergence and computation time of the algorithm. The detailed results of the utility analysis are explained in Appendix E.1.

Table 5.1.: Required characteristics compared to an excerpt of advantages and disadvantages of optimization algorithms, based on [103]

	Smoothness (Discontinuity)	Number n_p	Convergence
Required	+	high	o
SPX	o	middle	o
JAC	-	low	o
GA	+	high	-
SA	+	high	-
GN	-	low	+

5.4.2. Multi-criteria optimization

One frequent challenge of optimization problems is the parallel handling of several defined targets and the resulting conflicts between them, when more than one optimization target exist. This was already mentioned in Chapter 5.3 in Equation (5.18). Here, each target value is described by a function, which has to be minimized. The present thesis takes the CO₂ emissions and driving performance (e.g. acceleration time and maximum speed) into account. The optimization has to handle several optimization criteria.

In [103], a multi-criteria optimization is described for handling this problem. The approach of this method is based on an auxiliary function f_a . This function is a linear combination of all given objective functions f_i , as shown in Equation (5.25). In addition, the specific functions can be weighted by a factor w_i to shift the priority between target values. According to Equation (5.26), the sum of all weighting factors should be 1.

$$f_a = w_1 \cdot f_1 + w_2 \cdot f_2 + \dots + w_i \cdot f_i + \dots + w_n \cdot f_n \quad w_i \in \mathbb{R} \quad (5.25)$$

$$\sum_{i=1}^n w_i = 1 \quad (5.26)$$

5.4.3. Multi-level optimization

Technical systems often consist of several components, which must often be evaluated in terms of different criteria. General targets for the whole system, as well as targets for the individual components, have to be considered. One solution is to split the handling of the whole system and the components into different levels and then consider them step by step. In [104], this problem is explained using the example of an airplane. In the first level, the whole airplane is considered with general targets, such as safety or environmental sustainability. The second level considers a certain module and module targets, such as the eigenfrequency of a wing. The third level considers individual components, such as the stiffness of a wing ridge. With this approach, the targets for the whole airplane are broken down step by step into partial levels, which define new component-specific targets in each step.

Within this thesis, three levels exist, as shown in Figure 5.3. The first level is the fleet level, which takes into account the fleet-average CO₂ emissions targets. In addition, balancing sales volumes and global measures is important. The second level handles the vehicles individually. The consideration of the target conflict between various targets is the focus in this step. The last level concentrates on the optimization of one specific cycle for one individual vehicle.

The multi-level optimization is able to consider the optimization problem from the minimum cost of the whole fleet and the achievement of the market-specific fleet targets down to cycle-specific targets.

5.4.4. Automotive applications of optimization algorithms

Based on literature research, no other publication was found that addressed a comparable optimization problem. The analysis of solutions for the application of optimization problems in

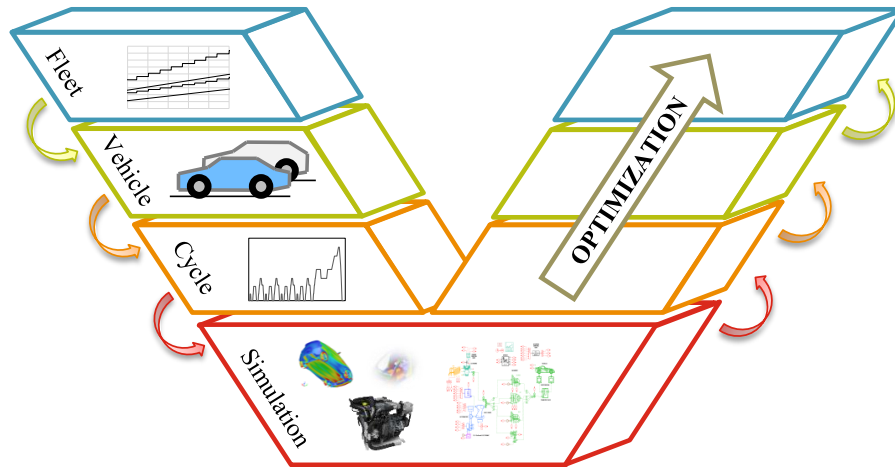


Figure 5.3.: Levels of the fleet optimization problem

This figure shows the multi-level approach for the optimization problem. First, the total vehicle fleet has to be broken down into individual vehicles and driving cycles. In the lowest level, the simulation and evaluation of the measures take place. The optimization has a reverse structure, whereby it considers the optimization of the driving cycles, the vehicle and finally the whole fleet.

other automotive examples should provide a basis for the optimization problem described in this thesis.

For example, [106] describes the optimization of a hybrid-electric vehicle operating strategy. Control variables are the parameters of the operating strategy (threshold values for battery SOC, torque and speed). The goal of the optimization is to reduce fuel consumption in a driving cycle. In addition, the exhaust gas emissions are considered as constraints. Here, fuel consumption and exhaust emissions can remain in conflict, depending on the operating points of the combustion engine. In addition, fixed target values for driving performance are considered. The author uses a genetic algorithm to solve the problem. A genetic algorithm alone is not capable of handling constraints and target conflicts. Two approaches are mentioned to consider constraints:

- Using a weighting and penalty function (multi-criteria optimization)
- Optimizing one target only and checking the validity of the other targets afterwards

The author uses both methods in his optimization approach. The penalty function is used to handle the fuel consumption and exhaust emissions. The achievement of the targets for driving performance is checked after an optimization iteration. In this paper, the optimization for fuel consumption and exhaust emissions is limited to one driving cycle and one vehicle.

In addition, [107] also describes the optimization of a hybrid-electric operating strategy. It is mentioned that the weakness of gradient-based algorithms is in finding a global optimum. Methods that are not based on gradients, such as PSO or GA, are recommended. In this paper, the goal is also to optimize the conflict between fuel consumption and exhaust emissions. The author mentions that a complete vehicle includes many design variables that influence fuel consumption and driving performance. For this reason, the number of parameters is limited to the electric motor size, final drive gear ratio, battery size and SOC boundaries.

In the third example, T. Krenek describes the optimization of fuel consumption of a hybrid vehicle in his master's thesis [105]. The control variables are the transmission shifting strategy, hybrid operation modes and SOC boundaries. He shows that every optimization algorithm

has advantages and disadvantages. A genetic algorithm achieves the best results on average, but can determine a local minimum. PSO and simplex methods can find better solutions, but the solution is strongly dependent on the initial solution. His approach is to use a hybrid optimization approach that combines several methods. The initial solution is generated using a *Monte-Carlo* algorithm. Then, the PSO considers the whole parameter space in the subsequent iteration steps. After a defined iteration step number, a *Genetic Algorithm* is used instead of the PSO. He also discusses the usage of a *tabu list*. A *tabu list* accesses previous calculations and is used to prevent the generation of previously considered solutions.

The optimization of an active vehicle chassis damper is described in [108]. Five chassis system design parameters are considered. The goal is to optimize three characteristics: ride comfort, road-holding ability and suspension working space. The ride comfort is evaluated via an objective function. The other two targets are described as boundary constraints. Here as well, a *Genetic Algorithm* is used to solve the problem. In addition, previously calculated solutions are stored in a lookup table. Thus, if a solution occurs a second time, a second calculation loop is prevented, in order to increase the computation efficiency of the method.

5.4.5. Specific aspects of the investigated optimization methods

As described in the previous sub-chapters, many optimization methods exist. However, the optimization algorithm itself is not the only deciding factor. In addition, the handling of targets, definition of the starting point and the combination of various methods will have an influence on the success of the optimization. For the final optimization approach, the following methodological aspects seem to be interesting:

- Using a stochastic optimization method as a base algorithm
- Combining various optimization methods to exploit advantages and reduce disadvantages of the individual methods
- Multi-criteria approach to handle the target conflict between fuel consumption and driving performance
- Multi-level structure to cover fleet targets and constraints, vehicle constraints and optimal cycle solutions
- Implementation of a *tabu list* to prevent the double evaluation of solutions

5.5. Interface between simulation and optimization

5.5.1. General approach

The algorithm framework to be developed consists of two parts: the simulation environment and the optimization method, which must be linked (see Figure 1.3). The simulation results provide the input for the optimization including the variation of variables. In addition, the simulation model has to validate and confirm a solution for the optimization. Figure 5.4 shows a general approach to solve such a linkage.

In the first step, the method uses an analysis model (2) for the calculation of the initial solution (1). In this thesis, the analysis model is the execution of the simulation model. The results of the calculation are evaluated (3) according to the optimization target (4). Based on the results,

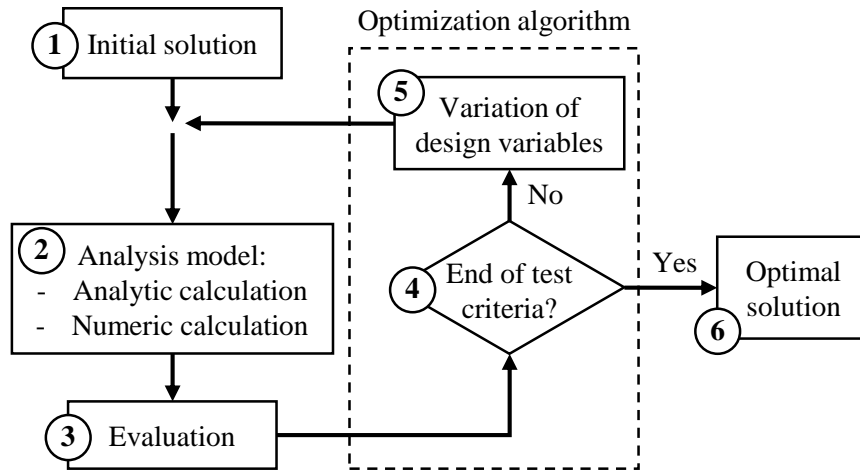


Figure 5.4.: Proposal for coupling an optimization with an analysis model for the calculation of the solution, based on [104]

the optimization algorithm varies parameters (5) to generate new solutions. With each new solution, the analysis model is repeated to calculate the updated result. The iteration loop is executed until an optimal solution (6) is found. This approach shows one method to combine the analysis model and the optimization. The advantage is that the analysis model is executed in every iteration. An exact result for a certain combination of variables is possible. However, this approach has two disadvantages. First, an execution of the simulation model (analysis model) in each iteration step and variable-combination increase the computation time. Depending on the complexity of the simulation model and the number of cycles, the simulation loop for one vehicle can take around half an hour. The total computation time also increases with the number of considered cycles n_c and number of vehicles n_v . Second, the variation of the parameters is based on an optimization algorithm. Some kind of information about the rating and influence of measures is needed to prioritize them in the optimization algorithm. A pre-processing of the variables is already needed here to get basic information about how to decide the importance of certain variables. As will be explained in Chapter 5.6.3.4, this decision is based on the cost ratio cr of each measure. For this information, the influence of each measure in each cycle and vehicle is already required before the optimization starts. Therefore, a simulation loop that includes the evaluation of each measure, vehicle and cycle must be performed beforehand.

Another solution for the optimization is mentioned in [104]. Here, the usage of a so-called “meta-model” during the iteration of the optimization step is recommended. The simplified meta-model replaces the execution of the initial complex model to reduce computation time. In the best case, the meta-model is a linear model and leads to low computation time.

To include this approach in the present optimization process, Figure 5.5 shows the adapted version using a meta-model. Based on the simulation results from a simulation matrix (7), the meta-model is derived (8). Using a cumulative approach, the meta-model is linear in the simplest case. Replacing the simulation model with the meta-model (2) leads to more time-efficient solution computations. In addition, the results are used as input for the prioritization of the design variables in the optimization algorithm (5).

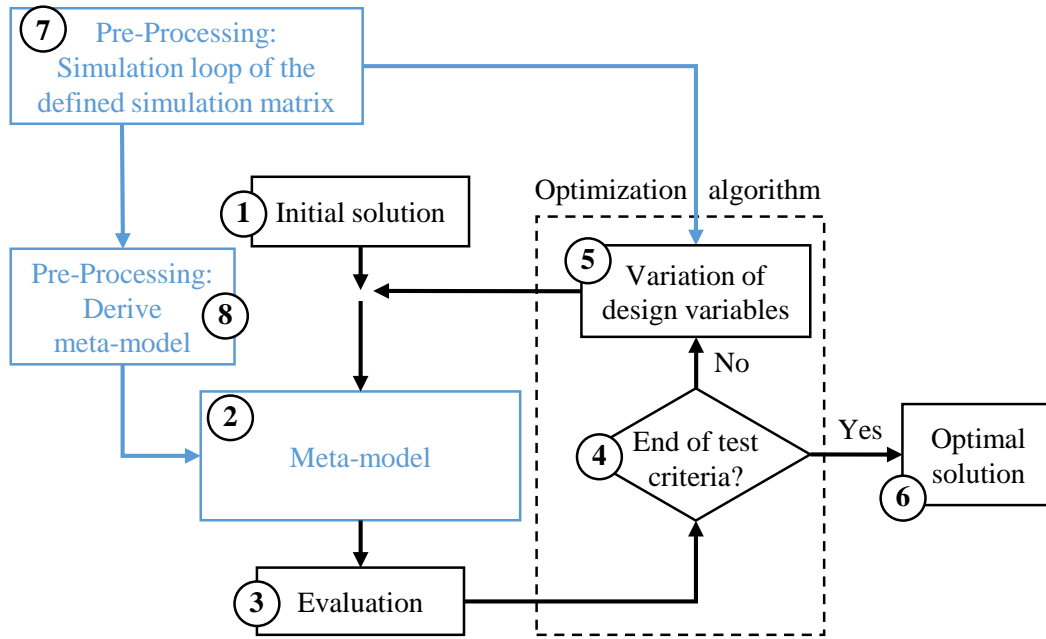


Figure 5.5.: Adapted proposal for coupling the optimization and simulation with a meta-model by adding process points (7) and (8) and using a meta-model (2) instead a complex analysis model

5.5.2. Meta-model

To avoid repeating time-intensive simulation loops within the optimization iteration, a meta-model should be used. The meta-model calculates the status values depending on the parameter vector, representing the selected measures. The basis of such an approach was already mentioned in Equation (5.20) in Chapter 5.3 and is illustrated in Figure 5.6, which shows a typical “walk down chart”. Starting from the baseline simulation result s_{bl} , the influences of certain measures m_{Δ_i} are added until a final status value s_m . For simplification, a linear correlation will be assumed. The individual calculated influences of the single measure are added. Interactions between measures which can lead to other results are initially neglected. Two results are required from the simulation loop: the baseline value s_{bl} for every considered vehicle-cycle configuration and the influence m_{Δ_i} of each measure i in the cycles and vehicles.

5.5.3. Analysis of interactions

One important factor for the validity of the meta-model is the correlation between its calculated results and the simulation result of the complex and more realistic model. The combination of measures can lead to interactions such that the real benefit is not equal to the theoretical benefit as computed by the meta-model, which is defined by the sum of the individual benefits. The influence of such interactions has to be discussed to guarantee the validity of the meta-model and to provide best input quality for the optimization. This effect of interactions is shown in Table 5.2. Four measures are listed: engine start-stop, intelligent generator control, cylinder deactivation and the reduction of the electrical power demand. In the first step, all four measures are evaluated individually, and the improvement of fuel consumption is simulated. In the next step, the four measures are combined, for example engine start-stop and generator control in the fifth line. On the one hand, the benefit of fuel consumption is evaluated by applying the

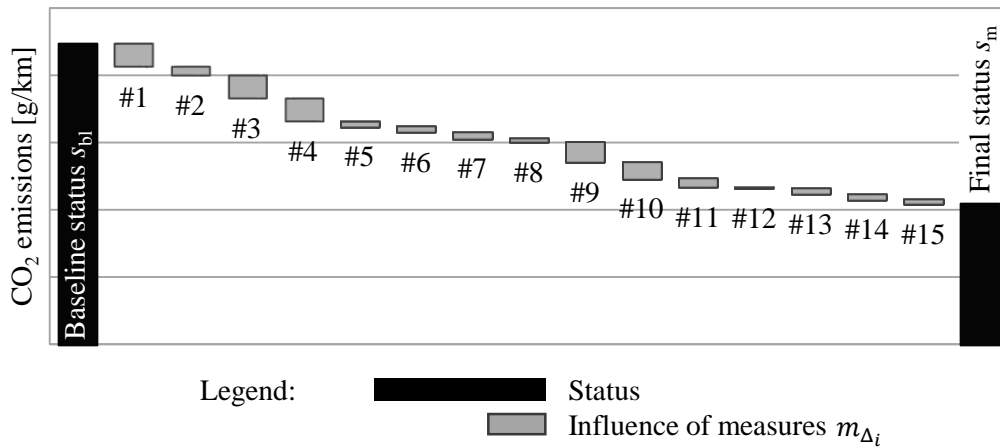


Figure 5.6.: Walk down chart as basis for the meta-model

This figure shows a so-called “walk down chart”. Starting from a baseline status s_{bl} , the influence of measures m_{Δ_i} are added. The result s_m is the final status based on the parameter vector. This approach is a linear calculation of all measures because no interactions between measures are considered.

combinations in the complex simulation model (e.g. simulation result of -0.43 l/100km for engine start-stop and generator control), and on the other hand, the benefit is calculated by using the meta-model, which considers each benefit individually without interactions caused by the combination of measures (e.g. addition of -0.21 l/100km for engine start-stop + -0.27 l/100km for generator control to -0.48 l/100km). This analysis is performed for every possible combination of the four measures considered. It turns out that for some combinations, the result of the meta-model is comparable to the simulation result of the complex model (e.g. a difference of -0.05 l/100km for engine start-stop and generator control), and for some combinations a different result occurs. To analyze which combinations result in a difference, such a comparison is needed for each possible combination, which also leads to a high simulation effort. Therefore, a method is required for deriving interactions between measures with low simulation effort. In addition, expert knowledge (engineering judgment, literature research) can be used as a basis for the definition of the interactions, in order to reduce the effort required for computational investigations. An example of possible interactions between technologies was shown in Figure 2.1 in Chapter 2.

The basis for the analysis of interactions between measures is the energy flow analysis, as explained in Chapter 4.6.4. Figure 5.5 showed the interaction between simulation and optimization. According to step (7), a simulation loop of the complete simulation matrix including all vehicles, cycles and measured is already done. Therefore, results exist before the first usage of the meta-model. One step in the simulation process also includes the evaluation of the energy flow in each simulation run (see Figure 4.18). Thus, without additional simulation effort, these energy flows can be used for a comparison. Table 5.3 shows the energy flow and distribution of the losses for various simulated measures. The second column shows the energy losses of the baseline status and is the reference for comparisons. The following columns show various measures. In the rows, the energy sinks are listed.

The analysis and comparison of the energy flow for the different measures is based on the correlation of the energy sinks. These simplified correlations are shown in Figure 5.7 with a reverse energy flow. Beginning with the cumulative driving resistance (aerodynamic resistance, rolling

Table 5.2.: Comparison of the combined influence of measures from the meta-model and the results of the complex model

Engine start-stop	Generator control	Cylinder deactivation	Reduced electrical power demand	Influence [l/100km] meta-model	Influence [l/100km] simulation	Difference [l/100km]
X				-0.21		
	X			-0.27		
		X		-0.18		
			X	-0.09		
X	X			-0.48	-0.43	-0.05
X		X		-0.39	-0.42	0.03
	X	X		-0.45	-0.37	-0.08
X	X	X		-0.66	-0.65	-0.01
X			X	-0.30	-0.31	0.01
	X		X	-0.37	-0.28	-0.09
X	X		X	-0.57	-0.51	-0.06
		X	X	-0.27	-0.28	0.01
X		X	X	-0.48	-0.52	0.04
	X	X	X	-0.54	-0.48	-0.06
X	X	X	X	-0.75	-0.73	-0.02

resistance, acceleration), the transmission losses have a multiplicative effect (“x”) because they are described by an efficiency factor. Thus, if the driving resistance is reduced, the transmission loss will also be reduced. The engine also has to supply the energy for the mechanical and electrical auxiliaries, in addition to the driving resistance (“+”). Here, the demand of electrical auxiliaries is also multiplicative overlaid (“x”) by the alternator efficiency factor, which defines the alternator loss. In addition, the losses are increased (“+”) by the coast consumption and the engine warm-up. The coast consumption describes the fuel consumption in phases when the engine has no load request and the fuel cut-off is not active. In addition, depending on the idle time in a driving cycle, the idle consumption is added (“+”) as an absolute value. Finally, the whole energy demand is overlaid by the engine efficiency factor that defines the engine losses described by a multiplicative correlation (“x”).

These interactions can also be seen in Table 5.3. In principle, the different measures have their influences on different energy sinks due to the additive and multiplicative correlation. For example, aerodynamics influences the aerodynamic resistance, but also the engine loss. In addition, the transmission losses are reduced, but due to the low portion of the total loss, the reduction of the transmission loss is negligible. Because the efficiency of the engine is significant lower than the efficiency of the transmission, the impact on the reduction of the engine losses is more important. As a second example, the reduction of weight has an influence on acceleration resistance, rolling resistance and the engine loss. The improvement of mechanical auxiliaries, for example, influences only the auxiliary loss and engine loss, but has no influence on transmission and driving resistance.

In order to analyze which measures are effected by each other, the energy sinks are compared to the baseline. If a difference occurs, they are marked in italics in Table 5.3. Measures which influence the same energy sinks are assumed to be “interactive”. For example, both weight

Table 5.3.: Energy sinks of a sample vehicle in an NEDC simulation and the influence of individual measures (Differences in energy sinks compared to the baseline are highlighted in italics.)

Energy sink / Energy loss [kWh]	Total										
	Baseline	6.88	7.00	7.02	6.85	6.77	6.86	6.96	6.89	6.91	6.98
Fuel		7.05	7.00	7.02	6.85	6.77	6.86	6.96	6.89	6.91	6.98
	<i>Engine</i>										
Cold-start loss	0.16	0.16	0.16	0.16	0.16	0.16	0.16	0.16	0.16	0.16	0.16
Coast consumption	0.05	0.05	0.05	0.05	0.05	0.05	0.05	0.05	0.05	<i>0.06</i>	0.05
Idle consumption	0.57	<i>0.53</i>	0.55	0.55	<i>0.34</i>	<i>0.28</i>	0.57	0.57	0.57	0.57	<i>0.54</i>
Engine loss	4.45	4.32	4.43	4.45	4.50	4.51	4.35	4.40	4.36	4.31	4.44
Engine efficiency [%]	28.1	28.7	27.9	28.0	28.0	28.0	27.6	27.9	27.7	28.6	27.9
	<i>Auxiliaries</i>										
Mechanical auxiliaries / Belt drive loss	0.08	0.08	<i>0.05</i>	0.08	0.08	0.08	0.08	0.08	0.08	0.08	0.08
Alternator loss	0.04	0.04	0.04	<i>0.02</i>	0.04	0.04	0.04	0.04	0.04	0.04	<i>0.03</i>
Electrical auxiliaries	0.12	0.12	0.12	0.12	0.12	<i>0.10</i>	0.12	0.12	0.12	0.12	<i>0.09</i>
Battery balance	0	0	0	0	0	<i>-0.03</i>	0	0	0	0	0
	<i>Power-train</i>										
Transmission / Drive-train loss	0.33	0.33	0.33	0.33	0.33	0.33	<i>0.32</i>	0.33	0.33	<i>0.32</i>	0.33
	<i>Vehicle</i>										
Rolling resistance / Wheel slip loss	0.33	0.33	0.33	0.33	0.33	0.33	<i>0.25</i>	0.33	<i>0.30</i>	0.33	0.33
Aerodynamic resistance	0.39	0.39	0.39	0.39	0.39	0.39	<i>0.39</i>	<i>0.35</i>	0.39	0.39	0.39
Acceleration vehicle	0.53	0.53	0.53	0.53	0.53	0.53	0.53	0.53	<i>0.49</i>	0.53	0.53

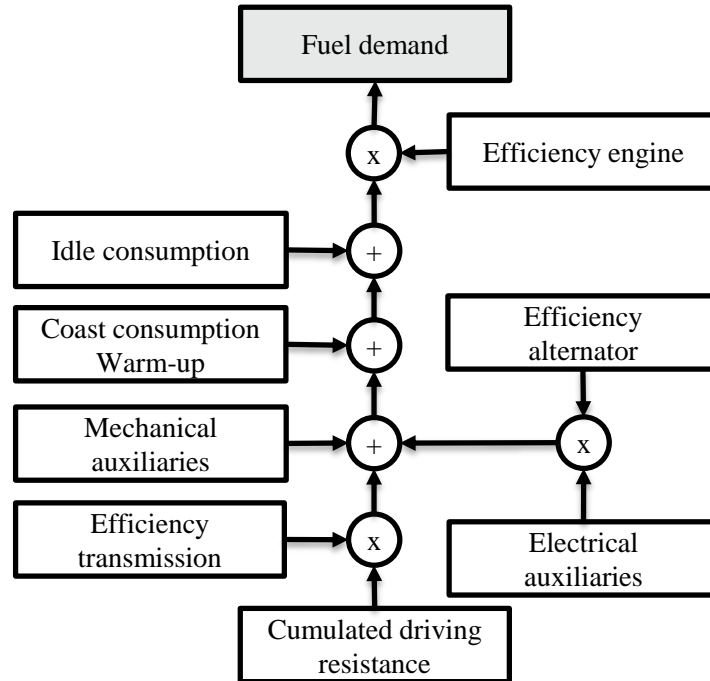


Figure 5.7.: Additive (“+”) and multiplicative (“x”) correlations of energy sinks

reduction and reduction of the rolling resistance influence the energy sink *rolling resistance*. According to Equation (3.9), the rolling resistance coefficient f_r is multiplied by the mass m_t . Due to this multiplication, an interaction can be assumed.

To reduce the effort and to omit small differences between simulation runs, the relevant sinks are additionally filtered by a threshold. Only if the absolute difference on a sink is above a defined threshold of 0.01 kWh, the sink will be considered in the next step (see differences in italics in Table 5.3).

Based on the filtered measures, a second evaluation step takes place. Each energy sink is investigated individually and will be described below with the examples of the sinks *rolling resistance* and *engine efficiency*. Both examples are shown in Table 5.4. The intention of the second step is to analyze the difference between the usage of the meta-model and the simulation of the complex model. The energy sink *engine efficiency* is influenced by the measures *cylinder deactivation*, *engine start-stop* and *gear ratio*. Four combinations are possible for the selected measures. The right side of the table shows the combination of measures for each combination. The measures *rolling resistance* and *weight reduction* influence the energy sink *rolling resistance*. Here, only one combination is possible. Two kinds of analyses are done. First, the meta-model calculates the results of the combination by adding the results of each individual measure. In the second analysis, the complex simulation model is used again. Every possible combination is parametrized in the simulation and executed. One point to be noted is that a measure can have several sub-variants, for example different steps of weight reduction. To reduce the effort, only the sub-variants with the highest influence on fuel consumption are used, for example the highest weight reduction and the lowest tire rolling resistance. Both the results of the meta-model and the simulation are compared. Table 5.4 shows this results. Based on this investigation, it can be seen that for *weight reduction* combined with *rolling resistance* the meta-model can be used because the difference can be neglected. In contrast, regarding the *engine efficiency*, a negligible interaction results if *start-stop* and *cylinder deactivation* are combined. However, when including

another *transmission gear ratio*, a difference is noticeable (up to 0.11 l/100km). In this case, a second simulation loop, is needed to analyze the interactions in detail. For selecting interactions for the second loop a threshold of 0.02 l/100km is defined. To this point, the comparison of the interactions is based only on the sub-variants with the highest influence on each measures. If an interaction occurs, the simulation loop is repeated with each combination of each sub-variant of the measures concerned. These simulation results are saved. Such an analysis is performed for every energy sink and also for each driving cycle.

Table 5.4.: Comparison of combined influence of measures (using the sub-variant with the highest influence) using the meta-model and simulation in l/100km

	Combination	Calculation meta-model	Simulation	Difference	Cylinder deactivation	Engine start-stop	Gear ratio	Rolling resistance	Weight reduction
Energy sink									
Selected sub-variant					1	5	3	4	12
Engine efficiency	1	6.58	6.60	<i>0.02</i>	x	x			
	2	6.63	6.68	<i>0.05</i>	x		x		
	3	6.32	6.32	0.00		x	x		
	4	6.14	6.24	<i>0.10</i>	x	x	x		
Rolling resistance	1	6.88	6.89	0.01				x	x

Related to this analysis, the meta-model will be adapted in the following way. If there is no interaction, then the calculation of the combined measures is still based on addition as a linear approach. If an interaction occurs, then the algorithm access the information on the simulated combinations. Based on the application of this method and the analysis of measures on examples, typical energy sinks which leads to interactions of measures are:

- Idle operation, auxiliaries and engine efficiency for CO₂ emission-related cycles
- Change of engine torque, gear ratio and weight for acceleration times
- Aerodynamic resistance for maximum speed

5.5.4. Final approach

The final approach for the simulation of the measures and interactions is shown in Figure 5.8. First, based on Chapter 4.6, the influences of each measure in each driving cycle and vehicle are evaluated. This includes the analysis of the energy flow (1) for each considered measure. In the second step (2), one representative vehicle is selected to analyze the interactions. The goal is to analyze the interaction in one vehicle in detail and transfer the results to the other vehicles. As described in the previous section, the influencing measures related to the same specific energy sinks are jointly analyzed (3). The important combinations of measures, using the sub-variant with the highest influence on the driving cycle, are compared (6) using an additional simulation loop with the complex model (4) and the calculation using the meta-model (5). Combinations of measures whose meta-model calculation do not match the simulation result of the complex model are extracted (7). A detailed simulation loop is executed while considering each sub-variant combination. Both the list of considered combinations and the simulation results are stored. This loop is repeated for each driving cycle (8) to analyze the interactions. The matching

of the meta-model including interactions and the simulation result will be discussed below using an example in Chapter 6.2.

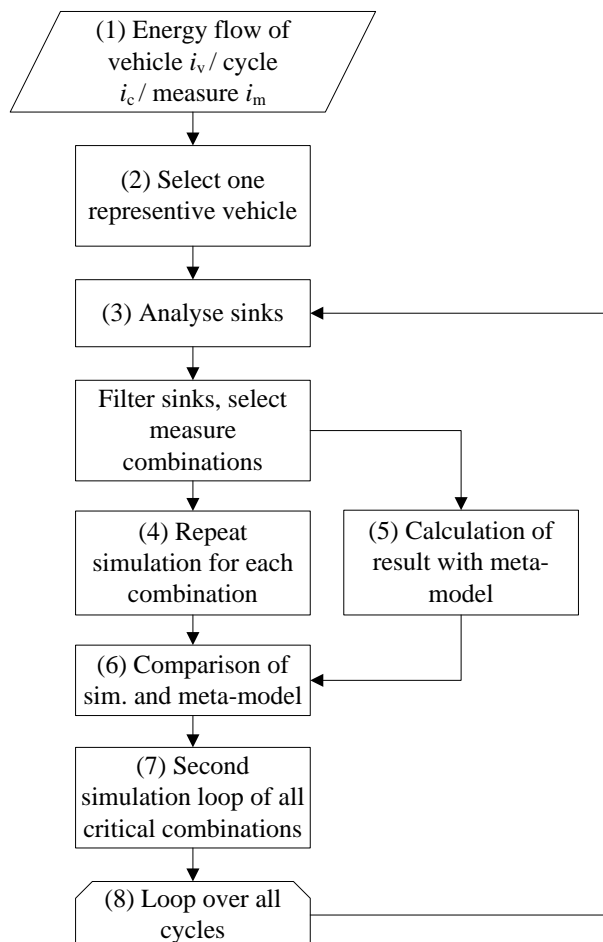


Figure 5.8.: Final approach for the simulation and analysis of the measures and interactions

5.6. Multi-step approach

5.6.1. Introduction

Figure 5.3 showed the different levels of the optimization problem. Below, the final optimization approach is derived with the same structure using three steps. The first step, the simplest, considers only the optimal selection for one driving cycle. This method can be used if the scope of work is the optimization of one cycle only, but it is also used as an input for the vehicle-based optimization. The second optimization, the vehicle-based optimization, addresses the targets of different driving cycles for one vehicle. In this level, the target conflicts between various given targets should be solved. In the final level, the fleet-based optimization handles more than one vehicle up to a complete fleet. This last level handles the target conflicts which occur when considering multiple vehicles.

5.6.2. Cycle-based optimization (CBO)

5.6.2.1. Starting point

The first step of the optimization method is the consideration of only one vehicle and one driving cycle. Figure 5.9 shows an example of a walk down chart to highlight the optimization task. The black bar on the left shows the baseline status s_{bl} in the driving cycle. Thereafter, a list of measures exists. The size of the bars represent their influence $M_{\Delta}(i_v, i_c, i_m)$ in the driving cycle. The black dashed line shows the defined target t of the vehicle i_v in the driving cycle. The measures are divided into two groups: the measures selected to achieve the target are indicated with a solid gray bar, and further potentials are indicated with a striped gray bar. The selection of measures defines the parameter vector \mathbf{m} . In addition to the walk down chart, the costs are also added within this diagram. The gray solid line and the gray dashed line represent the total costs $\sum_{i_m=1}^{n_m} c(i_m)$ with an increasing number of considered measures. Hereby, every measure is coupled with a cost value $c(i_m)$. The gray dotted line shows the cost ratio $cr(i_m)$ for each measure individually, according to Equation 5.27. The cost ratio is defined by dividing the cost c by the influence M_{Δ} of a measure i_m . In the first step in this example, the measures are unsorted. In addition, no sub-variants of the measures are considered here ($n_{svar}(i_m) = 1$).

$$cr(i_m) = \frac{c(i_m)}{M_{\Delta}(i_v, i_c, i_m)} \quad (5.27)$$

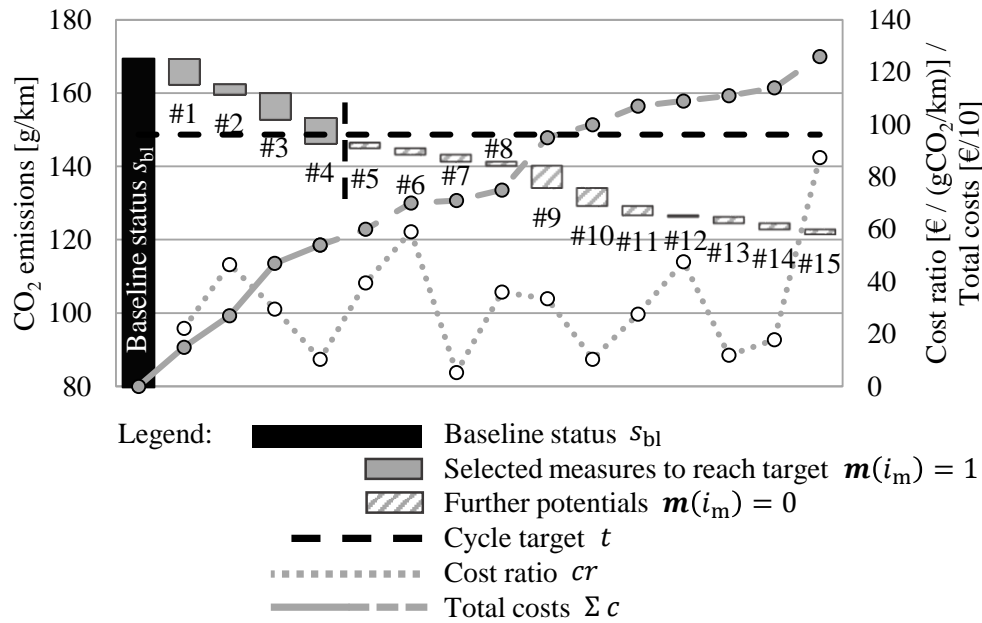


Figure 5.9.: Initial walk down chart

5.6.2.2. Initial solution - Sort by cost ratio

The focus of the method is on finding the optimal solution related to the costs. The first logical approach is to sort the measures by increasing cost-ratio. This means measures with higher influence and lower costs will be implemented first. The result can be seen in Figure 5.10. In

this figure, the gray solid line shows the total cost of the updated measure combination. In addition, the gray dotted line shows the total cost of the previous walk down chart from Figure 5.9 as a reference. It can be seen that the total costs are reduced, although more measures are integrated in this solution. In addition, it is evident that this solution has a target over-fulfillment, which means when selecting measure #1, the current status is lower than the black dashed target line.

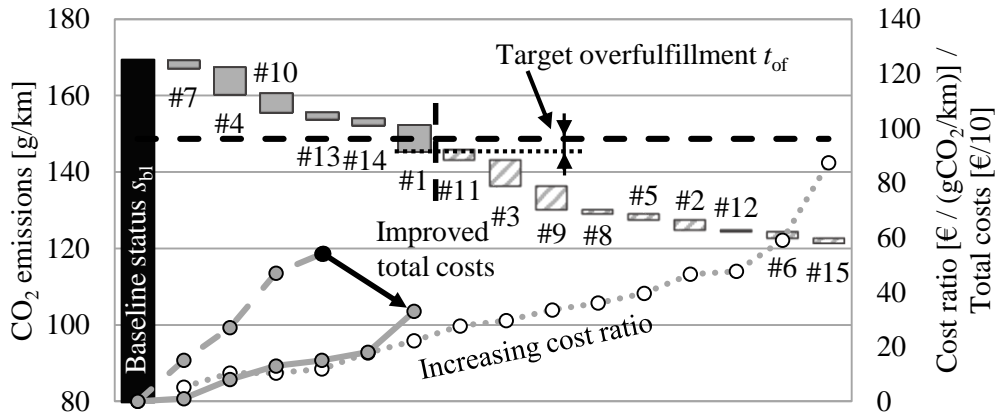


Figure 5.10.: Walk down chart - measures sorted by the cost ratio

Here, the question is whether a better solution can be found with a lower target over-fulfillment and lower costs. In addition, this first approach only considers measures without sub-variants. To adapt the method for the defined optimization problem, the method has to be extended with the following functions:

1. Include the influences of interactions between measures
2. Consider different steps of sub-variants of measures
3. Allow for the changing or deleting of measures in order to find the best relation between minimum target over-fulfillment and minimum costs.

5.6.2.3. Step 1 - Re-combination due to interactions

Based on the analysis performed in Chapter 5.5, the first step is to counter-check if interactions occur in the currently considered driving cycle. The goal is to reorganize the parameter vector by including interactions, while maintaining the same structure. This principle is shown in Figure 5.11. The upper part shows a set of measures in the first line, symbolized by the gray blocks. In the baseline vehicle, the state of these measures is “0”, which means they are not implemented. Different sub-variants can exist for a measure. In the simplest case, it is “0” (not used) or “1” (used). For other measures, more sub-variants may be available, such as different tires. The list of interaction shows which measures interact in the considered cycle. For example, start-stop and cylinder deactivation can interact in an NEDC. To consider such an interaction, the two measures are now combined and reorganized as one measure. All possible combinations of the sub-variants are combined and considered, as shown in Figure 5.11 (lower part).

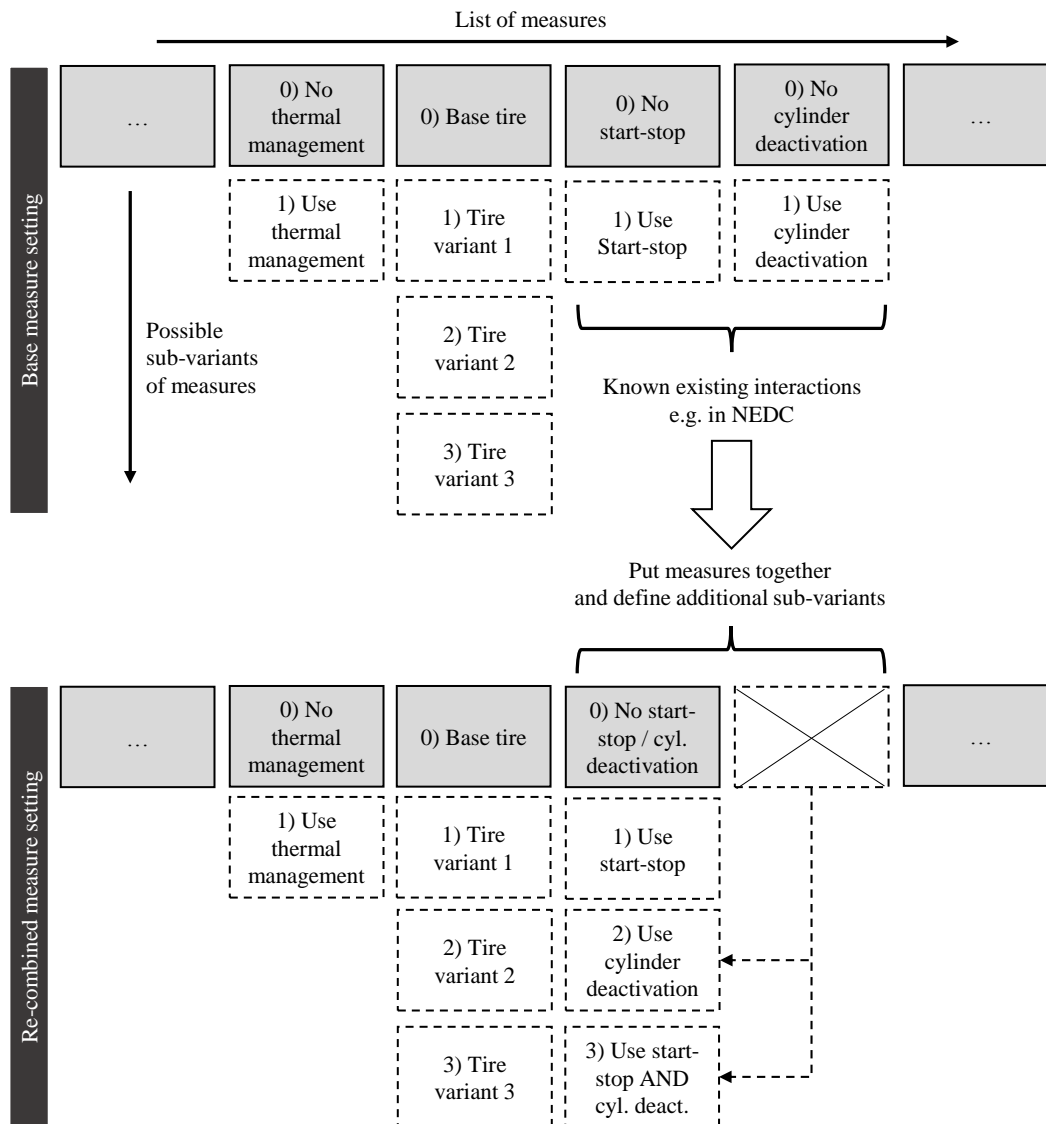


Figure 5.11.: Re-combination of measures and sub-variants due to interactions

5.6.2.4. Step 2 - Re-combination due to sub-variants

Figure 5.10 shows a walk down chart. Several measures are considered and analyzed according to their cost ratio. The problem is how to consider the different sub-variants of the measures. As shown in Figure 5.11, a measure can have various sub-variants, such as different possible tires. Figure 5.12 illustrates this with three walk down charts. The first chart shows the starting point. The bars for the individual measures are extended with the sub-variants, for example for #4, #14 and #9 in parallel. Here, the sub-variants have an “or” relation. Either #9 sub-variant 1 or sub-variant 2 can be used. The method of sorting the measures by the cost ratio does not work because every sub-variant can have another cost ratio. This is shown with the gray solid line. For example, the cost ratio of measure #14-1 is lower, and #14-3 is higher than the following measure #1. Considering one measure with its sub-variants, the influence on both the driving cycle and the cost ratio can vary.

In order to keep it as a “yes” or “no” decision (measure vector without sub-variants), the measures

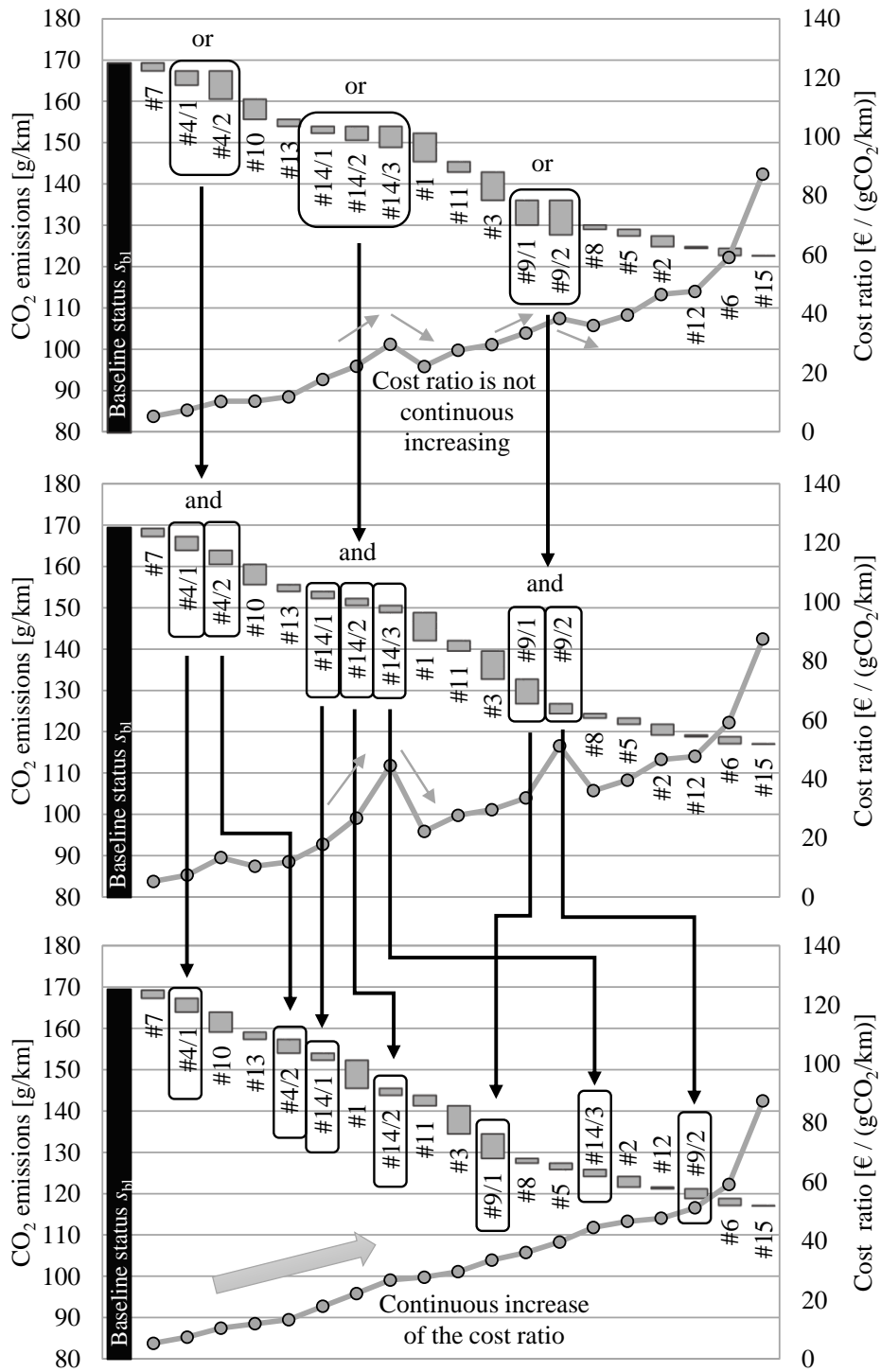


Figure 5.12.: Example for splitting the sub-variants

must be split. This split can be seen in the middle diagram of Figure 5.12. The sub-variants are transformed as shown in the example in Table 5.5. The left side shows the initial definition, which means the sub-variants are exchanged and connected by an “or” statement, either tire 1 or tire 2 or tire 3 is used. The cost ratios differ depending on the influence and the costs. In the next step, the measures are re-defined and connected by an “and” statement, but remain in place in terms of their relation to each other. It is assumed that first tire 1 will be implemented, after which it will be replaced by tire 2, and so on. Tire 2 is now re-defined by the difference between tire 1 and 2, as tire 3 is defined by the difference between tires 3 and 2. The benefit, costs and cost ratios are adapted.

Table 5.5.: Split of sub-variants into additional measures

Measure step	Benefit [$\frac{\text{gCO}_2}{\text{km}}$]	Cost [€]	Cost ratio [$\frac{\text{€} \cdot \text{km}}{\text{gCO}_2}$]	Change definition	Benefit [$\frac{\text{gCO}_2}{\text{km}}$]	Cost [€]	Cost ratio [$\frac{\text{€} \cdot \text{km}}{\text{gCO}_2}$]
(0) Base				(0) Base			
(1) Use tire 1	-1.6	30	18.8	(1) Use tire 1	-1.6	30	18.8
(2) Use tire 2	-3.2	75	23.4	(2) Replace tire 1 with tire 2	-1.6	45	28.1
(3) Use tire 3	-4.8	150	31.2	(3) Replace tire 2 with tire 3	-1.6	75	46.9

The process step can also be seen in Figure 5.13. The upper part shows the initial definition of measures with several sub-variants. They are re-defined according to the lower part of the figure. New measures are defined, which of course increases the total number of measures. Only two states (“yes” or “no”) for each measure are available now. The application of this effect can be seen in the middle walk down chart of Figure 5.12.

In the last step (lower diagram of Figure 5.12), the measures can be sorted again based on their cost-ratio, and the linear optimization method can be used. Because they are sorted according to the cost ratio, the order changes. For example, measure #14/3 moves to a position after measure #5. In addition, a precondition is included from now on. Thus, measure #14/2 can only be selected if measure #14/1 is also selected because sub-variant 2 is now based on sub-variant 1.

5.6.2.5. Step 3 - Pair exchange

To solve the problem of target-overfulfillment and the cost-optimal selection of measures, an algorithm is needed. The intention is to reduce both the target overfulfillment and also the total costs. The starting point for the algorithm is the definition of the initial solution, which is shown in Figure 5.14. This figure also highlights the important variables. The initial solution is generated, starting with an empty parameter vector $\mathbf{m} = \mathbf{0}$. All values are set to zero, which

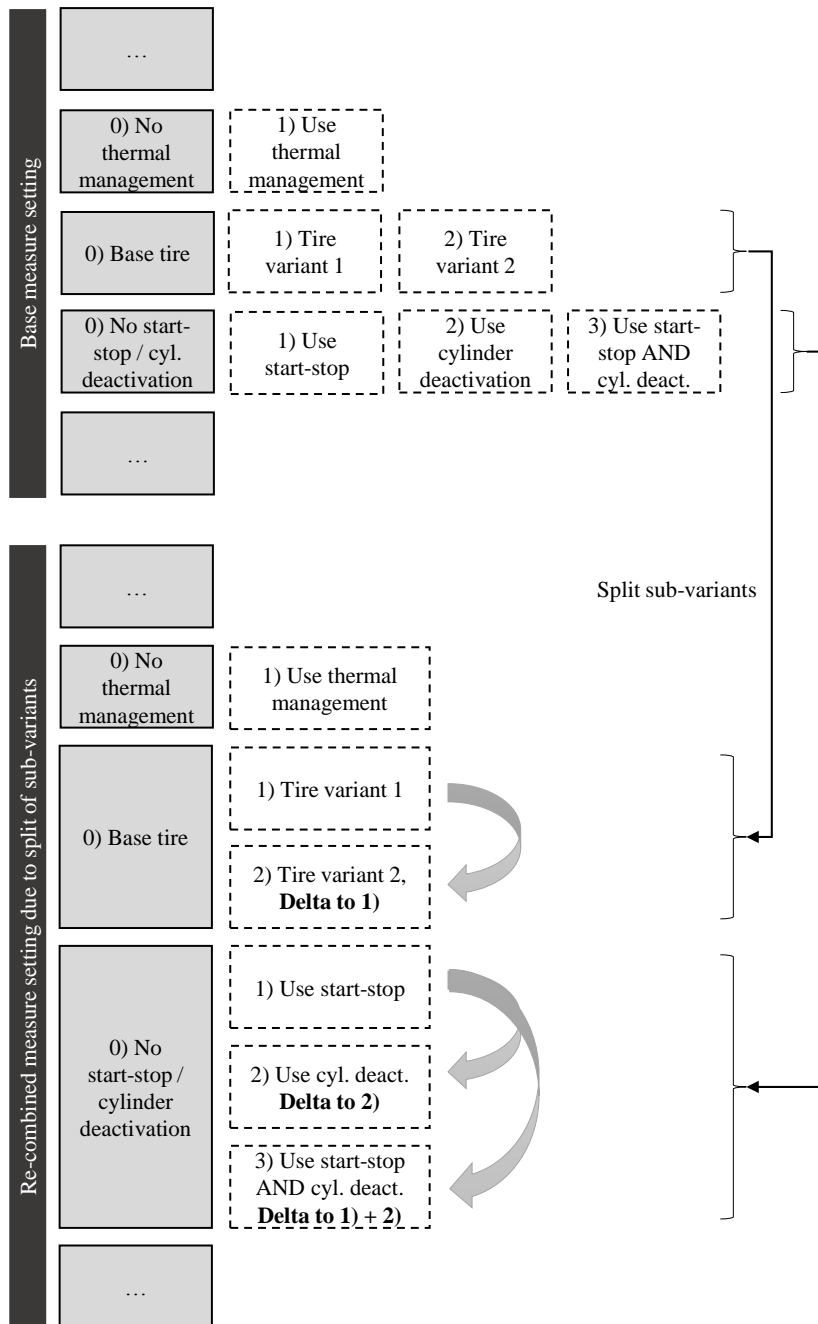


Figure 5.13.: Split of sub-variant to main-variants

means that no measure is selected. The basis is the sort of the measures according to their cost ratio (see step 2). Starting from the first measure $i_m = 1$, the measures are implemented until the target value is achieved. The last selected measure is the reference measure i_{ref} . Thus, if measures 1 to i_{ref} are implemented, the target is achieved, and if measures 1 to $(i_{\text{ref}} - 1)$ are implemented, the target is not yet achieved. An initial parameter vector is generated with a reference cycle status s_{ref} and the reference cost of the chosen measures c_{ref} . Here, the reference values are defined as follows. The reference status s_{ref} is the baseline status \mathbf{S}_{bl} of the considered vehicle i_v and driving cycle i_c plus the influence of the selected measures $\mathbf{M}_{\Delta}(i_v, i_c, i_m)$ from the first measure until the reference measure. The status value should be lower than the given target $\mathbf{T}_{\text{vc}}(i_v, i_c)$. The reference cost c_{ref} is defined as the cost c of all selected measures. The reference status and reference cost read

$$s_{\text{ref}} = \mathbf{S}_{\text{bl}}(i_v, i_c) + \sum_{i_m=1}^{i_{\text{ref}}} \mathbf{M}_{\Delta}(i_v, i_c, i_m) \leq \mathbf{T}_{\text{vc}}(i_v, i_c) , \quad (5.28)$$

$$c_{\text{ref}} = \sum_{i_m=1}^{i_{\text{ref}}} \mathbf{M}_c(i_v, i_c, i_m)$$

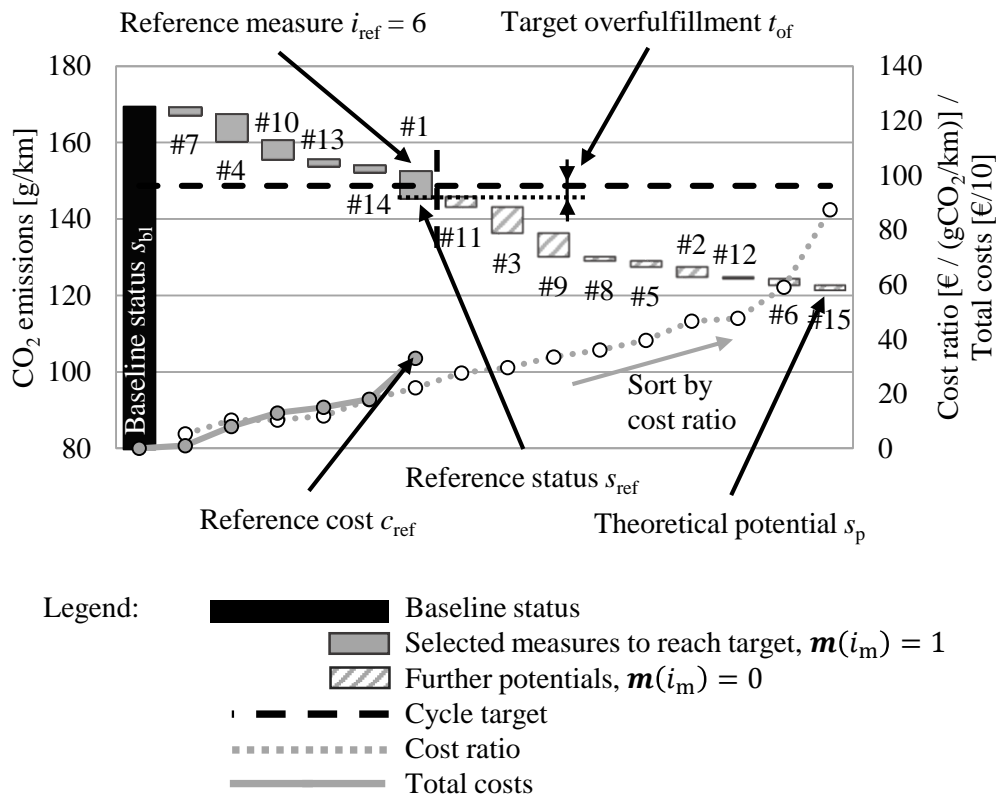


Figure 5.14.: Principle initial solution

In this example, the status s_{ref} of the initial solution is lower than the target. The target is overfulfilled, as described by the variable t_{of} , which reads

$$t_{\text{of}} = \mathbf{T}_{\text{vc}}(i_v, i_c) - s_{\text{ref}} . \quad (5.29)$$

The question is whether another parameter vector exists where both the costs and the difference between status and target are lower. Therefore, a re-combination algorithm is required. In this case, a *Tabu Search* method is used.

In general, a *Tabu Search* algorithm is a kind of neighborhood search and includes the history of the previous solutions. This approach is based on investigations on the neighborhood of a solution. Changing certain parameters yields a new solution. The best solution out of this neighborhood is used for the next iteration step. In addition, the idea is to use a “tabu list” to avoid revisiting previously considered solutions. The information regarding changed parameters will be saved. [109] [110]

In terms of the described optimization problem, the goal of the *Tabu Search* is to delete measures from the solution or to exchange measures. For example, when deleting a measure i_m^* , new measures have to be added in order to achieve the target. Here, more than one combination is possible, which define the possible neighborhood of the measure i_m^* . In the first step, valid solutions have to be found. A boundary constraint specifies that a valid solution should have lower costs than the reference solution \mathbf{m}^* . The initial parameter vector \mathbf{m}_{ref} is the starting point for the *Tabu Search*. Using a *Pair Exchange*, new parameter vectors are created. Each new solution has to fulfill the precondition of achieving the target, but with lower costs than the reference c_{ref} . Each identified solution is a new reference solution for the next iteration step. If no better solution is found, the last reference vector is defined as the optimal solution, and the algorithm stops.

Figure 5.15 illustrates the principle workflow of the *Pair Exchange* method in more detail. The state $\mathbf{m}(i_m)$ of a measure is defined as follows:

- “-1” = measure is not considered and not allowable
- “0” = measure is not considered yet, but allowable
- “1” = measure is used and allowed to disuse

Two major types of working steps are performed:

- The first simple step searches within the selected measures defined by $\mathbf{m}(i_m) = 1$. Measures may exist where the influence $\mathbf{m}_\Delta(i_m)$ is lower than the target overfulfillment t_{of} . Such measures can be excluded while still reaching the target and reducing the costs. In this step, measures can only be excluded. The working step can be defined as follows:

$$\text{exclude } i_m \text{ if } \mathbf{m}_\Delta(i_m) \leq t_{\text{of}} . \quad (5.30)$$

- The second step excludes selected measures $i_{m, s}$, as defined with $\mathbf{m}(i_m) = 1$, and includes unused measures $i_{m, u}$, defined by $\mathbf{m}(i_m) = 0$ instead. The intention is to find pairs which can be exchanged without inhibiting the ability to meet the target while reducing costs. Here, more than one measure can also be excluded and / or included, as long as the target is still reached. The statement can be defined as follows:

$$\text{exclude } i_{m, s} \text{ and include } i_{m, u} \text{ if } (\mathbf{m}_\Delta(i_{m, s}) - \mathbf{m}_\Delta(i_{m, u})) \leq t_{\text{of}} . \quad (5.31)$$

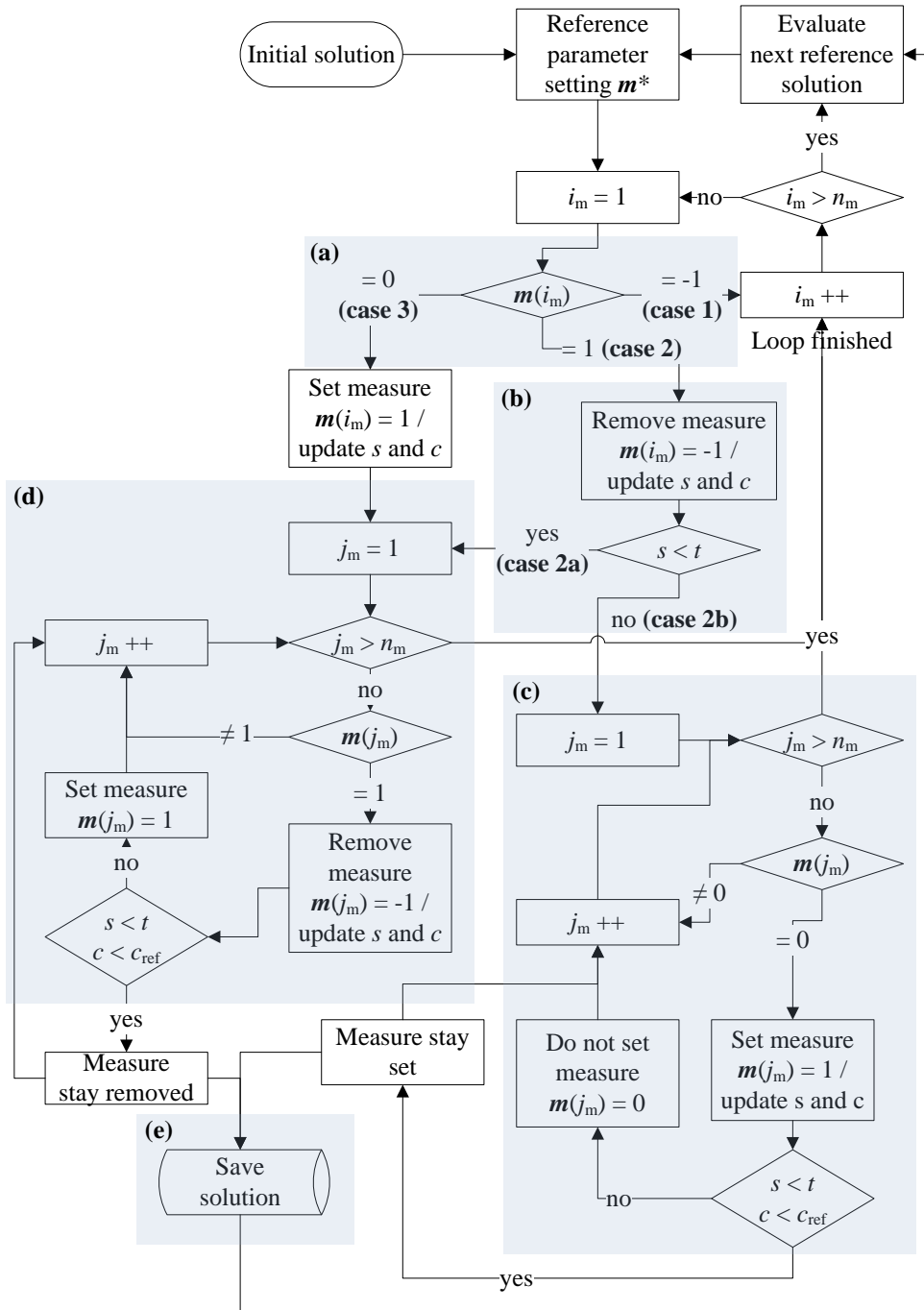


Figure 5.15.: Principle flow chart of the *Pair Exchange*

The implemented *Pair Exchange* is based on an iteration loop. For the first iteration, the initial parameter vector \mathbf{m}^* is used. A loop is started considering each measure i_m , which results in n_m sub-loops. The intention is to find other solutions by changing the state of measures. Based on the parameter state $\mathbf{m}(i_m)$, a branch (see solid area (a) in Figure 5.15) is included, as defined by the following three cases:

- Case (1) $\mathbf{m}(i_m) = -1$ means that the measure is already excluded by the tabu list and no longer considered. The loop goes to the next i_m .
- Case (2) $\mathbf{m}(i_m) = 1$ means that the measure is already included. The effect on the solution of excluding this measure must be checked.
- Case (3) $\mathbf{m}(i_m) = 0$ means that the measure is not included and can be selected. The effect on the solution of including this measure must be checked.

Case (1):

No further activities are performed in this case, and the algorithm selects the next i_m .

Case (2):

This routine will analyze the effect of excluding the selected measure i_m from the solution ($\mathbf{m}(i_m) = -1$). The new status s without this measure is calculated and compared to the target t (see solid area (b) in Figure 5.15). The routine is divided into two paths. The first path (case 2a) is used if the target is still achieved ($s < t$) when i_m is excluded. In this case, additional measures will be excluded until the target is no longer met. The goal is to reduce the costs by excluding measures such that their accumulated influences are lower than the target overfulfillment t_{of} . Here, the routine continues with case (3). The second path (case 2b) will now add new measures until the target is reached again. The routine runs a loop over all unused measures j_m (see solid area (c) in Figure 5.15), which are allowed to use ($\mathbf{m}(j_m) = 0$), as long as the cost of the new parameter vector is lower than the reference cost ($c < c_{ref}$) and until the target is reached ($s < t$). Here, the goal is to exchange the states of measures in order to find solutions with a lower target overfulfillment and lower costs. The identified solutions will be saved as new references (see solid area (e) in Figure 5.15).

Case (3):

This path analyzes the effect of including unused measures. In contrast to case 2, a new unused measure i_m is added to the solution ($\mathbf{m}(i_m) = 1$). This leads to a higher target-overfulfillment. An iteration is executed to consider selected measures j_m and stepwise removing them ($\mathbf{m}(j_m) = -1$) up to a minimal target overfulfillment (see solid area (d) in Figure 5.15). The goal is to exchange measures by including measures with a higher cost ratio but with lower total absolute costs for the whole solution. If this solution has lower costs than the reference cost ($c < c_{ref}$) while still achieving the target ($s < t$), it will be saved as a new reference (see solid area (e) in Figure 5.15). As a prerequisite for the iteration loops of j_m , it is defined that $i_m \neq j_m$.

After this loop, a set of new solutions n_S are available. If the number of new solutions n_S is zero, this means no new better solution has been found, the iteration loop is stopped. Otherwise, this routine is repeated with each new solution as a reference. For each solution, the removed measures are marked with “-1” so that they cannot be selected in the next loop.

Figure 5.16 shows the final approach of the flow chart for the cycle-based optimization. After sorting the measures based on cost ratio, the measures will be selected until the target is reached. Using a *Pair Exchange* algorithm, individual measures will be removed and added such that a solution with lower costs is found. If the algorithm does not find a better solution in an iteration step, the algorithm ends.

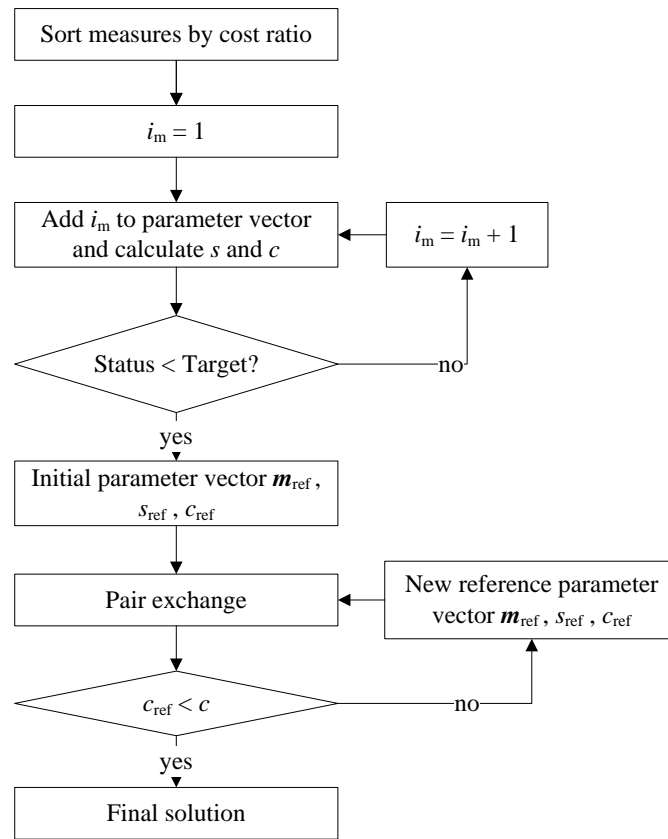


Figure 5.16.: General flow chart of the cycle-based optimization

5.6.2.6. Step 4 - Post-processing

The theoretical potential s_p is another important characteristic of the solution. The potential is defined as the value which can be achieved by implementing all available measures (see Figure 5.14). The input for the calculation is the tabu list of the reference solution. The tabu list includes the measures which are not allowed for further investigations ($m(i_m) = -1$), which reduces the possible solution space as a constraint. With a limited solution space, the number of available measures is also reduced, so the full potential is no longer possible. The impact of this restriction will be explained in more detail in Chapter 6.2.3. The information regarding the theoretical potential will be used below as an input for the vehicle-based optimization.

In sum, the result of the cycle-based optimization loop is the following variables:

- s_{opt} , the status of the optimal solution
- c_{opt} , the cost of the optimal solution and the implemented measures
- m_{opt} , the parameter vector of the optimal solution
- $s_{p, opt}$, the potential of all remaining measures due to the limited design space due to the tabu measures

5.6.2.7. Validation

In order to check the quality of the optimization method, the results must be compared to the global optimum. For the development of the optimization algorithm, a reduced number of vehicles was defined in the first step. To cover the vehicle range of a complete fleet for this validation, eight representative vehicles from all three markets, two segments and different engine and transmission configurations were defined with a reduced setting of measures. A calculation loop was generated to calculate the cost of each possible combination of measures. The result can be seen in Table 5.6. In the first step, the optimal solution was calculated for each vehicle for the fuel consumption targets using a time-intensive complete enumeration algorithm. This solution represents the global optimum. In the next step, the optimal solution was calculated using the described cycle-based optimization. The comparison shows that in all eight cases, the CBO is capable of identifying the global optimum. Besides the fuel consumption target, the global optimum for the performance targets was also compared using the cycle-based optimization and the complete enumeration algorithm with the same result. For example, about 8.5 million combinations of the measures are available for vehicle #5. However, only 2.5 million parameter vectors achieve the boundary constraint of reaching the given fuel consumption target. The calculation time for one vehicle using the complete enumeration algorithm was approximately 3 hours and 20 min. In comparison, the calculation time of the optimization algorithm was less than one second, which proves the advantage that optimization algorithms result in lower computation time.

Table 5.6.: Comparison of global optimum and optimum solution using the algorithm for a given fuel consumption target

Vehicle	Global optimum [€]	Optimum found by algorithm [€]
#5	465	465 ✓
#6	490	490 ✓
#7	560	560 ✓
#8	530	530 ✓
#15	250	250 ✓
#16	620	620 ✓
#17	450	450 ✓
#18	440	440 ✓

5.6.2.8. Summary

The cycle-based algorithm using a *Pair Exchange* method consists of the following steps:

- Re-organize measure vector with the sub-variants and interactions (to generate only “0” and “1” measure options)
- Calculation of the cost ratio
- Sort measures by cost ratio
- Select measures based on the cost ratio until the target is reached as an initial solution
- *Pair Exchange* to find a better solution with minimum target overfulfillment and lower cost

5.6.3. Vehicle-based optimization (VBO)

5.6.3.1. Starting Point

A vehicle in a development project is described by several targets, which be conflicting. Figure 5.17 shows the principle of target conflicts of the selection process of measures in the case of the target achievement for CO₂ emissions and driving performance. The upper diagram shows the CO₂ emission improvement. Using the CBO as an initial solution, the target is achieved by implementing the first four measures (#7, #4, #10 and #1). This solution represents the optimum solution with minimum costs only considering the NEDC. The lower diagram also shows two acceleration times, the acceleration from 0 to 100 kph with the light gray line, passing time from 80 to 120 kph with the dark gray line, and their defined target with the dashed lines. In addition, depending on the implemented measures, the status is improved step by step. Considering only the first four measures, it can be seen that the target for the acceleration time from 0 to 100 kph is achieved. In contrast, the target for the passing time from 80 to 120 kph is not achieved. Thus, additional measures have to be implemented to improve the passing time as well (e.g. measure #13, #14, #11 or #15). However, this remains in conflict with the optimum NEDC-based solution. The goal is to find the best combination considering not only the CO₂ emission, but also other complete-vehicle targets.

As explained in Chapter 5.4, a search method including random decisions should be used, whereby there are three typical options:

- *Genetic Algorithm* (GA)
- *Simulated Annealing* (SA)
- *Particle Swarm Optimization* (PSO).

A *Genetic Algorithm* considers several different parameter settings as a starting point. Thus, more than one solution is calculated on several places in the solution space. The solutions are optimized by random combinations of the parameter settings of two “parents”, which lead to a recombination. In addition, a mutation can be applied by randomly changing individual variables of the parameter vector. The parameters of the *Genetic Algorithm* are mainly based on bits (“0” and “1”). This is directly comparable to the selection of measures within the optimization problem of this thesis, where a “yes” or “no” decision for the implementation of measures has to be handled. [103] [109] [110] [111]

Simulated Annealing is comparable to the cooling process of physical bodies. Starting from the highest energy (warm body), the cool-down tries to find the state with the minimum energy. A neighborhood solution is generated by changing parameters to improve the defined objective function. The goal of the *Simulated Annealing* is to reduce the *temperature* step by step. The new solution is compared to the reference solution. If the new solution is better, it replaces the old reference solution. If the new solution is worse, the new solution is chosen depending on a defined probability, which is a function of time. This method is also comparable to the optimization problem, where the *temperature* of the body corresponds to the *cost* of the measures. Starting from the highest cost means that all defined targets are not reached. Step by step, measures are selected, which leads to a reduction of the costs. [103] [109] [110]

The last algorithm mentioned is the *Particle Swarm Optimization*. Different particles define a swarm. Each particle is defined by its position in the solution space and its speed vector. The intention is to adapt the speed vector of each particle in the direction to the global optimum. The speed vector can be adapted by the history (solutions of the last iteration steps), by a

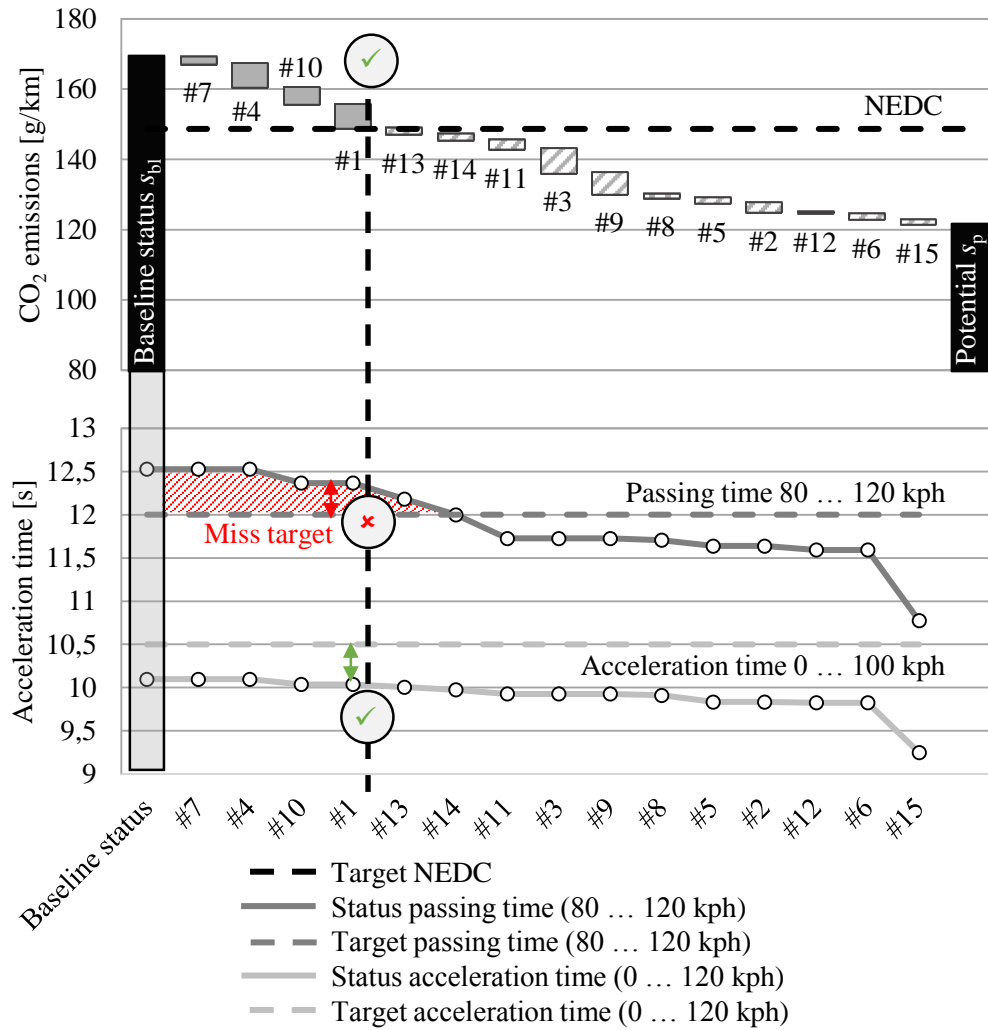


Figure 5.17.: Example of the target conflict between the NEDC-optimized selection of measures and the effect on other complete-vehicle targets

random change or by information from the neighbor particles. This approach also has analogies to the optimization problem of this thesis because a set of vehicles and targets (particles) define the whole fleet (swarm). [109] [111]

For the final approach, a mixture of all three ideas and influences will be used to combine the advantages of each approach.

5.6.3.2. Pre-processing and initial solution

At the beginning of each optimization algorithm is the definition of the initial solution. The definition of the initial solution is based on the *Simulated Annealing* procedure. Beginning from the highest *temperature*, the optimizer tries to reduce the temperature step by step. A similar approach is used in this case. The starting point for the algorithm is the baseline status, which is defined as no measures selected. This solution is the worst case because the gap between status and target is the maximum. The goal is that measures can be selected or excluded step by step until a final optimum solution is found. Thereby, it is important to specify on which basis

the measures should be selected and prioritized.

To derive a basis for the prioritization of measures, Table 5.7 shows the results of an sample vehicle, defined by different cycles. Every cycle has an initial baseline status s_{bl} and a target t . Considering the cycles individually and implementing all measures with a positive influence enables minimum potential s_p for each cycle. The table also shows three sample measures: engine start-stop, aerodynamic improvement and weight reduction. It can be seen that the benefit of the measures varies depending on the driving cycle. For defining a weighting of the measures, the ratio between the baseline status, the potential and the set target is of interest. This relationship is different for each cycle and describes the sensitivity related to the measures required to achieve the target. In addition, the targets and potentials differ so that it is necessary to weight the importance of the cycles. This is shown in Figure 5.18, which illustrates the ratio between the baseline status (no measures implemented), the potential (all measures with benefits implemented) and the target (solution to be found). Cycles where the target is closer to the baseline status are less important because only few measures are required to achieve the target. If some measures are not implemented, it is still possible to define other measures to reach the target. Cycles where the targets are closer to the potential than to the baseline status are crucial. Many measures have to be implemented into the vehicle to achieve the target. If some measures are not allowed to be implemented, then it can transpire that the target can no longer be achieved.

Table 5.7.: Example of the dependence between the influence of measures and cycles

	NEDC [l/100km]	Acc. 0...100 kph [s]	Acc. 80...120 kph [s]	Max. speed [kph]
Status s_{bl}	7.0	10.4	11.6	208
Target t	5.1	9.8	10.1	216
Potential s_p	3.9	9.4	6.5	226
Aerodynamic (c_d -0.03)	-0.1	-0.04	-0.23	5.0
Weight reduction (-100 kg)	-0.05	-0.48	-0.78	0.5
Engine start-stop	-0.17	0	0	0

Besides the weighting of cycles, the measures have to be weighted as well. As seen in Table 5.7, some measures have an influence on only one cycle, whereas others influence all cycles. In addition, the range of the influence is quite different. So for example, weight reduction has a high importance for the acceleration time. In contrast, aerodynamic improvement is important for the maximum speed. However, both measures have an influence on all four cycles considered. In contrast, an engine start-stop system only influences the CO₂ emission-related driving cycle (NEDC). The first step of weighting the importance of measures is related to the number of cycles where an influence exists, while the second step considers the range of influence. The calculation of the weighting will be described below. Measures with a high influence and a high number of cycles influenced are more important on the complete-vehicle level than measures with low influence and that influence only one cycle.

Furthermore, during the optimization process, measures will be selected. A decision must be made about which measure should be changed in a certain iteration step. In the optimization algorithm, the weighting information will be used to prioritize measures. The derivation of the weighting value is oriented on the idea of the *Particle Swarm Optimization*. Each cycle can be

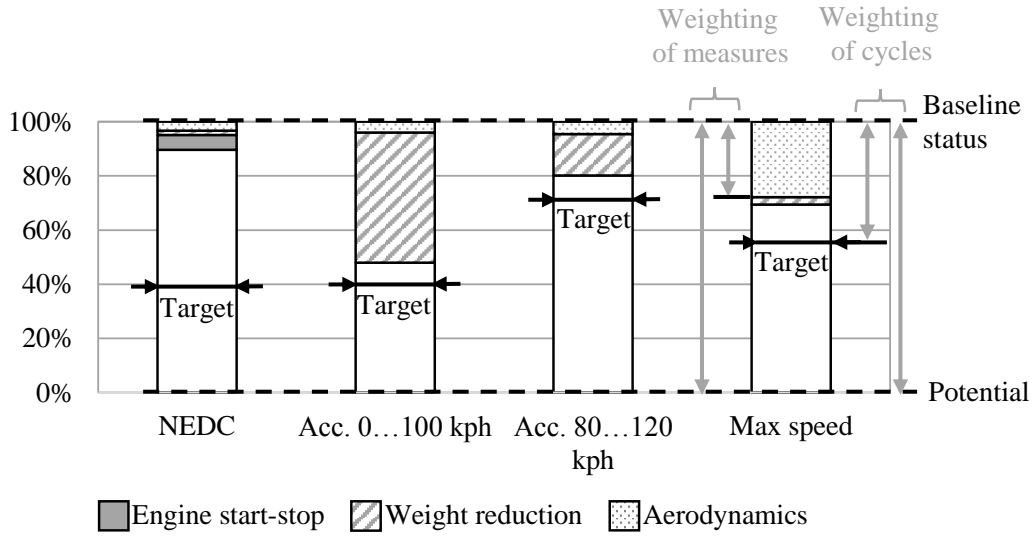


Figure 5.18.: Illustration of the different ranges between baseline status, potential and target of different cycles and the influence of different measures

This figure illustrates the concept for the weighting of cycles and measures. The target is set in relation to the status (defined as 100%) and the potential (defined as 0%). For a better overview, all units of measurements are ignored for comparison in this figure. The weighting of cycles is based on the relation between the difference between the target and the status compared to the difference between status and potential. The same procedure is used to weight measures. The influence of a measure is set in relation to the difference between status and potential.

seen as a individual particle trying to find its cycle-based optimum. For this reason, the CBO is executed separately for every cycle. Here, the following information from this loop is taken as an input:

- Possible potential s_p for each cycle (based on the tabu list, if available)
- The selected measures for the cycle-specific optimal solution m_{c_i}

Of course, the cycle-specific optimal solutions will differ. Another optimal combination of measures results for every cycle. All results have to be analyze in terms of similarities and differences in the selection of measures. The goal is to adjust the selection for all cycles in order to obtain an optimal solution for a vehicle.

The first step of the analysis is weighting the cycles among themselves. The weighting $cw(i_c)$ of a cycle i_c is described by the relation between the difference between the baseline status s_{bl} and target t towards the difference between the baseline status s_{bl} and the potential s_p , which reads

$$cw(i_c) = \frac{s_{bl}(i_c) - t(i_c)}{s_{bl}(i_c) - s_p(i_c)}. \quad (5.32)$$

The second step is the weighting mw of the measures. This weighting is performed for every measure individually. For measures i_m , each cycle i_c is considered individually in the first level. Because a measure can have sub-variants, the sub-variants with the minimum (= maximum negative value) and the maximum (= maximum positive value) influence are selected. The

weighting also considers the difference between the potential and baseline status in order to take into account the influence of a measure in contrast to the whole potential. The sub-variants with the minimum influence d_{\min} and the maximum influence d_{\max} are weighted in parallel, see Equations (5.33) and (5.34). In addition, the weighted influence is multiplied by the weighted cycle factor $\mathbf{cw}(i_c)$. The final rating value calculates the difference between d_{\min} and d_{\max} and is multiplied by the number of cycles $n_{c_{im}}$, where the measure has an influence. According to Equation (5.35), the result is a vector \mathbf{mw} including the weighting of each measure.

$$d_{\min}(i_c, i_m) = \min \left(\min_{1 \leq i_{svar} \leq n_{svar}} (\mathbf{M}_{\Delta}(i_c, i_m, i_{svar})), 0 \right) \cdot \frac{\mathbf{cw}(i_c)}{\mathbf{s}_{bl}(i_c) - \mathbf{s}_p(i_c)} \quad (5.33)$$

$$d_{\max}(i_c, i_m) = \max \left(\max_{1 \leq i_{svar} \leq n_{svar}} (\mathbf{M}_{\Delta}(i_c, i_m, i_{svar})), 0 \right) \cdot \frac{\mathbf{cw}(i_c)}{\mathbf{s}_{bl}(i_c) - \mathbf{s}_p(i_c)} \quad (5.34)$$

$$\mathbf{mw}(i_m) = \left| \max_{1 \leq i_c \leq n_c} (d_{\max}(i_c, i_m)) - \min_{1 \leq i_c \leq n_c} (d_{\min}(i_c, i_m)) \right| \cdot n_{c_{im}} \quad (5.35)$$

With the execution of the optimization iteration process, the weighting of each measure has to be repeated for every parameter vector in each iteration step. The selection of measures can influence the weighting, as explained in Figure 5.19. Within the process, measures are included or excluded from a parameter vector and thereby reduce the solution space. This causes a reduction of the current status and potential. The weighting \mathbf{mw} of the remaining measures changes. In this example, the weight reduction (striped bars) is included, and the aerodynamic improvement (dotted bars) is excluded. For the acceleration from 0 to 100 kph, the weight reduction has a significant influence on the status. This cycle now becomes less important because the difference between the updated status and the target decreases in comparison to the difference between the remaining potential. The opposite behavior can be seen at the maximum speed. When the aerodynamic improvement is excluded, one third of the potential is no longer available. This cycle now becomes more important because the ratio between the status and the target is reduced. A more detailed example for this calculation is explained in Appendix E.2.

5.6.3.3. Definition of children

After the initial solution, the definition of the children has to be considered during the execution of the iteration loop in the optimization process. The principle algorithm is shown in Figure 5.20. Based on the weighting of the cycles \mathbf{cw} and the measures \mathbf{mw} , one measure should be selected in each iteration step. The input for the calculation of the weighting is used from the CBO of each cycle considered. In a second decision, the measure should be included or excluded by adapting the parameter vector. If a measure is excluded, it can never be used as a measure again. If the measure is included, it must be used for all subsequent combinations. The status of all cycles \mathbf{s} is calculated based on the current parameter vector. If all cycles achieve their target ($\mathbf{s} < \mathbf{t}_v$), the loop is finished. Otherwise, the iteration continues. Thus, step by step, measures will be selected to reduce the difference between targets and the current status. The maximum number of iterations is limited to the number of available measures n_m .

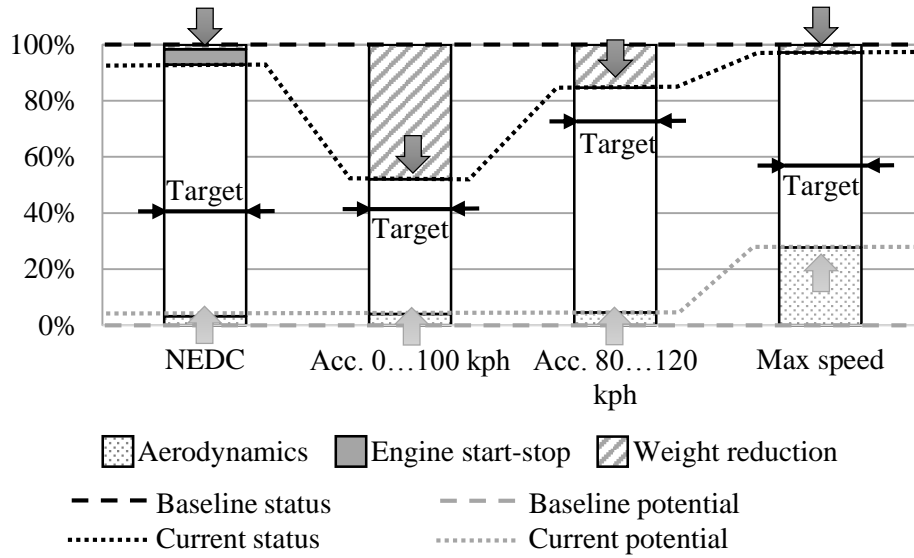


Figure 5.19.: Influence of the weighting caused by including and excluding measures

Typically, a *Genetic Algorithm* uses several parents in parallel. This enables a search for the global optimum in a wider range of the solution space. The “parents” are the initial parameter vectors of each optimization iteration. The procedure shown in Figure 5.20 is for one parent. Because n_{par} parents are defined, this procedure is executed for each parent parameter vector in parallel.

For the algorithm, two control parameters have to be defined:

- Number of parents n_{par}
- Number of children n_{child} .

Furthermore, two issues of the procedure explained in Figure 5.20 have to be discussed: the selection of one measure based on the weighting and the decision to include or exclude a measure.

For each parent, n_{child} children will be defined. A “child” is an adapted parameter vector based on the parameter vector of its parent. For each child, another measure will be selected for the adaptation of the parameter vector. The selection of a measure is based on a random selection. For the first child, the measure with the highest weighting according to the weighted parameter vector \mathbf{mw} is used. The measures for the other children ($2 \dots n_{\text{child}}$) are selected randomly. The probability distribution for the random decision is also influenced by the weighting factor. The basis for the probability distribution is a uniform distribution, but referred to the sum of all weighting. The portion of one measure correlates to its weighting. This means if all measures have the same weighting, a uniform distribution between all measures exists. If a measure has a weighting of two, then its probability is twice as high. Thus, measures with a higher weighting will be preferred.

The decision to include or exclude the chosen measures is solved such that all sub-variants will be evaluated. A measure can be excluded (value “-1”) or included with different sub-variants (value “1 ... n_{svar} ”). For each parent, n_{child} children-measures are defined. Each child also consists of $n_{\text{svar}}(i_m) + 1$ sub-children, which in each case sets another available sub-variant for the child-specific measure selected. Each child is defined by a parameter vector $\mathbf{m}_{\text{child}_i}$ defining the state of measures.

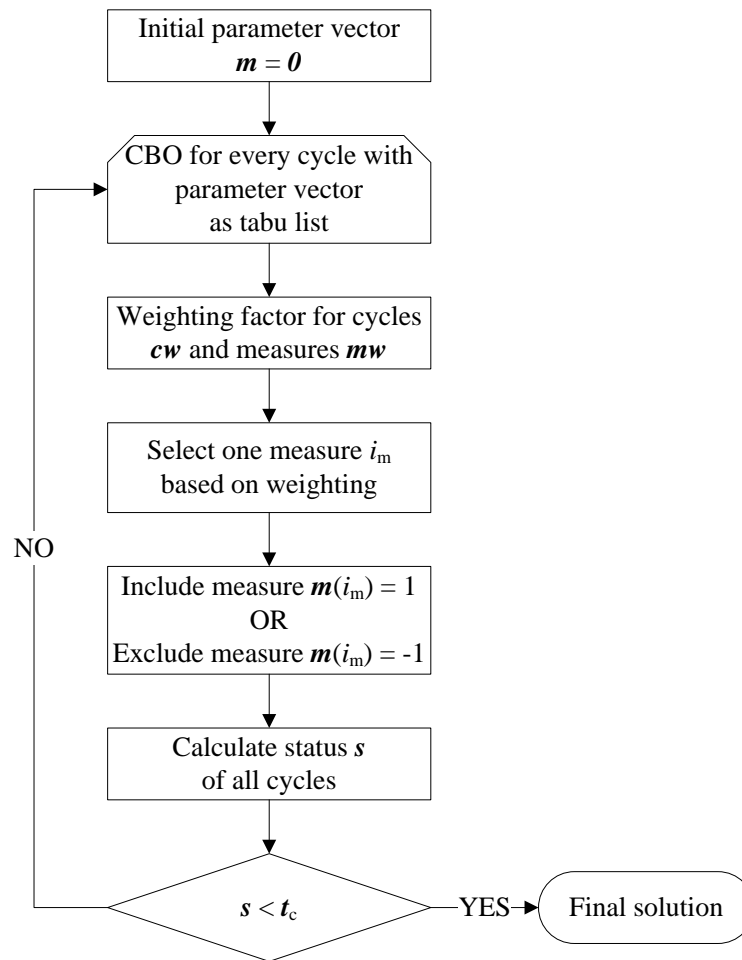


Figure 5.20.: Overview of the principle optimization algorithm

5.6.3.4. Selection of children

The described derivation of the children leads to more children compared than parents. For the next iteration step, only n_{par} parameter settings are allowed, and a reduction to n_{par} children from the whole children generation is needed. This selection is also based on a weighting, and two characteristic parameters are defined, which describe the solution corresponding to a child:

- Cost forecast - describes the cost of the required measures \Rightarrow this parameter should be minimized.
- Equality of cycle-specific solutions - describes the difference between the optimal solutions for each cycle. Measures whose states are different in the cycle-specific optimal solutions are combined to one representative value described by the variable er . \Rightarrow this parameter is a constraint and should be zero.

The CBO is used to derive these two parameters. The workflow is summarized in Figure 5.21. The child-specific parameter vector $\mathbf{m}_{\text{child}}$ is used as an initial solution for the evaluation of the individual optimal solution vectors for each cycle. The CBO is executed for each cycle, and the solutions are compared among themselves. The solution vector can differ for each cycle. The assumption is that all of these measures have to be implemented to achieve all targets. This is a simplified assumption at this point because no inter-cycle interactions are considered. In the

worst case, all of these measures have to be implemented. This definition is illustrated in Figure 5.22. Thus, the costs of this solution are based on all measures used in all cycles.

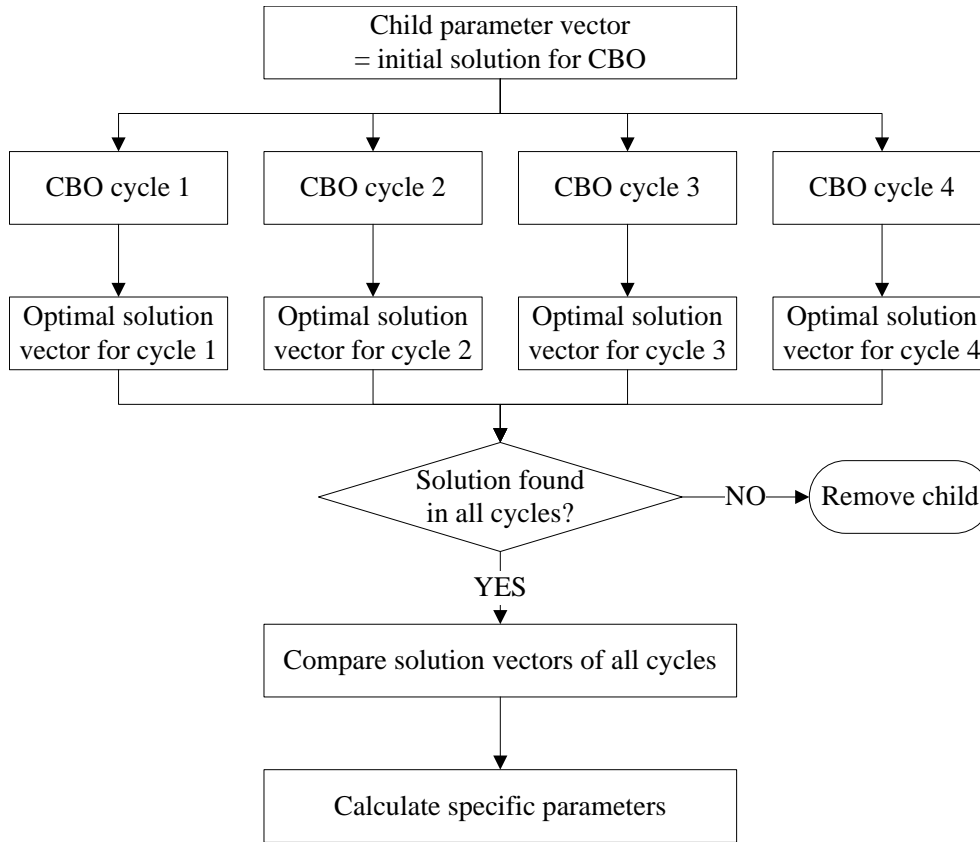


Figure 5.21.: Workflow for the evaluation of the specific parameters

After the execution of the CBO for each driving cycle, a checking function is implemented. If the CBO algorithm does not find a solution for a cycle where the target can be reached (e.g. because too many measures are excluded by the child-parameter vector), this child is removed and no longer considered as a possible solution in the subsequent steps.

The cycle-specific solutions from the CBO are also used for the equality rating. By comparing all results, the measures whose states are not the same in all cycle-specific solutions are selected. In the example in Figure 5.22, the solutions differ in seven out of eight measures used. The difference is described by a number, the so-called equality rating er . This quantity is based on the weighted influence mw of each measure, but only from the measures whose states are different in the cycle-specific solutions. In this case measure #7 is not considered in the equality rating er because the measure is selected in all cycle-specific solutions. The goal is that each cycle will ultimately have the same solution. To compare with other child solutions, the sum of the weighted measures is calculated. This value is defined as the equality rating er . A low sum means that the cycles differ only in few measures with low influence. A high value means that many measures with a high influence are different for the cycles. A sum of “zero” means that a final solution is found where all solution vectors for each cycle are the same, and all targets are met. A more detailed explanation of an example is given in Appendix E.2.

This two characteristic values are calculated for every child. The goal is to minimize the costs and to reduce the equality rating er to zero. For the selection of the children, both parameters have to be considered simultaneously. The final selection of the children is based on a *Pareto*

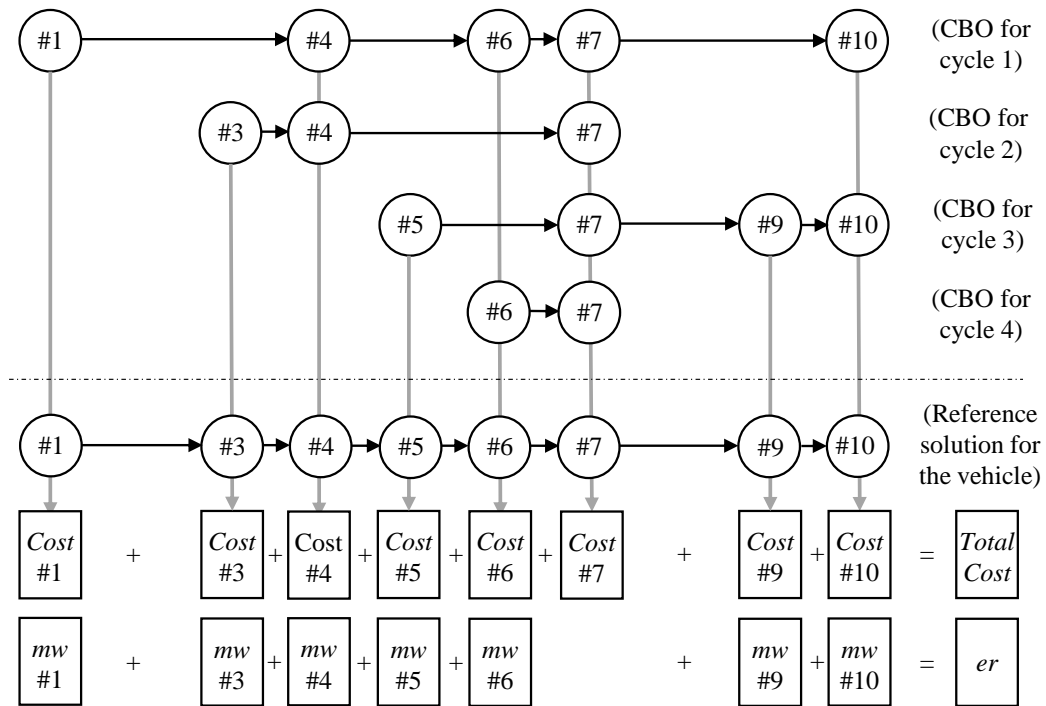


Figure 5.22.: Illustration of the evaluation of the children-specific parameters

Front. The *Pareto Front* is a set of children (solutions) defined as follows: a solution $\mathbf{m}_{\text{child}}^*$ belongs to the *Pareto Front* if and only if there is no other solution $\mathbf{m}_{\text{child}}$ for which the value of the target function and the costs are both smaller than the respective values corresponding to solution $\mathbf{m}_{\text{child}}^*$ [109]. An example of the *Pareto Front* is shown in Figure 5.23.

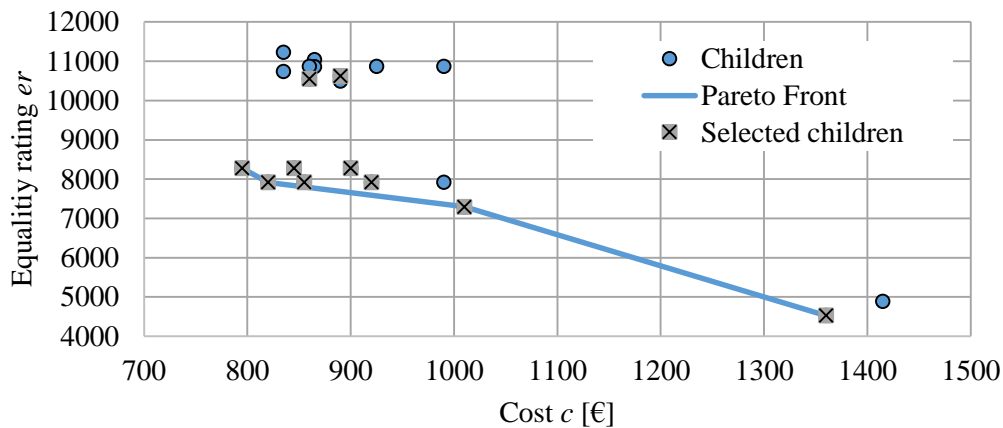


Figure 5.23.: Illustration of the *Pareto Front*

The *Pareto Front* is used to reduce the number of children to the maximum allowed number of parents n_{par} . First, the two extreme points of the *Pareto Front* are selected, the child with the lowest cost and the child with the lowest equality rating [109]. In the second step, out of this *Pareto Front*, a defined number of children are chosen by a random selection. The basis for the probability distribution is a uniform distribution, which is comparable to the random selection of measures in Chapter 5.6.3.3. The uniform distribution is influenced by a weighting

of the child. In this case, the weighting is the distance to the *Pareto Front*. Solutions located on the *Pareto Front* have the lowest distance and will be preferred. However, due to the random selection, solutions which are not directly on the *Pareto Front* can also be selected.

5.6.3.5. Mutation and end-of-iteration criteria

One key point of this approach is that in each iteration step one measure is fixed. A post hoc change of a fixed measure is not possible. To provide some flexibility and allow for changes in already decided measures, a mutation step is included after the selection of the children. This step can allow a solution to leave a local minimum. Here, one of the fixed measures is randomly selected, depending on the weighting of the measure mw . The measure is reset, and the selection process of sub-variants of this measure is investigated again. The cost of the child is set as a reference. If one sub-variant out of the selected measures with a lower cost value is found, then this sub-variant is fixed and defines the new child solution. Otherwise, the reference child is kept. Finally, the selected children represent the new parent solution for the next iteration step.

If a child has an equality rating of zero ($er = 0$), then this solution is saved as one final solution. The loop terminates if n_{par} solutions are found or if the counter of the loop achieves the maximum number of measures n_m . Out of the n_{par} final children solutions, the solution with the lowest total cost is selected and defined as the optimum solution.

5.6.3.6. Validation

As previously discussed in the CBO (see Chapter 5.6.2.8), with this vehicle-based optimization approach the quality of the optimum solution was also checked. The calculation loop to evaluate the global optimum was extended to calculate the cost of each possible combination of measures and identify solutions which achieve all given vehicle targets. The results can be seen in Table 5.8. In the first step, the global optimum was calculated for each vehicle on vehicle level using a time-intensive calculation loop based on a complete enumeration. The results are shown in the second column. In the next step, the optimum solution was calculated using the described vehicle-based optimization, as shown in the third column. The comparison shows that in five out of eight cases, the algorithm found the global optimum.

Table 5.8.: Comparison of the global optimum and optimum solution found by using the optimization algorithm on vehicle level

Vehicle	Global optimum [€]	Optimum found by algorithm [€] (1 st loop)	Optimum found by algorithm [€] (2 nd loop)
#5	775	825	825
#6	455	455	455 ✓
#7	560	630	560 ✓
#8	480	480	480 ✓
#15	420	420	420 ✓
#16	710	710	710 ✓
#17	700	740	700 ✓
#18	600	600	600 ✓

The reason for this can be found in the complexity of the optimization problem, the size of the solution space and the defined convergence time. There is no guarantee that a stochastic optimization will end in a global optimum. Stochastic optimization algorithms can also end in a local optimum. The first optimization loop starts from an initial solution where no measures are defined. The optimization ends in n_{par} solution, where the best is defined as the optimum. This first loop takes the whole solution space into account. One approach which might lead to increased efficiency in the search for an optimal solution over a high dimensional solution space is the clustering of the solution space. The possible solution space has to be reduced step by step. To achieve this, a second optimization loop is integrated. The definition of the initial solution for the second loop is important.

The initial solution for the second loop is based on the results of the selected measures of the first loop. From the first loop, up to n_{par} solutions exist, which differ in the selection of measures. Some selected measures can be found in each solution and some cannot. It is assumed that measures which are selected in each solution are very important. They are selected and fixed as an initial solution for the second loop. This means their status is fixed and can no longer be changed. The second loop now considers the reduced solution space. The results of the second optimization loop are shown in the fourth column of Table 5.8. For two vehicles, an additional improvement is achieved by using this second optimization loop with a reduced solution space.

For vehicle #5, about 8.5 million combinations are available, of which only about 210,000 parameter settings are in the valid solution space. The calculation time for one vehicle using the complete enumeration-based calculation was around 4 hours. The calculation time for the described optimization algorithm was less than 3 minutes, depending on the defined number of parents and children. To evaluate the quality of the solution, the difference between the global optimum and the local optimum identified by the algorithm was analyzed. For this analysis, the cost of each possible solution was computed. The global optimum has a cost of €775, and the worst possible valid solution has a cost of €1870. The optimum solution found by the optimization is €825, which is €50 higher than the global optimum. Compared to the worst solution, 95% of the cost potential is achieved. The calculated percentage of the possible solution over the costs are shown in Figure 5.24. Although the identified solution is €50 worse than the global optimum, the identified solution is the 20th best optimum solution from around 210,000 possible solutions. The optimization approach is capable of finding a solution within 0.01% of the best solutions in this example with a 99% reduction in the computation time.

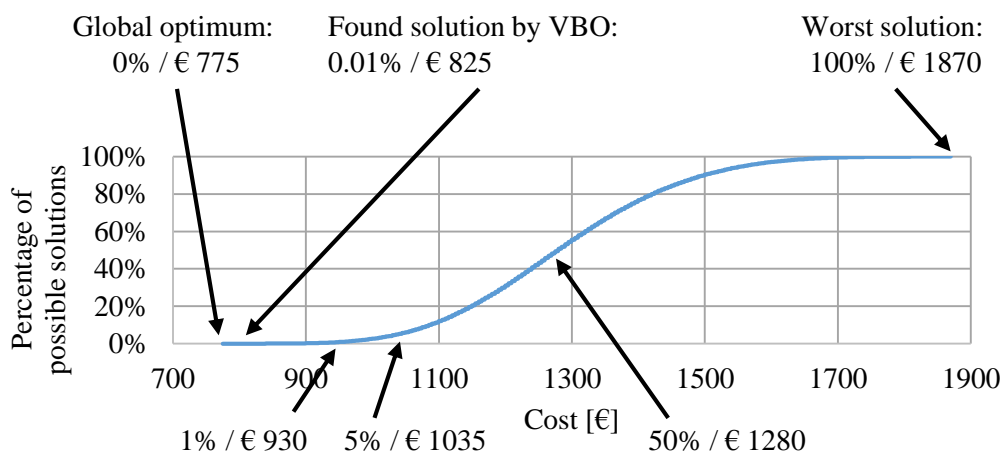


Figure 5.24.: Distribution of possible solutions

Another possible way to reduce the solution space is to fix measures with a high sensitivity and influence in different driving cycles. A high measure sensitivity means, for example, if a transmission type 1 improves CO₂ emissions, but worsens driving performance, and a transmission type 2 improves driving performance, but worsens CO₂ emissions. If such a measure is fixed with a bad sub-variant during the optimization iteration, it is difficult for the optimization to leave a local optimum. In this case, two parallel optimization loops can be executed; for example, one loop with transmission type 1 as a fixed initial solution and the second loop with transmission type 2. Finally, such analyses can prove the validity of the identified optimum and must be compared with expert knowledge. By using such a sensitivity analysis to adapt the sub-variant of the transmission gear ratio of vehicle #5, the optimization algorithm was also able to find this global optimum.

5.6.3.7. Summary

The final approach can be seen in Figure 5.25. From a number n_{par} parents, a set of children are generated by selecting a measure. For each child, characteristic values for the cost and the equality constraint are calculated. These two parameters define a *Pareto Front*. From this front, the best solutions are selected. Next, using a mutation step for each child, one selected measure is changed again. Finally, for every child a check is made to determine if all cycle targets are still attainable. The children are defined as new parents, and the iteration continues. If all cycle targets t_v are achieved, the child is defined as a final solution. If n_{par} final solutions are found, the algorithm ends. The algorithm ends after n_m iteration steps, at the latest.

5.6.4. Fleet-based optimization (FBO)

5.6.4.1. Principle

For the fleet-based algorithm, the same methods as for the VBO are used. A vehicle is defined by driving cycles and targets. A fleet consists of at least two vehicles. Each vehicle is then defined again by targets. So the fleet can also be defined by a set of vehicle targets. Due to this abstraction, the goal of the optimization method is that the difference between one vehicle and a fleet (multiple vehicles) is only the number of cycle-specific targets that have to be handled and achieved.

Compared to the vehicle-based optimization, the fleet-based algorithm has to be extended with the following steps:

- Summarized vehicle targets
- Fleet-average CO₂ emissions targets instead of vehicle-specific targets
- Vehicle-specific measures

5.6.4.2. Summarized targets

The first step is the definition of the targets. Equation 5.18 showed an example of the definition of the targets for one vehicle. For the fleet problem, the target vector t_v has to be extended with other vehicles and driving cycle targets, as shown with an exemplary vector t_f in Equation 5.36.

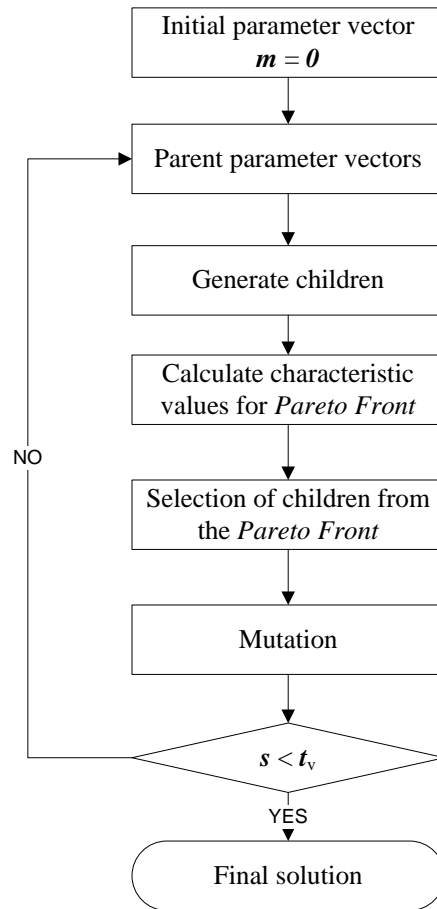


Figure 5.25.: Summary of the optimization algorithm for the vehicle level

$$\mathbf{t}_f = \begin{pmatrix} t_{v_1, c_{NEDC}} \\ t_{v_1, c_{EPA2}} \\ t_{v_1, c_{t.0.100}} \\ t_{v_1, c_{t.80.120}} \\ t_{v_1, c_{vmax}} \\ t_{v_2, c_{NEDC}} \\ t_{v_2, c_{EPA2}} \\ t_{v_2, c_{t.0.100}} \\ t_{v_2, c_{t.80.120}} \\ t_{v_2, c_{vmax}} \\ \dots \\ t_{v_{n_v}, c_{NEDC}} \\ t_{v_{n_v}, c_{EPA2}} \\ t_{v_{n_v}, c_{t.0.100}} \\ t_{v_{n_v}, c_{t.80.120}} \\ t_{v_{n_v}, c_{vmax}} \end{pmatrix} \quad (5.36)$$

5.6.4.3. Fleet-average CO₂ emissions target

The second step is the consideration of the market-specific fleet targets. Chapter 3.2 described the principle fundamentals and influences for the calculation of the fleet CO₂ emissions. The fleet targets are calculated depending on the sales volume, footprint or weight and year. Overlaid on this target is the influence of credits (e.g. ECO innovations, off-cycle credits). The field of application for the optimization can be the consideration of the whole fleet or only a selection of the fleet vehicles. In addition, a vehicle platform can be taken into account. A platform consists of vehicles which share the same technical basis but have different components (e.g. engine, transmission) or different bodies. Here, a difference between the overall fleet and the considered platform has to be taken into account.

If the whole fleet is not considered in the optimization, the fleet-average target has to be broken down to the platform level. This breakdown is shown in Figure 5.26. Considering the footprint or weight and the sales volume, the overall fleet target for a defined year can be calculated according to the regulations. The first influences on the final target are credits for low-emission vehicles, ECO innovations or off-cycle technologies. The second influence is the distribution of the fleet. The fleet-average target has to be balanced between all vehicles and also between the several model platforms based on the sales volume distribution. For example, a compact car with hybrid power-train, whose CO₂ emissions are below its reference target, can compensate for a sports utility vehicle (SUV), whose CO₂ emissions are above the reference target. The target setting for a certain platform can differ. The sales volume and the production time are additional influences. Figure 5.27 illustrates this aspect. The various platforms of a fleet have different production duration, which influences the overall vehicles in the fleet considered for the calculation of the fleet target (e.g. vehicle A is considered from 2015 to 2019). If the task is to develop vehicle C, every model year has to be evaluated. For example, if platform A has a very high CO₂ emission status, the target in 2019 can be stricter than in 2020 because platform C has to compensate for platform A. The target setting for C has to be discussed for every year and must take into account the whole fleet.

Based on this information, the strategy is first to calculate the average fleet target FT_{avg} based on the assumed sales volumes $svol_{total}$ and credits crd . It is assumed that the other vehicles still on the market are fixed with their CO₂ emission status FS_{rmf} . This part of the fleet has a sales volume $svol_{rmf}$. The status of the fleet FS_{rmf} and the fleet-average target FT_{avg} can result in a difference. This difference ΔT_{pf} is the input for the target T_{pf} of the considered platform / vehicles for the optimization problem. The considered platform has a sales volume $svol_{pf}$. The target FT_{pf} reads

$$FT_{pf} = \frac{(FT_{avg} - crd) \cdot svol_{total} - FS_{rmf} * svol_{rmf}}{svol_{pf}} . \quad (5.37)$$

This analysis is performed for every market i_{mkt} and considered year i_y . Thereby, all listed parameters (fleet targets, credits, sales volume) depend on the market and year. The variable ΔT_{pf} is the difference between the average platform target FT_{pf} according to the regulation, depending on the platform-average curb vehicle weight or footprint, and reads

$$\Delta T_{pf} = FT_{pf} + T_{pf} . \quad (5.38)$$

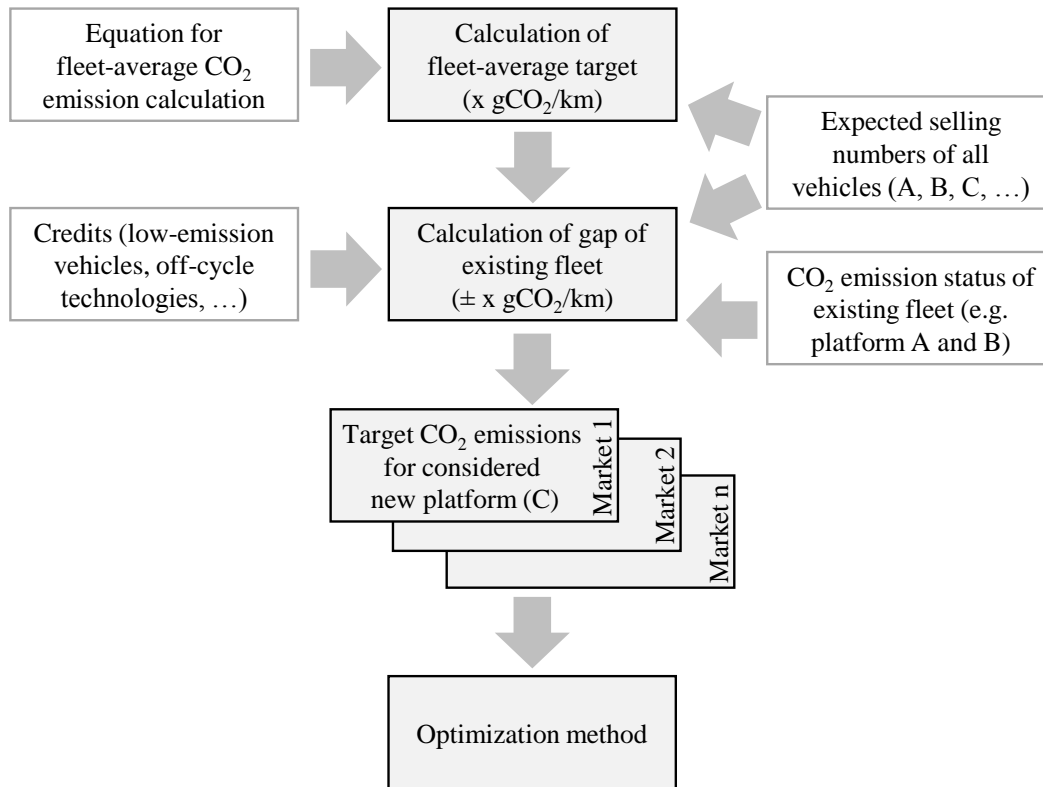


Figure 5.26.: Calculation and breakdown of the fleet-average target to the platform level to be investigated

Figure 5.28 illustrates the difference ΔT_{pf} using an example. The gray solid line shows the theoretical platform-average target FT_{pf} based on the EU fleet regulation, taking only the sales volume and curb weight of the platform vehicles into account. The black dashed line shows the final platform-average target T_{pf} considering a delta from the remaining fleet. Depending on the fleet, the requirement for the platform can be a stricter or a lenient target in comparison to its theoretical legal requirement.

Due to the fleet-average target, the vehicle-specific CO₂ emissions targets are not of primary interest. Thus, the target vector \mathbf{t}_f has to be adapted as described below. The vector \mathbf{t}_f in Equation (5.39) provides an example. All vehicle-specific CO₂ emissions targets are removed. The fleet targets for the markets and years are added to Equation (5.36). For example, $t_{\text{mktEU}, c_{2016_CO_2}}$ stands for the European market and the CO₂ emissions fleet-average target for 2016. If the vehicle-specific targets for CO₂ emissions are of interest, they can remain in the target vector. This can be the case if there is also a vehicle-specific target existing, as it is the case for the Chinese regulation.

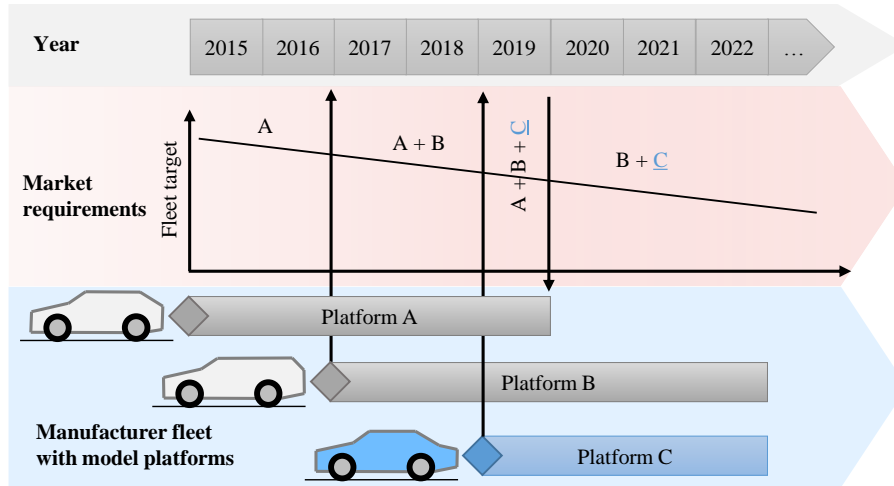


Figure 5.27.: Influence of production duration on the constitution of the fleet-average target calculation

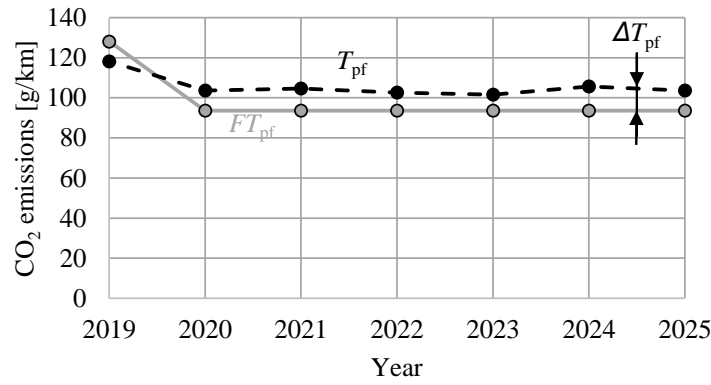


Figure 5.28.: Example of the difference between theoretical legal weight-based reference platform target and selected platform target depending on the remaining fleet

$$\mathbf{t}_f = \begin{pmatrix} t_{v_1, c_{t.0.100}} \\ t_{v_1, c_{t.80.120}} \\ t_{v_1, c_{vmax}} \\ t_{v_2, c_{t.0.100}} \\ t_{v_2, c_{t.80.120}} \\ t_{v_2, c_{vmax}} \\ \dots \\ t_{v_{n_v}, c_{t.0.100}} \\ t_{v_{n_v}, c_{t.80.120}} \\ t_{v_{n_v}, c_{vmax}} \\ t_{mkt_{EU}, c_{2016_CO_2}} \\ t_{mkt_{EU}, c_{2017_CO_2}} \\ \dots \\ t_{mkt_{USA}, c_{2016_GHG}} \\ t_{mkt_{USA}, c_{2017_GHG}} \\ \dots \end{pmatrix}^T \quad (5.39)$$

5.6.4.4. Vehicle-specific measures

Listing 4.4 provided an overview of the definition and description of measures. Two kinds of definitions for the measures are required: first, the differentiation of a measure as a so-called “global” or “local” measure (“*M_global*”); and second, the specification of which vehicles, engines or transmissions a measure is possible for. A measure cannot be used for every vehicle. In the VBO, this influence is not of interest because the possibility of using measures is specified as an input.

According to the first required definition, it has to be specified whether a measure is fleet-global or vehicle-local. Thus, we distinguish between measures to be implemented in all vehicles where the measures are allowed to be implemented or measures that can be implemented individually in a vehicle. For example, a tire selection is vehicle-specific. Different tires can be used for different vehicles. Therefore, the measure of improving the rolling resistance of the tire is also specific for every vehicle. This measure is defined as a local measure. In contrast, an improvement of an engine (e.g. direct injection) is a global measure. The intention here is that all vehicles with the same base engine will be only collectively improved related to measures in the engine. If one vehicle requires an improvement of the engine to achieve its CO₂ emissions target, other vehicles with the same engine must implement this measure as well, which results in a global measure.

Based on this influence, the list of measures and the parameter vector \mathbf{m} have to be adapted, see for example in Equation (5.40). In this case, an engine start-stop and tire rolling resistance are defined as local measures. Thus, they can be selected for every vehicle individually by the optimization algorithm. They have to be extended for every vehicle individually. Weight reduction and direct injection are global measures. They are considered only once because once they are selected, they have to be implemented in every vehicle.

$$\mathbf{m}_f = \begin{pmatrix} s_{\text{ess}, v_1} \\ s_{\text{ess}, v_2} \\ s_{\text{ess}, v_3} \\ s_{\text{wr}, f} \\ s_{\text{trr}, v_1} \\ s_{\text{trr}, v_2} \\ s_{\text{trr}, v_3} \\ s_{\text{di}, e_1} \\ \dots \end{pmatrix} \quad (5.40)$$

Considering the adapted target vector \mathbf{t}_f and parameter vector \mathbf{m}_f , the input data for the optimization also have to be adapted. The costs and influences of the measures have to be adapted according to the sales volume. When considering a fleet target, it is not important how much an engine start-stop system improves one vehicle related to its CO₂ emission and how much it will cost for one vehicle. From this point on, the question is how much the fleet-average CO₂ emissions are improved and what are the additional costs in terms of the complete fleet if the engine start-stop is implemented in vehicle #1. According to Equations (5.41) and (5.42), both the cost c_f and the influence m_Δ of the measures have to be adapted according to the sales volume $svol_m$ where the measure can be implemented and the total sales volume of the whole platform considered $svol_{\text{total}}$.

$$\mathbf{c}_f(i_m) = \mathbf{c}(i_m) \cdot \frac{svol_m(i_m)}{svol_{total}} \quad (5.41)$$

$$\mathbf{m}_{\Delta, f}(i_m) = \mathbf{m}_{\Delta} \cdot \frac{svol_m(i_m)}{svol_{total}} \quad (5.42)$$

5.6.4.5. Post-processing using VBO

The workflow of the VBO described the usage of a second optimization loop so as to find a better solution with a reduced solution space. With the change from vehicle to fleet optimization, the solution space also increases. Here, a second optimization loop can be used as well to reduce the solution space and to help the optimization method find the global optimum efficiently. The basis for the initial solution of the second optimization loop is the differentiation into global and local measures. Out of the optimum solution of the FBO, all global measures are analyzed. The state of the global measures (selected / unselected) is fixed and taken as an initial solution for the second loop. In the second loop, each vehicle is then optimized individually by considering only vehicle-specific measures with the VBO. Global measures which influence certain vehicles are fixed. The selection of local measures is independent between the vehicles. Thus, the solution space is reduced from the whole fleet to local measures of individual vehicles.

5.6.5. Overview of the optimization steps

The last three sub-chapters described the three optimization steps. The steps and their interaction are summarized in Figure 5.29. The cycle-based optimization (CBO) is used if only one vehicle and one driving cycle target are considered. In addition, this method is part of the vehicle-based optimization (VBO) for the evaluation of the characteristic parameters (costs and equality ratio) for the *Pareto Front*. The VBO is used if only one vehicle is to be optimized, but with various driving cycle targets. Finally, the fleet-based optimization (FBO) is used to handle multiple vehicles. As part of the FBO, the VBO is used for a post-processed second optimization loop with a reduced solution space. In Chapter 6, the described optimization approach will be applied to several examples. Different scenarios will be investigated in order to illustrate the multi-level approach.

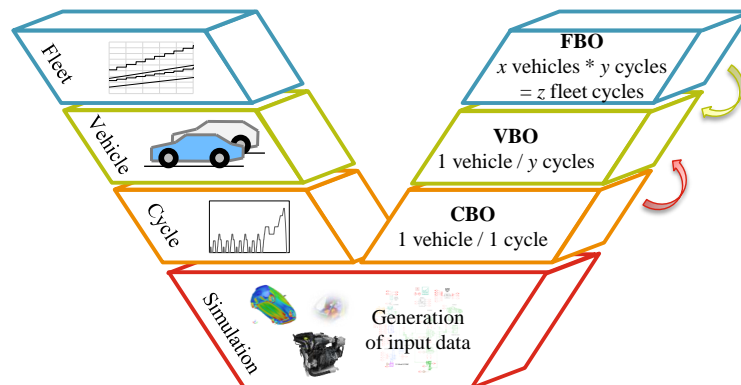


Figure 5.29.: Summary of the optimization steps and their interaction

6. Results

6.1. Definition of the considered vehicles, platform and fleet

In the following sub-chapters the application of the method to fictional vehicles, platforms and fleets will be demonstrated. The selected scenarios are only excerpts of possible applications and are only intended to illustrate the strength of the developed method.

One of the three inputs for the optimization is the vehicle matrix. The vehicle matrix describes the vehicles considered and their characteristic parameters in more detail. The definitions of the vehicles, platforms and fleets are fictional, but should be comparable to real data. To evaluate the application of the optimization algorithm in different scenarios, the fleet must meet the following requirements:

- Different markets: EU, China, USA
- Representative sales volume distribution including the top-selling vehicles in each market
- Consideration of one platform in more detail with various engine / transmission configurations

For the fictional fleet, the EU, China and USA markets were selected. EU and China are chosen because both markets use the same test cycle (NEDC) but have different legal fleet targets for fuel consumption and CO₂ emissions. Moreover, the composition of the typical fleet is also different. The interesting aspect of the EU market is the change of the test driving cycle from the NEDC to the WLTC. The US market was also selected in order to analyze the difference to another driving cycle.

Based on the IHS Sales and Production Database [112], the distribution of the segments and bodies was analyzed. The definition of vehicle segments is based on the car classification of the European Commission [90] [91]. An overview of vehicle segments, including examples, is given in [7]. The international standard *ISO 3833* [12] and the European Commission regulation *EC No. 678/2011* [13] provide the definition for the types of road vehicles (e.g. sedan, station wagon), referred to hereafter as “bodies”. The goal is to find the segment-body configurations with a fleet share of higher than 60%. A vehicle segment divides vehicles into different groups, primarily separated by the vehicle size. The fleet is divided into various segments. A segment can be divided into several bodies. Finally, a segment-body configuration can also consist of different engine-transmission configurations.

Figure 6.1 shows the composition of a typical European fleet with a high variation of segments and bodies. The most important combinations are A-segment hatchback (8%), B-segment hatchback (21%), C-segment hatchback and wagon (19%), C-segment SUV (9%) and C and D-segment VAN (14%). Together, these vehicles represent 71% of the whole fleet. Figure 6.2 shows the composition of a typical US fleet with a smaller variation of segments and bodies. Excluded in this consideration are light-duty trucks. The focus is on passenger cars. The influence of A and B-segment vehicles is negligible. The most important combinations are C-segment sedan and hatchback (22%), C and D-segment SUV (27%) and D-segment sedan (22%). Together,

these vehicles represent 71% of the whole fleet. Finally, Figure 6.3 shows the composition of a typical Chinese fleet, also with a smaller variation of segments and bodies. Excluded in this consideration are the A-segment mini-VANs. Here, the focus is also on passenger cars. The most important combinations are C-segment sedan and hatchback (38%), C and D-segment SUV (14%) and D-segment sedan (12%). Together, these vehicles represent 64% of the whole fleet.

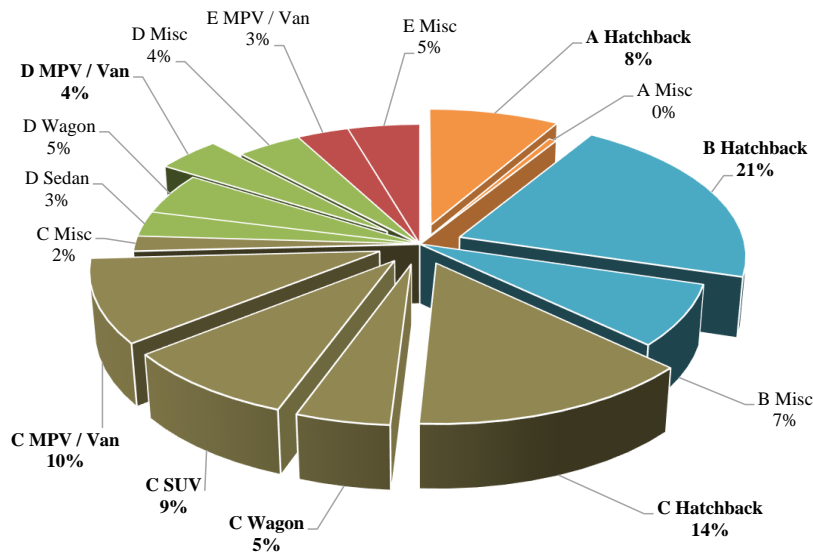


Figure 6.1.: Composition of an average EU fleet of passenger cars

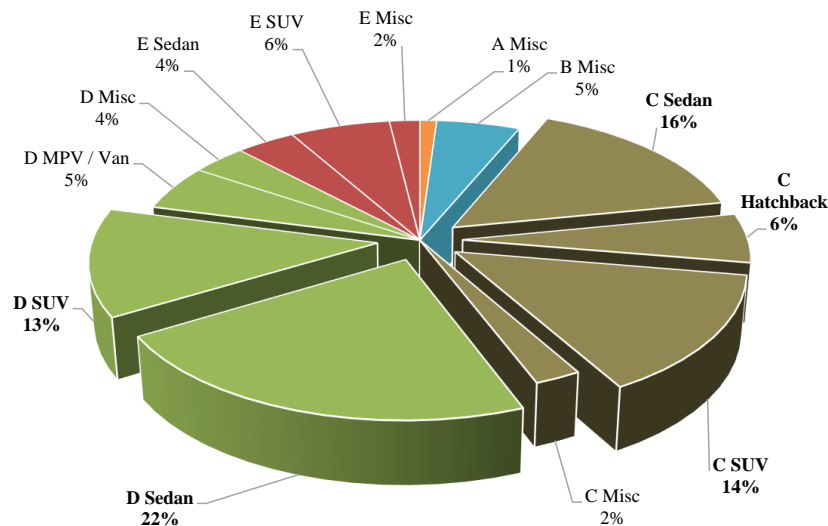


Figure 6.2.: Composition of an average US fleet of passenger cars

For simplification purposes, only one type of body is used for each segment for the following

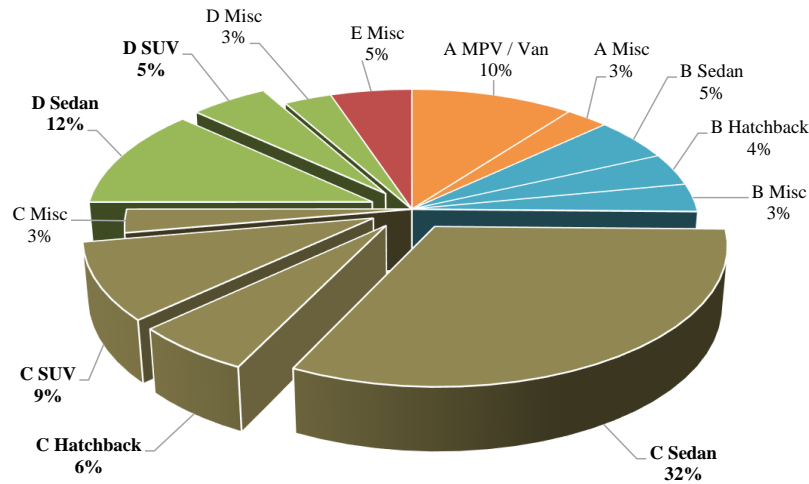


Figure 6.3.: Composition of an average Chinese fleet of passenger cars

investigations. For example, the European C-segment is composed of the hatchback and the wagon. After the selection of the important segments, the next step is to define the engine / transmission configurations. To this end, the production volumes of a global manufacturer that operates on all three considered markets with the chosen segment-body configurations were analyzed. The data on the production volumes is also based on the IHS Sales and Production Database [112]. Out of the sales distribution of the detailed fleet, the typical engine / transmission configurations were selected. The goal is to select a minimum share of 66% of each segment. The result can be seen in Table 6.1. The vehicles are described by the engine type, classified as Diesel engine (D) or gasoline engine (G), the power, and the transmission type, classified as MT or AT.

Analyzing the statistics, it can be seen that many engine / transmission combinations and segments are available in the EU. Both gasoline and Diesel engines are used. The focus on transmission is set to manual transmissions. For C-segment vehicles, the body in Europe is typically a hatchback. In contrast, fewer segments are important in the US and Chinese markets. The typical vehicles are quite similar in both markets. Here, the focus is on gasoline engines with automatic transmission. The typical highest-selling vehicles correlate in the US and Chinese market. A small difference can be found in the amount of engine power. For the C-segment, mostly a sedan body is used here.

In order to analyze a vehicle platform in more detail, the engine / transmission configurations for a European C-segment vehicle were considered, as summarized in Table 6.2. In this example, only one kind of body with different engine / transmission configurations are considered as a platform. A detailed description of the complete fleet and its vehicle parameters is given in Appendix D.1. Below, the vehicles will be numbered consecutively from #1 to #26.

The second input for the optimization are the measures. Measures for reducing CO₂ emissions were already discussed in Chapter 3.3. The measures used for the optimization in the following examples are described in Appendix D.2 in more detail.

Table 6.1.: Composition of the whole fleet including engine / transmission configurations based on data from one manufacturer

A-seg. (hatchback)	B-seg. (hatchback)	C-seg. (hatchback, sedan, wagon)	SUV (C and D-seg.)	D-seg. (sedan)	VAN (C and D-seg.)
EU					
G 60 kW MT (77%)	D 60 kW MT (20%) G 60 kW MT (56%) = 76%	D 80 kW MT (23%) G 100 kW MT (43%) G 130 kW MT (10%) = 76%	D 120 kW MT (43%) D 120 kW AT (17%) G 130 kW MT (27%) = 87%		D 80 kW MT (60%) G 100 kW MT (27%) = 87%
China					
		G 100 kW MT (35%) G 100 kW AT (65%) = 100%	G 220 kW AT (100%)	G 100 kW AT (37%) G 130 kW AT (39%) = 76%	
US					
		G 130 kW AT (76%)	G 220 kW AT (100%)	G 130 kW AT (28%) G 220 kW AT (68%) = 96%	

Table 6.2.: Detailed composition of a European C-segment based on data from one manufacturer

Engine	Transmission	Distribution
D 80 kW	MT	23%
G 100 kW	MT	43%
G 130 kW	MT	10%
D 120 kW	MT	5%
D 120 kW	AT	1%
G 60 kW	MT	5%
G 100 kW	AT	9%
G 130 kW	AT	3%
G 220 kW	MT	1%

6.2. Example: Optimization of a vehicle

The first case study covers the optimization of one vehicle. In different optimization steps, various boundary constraints for the optimization will be considered. The intention is to show that different optimal solutions for the selection of measures will occur depending on the given boundary constraints. To this end, vehicle #5 (C-segment vehicle with 100 kW gasoline engine and manual transmission) is used for the sample application of the cycle- and vehicle-based optimization.

6.2.1. Cycle-based optimization on NEDC

In the first level, only the fuel consumption described by the NEDC is analyzed. No other vehicle attributes are taken into account. Focusing on the NEDC, Figure 6.4 shows the complete walk down chart, starting from the baseline fuel consumption of 7.0 l/100km up to a theoretical potential including all available measures. The measures used and their possible sub-variants are explained in more detail in Appendix D.2. Here, the bars show the maximum range of the sub-variants of the measures. The solid gray bars illustrate benefits, while gray striped bars indicate a negative impact. To calculate the theoretical potential, only the sub-variants with the highest benefit of each measure are used. In this first step of this analysis, no interactions between the measures were considered. The interactions were evaluated using the second simulation loop described in Chapter 5.5. The calculated and summarized interactions are shown with the black dotted bar, which leads to an increase of the theoretical potential. This analysis was performed using the meta-model described in Chapter 5.5. To validate the meta-model, the right black striped bar shows the result of a checking simulation, which considers all of these measures and uses the complex simulation model. The difference between the potential calculated using the meta-model and the simulated potential is around 0.1 l/100km. This value is acceptable considering that this corresponds to 3% of the total potential.

Using the cycle-based optimization procedure (see Chapter 5.6.2.8) the first step is to split the sub-variants and the interactions. Due to the split, the number of total steps increases. The complete extended walk down chart for this vehicle and the measures considered can be seen in Figure 6.5. The steps are sorted by cost ratio. The solid gray bars are steps with a positive effect, and the gray striped bars are steps with a negative impact. The dash-dotted line shows the target, which is set to 5.0 l/100km in this example. The black dotted line indicates the initial solution, based on the sorted cost ratio. It can be seen that this solution leads to a target overfulfillment.

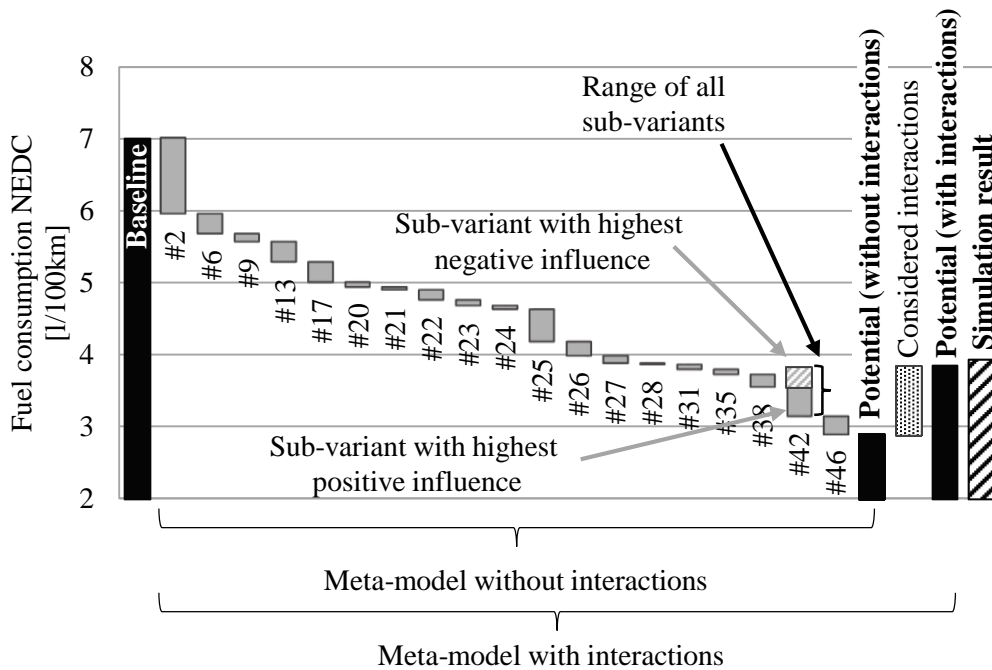


Figure 6.4.: Walk down chart for NEDC from baseline status to the potential

Based on this initial solution, the cycle-based optimization was executed to find a better solution. The solutions derived from the *Pair Exchange* algorithm are described by two parameters: the total costs of the selected measures and the target overfulfillment. The intention is to reduce the costs by minimizing the target overfulfillment, which is illustrated in Figure 6.6. The initial solution has a cost of €890 and a target deviation of around 0.27 l/100km. The optimal solution identified has a cost value of €560 with a target deviation of 0.01 l/100km. In this example, this results in an improvement of €330, or a 37% reduction of cost using the optimization approach for this problem. The NEDC-optimal solution for a given target is shown in Figure 6.7. Measures are added to the initial solution vector until the target is achieved. For a better overview, this figure shows a reduced walk down chart. The measures which are not used in the optimal solution are combined to one bar to show the remaining achievable potential for fuel consumption. In this illustration, the chosen sub-variants are added to the number of the measures.

6.2.2. Sensitivity analysis

Figure 1.4 in Chapter 1.3 explained the usage of the method with respect to the vehicle development process. The intention is to use such an investigation in early development phases when the degree of freedom of components and parameters is high. The advantage is that many measures are still possible. The disadvantages in early development phases are the availability of accurate input data for the simulation model, the limited possibility of validating the simulation with measurements, and the input for cost estimations. These limitations conflict with the demand for exact input values, which are required in order to use a mathematical method. The input data can change over the development time, and the benefit of measures can also depend on the final implementation. As an example, the engine calibration on the real vehicle can have an influence. To quantify such influences in the early development phases, and to evaluate the va-

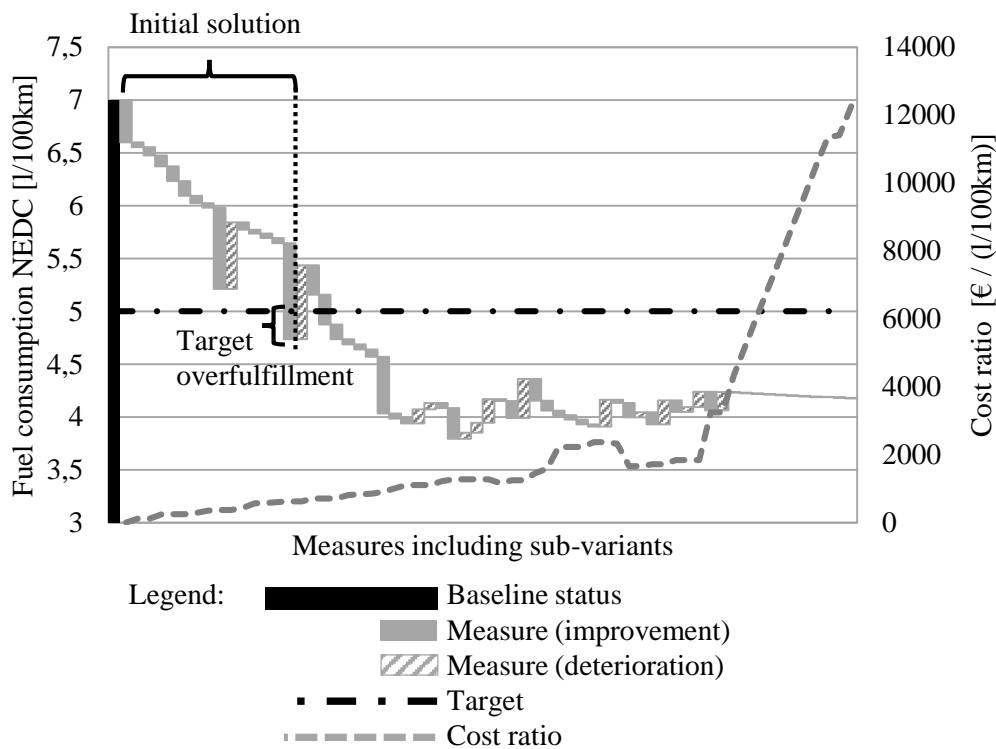


Figure 6.5.: Complete walk down chart including split sub-variants and interactions, sorted by cost ratio

lidity of the identified optimal solution, a sensitivity analysis can be performed. In this example, the sensitivity was defined by varying the following steps:

- Increase / decrease the baseline status by 5% \Rightarrow risk of limited access to input data and vehicle measurements for the model validation
- Increase / decrease the costs of each measure by 20% (each measure was considered in its own calculation loop) \Rightarrow risk of uncertainty of input data
- Increase / decrease the influence of each measure by 20% (each measure was considered in its own calculation loop) \Rightarrow risk of uncertainty of input data
- Omit each measure completely \Rightarrow risk that a measure will be eliminated in a later phase

A separate optimization loop was executed for each of the points listed, and the optimal selection of measures was compared. The result can be seen in Figure 6.8. Measures which are colored in gray with a black frame are selected in every loop. The gray bars without frames represent measures which are not selected in every loop. The percentage value shows how often they are used in all loops. The measures between the baseline and the final status bar are the optimal selection of measures for the initial optimization loop. The analysis of this example can be interpreted as follows:

- 8 out of 11 initially selected measures remain constant
- 1.8 out of 1.9 l/100km reduction of fuel consumption remains constant
- 88% of the estimated cost (from €490 to €560) remains constant

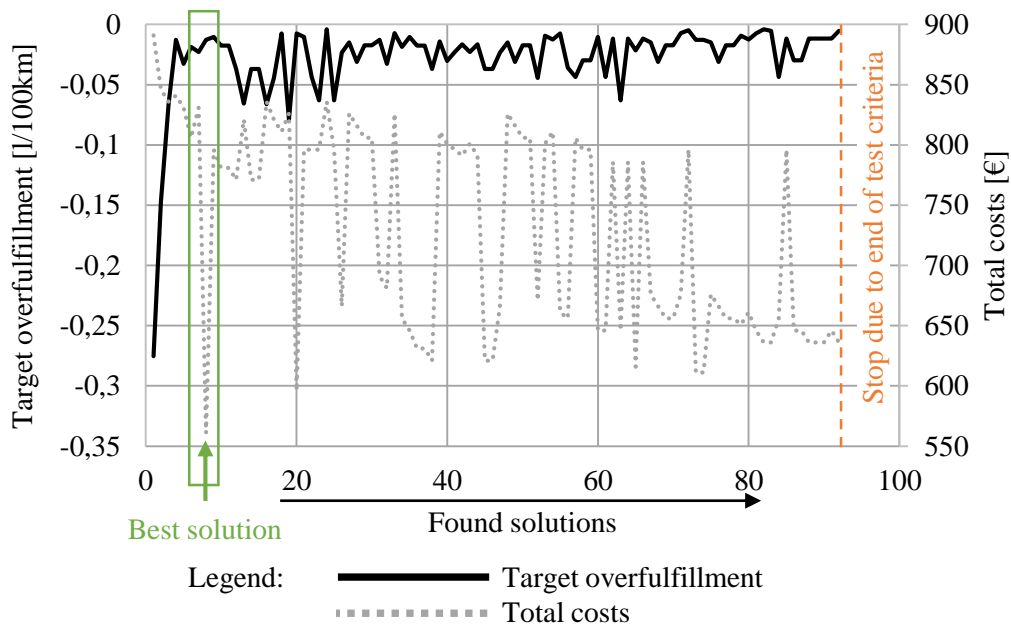


Figure 6.6.: Costs and target overfulfillment of the identified solutions using the *Pair Exchange* approach

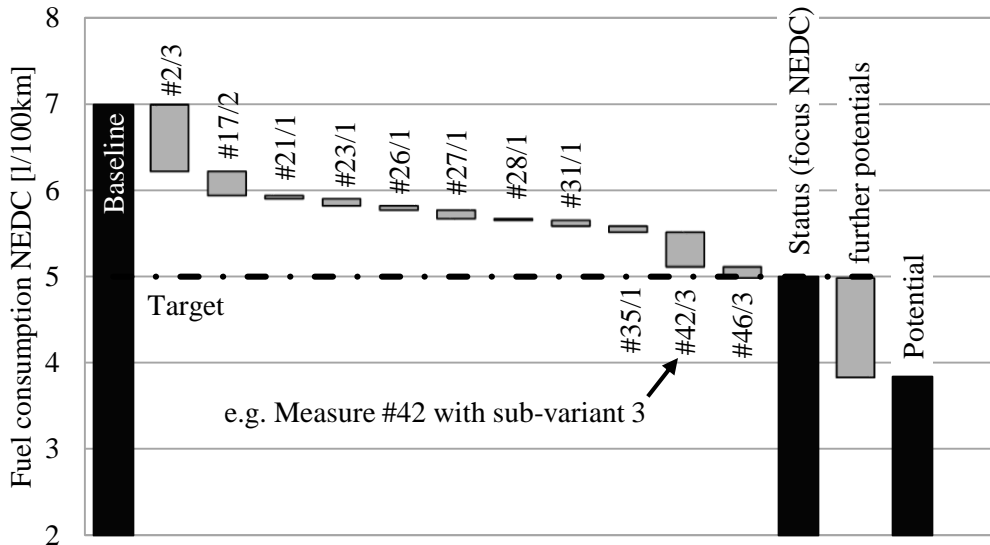


Figure 6.7.: Reduced walk down chart for NEDC from baseline to target with optimized measure selection

Such sensitivity analyses can be used to check the robustness of the solutions in early development phases. In this example, for every measure the same variation range of costs and influence is assumed. In a real vehicle development project, the parameters for the sensitivity analysis can be adapted based on expert knowledge.

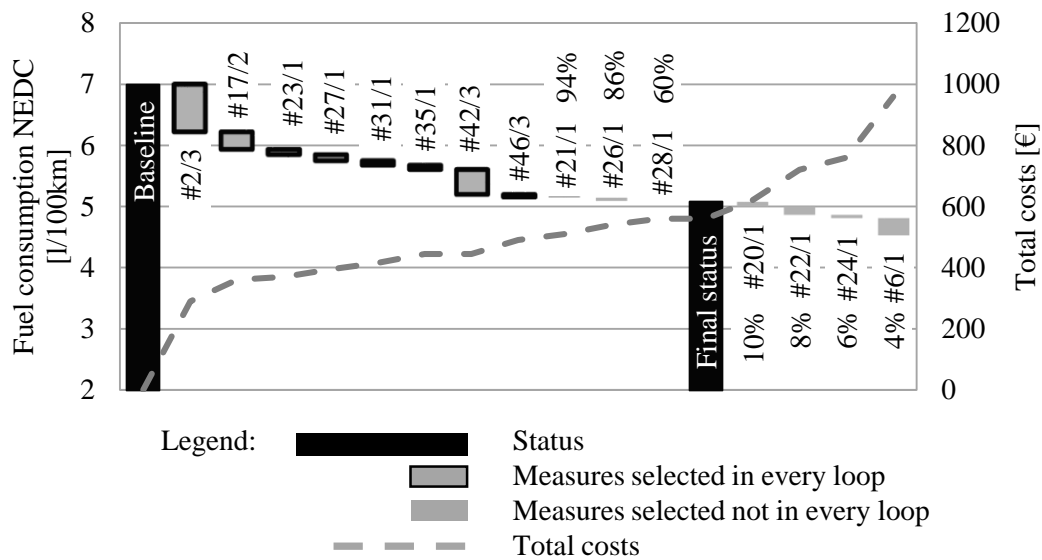


Figure 6.8.: Sensitivity analysis

6.2.3. Effect of NEDC-optimal selection on other cycles

Chapter 5.6.3.7 showed in Figure 5.17 an example of how the NEDC-optimized selection of measures can lead to missing the target on other driving cycles, such as driving performance. A typical example of this involves the transmission gear ratios. A long gear ratio has benefits for fuel consumption, but disadvantages for driving performance. Figure 6.4 already showed the walk down chart for the NEDC down to the theoretical potential including all measures. To complete the picture, Figure 6.9 shows the walk down chart for other driving cycles: acceleration from 0 to 100 kph, passing time from 80 to 120 kph and maximum speed. These walk down charts show which potential is available in the driving cycles. The potential was calculated again by adding each measure, including the interactions analyzed. A checking simulation as performed to validate this meta-model for every cycle with the complex model, as shown in the last bar. In all cycles, the meta-model including all measures shows good accuracy compared to the simulation with the complex model. For example, the difference in diving performance is less than 0.1 s. In this walk down chart, two measures, #38 (weight reduction) and #42 (transmission gear ratio), are of interest for the driving performance due to their high leverage.

Figure 6.7 showed the optimal selection of measures focusing only on NEDC. Based on this selection, the status of the other targets was calculated. The result is shown in Figure 6.10. Starting from the baseline, the NEDC-optimal selection of measures was added to the driving performance cycles, which yields a status value. In addition, the walk down charts show two further status values. First, the penultimate bar shows the remaining potential which enables by the pre-selection of measures. Second, the theoretical potential based on Figure 6.9 is shown in the last bar. This potential is no longer available due to the pre-selection of the NEDC-optimal solution. In this example, the target for each performance attribute is set to the baseline value. This approach means that the optimization of fuel consumption should have no negative impact on driving performance. It can be seen that two performance targets (acceleration from 0 to 100 kph and from 80 to 120 kph) are not achieved. While the acceleration from 0 to 100 kph still has the potential to achieve the target by adding further measures, this will not be possible for the passing time from 80 to 120 kph. The major reason is the selection of measure #42

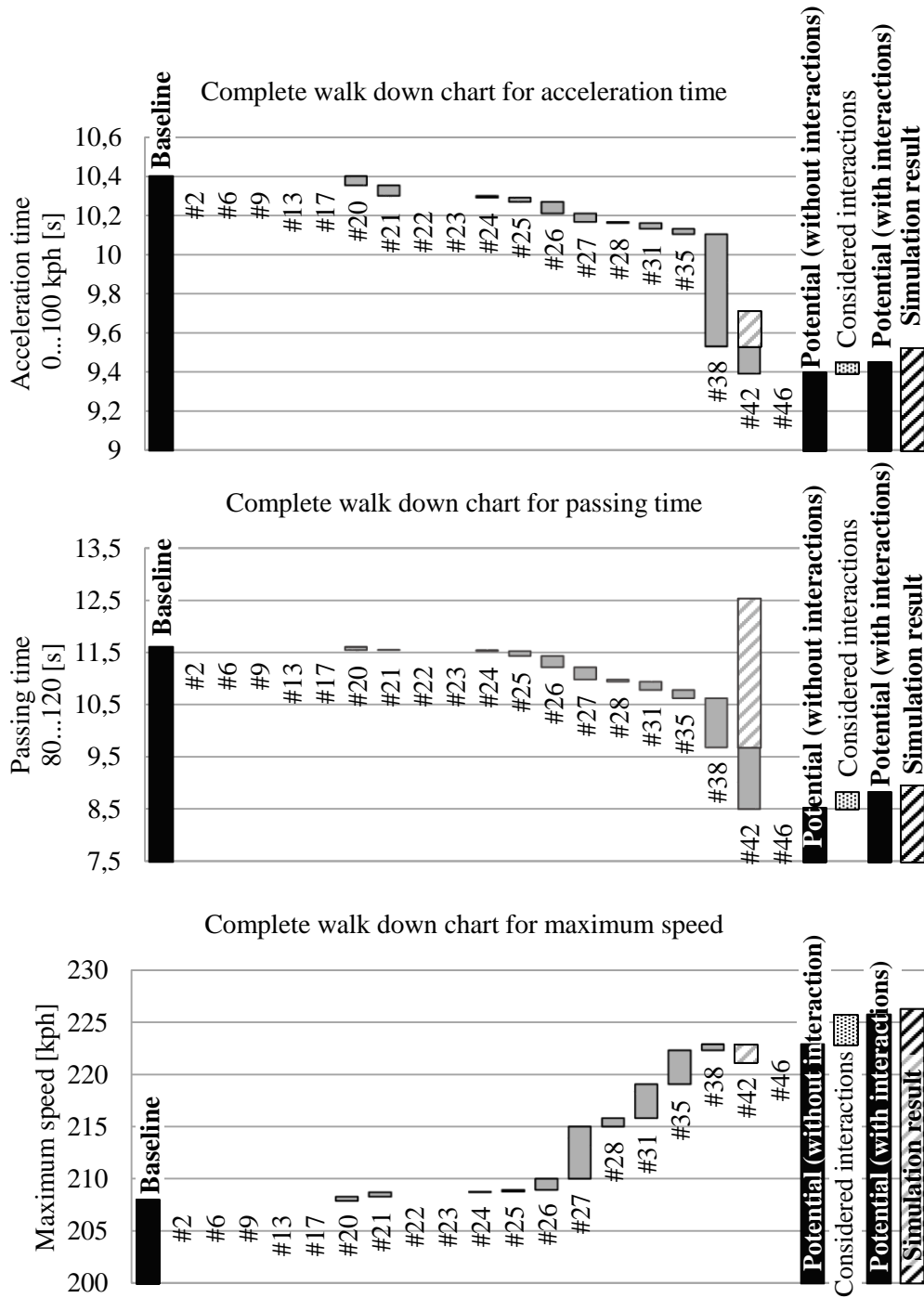


Figure 6.9.: Walk down chart for driving performance targets from baseline status to the theoretical potential

(transmission gear ratio) with sub-variant 3. When focusing only on the NEDC, the transmission will be optimized for fuel consumption, which means selecting a long gear ratio. However, a long gear ratio has a negative impact on driving performance, as it can be seen here. This summary explains why a complete-vehicle approach which takes several targets into account is needed to optimize fuel consumption.

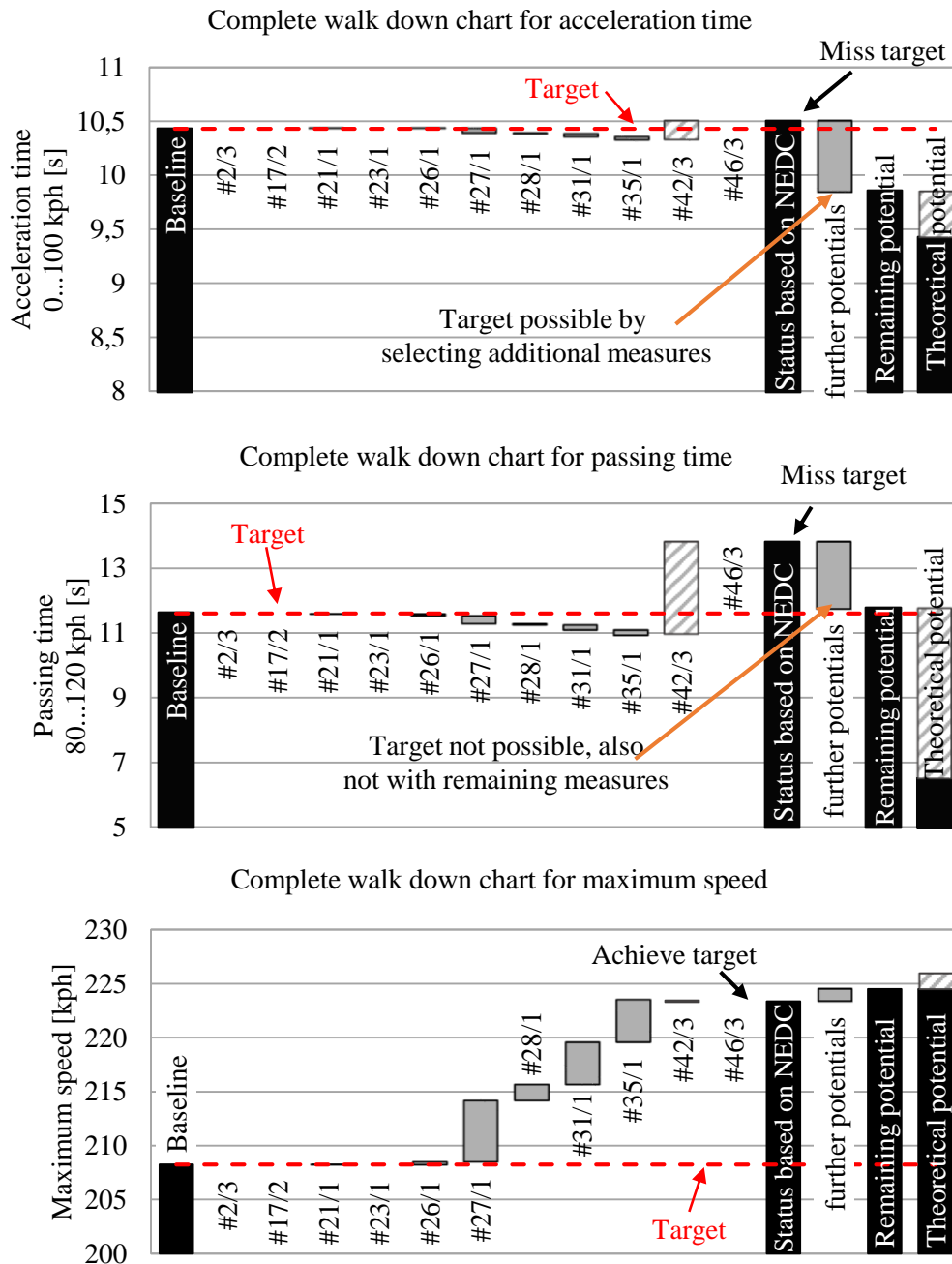


Figure 6.10.: Walk down chart for other performance targets based on NEDC-optimized selection of measures

6.2.4. Vehicle-based optimization

To consider other vehicle targets beside the NEDC, the vehicle-based optimization (see Chapter 5.6.3.7) should be used. In this example, four targets are defined. The targets for the three driving performance cycles are set to the baseline value. This means the optimization of fuel consumption should have no negative impact on driving performance. The results can be seen in Table 6.3. The table shows the selected sub-variants of measures compared between NEDC-based and vehicle-based optimization. Measures marked in gray remain constant, measures

printed in italics changed their sub-variants, and measures in black bold print are new in the vehicle-optimal selection. The results for the driving cycles are shown in the last four lines. In the NEDC-based optimization, two performance targets are not met, which are marked with brackets. In the vehicle-based optimization, all targets are achieved. The last two columns show the delta between the NEDC-optimal selection of measures and the vehicle-optimal selection in the driving cycles for the NEDC and the passing time. The largest deviation between target and status can be found in the passing time from 80 to 120 kph. The difference is around 2.2 s starting from the NEDC-optimized solution. In order to compensate for this difference, the vehicle-based optimization selects other measures. Improvements in passing time are obtained by adding measures #26, #38 and #42. In contrast, the changed transmission ratio (measure #42) has a negative impact on fuel consumption, which has to be compensated for. Thus, to achieve the NEDC target again, additional measures (#22 and #24) are selected. The altered selection of measures results in a cost increase of €200 in this example.

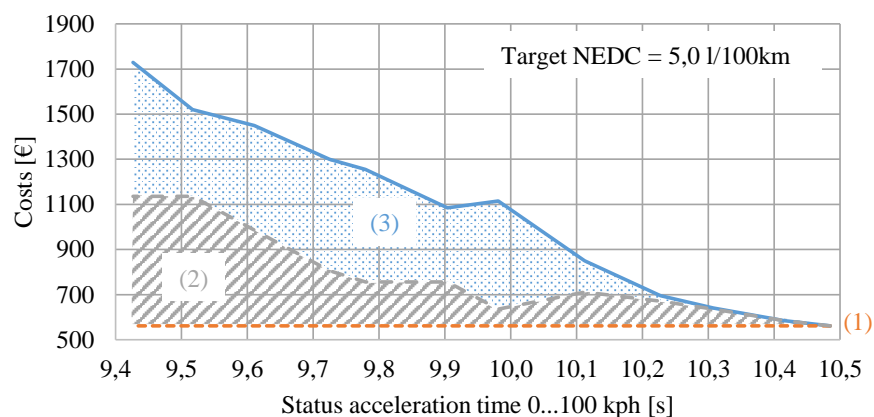
Table 6.3.: Comparison of the NEDC-based and vehicle-based optimization

Optimization level / Measure	NEDC-optimized sub-variants	Vehicle-optimized sub-variants	Influence on NEDC [l/100km]	Influence on passing time [s]
#2	3	3		
#17	2	2		
#21	1	1		
#22	-	1	-0.14	-
#23	1	1		
#24	-	1	-0.05	-
#26	1	2	-0.05	-0.1
#27	1	1		
#28	1	1		
#31	1	1		
#35	1	1		
#38	-	1	-	-0.1
#42	3	2	+0.24	-2.0
#46	3	3		
Total costs [€]	560	760		
NEDC [l/100km] target = 5.0	5.0	5.0		
Acc 0 ... 100 kph [s] target = 10.4	(10.5)	10.4		
Acc 80 ... 120 kph [s] target = 11.6	(13.8)	11.6		
Max speed [s] target = 208	223	222		

6.2.5. Influence of target setting

The previous chapter showed an example of how the selection of measures changes when the goal is to avoid a negative impact on driving performance. The focus to this point was on improving

fuel consumption. As another task, the additional improvement of the driving performance can be considered. In this example, the starting point is the solution presented in the previous chapter. The target for the NEDC remains constant at 5.0 l/100km. In the next step, the target for the driving performance from 0 ... 100 kph is reduced step by step to the minimal possible value. In each step, the vehicle-based optimization loop is executed to analyze the influence on the selection of measures. The results can be seen in Figure 6.11. In this figure, measures #38 (weight reduction) and #42 (transmission gear ratio) are highlighted. Both measures have a higher influence on driving performance than the others (see Figure 6.9). In addition, as the performance target decreases, these measures become more and more important, while the costs increase. The upper diagram in Figure 6.11 shows different portions of costs. The dashed line on the bottom (1) is the reference cost without considering the performance targets. The gray striped area (2) shows the influence of the cost due to weight reduction. The blue dotted area (3) shows the costs of the additional required measure. In summary, the optimal selection of measures and the resulting costs are highly dependent on the given vehicle targets.



Acc. time [s]	Selected measures																	
	2	6	13	17	20	21	22	23	24	25	26	27	28	31	35	38	42	46
10,5	3	0	0	2	0	1	0	1	0	0	2	1	0	1	1	0	3	2
10,4	3	0	0	2	0	1	0	1	0	0	1	1	0	1	1	2	3	3
10,3	3	0	0	2	0	2	0	1	0	0	1	1	0	1	1	3	3	3
10,2	3	0	0	2	1	2	0	1	0	0	1	1	0	1	1	4	3	1
10,1	3	0	0	1	1	2	0	1	0	0	4	1	0	1	1	5	3	1
10,0	3	1	1	2	1	1	0	1	0	0	2	1	0	1	1	3	1	3
9,9	3	1	0	2	1	2	0	1	0	0	3	1	0	1	1	6	0	2
9,8	3	1	1	2	1	2	0	1	0	0	2	1	1	1	1	6	1	2
9,7	3	1	0	2	1	2	1	1	1	0	3	1	0	1	1	7	1	3
9,6	3	1	1	2	1	2	0	1	0	0	1	1	0	1	1	10	1	3
9,5	3	0	1	2	1	2	1	1	0	0	1	1	1	1	1	12	1	3
9,4	3	0	0	2	1	2	0	0	1	4	4	1	1	1	1	12	1	1

Figure 6.11.: Impact on costs and selection of measures with relation to the acceleration time target

6.2.6. Discussion of the results

These scenarios show that the optimal selection of measures and the resulting costs are highly dependent on the given boundary constraints. In this case, the boundary constraints were defined only for the vehicle targets in the first step.

6.3. Example: Optimization of a platform

The previous chapter explained the application of the optimization approach on one vehicle. The next step is to extend the usage to more than one vehicle. The minimum example of using multiple vehicles is the consideration of a vehicle platform. In this example, all C-segment vehicles sold in the EU market are used (see vehicle description in Appendix D.1). Overall, nine vehicles with different engine / transmission configurations and sales volumes are considered. The following example illustrates how the selection of measures changes from vehicle-specific optimization to a platform optimization. Here, the following influences and steps are considered:

1. Including global measures
2. Including a sales volume distribution
3. Removing the vehicle-specific CO₂ emissions targets by replacing them with one overall platform-average CO₂ emissions target

Furthermore, three additional scenarios will be discussed in this case study. The influence on the optimal solution due to the change of the CO₂ emission-related driving cycle from the NEDC to the WLTC will be analyzed. When considering a fleet, another interesting question is the distribution of the vehicle-specific CO₂ emission targets derived from the fleet-average target. In the case of a newly available technology, the change of this distribution for an optimal solution will be discussed. The last example is an investigation of the overall production time. Since a vehicle platform is in production for more than one year, a defined time period and the fleet-average CO₂ emissions target of several years have to be met. A reduction of the target from year to year is expected. In addition, the application of the optimization algorithm for this influence will be checked.

6.3.1. Transition from vehicle to platform level

The transition from individual vehicles to multiple vehicles changes the primary optimization target. All legal regulations for CO₂ emissions or fuel economy are based on a fleet-average target. The platform-average status value of the simulated C-segment vehicles for CO₂ emissions is 159.2 g/km. Based on the defined curb vehicle weight of the vehicle, the theoretical platform-average target is 93.3 gCO₂/km in 2022, in accordance with the sales volume distribution shown in Table D.2 in Appendix D.1. Taking into account an assumed given fictional offset of 28.4 gCO₂/km from the remaining fleet, the target for the platform is defined as 121.7 gCO₂/km in this case study. Figure 6.12 shows the baseline status of the platform vehicles with the blue bubbles with a solid frame. The size of the bubbles represents the sales volume distribution. The red dashed line is the mass-dependent reference target, including the defined offset. The arrow shows the platform-average baseline status and target. The green bubbles with a dashed frame show the specified initial vehicle-specific targets. In the first approach, the goal is to reduce the CO₂ emissions of all vehicles by the same relative amount.

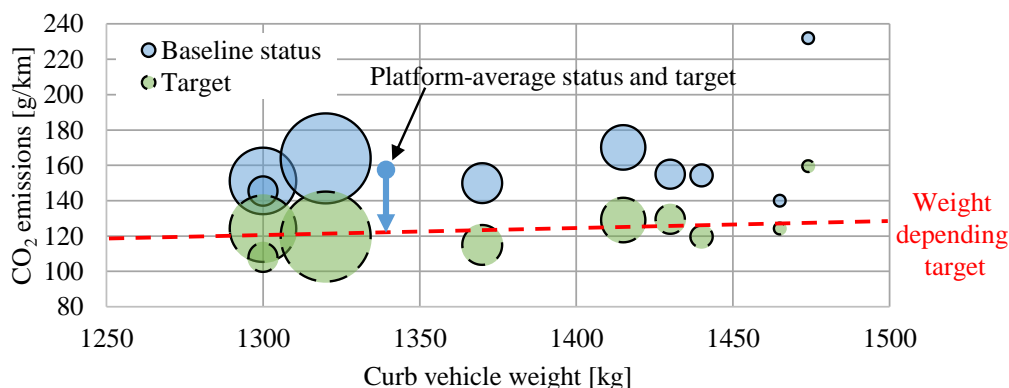


Figure 6.12.: Distribution of the vehicles of the platform and the defined platform-average target

Five optimization steps were analyzed with this platform. The differences and boundary constraints of the optimization steps are summarized in Table 6.4.

Table 6.4.: Boundary constraints of the optimization steps considered

Step	1	2	3	4	5
NEDC target of individual vehicles	x	x	x	x	
NEDC platform-average target					x
Performance targets of individual vehicles		x	x	x	x
Differentiation into global / local measures			x	x	x
Sales volume distribution				x	x
Optimization step used	CBO	VBO	FBO	FBO	FBO

In the first step (1), each vehicle was optimized individually. The focus was on the cycle-based optimization to achieve only the NEDC target. This restriction leads to the best possible costs because no boundary constraints were considered. In order to evaluate this solution in the context of other vehicle targets, the statuses of the performance cycles were calculated with the NEDC-optimal solution vector. The actual statuses of the performance targets were compared to their baseline statuses. The goal of this comparison is to ensure that the improvement of CO₂ emissions has no negative impact on driving performance. The detailed statuses of the driving cycles can be seen in Table E.6 in Appendix E.3. It is obvious that two out of nine acceleration time targets and eight out of nine passing time targets are not met.

Considering the unmet performance targets as boundary constraints, the optimization level was extended to the vehicle-based optimization including the NEDC and the performance targets in the next step (2). In this step, each vehicle was still optimized individually. The targets for the driving performances were set to the baseline values. In this vehicle-based analysis, all performance targets are achieved. The next boundary constraint is the consideration of interactions between vehicles in form of global measures. To this end, the measure vectors of all vehicle were compared. When considering interactions between vehicles, the differentiation of the measures into global and local measures is important. Local measures are technologies which can be specified for every vehicle individually. In contrast, global measures are selected out of a modular assembly (e.g. engine). These global measures and the selected sub-variants have to be the same in all vehicles considered. The detailed results are shown in Table E.7 in

Appendix E.3. By analyzing the selection of the global measures of the parameter vectors of the vehicles, it is evident that seven out of 15 global measures have a different selection in the sub-variants.

With the transition from the vehicle-specific consideration to the fleet-based optimization, the common selection of sub-variants of global measures is important. In the third step (3), the vehicle-specific optimization was extended to the fleet-based optimization. Here, the sales volume distribution was not considered in step (3), but it was considered in the fourth step (4).

For the introduction of the fleet optimization, the targets for the CO₂ emissions must also be discussed. The target is a fleet-average CO₂ emission value, weighted by sales volume distribution and the curb vehicle weights of the vehicles. To reduce the overall platform-average costs and improve the selection of measures, the target for each vehicle can vary. This was done in the last optimization step (5). The vehicle-specific CO₂ emissions targets were replaced by one platform-average target. The solution of this fleet-based optimization leads to another status and distribution of the vehicle-specific CO₂ emissions targets. More detailed results can be found in Table E.8 in Appendix E.3.

For all five optimization steps, the costs of the selected measures are analyzed and summarized in Figure 6.13. The vehicle-specific costs are shown in the gray lines, and the fleet-average costs per vehicle are shown in the black line. It can be seen that the fleet-average costs increase from step 1 to step 4 as a result of additional boundary constraints. These boundary constraints lead to different required selections of measures. In this context, the largest influence was the consideration of other vehicle attributes from step 1 to 2. However, the inclusion of the global measures and the sales volume as a weighting will also increase the costs. The last optimization step for including the fleet-average target will improve the fleet-average cost. The targets of the various vehicles are changed so as to improve the optimal selection of measures with respect to the overall fleet costs. For some vehicles, the target becomes more strict, and the costs increase, while other vehicles end up with less strict targets with lower costs. The reason for this can be found by analyzing the specific costs, as shown in Figure 6.14. According to Equation (6.1), the specific costs c_{spec} are the relation of the total costs to the reduction of CO₂ emissions including all selected measures \mathbf{m} . In this figure, it can be seen that the specific costs become more equal across all vehicles. While the ratio of the specific costs in step (4) ranges from 11 to 40 € per gCO₂/km, the range in step (5) is reduced from 9 to 27. The remaining differences result from the measures available for each vehicle and the consideration of the vehicle performance targets, which must also be achieved in the fleet optimization.

$$c_{\text{spec}} = \frac{\sum_{i_m=1}^{n_m} (\mathbf{M}_c(i_m, \mathbf{m}(i_m)))}{\sum_{i_m=1}^{n_m} (\mathbf{M}_\Delta(i_m, \mathbf{m}(i_m)))} \quad (6.1)$$

Finally, the impact of the fleet-average-based derivation of the vehicle-specific status is highlighted in Figure 6.15. In addition to Figure 6.12, this figure shows vehicle targets derived by the fleet-based method in the red bubbles with the dotted frame. Comparing the green dashed bubbles of the initial target setting (step (1) to (4)) with the red dotted bubbles of the fleet-optimized target (step (5)), a change in the targets can be seen.

Based on this information, an interesting question is whether the focus on the reduction of the fleet-average CO₂ emissions can be placed on the top-selling vehicles or if all vehicles have to be taken into account and improved. Figure 6.16 shows the correlation between the reduction of CO₂ emissions for each vehicle based on the fleet-average optimization. The reduction shown is the difference between the baseline status and the fleet-optimized target for each vehicle after

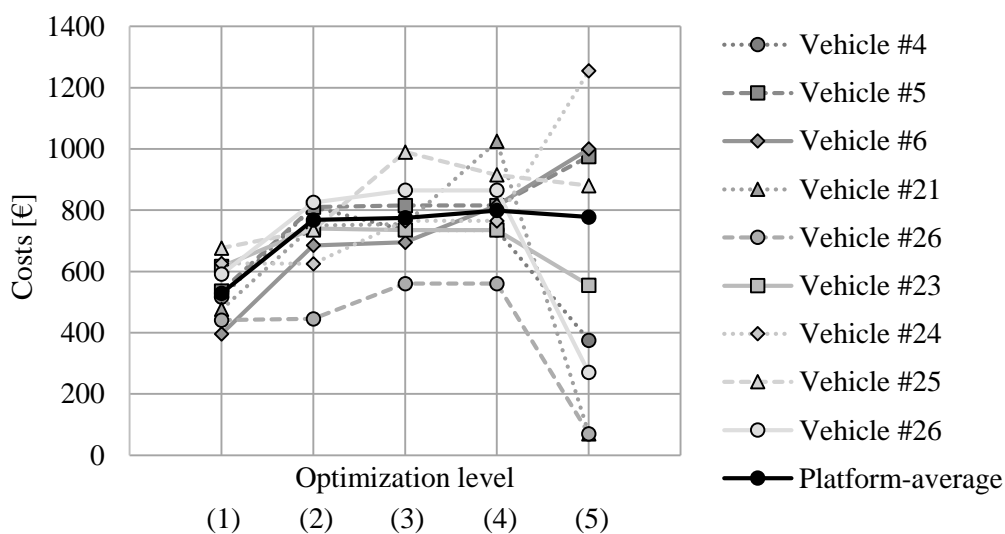


Figure 6.13.: Vehicle and platform-average costs depending on optimization level

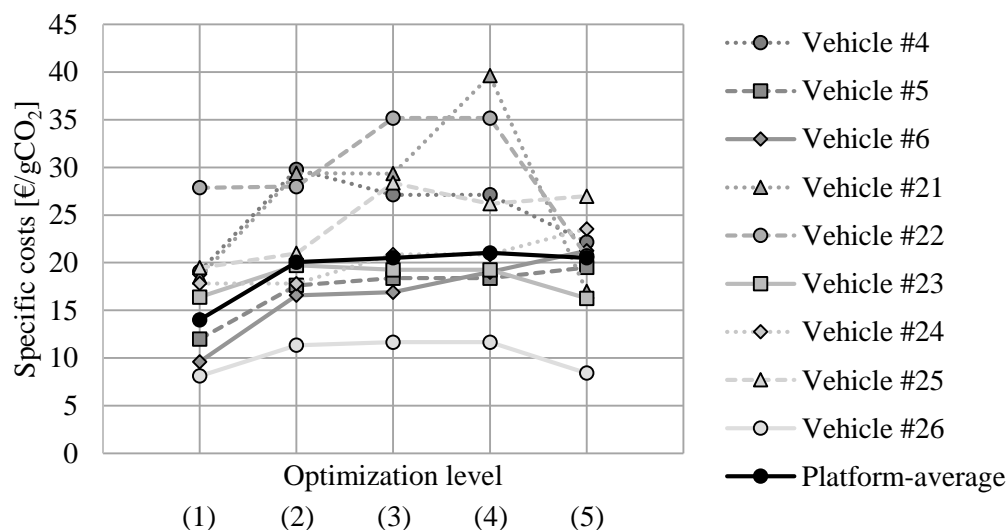


Figure 6.14.: Vehicle and platform-average specific costs depending on optimization level

the application of the FBO according to Figure 6.15. Based on the data points, two linear regression lines are shown in the figure: a solid line for gasoline vehicles and a dashed line for Diesel vehicles. Because the regression lines have an increasing behavior, an approximate correlation of the reduction of CO₂ emissions and sales volume can be seen in this example. The reason for this is related to the weighting of measures. Measures used for a vehicle with a high sales volume have a higher leverage on the fleet-average target and will be selected with a higher priority by the optimization algorithm. A higher difference can be found when comparing gasoline and Diesel engines. The reason is the availability of measures for reducing CO₂ emissions. As shown in Chapters 3.3.3.1 and 3.3.3.2, gasoline engines still have a higher potential to improve engine efficiency. In contrast, the improvement of Diesel engines is limited, so fewer measures are available in this example.

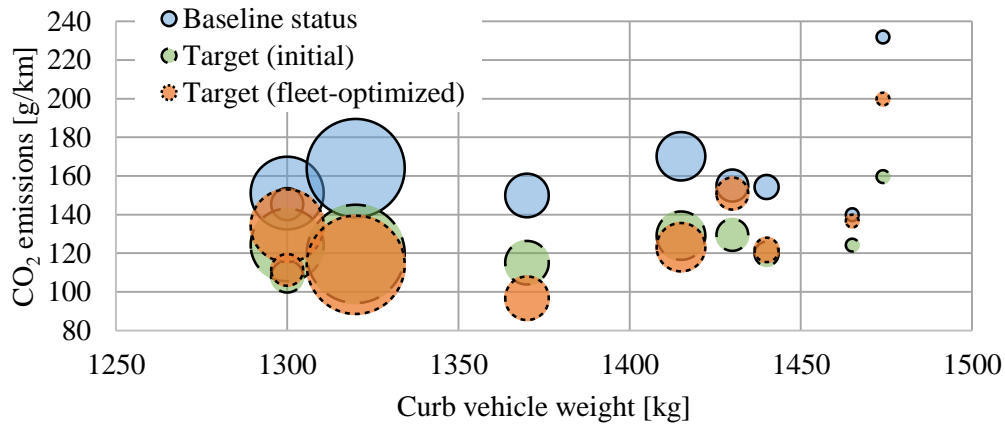


Figure 6.15.: Distribution of the platform-vehicles' baseline statuses, the platform-vehicles' initial targets and the platform-vehicles' optimized targets

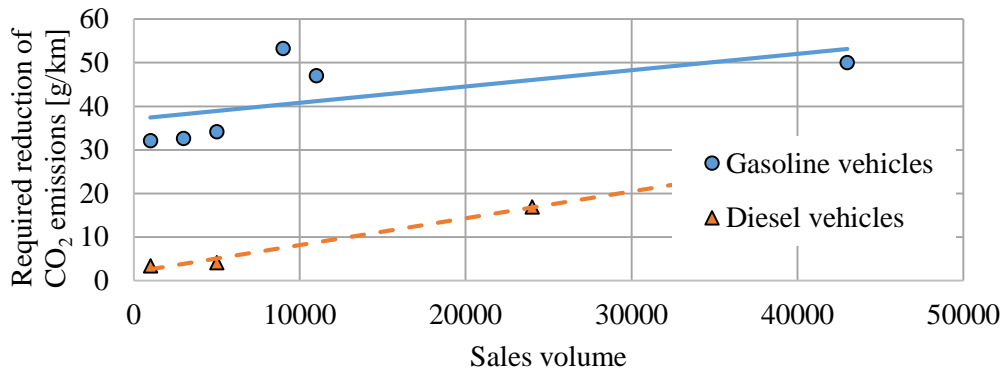


Figure 6.16.: Reduced CO₂ emissions depending on the sales volume using the fleet-based optimization based on a platform-average target

6.3.2. Influence on the optimal solution for NEDC vs WLTC

In the EU, the test cycle and test procedure for the evaluation of CO₂ emissions will change from the NEDC to the WLTC. This example investigates the usage of the algorithm to analyze this influence related to the achievement of the fleet target for CO₂ emissions. The fleet-based optimization with a fleet-average CO₂ emissions target was executed once using the NEDC and once using the WLTC. Table D.1 in Appendix D.1 shows in the baseline results for both the NEDC and the WLTC for every European vehicle. It can be seen that in this fictional fleet, the status for the WLTC is often lower than the NEDC status. This also leads to a lower fleet-average CO₂ emission status of 143.4 g/km for the WLTC compared to 159.2 g/km for the NEDC. Due to the lower required CO₂ emission reduction, using the same platform-average target of 121.7 g/km in both cases also decreases the costs for achieving the target. Fewer measures are required in the case of the WLTC. The cost for the optimum selection to achieve the fleet-average target decreases from €778 for the NEDC to €546 for the WLTC.

Using the NEDC as a reference for the CO₂ emissions optimization, the baseline status of 159.2 g/km and the target of 121.7 g/km lead to a delta of 37.5 g/km. In a second comparison, the target for the WLTC investigation is now reduced to the same delta of 37.5 g/km.

Based on the baseline status of 143.4 g/km, the new fleet-average target for the WLTC is set to 105.9 g/km. As a result, the cost for the target achievement increases from €778 per vehicle for the NEDC-based fleet-average optimization to €1167 per vehicle for the WLTC-based fleet-average optimization. There are two reasons for this change. The first reason is the difference between the CO₂ emissions benefits of the measures. Figure 4.2 in Chapter 4.2 already emphasized that the aerodynamic potential can be different for each driving cycle, for example. Due to the changes in the benefit, the prioritization of measures also changes. The optimal parameter vectors of the NEDC and WLTC differ mainly in the following parameters:

- Reduced implementation of engine start-stop system and generator control: Lower vehicle standstill time in the WLTC and the correction of the battery energy balance results in less influence in the WLTC.
- Increased implementation of aerodynamic measures: Due to the higher maximum and average speeds, the aerodynamics have a bigger influence.
- Higher weight reduction: Due to the fact that the WLTC has no test weight classes, every kg of weight reduction is noticeable in CO₂ emissions.
- Different gear ratio selection: Due to the vehicle-specific adaptation of the gear-shifting for manual transmission, the tendency towards a longer gear ratio to reduce fuel consumption is not pronounced in the WLTC, as is the case in the NEDC.

Because the costs of the measures themselves remain constant, the cost ratio of each measure will change due to the altered influence. Based on the altered cost ratio of each measure, a different optimal parameter vector will be available in the WLTC than that available in the NEDC.

The second reason can be found in the different baseline statuses and theoretical potentials in the driving cycles. Figure 6.17 shows the difference between NEDC and WLTC for each vehicle in the platform. The comparison is based on two reference values. The value “100%” represents the baseline status in the NEDC of each vehicle. The value “0%” is the theoretical potential for improving CO₂ emissions in the NEDC. The change of the driving cycle will first change the baseline status. The solid light gray bars show an improvement in the baseline status, and the black striped bars show an increase in the baseline status. In addition, due to the changed benefits of each measure, the theoretical potential will also change. In this case, the potential decreases for every vehicle shown with the light gray striped bars. The solid black bar in between shows the remaining potential for the WLTC. For example, for vehicle #4 the NEDC has 100% as a reference. Due to the decrease in the baseline status and the increase in the potential in the WLTC, only around 60% remains. In this example, the potential is reduced for all vehicles in the WLTC. This means that to achieve the same absolute amount of reduction as the NEDC, more measures have to be implemented into the WLTC vehicles. Ultimately, this leads to an increase in costs.

In summary, no general statement about the effect of the change from the NEDC to the WLTC can be made out of this analysis. The only rationale is that the prioritization of measures will change due to the changed benefit for CO₂ emissions. This rationale is also verified by expert analysis of the simulation results, which validates the method. The outcome of this example is that changing the baseline status and target has a higher influence on the selection of measures than changing of the driving cycle.

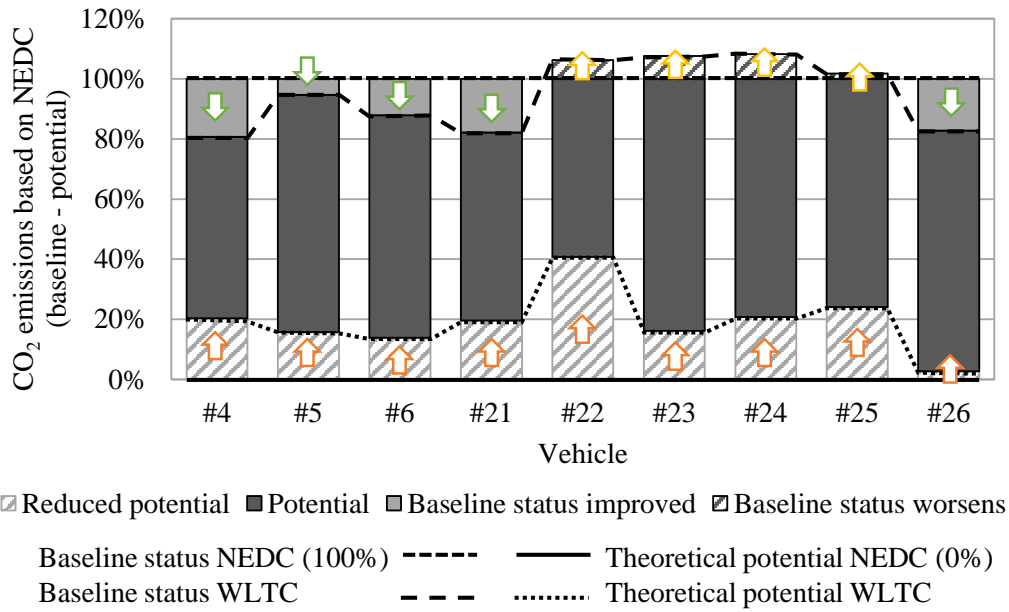


Figure 6.17.: Comparison of baseline status and potential of CO₂ emissions of NEDC and WLTC

6.3.3. Influence of new technologies

The optimization method can also be used to analyze the potential of new technologies to improve CO₂ emissions. A current well-discussed measure is the influence of a 48-V-mild hybridization to achieve the fleet target. In this analysis, the measure for a 48-V-mild-hybrid will be included as available measure for every vehicle. The measure for the mild-hybrid is defined with three sub-variants for different parallel architectures (P0, P1 and P2). The intention is to investigate how the selection of measures and the target setting of the vehicle-specific CO₂ emissions will be altered. Using the new measures, the fleet-based optimization of the platform was executed. In addition to the analysis in Chapter 6.3.1, this example is defined as step (5*). The results of this analysis are shown in Figure 6.18, which is the extension of Figure 6.15 with the results including the new measure. The figure shows three groups: the baseline status in the blue bubbles with the solid frame, the fleet-optimized target setting (without consideration of 48-V-mild-hybrid) in the red bubbles with the dotted frame, and the fleet-optimized target setting (with consideration of 48-V-mild-hybrid technology as possible measure) in the gray bubbles with the dashed frame. The result of the optimization shows that the measure of a 48-V-mild-hybrid system is selected in only one of the nine vehicles. This vehicle is the top-selling vehicle #5. The reduction in CO₂ emissions due to the 48-V-mild-hybrid potential multiplied by the high sales volume leads to a high leverage in the fleet-average calculation. The required CO₂ emissions reduction for the other vehicles can be reduced, which leads to fewer measures required to fulfill the targets. The result for the costs of each vehicle can be seen in Figure 6.19. On the one hand, due to the integration of the 48-V-mild-hybrid system, the costs of vehicle #5 increases. On the other hand, due to the lower required reduction of the other vehicles, their costs are reduced. Overall, the fleet-average costs decrease from €778 to €765 in this example.

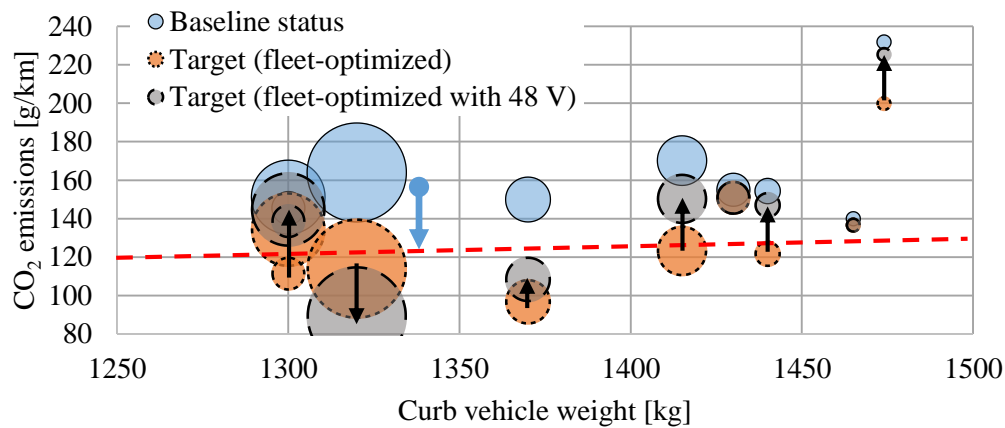


Figure 6.18.: Target breakdown of the vehicle-specific CO₂ emissions of the platform with a 48 V hybridization as an additional measure

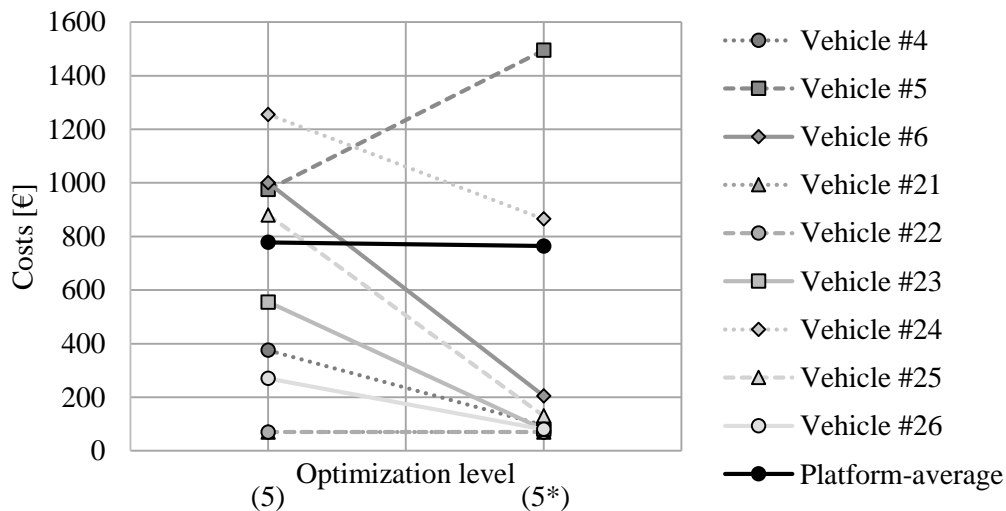


Figure 6.19.: Costs of vehicles and platform-average costs depending on optimization level, including the 48-V-mild-hybrid potential

6.3.4. Influence of sales volume by year

The previous optimization examples focused on one fleet-average target for one year. Depending on the market and the fleet sales distribution, the target can change depending on the year of production of a platform. In addition, both the sales volume distribution and the start of production of the various platform vehicles can vary depending on the year. In this context, the algorithm is also able to account for such an optimization challenge. In this example, the sales volume was changed over a time period of six years. The assumed sales volume distribution is shown in Table D.2 in Appendix D.1. Instead of one fleet target, six fleet-average CO₂ emissions targets are now defined for each year. The result is illustrated in Figure 6.20. The black dotted line shows the fleet-average baseline status depending on the year. Because the sales volume of each vehicle changes every year, the fleet-average status also varies. For each year, a target was defined, indicated with the black solid line. In this study, the target was reduced every year by 2 gCO₂/km. This target provides the input for the optimization algorithm. The resulting

average status after the optimization is shown with the black dashed line. The algorithm tries so select the measures to achieve the target in every year. The strictest target is in 2025. Meeting the target in 2025 also leads to the status in other years being below the target. This leads to a target overfulfillment, as indicated by the solid gray area. The solid gray line shows the vehicle-average costs by year. The gray square shows the reference considering only the target for 2022. This target was selected in the previous analysis in the optimization step 5 in Figure 6.13. It can be seen that meeting the target over several years will increase the costs again. The reason for this is the target achievement for 2025. As this selection of measures influences the selection for 2022 and the other years, the overall production time period has to be taken into account for the optimal selection of measures.

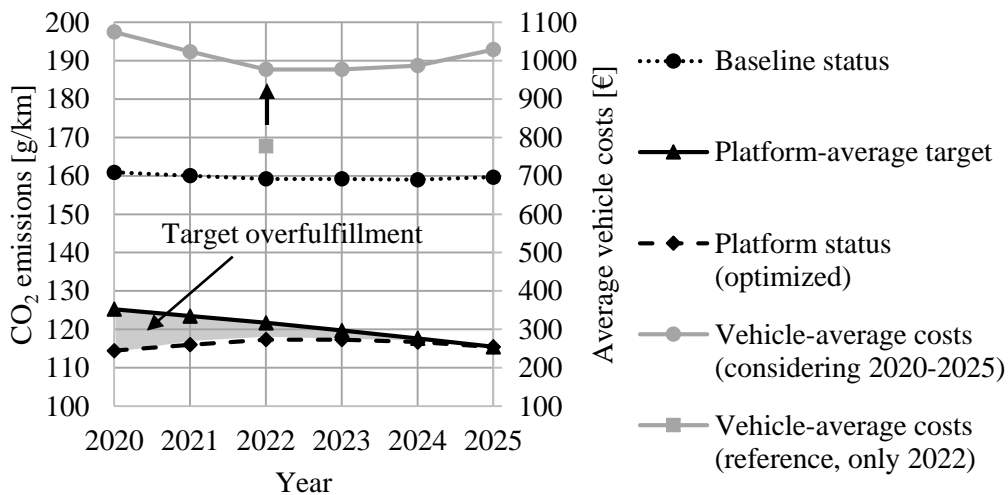


Figure 6.20.: CO₂ emissions baseline status, targets and expected costs depending on year

6.3.5. Discussion of the results

In summary, the results of these case studies prove the statements of the results of Chapter 6.2. The optimal selection of measures depends on the defined boundary constraints. These examples focused on the boundary constraints of the whole fleet. Both the optimal selection of measures and the vehicle-specific target setting of CO₂ emissions are highly dependent on the baseline status, the fleet-average target, sales volume distribution and the measures available for each vehicle.

Another conclusion related to the validity of the optimization algorithm is the prioritization of measures in the context of a sales volume distribution. The sales volume distribution changes the weighting of measures. A measure which to be implemented in a vehicle with a high sales volume will be preferred over other measures with an approximately equal cost ratio. Thus, the improvement of vehicles with a high sales volume will be prioritized when using this FBO algorithm.

6.4. Example: Optimization of a fleet

This example covers a fleet consisting of different segments for the European, US and Chinese markets. Two case studies are considered. For the first study, the focus is only on the European

vehicles. The intention is to analyze the selection of measures and the target breakdown of the CO₂ emissions from the fleet-average target to vehicle-specific targets in the context of different segments. The second study considers the partial fleet of the three markets in a holistic context. The goal is to analyze how the targets of different markets and the interactions between vehicles influence the selection of measures.

6.4.1. Interactions due to different segments

In the first step, only the European vehicles are considered. The fleet consists of eleven vehicles out of the complete fleet of vehicles #1 to #20. The detailed configuration can be found in Appendix D.1. The focus was on achieving the fleet-average CO₂ emissions target. The boundary constraint was defined such that the improvement of CO₂ emissions for every vehicle should have no negative impact on the vehicle-specific driving performances. The sales-weighted baseline status of the fleet is 157 gCO₂/km. The fleet-average target was set to 122.7 gCO₂/km.

Figure 6.21 shows the result of the fleet-based optimization. The baseline status of each vehicle is illustrated with the blue bubbles with a solid frame, and the derived vehicle targets that lead to the achievement of the given fleet-average target are shown with the red bubbles with a dotted frame. The dashed line shows the weight-dependent target based on the EU fleet regulation and a given offset. The arrow shows the fleet-average baseline value of 157 gCO₂/km. The fleet-average target is set to 122.7 gCO₂/km, which corresponds to a reduction of 50% compared to the total potential for implementing all measures.

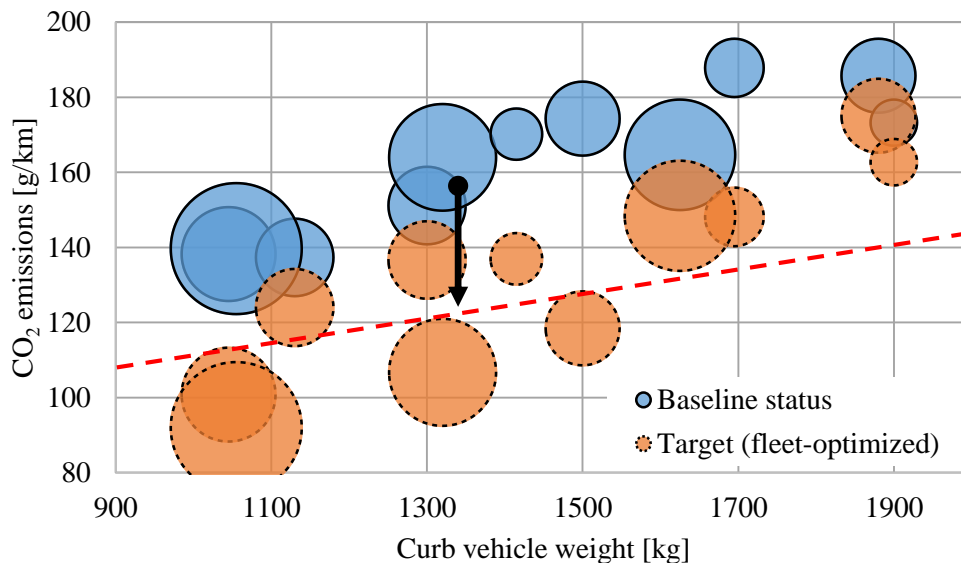


Figure 6.21.: Vehicle status and target based on fleet-average target breakdown

The result of the required reduction of CO₂ emissions depending on the segment is shown in Figure 6.22. The result is comparable to the example of the platform optimization (see Chapter 6.3.1). A small correlation with the sales volume is noticeable. Therefore, a linear regression with the solid line for gasoline vehicles and the dashed line for Diesel vehicles is shown. A higher differentiation between Diesel and gasoline vehicles can be seen due to the higher number of possible measures for gasoline vehicles, as already discussed in Chapter 6.3.1 (see Figure 6.16).

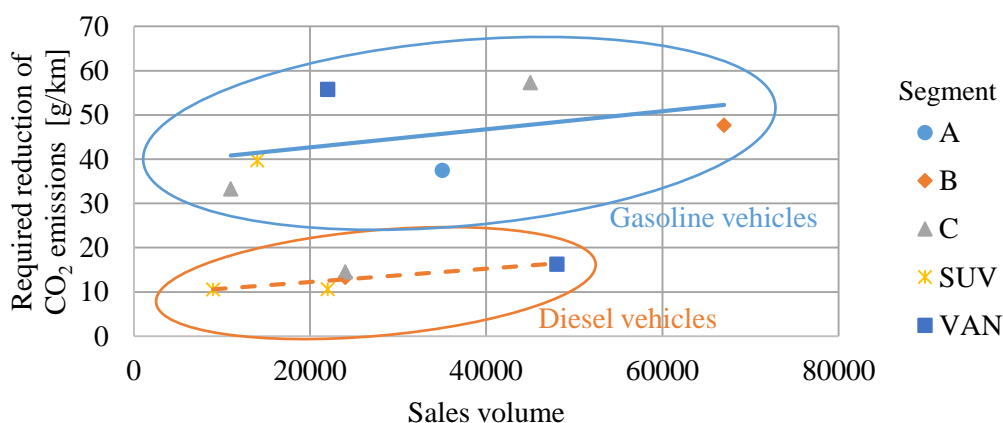


Figure 6.22.: Required reduction of CO₂ emissions depending on sales volume of the vehicles with a focus on comparing segments

6.4.2. Interactions due to different markets

In the final step, the fleet was extended to the three markets. This fleet now consists of twenty vehicles. The detailed configuration can be found in Appendix D.1. From this list, vehicles #1 to #20 were used, consisting of eleven vehicles for the EU market, five vehicles for the Chinese market and four vehicles for the US market. The challenge in this example is related to the different legal regulations. Both the starting point and the market-specific fleet-average targets are different. Table 6.5 shows a summarized comparison. In this example, an equal reduction in all markets was specified.

Table 6.5.: Comparison of the baselines and targets of the three markets considered

Market	EU	CN	US
Number of vehicles	11	5	4
Fleet-average baseline status	157.0 gCO ₂ /km	7.3 l/100km	285.3 gCO ₂ /mi
Defined fleet-average target	122.7 gCO ₂ /km	5.6 l/100km	217.7 gCO ₂ /mi
Required reduction	-34.3 gCO ₂ /km (-23%)	-1.7 l/100km (-23%)	-65.4 gCO ₂ /mi (-23%)
Average status after optimization	122.7 gCO ₂ /km	5.6 l/100km	217.7 gCO ₂ /mi

To show the influence resulting for the different markets, on the first level each market was optimized individually. This first level did not consider interactions for the selection of measures between the vehicles of different markets. However, because the selection of global measures also has an influence between vehicles on certain markets, this influence also has to be considered. Therefore, on the second level all three markets were optimized in one optimization loop. The result for the selection of global measures can be seen in Table 6.6. This table focuses only

on the comparison of global measures; local measures are not shown. The columns show the number of measures defined as global. The three columns in the middle show the results for the market-specific optimizations for the EU, China and US. The last column shows the result of the complete-fleet optimization, including the interactions between all markets. The measures where the selection of the market-specific optimization is equal to the fleet optimization are marked in gray. The numbers show the selected sub-variants in columns two to four. A dash (“-”) means that this measure is not used in any vehicle for this market or that it is only available for one vehicle. As a result, it can be seen that 19 out of 33 measures correlate. For the other 14 measures, differences between the individual market optimizations and the complete-fleet optimization occur. Thus, the task of the optimization loop including all markets is to adjust the global measures for each vehicle.

Based on this adjustment, Figure 6.23 shows the impact on the vehicle-average cost to achieve the given targets. The change from market-specific optimization (1) to complete-fleet optimization (2) will increase the cost due to the alignment of global measures. The gray lines show the various markets, and the black line shows the overall fleet-average cost.

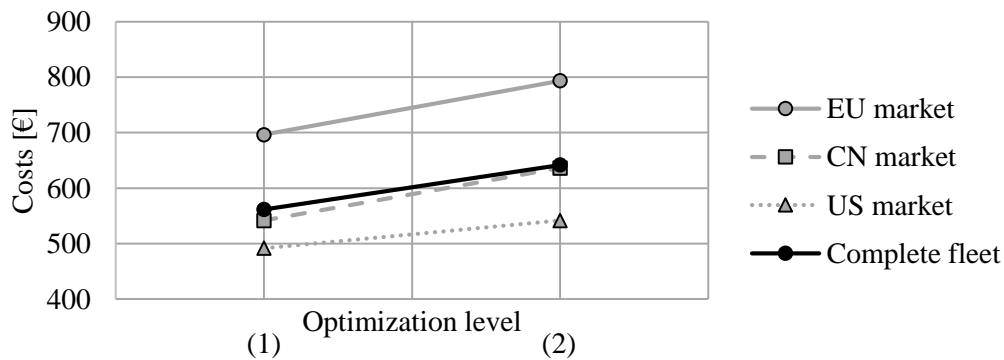


Figure 6.23.: Vehicle-average costs by fleet optimization level

6.4.3. Discussion of the results

The examples in this sub-chapter also validate the statements about the results of Chapters 6.2 and 6.3. The optimal selection of measures depends on the defined boundary constraints. In these case studies, the focus was set to the selection of global measures in the context of a larger fleet sold in various markets. In this way, it is proven that for a certain development project, the whole vehicle fleet has to be taken into account, including boundary constraints, in order to achieve the fleet emissions targets with optimized costs.

Table 6.6.: Number of selected global measures depending on fleet-optimization level

Measure	EU only	CN only	US only	Overall
# 1	3	-	-	4
# 2	3	3	-	3
# 3	1	-	1	0
# 4	-	-	1	1
# 5	0	-	-	1
# 6	1	0	-	0
# 7	-	-	0	0
# 8	-	-	2	2
# 9	0	0	-	0
# 10	0	-	0	0
# 11	-	-	0	0
# 12	1	-	-	1
# 13	1	0	-	1
# 14	1	-	0	0
# 15	-	-	0	0
# 16	2	-	-	2
# 17	2	2	-	2
# 18	2	-	2	2
# 19	-	-	2	2
# 21	1	0	0	0
# 22	1	0	0	0
# 23	1	1	1	1
# 30	1	-	-	1
# 31	1	1	-	1
# 32	1	-	-	1
# 33	-	1	0	1
# 34	1	-	-	1
# 35	1	1	0	1
# 37	1	-	-	0
# 38	2	0	-	0
# 39	0	-	-	4
# 40	-	0	0	0
# 41	1	-	-	0

7. Discussion

Practical benefit and results

The state-of-the-art analysis (Chapter 2) described the missing link in the available literature between the achievement of the fleet-average CO₂ emissions targets and the optimization of a specific vehicle in terms of costs. The question of how to provide this link by using simulation techniques and an optimization method was the major motivation for this thesis. In summary, the following points were defined for improving the state-of-the-art:

- Combine the high-level strategy for achieving the fleet-average CO₂ emissions targets with the analysis of specific vehicles
- Consider boundary constraints, such as avoiding negative impact on driving performance
- Reduce vehicle and total-fleet costs as the major optimization goal
- Derive an optimization approach and show the need for this approach

Based on the state-of-the-art analysis, no comparable method was found in the literature which could be used as starting point. Therefore, the task was to develop an approach to solve the challenges listed. The points mentioned and goals of this thesis were implemented by using a simulation environment and an optimization algorithm, as described in detail in Chapters 4 and 5. Chapters 6.2 to 6.4 show several cases for the application of the developed optimization approach. The major intention of the case studies, other than to validate the functionality of the developed optimization approach, is to show the need for such a complex tool in terms of future practical applications. Thus, Figure 6.13, for instance, highlights the influence on the expected costs due to different optimization levels. The greatest influence on the costs and optimal selection of measures results from considering additional vehicle attributes, such as driving performance. However, the differentiation into global and local measures and the sales volume distribution also have an influence. Finally, the target breakdown from a fleet-average target to vehicle-specific targets also influences the costs and therefore needs to be optimized. The studies also show that no general tendency for the target breakdown of the CO₂ emissions target is noticeable (e.g. see Figure 6.22). One obvious tendency is that top-selling vehicles are preferred for the reduction of CO₂ emissions related to the fleet-average target. However, as discussed in Chapter 6.3.5, this effect is caused by the principle of the algorithm, which selects measures with a high influence on many measures with a higher probability. The overall conclusion from the all examples is that the optimal selection and combination of measures to achieve the optimal costs is highly dependent on the given boundary constraints. For example, since the selection of a gear ratio or weight reduction can have an effect on a given driving performance target, the optimal selection differs when considering additional targets. These selected examples highlight the need to apply the developed optimization approach. The cost-optimum selection of measures for specific vehicles can vary depending on additional vehicle attributes, global measures and fleet influences. No general statement in terms of general high-level analyses about an optimum solution could be derived and transferred to other vehicle selections. The selection of measures has to be analyzed for every vehicle, platform or fleet configuration individually based on the available measures

and boundary constraints, which demonstrates the need for the application of such a complex method.

Quality assessment of the developed method

The developed method consists of two parts: the simulation and the optimization.

The simulation is needed to evaluate the input data for the optimization. The physics behind the simulation of CO₂ emissions and driving performance have already been amply discussed in the literature. In this thesis, a commercial tool was used for the simulation. The baseline simulation model with the given input data was validated with measurements on a test bench and on the test track. The validity of the simulation model was validated and achieved with good accuracy. The question for the accuracy of a development project is more related to the input data than to the simulation model. The accuracy is only as good as the input data. To provide accurate simulation results for further vehicle projects, an individual validation of the baseline model is needed in each case. This prerequisite is usually fulfilled, since the majority of vehicle development projects generate validated simulation models. Thereafter, the focus was set on the adaptation of the simulation model to evaluate the influence of common measures for the reduction of CO₂ emissions. At the beginning of the project, the plan was to check some adapted features of the simulation model (e.g. start-stop system, generator control) with measurements as well. However, the vehicles and equipment required for the measurements were not available in time. Thus, one remaining point for the simulation model is the validation of the measures implemented in the model.

The next point related to the simulation is handling the large amount of input data and simulation runs. Each measure has to be simulated for each combination of each vehicle and driving cycle. Here, the fact that each measure has to be evaluated for each vehicle is important. No general statement can be made about the benefits of measures. This was demonstrated by two examples: the influence of an engine start-stop system (see Figure 4.1) and aerodynamics (see Figure 4.2). The influences are quite different to the values proposed in the literature as those from the simulations of various vehicles. Therefore, to prepare accurate input data for the optimization, a vehicle-specific evaluation of measures is needed. This yields a 3-dimensional simulation matrix. Depending on the number of vehicles, cycles and measures, up to several hundred simulation runs are required. It is not possible to handle such a high number of simulation runs without automation, which necessitated the programming of an automated model environment. The vehicles, driving cycles and measures to be considered have to be defined in scripts. Once programmed, the script will automatically run all defined combinations. Thus, the simulation runs can be executed without further user interaction, which provides advantages in the prevention of user input error, automatic documentation of the simulation results and a time benefit for the user.

To create the optimization algorithm, common optimization methods for other automotive applications were analyzed. After the abstraction of the optimization problem within this thesis, the usage of stochastic algorithms proved to fit best. To break down the optimization problem and reduce the solution space, the algorithm was designed with three steps, including cycle, vehicle and fleet optimization. The optimization approach was validated by comparing the optimum determined by the algorithm with the global optimum. Here, the global optimum was evaluated by a time-intensive calculation of each possible combination in the form of a complete enumeration approach. Due to the high number of combinations, it is not possible to validate the accuracy of the fleet-based optimization with multiple vehicles. Either a very time-intensive calculation loop for the evaluation of each possible combination or a second optimization method has to

be developed for the validation. At this stage, the validation of the fleet-based optimization can only be performed by expert engineering judgment. For example, the altered selection of the optimal combination of measures, comparing the fleet optimization of the NEDC and the WLTC, represents the expectation based on the characteristics of the measures. In addition, the prioritization of aerodynamics measures and altered selection of the gear ratios due to the WLTC are logical. Finally, it is also not possible to validate the results of the method on practical examples. The first reason is the definition of the fleet, which is based on fictional data due to the confidentiality of such data. Related to this fact, it has already been mentioned that the optimal selection of measures depends on the given boundary constraints and targets. Therefore, the results of the fictional fleet cannot be transferred one-to-one to another manufacturer's fleet. In a first step, this method has to be repeated using real vehicle fleet data from a real manufacturer. However, in this context, the result will be influenced by the second factor, the complete-vehicle development. The complete-vehicle development involves many parties, such as the energy management (CO₂ emissions, driving performance), thermal management, vehicle safety, power-train (exhaust emissions) and driving dynamics (driving comfort). Therefore, the selection of components and decisions about measures in real vehicle development are not only driven by the CO₂ emissions. Even if a list of selected measures were available from a manufacturer, each decision would have to be discussed in this development context. Due to the nature of the information required, the final validation of the method on a real vehicle can only be performed by manufacturers themselves, which was not possible within this thesis.

Nevertheless, the presented method is a mathematical numerical and stochastic approach. The ability to generate solutions that are near the global optimum was proven by reduced examples (see Figure 5.24). Overall, it is challenging to find the global optimum in this large and complex solution space. Anyhow, for one investigated example of the vehicle-based optimization, the algorithm was able to find a solution within 0.01% of the best solutions. However, if an optimization approach is able to find the global optimum, the solution has to be discussed with respect to practical background. A mathematical method can find the optimum based on the given input data. In reality, and in the context of the vehicle development process (see Figure 1.4), it cannot be assumed that fixed input data will be available from the beginning of the project. Here, the claim regarding the quality of the output from the method stays in contrast to the availability of accurate input data. The quality and availability of the input, the costs and the simulation input data increase as the development time proceeds. On the other hand, such investigations are needed as early as possible in the development process, in order to profit from a high degree of freedom when selecting measures to improve CO₂ emissions. In addition, decisions regarding measures and components in a complete-vehicle development project are not only driven by CO₂ emissions. Other aspects, such as vehicle safety, design or heat protection, must also be considered. For this reason, an optimization algorithm that finds the global optimum in every case is not needed from a practical standpoint. Furthermore, the developed tool and optimization algorithm is intended to provide a solution to the expert to support analyses and interpretations. Therefore, the required accuracy of the approach was demonstrated and validated. In a second step, the expert can perform sensitivity analyses and define additional boundary constraints in order to reduce the solution space and to make the results plausible.

The proposed workflow for using this optimization approach during the development is as follows:

1. Initial simulation loop with a validated simulation model; definition of possible measures and costs assumptions
2. First optimization loop
3. Expert interpretation of results (e.g. by using sensitivity analyses); discussion of results

with other complete-vehicle disciplines

4. Detailing and validation of the simulation model (e.g. new measurements, new input data)
5. Adjusting the possible measures based on discussions of point 3 (define new measures, delete measures which were rejected by other disciplines); adjusting costs
6. Second and further optimization loops (repeat workflow points 2 to 5 in each optimization loop)

Proposed practical applications of the developed method

The described method was implemented in a commercial simulation tool by using scripts. It can be used in the future as an expert tool. Possible applications are the optimization of specific vehicles or a set of vehicles, including the described interactions and boundary constraints. It is also possible to use this optimization method to break down vehicle-specific CO₂ emissions targets from a given fleet-average target. This step can be used for a detailed optimization, as well as to generate an initial solution of the target distribution for further discussions in projects. Furthermore, current and future measures and their importance for CO₂ emissions reduction can be rated. Additional sensitivity analyses generated by changing input parameters or boundary constraints can support the expert in evaluating the measures and estimating the advantages and disadvantages of possible combinations. The method was also created as a flexible and scalable tool. Thus, it is possible to include additional markets, driving cycles, vehicles and measures. One open point in this context is the validation of the method with a larger solution space.

8. Summary

This thesis dealt with the development of a method to quantify measures for the achievement of the CO₂ emissions targets of a defined selection of vehicles. Depending on the number of vehicles and measures, up to several million combinations are possible. The aim is to select an optimum combination of the available measures. The focus thereby is on reducing the total costs.

Based on an analysis of the state-of-the-art in Chapter 2, methods and approaches for meeting future CO₂ fleet emissions targets, as well as vehicle-specific considerations, were evaluated as a starting point for this thesis. In the literature, the topic of CO₂ fleet emissions is either discussed only on a general fleet-average level or only for considering one vehicle in detail. In addition, the cost of reducing CO₂ fleet emissions has not been used as an input for optimization approaches. No method was found in the literature that combined a general fleet-average-level consideration with a breakdown of targets and measures for defined specific vehicles. Within this thesis, the task was to develop an optimization approach to provide this link.

As input for the method, Chapter 3 addressed the background for the market-specific fleet regulations for CO₂ emissions and provides an overview of technologies available for improving CO₂ emissions on the complete-vehicle level. The regulations for the three regions with the highest market share (i.e. Europe, China and USA) were explained, and the driving cycles for the evaluation of CO₂ emissions were described. It was evident that both the driving cycles for CO₂ emissions and the market-specific regulations differ. Therefore, the optimal selection of measures depends on the market. Based on the energy flow of a vehicle, the important components and systems related to CO₂ emissions were defined. In further steps, current technologies for improving these components and systems and, ultimately, the CO₂ emissions were discussed. Because the fleet-average CO₂ emissions targets cannot be met by implementing one or two measures, it is necessary to consider various technologies on the complete vehicle.

The developed optimization method itself consists of two parts. The first part is the simulation, as described in Chapter 4. The simulation is used for the evaluation of measures for improving CO₂ emissions. The simulation provides the input data for the optimization. Beginning from a baseline simulation model, the model was adapted to evaluate common technologies for improving CO₂ emissions according to Chapter 3. To provide the most accurate results possible, the simulation model was validated with measurements done on a test bench and on a test track. The optimization task can consider multiple vehicles, driving cycles and measures. This results in a large number of required simulation runs. To handle the simulation matrix, an automated simulation environment based on scripts was generated. The reason for the high effort required to generate the input data for the optimization is the accuracy. Using fictional examples, it was proven that the influences of a measure in the literature references and the simulation results of several vehicles vary. No general statements are possible about the exact influences of measures. The improvement of CO₂ emissions must be evaluated for every vehicle individually, in order to provide maximum accuracy.

The second part is the optimization algorithm, as described in Chapter 5. Based on the analysis of the usage of optimization methods in other automotive applications, a discussion of the advantages and disadvantages of various optimization algorithms, and the abstraction of the

optimization task, the usage of meta-heuristics and stochastic algorithms showed the best suitability. An important interface is the linkage between the simulation runs and the generation of solutions of combinations of measures during the optimization process. To improve the computation time, a meta-model was derived. The meta-model is a linear summation of the benefits of individual measures, but it also takes into account interactions caused by the combination of measures. The influence of individual measures is simulated before the optimization. Based on an energy flow analysis of the measures and differentiation into energy sinks, interactions between measures can be detected. These interactions are considered in the meta-model to increase the accuracy of the meta-model compared to the complex simulation model. The overall optimization approach is designed in three steps: cycle-based, vehicle-based and fleet-based optimization. The challenge is to include several boundary constraints and interactions between measures, targets and vehicles. The cycle-based optimization (CBO) is based on the cost ratio of measures and a *Pair Exchange* method. The aim is to find the cost-optimal solution for one vehicle and one cycle, while considering other interactions caused by the combinations of measures. The vehicle-based optimization (VBO) is based on stochastic algorithms. Here, an algorithm influenced by *Genetic Algorithm*, *Simulated Annealing* and *Particle Swarm Optimization* was derived. This optimization step still considers only one vehicle, but with several cycles, and it solves the problem of target conflicts between cycles. The quality of the optimization results was validated by comparing the results of the optimization with the global optimum. The global optimum was calculated using a complete enumeration algorithm to calculate each possible solution. In summary, in some cases, the algorithm did not find the global optimum, which is due to the huge solution space among other factors. To obtain a better solution, a second optimization loop was included with a reduced solution space. In addition, including sensitivity analyses based on expert knowledge can also reduce the solution space in order to obtain the optimum solution. The last step is the fleet-based optimization (FBO). It was determined that the difference between the optimization of one vehicle and multiple vehicles can be abstracted to the number of cycles and their targets. Thus, the same approach was used for the FBO as for the VBO. The aim of this step is to handle the differentiation into global and local measures and the target breakdown of a given fleet-average target into vehicle-specific CO₂ emission targets. Instead of vehicle-specific CO₂ emissions targets, now fleet-average CO₂ emissions targets based on market and year are defined.

The final result of the method is a combination of measures for each vehicle, the proposed status of the considered driving cycles (e.g. CO₂ emissions and driving performance) and the resulting vehicle costs. To show the application of the optimization method, a fictional vehicle fleet was simulated and some investigations on case studies were done in Chapter 6. The intention was to prove the applicability of the algorithm and the need for such a complex method. Different scenarios were investigated, starting from the analysis of one vehicle up to the evaluation of the interactions caused by a vehicle fleet. The results show that the cost-optimum selection of measures is highly depending on the given boundary constraints such as driving performance. These investigations show, that the algorithm can be used for the cost optimization of one or multiple vehicles. But also the target breakdown from the fleet-average CO₂ emissions target down to vehicle-specific targets is a possible application. So the algorithm can be used to derive a first definition of complete-vehicle targets in early development phases.

Since no similar optimization method was found in the literature that could be used as starting point, the intention in this thesis was to develop a novel approach for the described optimization problem. To reduce the complexity of the overall optimization problem, the task was simplified in some points. Thus, the following list contains some possible extensions that would make the method more functional but were not considered in this first approach, and also shows the defined limitations, assumptions and boundaries:

-
- Variable cost, for example depending on the economy of scale of measures and year [22] (This thesis only considers fixed costs.)
 - Definition of dates from which a measure is available [22] [24] (In this thesis, measures are available at all times.)
 - Adding further vehicle attributes, such as driving comfort, exhaust emissions, drivability (In this thesis, only driving performance is considered as a boundary constraint.)
 - Additional weighting of measures due to influence on other vehicle attributes and disciplines or due to development risks [24]
 - Further detailing of the sub-components of the simulation model
 - Extension with alternative power-trains, such as hybrid and electric vehicles (In this thesis, only conventional and mild-hybrid vehicles are considered.)

One possible question for further investigation could be to use this method for power-train dimensioning of hybrid and electric vehicles, for example. To reduce the CO₂ emissions of passenger cars, governments also consider regulations to promote the sale of electric vehicles. The increased market share of alternative vehicles expected for the future will also increase the importance of electric vehicles for common platforms. For example, by adapting this optimization algorithm, such a method could be used to investigate the achievement of driving performance and driving range targets for battery-electric vehicles sharing the same platform, including traction batteries and electric motors.

In addition, it is possible to extend the method with additional vehicle attributes. Here, two possibilities exist. Either the vehicle attributes and the influences of measures can be described without simulation as a fixed value, which is already possible with the method, or the method has to be extended via additional coupling of further simulation tools, such as for the evaluation of driving comfort. A typical example is tire selection. With a low rolling resistance, CO₂ emissions can be improved, but the brake balance, acoustic, durability and vehicle dynamics must also be evaluated in the complete-vehicle context. Therefore, either further and more detailed simulation models in AMESim are needed, or new maneuvers with the existing models have to be defined, or other simulation tools can be used as long as an interface to Scilab exists.

Chapter 7 discusses the quality assessment of the developed method, among other topics. The compromise between the availability of input data, the ability to find the global optimum and the expected quality of the output is of interest. Since in a complete-vehicle development the discussion about measures is not driven only by CO₂ emissions, the method is intended to provide the expert with an initial solution as a basis for further discussions, rather than a 100% mathematically correct solution. Therefore, the accuracy of the algorithm was proven. Finally, based on the method, a tool was developed. This tool can be used as an expert tool by engineers in a vehicle development project. In addition, with sensitivity analysis or the variation of boundary constraints, this tool can help to understand and develop plausible solutions during the development.

As a final conclusion, a novel method for the optimization of CO₂ fleet and vehicle-specific emissions was developed. The method is implemented in scripts so that experts can use it for early decisions in vehicle development. The incomplete validation of the overall method has to be discussed in the context of the practical application of the method. The accuracy of an optimization result can only be discussed with respect to the accuracy of the given input data and the usage of the result. Thus, accurate input data is critical during early development phases, and the result must ultimately be discussed with other development disciplines. The

final selection of technologies is not only driven by CO₂ emissions. Therefore, the developed method provides a valuable tool to support the work of experts in vehicle development. By using sensitivity analysis and altering boundary constraints, the tool can help the expert to understand the optimal solution. The tool offers the ability to derive vehicle-specific CO₂ emissions targets from a given fleet-average target. A comparable tool was not found in the literature.

List of Figures

1.1. Distribution of global anthropogenic CO ₂ emissions (based on [5])	1
1.2. Study on the market share of power-train types with a moderate and slight increase of alternative power-trains (based on [6])	3
1.3. Overview and content of the doctoral thesis	4
1.4. Role of virtual methods in vehicle development	6
2.1. Overview of interactions between technologies [7]	9
3.1. Overview of existing CO ₂ emissions or fuel economy regulations [25]	13
3.2. Fleet target in the EU, based on year and curb vehicle weight [27] [28]	15
3.3. Speed profile of NEDC and WLTC	17
3.4. Fleet targets in China, based on curb vehicle weight, stage and power-train type [39] [40] [41] [42]	18
3.5. Fuel economy fleet targets for passenger cars according to NHTSA, based on year and footprint [22]	21
3.6. Greenhouse gas emissions fleet targets for passenger cars according to EPA, based on year and footprint [22]	21
3.7. Speed profiles of FTP75 and HWFET	22
3.8. Simplified energy flow and sinks in a vehicle	24
3.9. Example of the energy loss distribution in a vehicle (NEDC) based on simulation	25
3.10. Illustration of a specific fuel consumption map with typical technologies for improving fuel efficiency and their map regions where the improvement is expected (based on [54])	25
3.11. Components of the power-train sub-system	30
3.12. Contribution of various vehicle components to the aerodynamic drag c_d [84]	34
3.13. Hybrid power-train with different parallel architectures	37
4.1. Range of the influence of an engine start-stop system, based on various literature sources and simulation results	40
4.2. Influence on CO ₂ emissions of an aerodynamic drag reduction c_d by 30 points by vehicle segment and driving cycle based on simulation of fictional vehicles	41
4.3. Interactions and workflow between simulation model (1), scripting (2) and database (3)	42
4.4. Multi-physics interfaces of an electric motor model (based on [97])	43
4.5. Principle signal flow of the simulation model used	44
4.6. Excerpt from the global parameter list in the AMESim simulation model	45
4.7. Initial simulation model for a vehicle with manual transmission	46
4.8. Adapted simulation model	47
4.9. Sub-system driver including driver model and hill-hold control	48
4.10. Sub-system internal combustion engine including engine control unit	49
4.11. Sub-system auxiliaries	51
4.12. Sub-system power-train and the visualization of potential power flows	53

4.13. Vehicle sub-system	55
4.14. Sub-system cooling circuit	56
4.15. Adapted sub-systems for auxiliaries and power-train due to hybridization	58
4.16. Comparison of simulation and measurement, maneuver: NEDC	61
4.17. Comparison of simulation and measurement, maneuver: Full-throttle acceleration from 50 to 100 kph with locked 4 th gear	63
4.18. Script-based execution of simulation loops including the setting of variables	65
4.19. Execution of a simulation loop for vehicles and cycles	66
4.20. Interaction of simulation and scripting during the execution of a driving cycle simulation loop	70
4.21. Sample Scilab-plot for an NEDC and a full-throttle acceleration simulation	72
4.22. Measurement points for energy flow analysis (engine, auxiliaries, power-train)	75
4.23. Measurement points for energy flow analysis (vehicle)	76
5.1. Overview of non-linear optimization algorithms, based on [103]	83
5.2. Example of fuel consumption and costs depending on parameter vectors	84
5.3. Levels of the fleet optimization problem	87
5.4. Proposal for coupling an optimization with an analysis model for the calculation of the solution, based on [104]	89
5.5. Adapted proposal for coupling the optimization and simulation with a meta-model by adding process points (7) and (8) and using a meta-model (2) instead a complex analysis model	90
5.6. Walk down chart as basis for the meta-model	91
5.7. Additive (“+”) and multiplicative (“x”) correlations of energy sinks	94
5.8. Final approach for the simulation and analysis of the measures and interactions	96
5.9. Initial walk down chart	97
5.10. Walk down chart - measures sorted by the cost ratio	98
5.11. Re-combination of measures and sub-variants due to interactions	99
5.12. Example for splitting the sub-variants	100
5.13. Split of sub-variant to main-variants	102
5.14. Principle initial solution	103
5.15. Principle flow chart of the <i>Pair Exchange</i>	105
5.16. General flow chart of the cycle-based optimization	107
5.17. Example of the target conflict between the NEDC-optimized selection of measures and the effect on other complete-vehicle targets	110
5.18. Illustration of the different ranges between baseline status, potential and target of different cycles and the influence of different measures	112
5.19. Influence of the weighting caused by including and excluding measures	114
5.20. Overview of the principle optimization algorithm	115
5.21. Workflow for the evaluation of the specific parameters	116
5.22. Illustration of the evaluation of the children-specific parameters	117
5.23. Illustration of the <i>Pareto Front</i>	117
5.24. Distribution of possible solutions	119
5.25. Summary of the optimization algorithm for the vehicle level	121
5.26. Calculation and breakdown of the fleet-average target to the platform level to be investigated	123
5.27. Influence of production duration on the constitution of the fleet-average target calculation	124
5.28. Example of the difference between theoretical legal weight-based reference plat- form target and selected platform target depending on the remaining fleet	124

5.29. Summary of the optimization steps and their interaction	126
6.1. Composition of an average EU fleet of passenger cars	128
6.2. Composition of an average US fleet of passenger cars	128
6.3. Composition of an average Chinese fleet of passenger cars	129
6.4. Walk down chart for NEDC from baseline status to the potential	132
6.5. Complete walk down chart including split sub-variants and interactions, sorted by cost ratio	133
6.6. Costs and target overfulfillment of the identified solutions using the <i>Pair Exchange</i> approach	134
6.7. Reduced walk down chart for NEDC from baseline to target with optimized mea- sure selection	134
6.8. Sensitivity analysis	135
6.9. Walk down chart for driving performance targets from baseline status to the theoretical potential	136
6.10. Walk down chart for other performance targets based on NEDC-optimized selec- tion of measures	137
6.11. Impact on costs and selection of measures with relation to the acceleration time target	139
6.12. Distribution of the vehicles of the platform and the defined platform-average target	141
6.13. Vehicle and platform-average costs depending on optimization level	143
6.14. Vehicle and platform-average specific costs depending on optimization level . . .	143
6.15. Distribution of the platform-vehicles' baseline statuses, the platform-vehicles' ini- tial targets and the platform-vehicles' optimized targets	144
6.16. Reduced CO ₂ emissions depending on the sales volume using the fleet-based op- timization based on a platform-average target	144
6.17. Comparison of baseline status and potential of CO ₂ emissions of NEDC and WLTC	146
6.18. Target breakdown of the vehicle-specific CO ₂ emissions of the platform with a 48 V hybridization as an additional measure	147
6.19. Costs of vehicles and platform-average costs depending on optimization level, in- cluding the 48-V-mild-hybrid potential	147
6.20. CO ₂ emissions baseline status, targets and expected costs depending on year . .	148
6.21. Vehicle status and target based on fleet-average target breakdown	149
6.22. Required reduction of CO ₂ emissions depending on sales volume of the vehicles with a focus on comparing segments	150
6.23. Vehicle-average costs by fleet optimization level	151
A.1. NEDC test sequence for hybrid vehicles	XX
A.2. WLTP calculation process for the gear profile of a vehicle with manual transmission	XXI
A.3. FTP72 test sequence for hybrid vehicles	XXVIII
B.1. Principle of the down-scaled system efficiency map due to cylinder deactivation (based on [51])	XXX
B.2. Mechanical efficiency depending on bmp (based on [51])	XXXI
C.1. Principle flow chart for engine start and stop logic	LII
C.2. Principle flow chart for a generator control	LIII
C.3. Principle flow chart for a cylinder deactivation control	LIII
C.4. Measurement points	LIV
C.5. Layout of the 4WD chassis dyno used [Source: Magna Steyr test bench description]	LVI

- C.6. Specification exhaust measuring system [Source: Magna Steyr test bench description] LVI
- C.7. Comparison of simulation and measurement, maneuver: WLTC LVII
- C.8. Comparison of simulation and measurement, maneuver: Full-throttle acceleration from 0 to 100 kph LVIII
- C.9. Comparison of simulation and measurement, maneuver: Full-throttle acceleration from 60 to 100 kph in D Mode LIX

- E.1. Example of a *Pareto Front* for the selection of children LXXXIII

List of Tables

3.1. Parameters for calculating the vehicle target, based on year [27] [28]	15
3.2. Monetary penalty $P_y(gap)$ for exceeding the fleet target based on year and gap .	16
3.3. Phase-in factors for fleet targets [39] [40] [41] [42]	19
3.4. Classification of hybridization levels based on functionality and power range [33]	36
4.1. Lookup table for vehicle states	74
4.2. Energy sinks of a sample vehicle in an NEDC simulation	76
5.1. Required characteristics compared to an excerpt of advantages and disadvantages of optimization algorithms, based on [103]	85
5.2. Comparison of the combined influence of measures from the meta-model and the results of the complex model	92
5.3. Energy sinks of a sample vehicle in an NEDC simulation and the influence of individual measures (Differences in energy sinks compared to the baseline are highlighted in italics.)	93
5.4. Comparison of combined influence of measures (using the sub-variant with the highest influence) using the meta-model and simulation in l/100km	95
5.5. Split of sub-variants into additional measures	101
5.6. Comparison of global optimum and optimum solution using the algorithm for a given fuel consumption target	108
5.7. Example of the dependence between the influence of measures and cycles	111
5.8. Comparison of the global optimum and optimum solution found by using the optimization algorithm on vehicle level	118
6.1. Composition of the whole fleet including engine / transmission configurations based on data from one manufacturer	130
6.2. Detailed composition of a European C-segment based on data from one manufacturer	131
6.3. Comparison of the NEDC-based and vehicle-based optimization	138
6.4. Boundary constraints of the optimization steps considered	141
6.5. Comparison of the baselines and targets of the three markets considered	150
6.6. Number of selected global measures depending on fleet-optimization level	152
A.1. Super-credit-factor by year for vehicles with less than 50 gCO ₂ /km [27] [28] . . .	XVII
A.2. Phase-In: Percentage of registered vehicles considered by year [27] [28]	XVII
A.3. Test weight classes for the NEDC [34]	XIX
A.4. Overview of vehicle and fleet targets for China by year	XXII
A.5. Fuel consumption limitations in l/100km [39] [41] [40] [42]	XXIII
A.6. Credits for vehicles [41] [42]	XXIV
A.7. Characteristic parameters for the fuel economy target	XXV
A.8. Characteristic parameters for the greenhouse gas target	XXV
A.9. Credits for vehicles	XXVI
A.10.A/C efficiency credits [22]	XXVI

A.11.Off-cycle technologies [22]	XXVII
A.12.Thermal control technologies [22]	XXVII
A.13.Test weight classes for the FTP/HWFET	XXVII
B.1. Overview of measures to increase the efficiency of the gasoline engine	XXXII
B.2. Overview of measures to increase the efficiency of the Diesel engine	XXXVII
B.3. Overview of measures for improving energy demand of auxiliaries	XXXVIII
B.4. Electrical power demand of consumers (for minimum auxiliaries)	XL
B.5. Overview of measures for reducing transmission losses	XLI
B.6. Overview of measures for weight reduction	XLIII
B.7. Overview of measures for aerodynamic improvement	XLIV
B.8. Overview of measures to reduce the tire rolling resistance	XLVI
B.9. Overview of potential pf start-stop and generator control	XLVII
B.10.Overview of potential for mild-hybrid (48 V)	XLIX
C.1. Measurement points	LIV
D.1. Definition of the vehicles	LXVIII
D.2. Sales volume by year, in thousands	LXXIV
D.3. Definition of the measures	LXXV
E.1. Utility analysis of optimization algorithms	LXXIX
E.2. Initial solution	LXXX
E.3. Calculation example for the weighting factor	LXXXI
E.4. <i>Pareto Front</i>	LXXXII
E.5. Example of a parent after 6 th iteration step	LXXXIII
E.6. Results of the vehicle-specific NEDC-based optimization and impact on driving performance	LXXXIV
E.7. Comparison of global measures if vehicles are optimized individually	LXXXV
E.8. Influence of the NEDC fleet-average target optimization on vehicle targets	LXXXV

Listings

4.1. Exemplary source code to describe vehicle #1	67
4.2. Exemplary source code for vehicle body data	68
4.3. Exemplary source code to describe a cycle	69
4.4. Exemplary source code to describe a measure	73
C.1. Exemplary source code for engine data	LX
C.2. Exemplary source code for transmission data	LXI
C.3. Exemplary source code for wheel data	LXI
C.4. Exemplary source code for control logic data	LXI
C.5. Exemplary source code for auxiliary data	LXII
C.6. Exemplary source code to describe a measure	LXIII

Bibliography

- [1] Das Kyoto-Protokoll - Ein Meilenstein für den Schutz des Weltklimas. Technical report, Bundesministerium für Umwelt, Naturschutz und Reaktorsicherheit, 2005.
- [2] M. Lunanova. *Optimierung von Nebenaggregaten - Maßnahmen zur Senkung der CO₂-Emissionen von Kraftfahrzeugen*. Vieweg+Teubner Verlag, Wiesbaden, 2009.
- [3] I. Meyer, S. Kaniovski, and J. Scheffran. Scenarios for regional passenger car fleets and their CO₂ emissions. *Elsevier - Energy Policy*, 41:66–74, 2012.
- [4] Redrawing the Energy-Climate Map - World Energy Outlook Special Report. Technical report, International Energy Agency, 2013.
- [5] H. Wallentowitz, A. Freialdenhoven, and I. Olschewski. *Strategien in der Automobilindustrie - Technologietrends und Marktentwicklung*, page 11 and 175. Vieweg+Teubner Verlag, Wiesbaden, 2009.
- [6] G. Pasaoglu, M. Honselaar, and C. Thiel. Potential vehicle fleet CO₂ reductions and cost implications for various vehicle technology deployment scenarios in Europe. *Elsevier - Energy Policy*, 40:404–421, 2012.
- [7] CO₂-Reduzierungspotentiale bei Pkw bis 2020. Technical report, Bundesministerium für Wirtschaft und Technologie, 2012.
- [8] A. Bandivadekar, L. Cheah, C. Evans, T. Grodde, J. Heywood, E. Kasseris, M. Kromer, and M. Weiss. Reducing the fuel use and greenhouse gas emissions of the US vehicle fleet. *Elsevier - Energy Policy*, 36:2754–2760, 2008.
- [9] L. Cheah and J. Heywood. Meeting U.S. passenger vehicle fuel economy standards in 2016 and beyond. *Elsevier - Energy Policy*, 39:454–466, 2011.
- [10] H. Ma, F. Balthasar, N. Tait, X. Riera-Palou, and A. Harrison. A new comparison between the life cycle greenhouse gas emissions of battery electric vehicles and internal combustion vehicles. *Elsevier - Energy Policy*, 44:160–173, 2012.
- [11] C. Silva, M. Ross, and T. Farias. Analysis and simulation of “low-cost” strategies to reduce fuel consumption and emissions in conventional gasoline light-duty vehicles. *Elsevier - Energy Conversion and Management*, 50:215–222, 2009.
- [12] International organization for standardization. International Standard ISO 3833 - Road vehicles - Types - Terms and definitions, 1977.
- [13] European Community. Replacing annex II and amending annexes IV, IX and XI to directive 2007/46/EC (Regulation (EC) No. 678/2011), 2011.
- [14] A. Neßler. Optimierungsstrategien in der modellbasierten Dieselmotorenentwicklung. Master’s thesis, Berlin University of Technology, 2015.
- [15] R. Fischer, F. Küçükay, G. Jürgens, and B. Pollak. *Das Getriebebuch*, pages 28–33. Springer Fachmedien Wiesbaden, 2nd edition, 2016.

- [16] M. Muffatto. Introducing a platform strategy in product development. *Elsevier - Production Economics*, 60-61:145–153, 1999.
- [17] M. Brylawski. Automotive platform sharing’s potential impact on advanced technologies. [https://d231jw5ce53gcq.cloudfront.net/wp-content/uploads/2017/05/RMI_Document_Repository_Public-Reports_T99-10_UncommonKnwldg.pdf]. Accessed: 2017-09-12.
- [18] U. Seiffert and G. Rainer. *Virtuelle Produktentstehung für Fahrzeug und Antrieb im Kfz - Prozesse, Komponenten, Beispiele aus der Praxis*. Vieweg+Teubner Verlag, Wiesbaden, 2008.
- [19] G. Fontaras and Z. Samaras. On the way to 130 g CO₂/km - Estimating the future characteristics of the average European passenger car. *Elsevier - Energy Policy*, 38:1826–1833, 2010.
- [20] C. Haupt. *Ein multiphysikalisches Simulationsmodell zur Bewertung von Antriebs- und Wärmemanagementkonzepten im Kraftfahrzeug*. PhD thesis, TU München, 2012.
- [21] J. v. Grundherr, R. Misch, and H. Wigermo. Verbrauchssimulationen für die Fahrzeugflotte. *ATZ*, pages 168–173, 03 2009.
- [22] US Government Federal Register. 2017 and Later Model Year Light-Duty Vehicle Greenhouse Gas Emissions and Corporate Average Fuel Economy Standards from December 1st 2011 (Federal Register Vol. 76 No. 231 Page 74854-75420), 2011.
- [23] D. Tscharnuter. *Optimale Auslegung des Antriebsstrangs von Kraftfahrzeugen - Modellbildung, Simulation und Optimierung*. PhD thesis, TU München, 2000.
- [24] Engineering-Economic Analyses of Automotive Fuel Economy Potential in the United States. Technical report, OAK Ridge National Laboratory, 2000.
- [25] CO₂-Emissionsreduktion bei Pkw und leichten Nutzfahrzeugen nach 2020 - Abschlussbericht 123320. Technical report, RWTH Aachen, Institut für Kraftfahrzeuge, 2014.
- [26] A. J. Martyr and M. A. Plint. *Engine Testing - The Design, Building, Modification and Use of Powertrain Test Facilities*, pages 324–353 and 368–394. Elsevier, 4th edition, 2012.
- [27] European Community. Setting emission performance standards for new passenger cars as part of the Community’s integrated approach to reduce CO₂ emissions from light-duty vehicle (Regulation (EC) No. 443/2009), 2009.
- [28] European Community. Amending Regulation (EC) No. 443/2009 to define the modalities for reaching the 2020 target to reduce CO₂ emissions from new passenger cars, 2014.
- [29] Deutsche Autohersteller und die Reduzierung von CO₂ bei Neuwagen - EU-Klimafahrtenbuch 2012 für PKW. Technical report, Bund für Umwelt und Naturschutz Deutschland, 2007.
- [30] H. Wallentowitz, A. Freialdenhoven, and I. Olschewski. *Strategien zur Elektrifizierung des Antriebsstranges - Technologien, Märkte und Implikationen*, pages 6–17, 36–44 and 95–97. Vieweg+Teubner Verlag, Wiesbaden, 2010.
- [31] Passenger Vehicle Greenhouse Gas and Fuel Economy Standards: A Global Update. Technical report, International Council on Clean Transportation, 2007.
- [32] Global Overview on Fuel Efficiency and Motor Vehicle Emission Standards: Policy Options and Perspectives for international Cooperation. Technical report, United Nations, Department of Economic and Social Affairs, 2011.

- [33] P. Hofmann. *Hybridfahrzeuge - Ein alternatives Antriebskonzept für die Zukunft*, pages 19, 68, 75 and 201. Springer Verlag, Wien, 2010.
- [34] Economic Commission for Europe Regulation. Regulation No. 83 Revision 5 - Uniform provision concerning the approval of vehicles with regard to the emission of pollutants according to engine fuel requirements, 2015.
- [35] Economic Commission for Europe Regulation. Regulation No. 101 Revision 3 - Uniform provision concerning the approval of passenger cars powered by an internal combustion engine, or powered by a hybrid electric power train with regard to the measurement of the emission of carbon dioxide and fuel consumption and / or the measurement of electric energy consumption and electric range, and of categories M1 and N1 vehicle powered by an electric power train only with regard to the measurement of electric energy consumption and electric range, 2013.
- [36] European Commission - Discussion paper - Adapting the eco-innovations regime to WLTP. [<https://circabc.europa.eu/sd/a/f3e7612b-1dbf-4633-bca8-c51c709c4ad0/2015-09-15%20Discussion%20paper%20EI%20WLTP.pdf>]. Accessed: 2017-06-05.
- [37] European Commission - NEDC/WLTP correlation process - Meeting of TCMV on 17 November 2015. [<https://circabc.europa.eu/webdav/CircaBC/GROW/wltp/Library/WLTP/EU-WLTP/AdminWG%20for%20WLTP%20transposition/AdminWG%20Meeting%2023-24%20Nov%202015/Correlation%20process%20TCMV.ppt>]. Accessed: 2017-06-05.
- [38] Economic Commission for Europe. ECE/TRANS/WP.29/GRPE/2016/03 - Proposal for amendments to global technical regulation No. 15 on Worldwide harmonized Light vehicles Test Procedure (WLTP), 2016.
- [39] Chinese National Standard. GB 19578-2004 - Limits on Fuel Consumption for Passenger Cars, 2004.
- [40] Chinese National Standard. GB 27999-2011 - Fuel Consumption Evaluation Methods and Targets for Passenger Cars, 2011.
- [41] Chinese National Standard. GB 19578-2014 - Limits on Fuel Consumption for Passenger Cars, 2014.
- [42] Chinese National Standard. GB 27999-2014 - Fuel Consumption Evaluation Methods and Targets for Passenger Cars, 2014.
- [43] Z. Wang, M. Wang Y. Jin, and W. Wu. New fuel consumption standards for Chinese passenger vehicles and their effects on reductions of oil use and CO₂ emissions of the Chinese passenger vehicle fleet. *Elsevier - Energy Policy*, 38:5242–5250, 2010.
- [44] China Passenger Vehicle Fuel Consumption Development Annual Report. Technical report, The Innovation Center for Energy and Transportation (iCET), 2014.
- [45] Chinese National Standard. GB 19233-2008 - Measurement Methods of Fuel Consumption for Light-duty Vehicles, 2008.
- [46] Chinese National Standard. GB 19753-203 - Measurement Of Energy Consumption Of Light-duty Hybrid Electric Vehicles, 2013.
- [47] A. E. Atabani, I. A. Badruddin, S.Mekhilef, and A.S. Silitonga. A review on global fuel economy standards, labels and technologies in the transportation sector. *Elsevier - Renewable and Sustainable Energy Reviews*, 15:4586–4610, 2011.

- [48] B. M. Al-Alami and T. H. Bradley. Analysis of corporate average fuel economy regulation compliance scenarios inclusive of plug in hybrid vehicles. *Elsevier - Applied Energy*, 113:1323–1337, 2014.
- [49] US Federal Regulation. 40 CFR Part 600 - Fuel Economy and Greenhouse Gas Exhaust Emission of Motor Vehicles, 2015.
- [50] Society of Automotive Engineers. SAE J 1711 - Recommended Practice for Measuring the Exhaust Emission and Fuel Economy of Hybrid-Electric Vehicles, Including Plug-In Hybrid Vehicles, 2nd edition 2010.
- [51] R. Golloch. *Downsizing bei Verbrennungsmotoren - Ein wirkungsvolles Konzept zur Kraftstoffverbrauchssenkung*, pages 52–138. Springer Verlag, Berlin, Heidelberg, 2005.
- [52] Advanced Automotive Technology - Visions of a super-efficient family car. Technical report, United States. Congress. Office of Technology Assessment, 1995.
- [53] Technologies to improve light-duty vehicle fuel economy. Technical report, Energy and Environmental Analysis, INC., 2007.
- [54] P. Kapus. Lowest Consumption and Highest Performance - a Contradiction? - Outlook on the Future of the Gasoline Engine. Lecture notes. 2014. Accessed: 2017-04-08.
- [55] G. P. Merker, C. Schwarz, and R. Teichmann. *Grundlagen Verbrennungsmotoren - Funktionsweise, Simulation, Messtechnik*, pages 47–48 and 379–550. Vieweg+Teubner Verlag Wiesbaden, 6th edition, 2012.
- [56] G. Merker, C. Schwarz, G. Stiesch, and F. Otto. *Verbrennungsmotoren - Simulation der Verbrennung und Schadstoffbildung*. B. G. Teubner Verlag, Wiesbaden, 3rd edition, 2006.
- [57] H. Kudo, I. Hirose, T. Kihara, M. Yamakawa, and M. Hitomi. Mazda Skyactiv-G 2.0L Gasoline Engine. In *Aachen Colloquium - Automobile and Engine Technology*, pages 111–150, 2011.
- [58] M. Weilemann, P. Soltic, and S. Hausberger. The cold start emissions of light-duty-vehicle fleets: A simplified physics-based model for the estimation of CO₂ and pollutants. *Elsevier - Science of the Total Environment*, 444:161–176, 2013.
- [59] B. C. Singer, T. W. Kirchstetter, R. A. Harlay, G. R. Kendall, and J. M. Hesson. A fuel-based approach to estimate motor vehicle cold-start emissions. *Journal of the Air and Waste Management Association*, 49:125–135, 1999.
- [60] M. Higashitani, K. Yamada, K. Yoshijima, and H. Kobayashi. Zweikammerölwanne zur Verbesserung des Motoraufwärmverhaltens. *MTZ*, pages 996–999, 12 2012.
- [61] C. Gamsjäger, J. Hager, V. Kordesch, and W. Öller. Intelligent Heat Management - A Chance for further reduction of Emissions and Fuel Consumption. In *Aachen Colloquium - Automobile and Engine Technology*, pages 871–888, 2012.
- [62] A. Wimmer, P. Unterguggenberger, A. Eder, and F. Schedel. Simulation von Maßnahmen zum Wärmemanagement. *ATZ*, pages 958–963, 12 2011.
- [63] R. Struzyna, R. Span, and W. Eifler. Utilization of Waste Heat through Thermodynamic Cycles. In *Aachen Colloquium - Automobile and Engine Technology*, pages 527–558, 2011.
- [64] K. Osawa, N. Yamamoto, S. Inoue, A. Kato, and T. Aoyagi. Fuel Consumption Improvement Expansion of Stop/Start. In *Aachen Colloquium - Automobile and Engine Technology*, pages 1433–1450, 2011.

- [65] F. Caresana, M. Bilancia, and C. M. Bartolini. Numerical method for assessing the potential of smart engine thermal management: Application to a medium-upper segment passenger car. *Elsevier - Applied Thermal Engineering*, 31:3559–3568, 2011.
- [66] B. Knauf and E. Pantow. Auslegung eines Kühlsystems mit elektrischer Kühlmittelpumpe. *MTZ*, pages 878–884, 11 2005.
- [67] P. Pfeffer and M. Harrer. *Lenkungshandbuch - Lenksysteme, Lenkgefühl, Fahrdynamik von Kraftfahrzuegen*, pages 325–403. Vieweg+Teubner Verlag, Wiesbaden, 2011.
- [68] K. Reif. *Automobilelektronik - Eine Einführung für Ingenieure*, pages 185–236. Friedr. Vieweg & Sohn Verlag, Wiesbaden, 2nd edition, 2007.
- [69] H. Wallentowitz and K. Reif. *Handbuch Kraftfahrzeugelektronik - Grundlagen, Komponenten, Systeme, Anwendung*, pages 33–38 and 301–309. Friedr. Vieweg & Sohn Verlag, Wiesbaden, 2006.
- [70] R. Hecke, S. Ploumen, and L. Bartsch. Erhöhte Rekuperation kinetischer Energy in Mikro-Hybrid Fahrzeugen. In *Aachen Colloquium - Automobile and Engine Technology*, pages 1279–1290, 2009.
- [71] T. Christ. *Rekuperation in elektrischen Energiebordnetzen von Kraftfahrzeugen*. PhD thesis, TU Berlin, 2006.
- [72] E. Kirchner. *Leistungsübertragung in Fahrzeuggetrieben - Grundlagen der Auslegung, Entwicklung und Validierung von Fahrzeuggetrieben und deren Komponenten*, pages 77–100. Springer Verlag, Berlin, Heidelberg, 2007.
- [73] X. Zhang and C. Mi. *Vehicle Power Management - Modeling, Control and Optimization*, pages 89–94. Springer Verlag, London, 2011.
- [74] R. Ahlawat, H. K. Fathy, B. Lee, J.L. Stein, and D. Jung. Modelling and simulation of a dual-clutch transmission vehicle to analyse the effect of pump selection on fuel economy. *Vehicle System Dynamics: International Journal of Vehicle Mechanics and Mobility*, 48(7):851–868, 07 2010.
- [75] J. Looman. *Zahnradgetriebe - Grundlagen, Kontruktion, Anwendung in Fahrzeugen*, pages 184–240 and 457–463. Springer Verlag, Berlin, Heidelberg, 3rd edition, 2009.
- [76] K. Reif. *Koventioneller Antriebsstrang und Hybridantriebe - mit Brennstoffzellen und alternativen Kraftstoffen*, pages 10–22, 98–142. Vieweg+Teubner Verlag, Wiesbaden, 2010.
- [77] T. Schütz. *Hucho - Aerodynamik des Automobils*. Springer Fachmedien Wiesbaden, 6th edition, 2013.
- [78] T. Laue, M. Goede, and O. Schroeter. Optimierung von Leichtbau und Energieeffizienz zur nachhaltigen CO₂-Reduktion. In *Aachen Colloquium - Automobile and Engine Technology*, pages 853–864, 2009.
- [79] B. Heißig and M. Ersoy. *Fahrwerkhandbuch - Grundlagen, Fahrdynamik, Komponenten, Systeme, Mechatronik, Perspektiven*, pages 35–65. Friedr. Vieweg & Sohn Verlag, Wiesbaden, 2007.
- [80] J. Liebl, M. Lederer, K. Rohde-Brandenburger, J.-W. Biermann, M. Roth, and H. Schäfer. *Energiemanagement im Kraftfahrzeug - Optimierung von CO₂-Emissionen und Verbrauch konventioneller und elektrifizierter Automobile*, pages 102–106. Springer Fachmedien Wiesbaden, 2014.

- [81] W.-H. Hucho. *Aerodynamik der stumpfen Körper - Physikalische Grundlagen und Anwendungen in der Praxis*, pages 264–305. Vieweg+Teubner Verlag, Wiesbaden, 2nd edition, 2011.
- [82] S. Leitman and B. Brant. *Build Your Own Electric Vehicle*. McGraw-Hill, 2nd edition, 2009.
- [83] Technology Roadmap - Fuel Economy of Road Vehicles. Technical report, International Energy Agency, 2012.
- [84] M. Bollig. Der Weg zu Efficient Dynamic 2.0. *ATZ*, pages 10–16, 04 2014.
- [85] K. Reif. *Bremsen und Bremsregelsysteme*, pages 20–35. Vieweg+Teubner Verlag, Wiesbaden, 2010.
- [86] M. Vennebörger, C. Strübel, B. Wies, and K. Wiese. Leichtlaufreifen für PKW mit niedrigem CO₂-Ausstoß. *ATZ*, pages 572–577, 07 2013.
- [87] Economic Commission for Europe Regulation. Regulation No. 100 Revision 2 - Uniform provisions concerning the approval of vehicles with regard to specific requirements for the electric power train, 2013.
- [88] M. Nalbach, A. Körner, and C. Hoff. Der 48-V-Mikro-Hybrid - Ein neues Leistungskonzept. *ATZ*, pages 296–300, 04 2013.
- [89] M. Timmann, M. Renz, and O. Vollrath. Herausforderungen und Potenziale von 48-V-Startsystemen. *ATZ*, pages 216–220, 03 2013.
- [90] European Community. Motor vehicle distribution and after-sales services in the European Union (Regulation (EC) No. 1400/2002), 2002.
- [91] European Community. Case No IV/M.1406 HYUNDAI / KIA - Notification of 17 February 1999 pursuant to Article 4 of Council Regulation (EEC) No. 4064/89, 1999.
- [92] D. Schröder. *Elektrische Antriebe - Regelung von Antriebssystemen*, pages 1049–1087. Springer-Verlag GmbH Berlin Heidelberg, 4th edition, 2015.
- [93] S. Hopfgarten. Objektorientierte Simulation. Lecture notes. [https://www.tu-ilmenau.de/fileadmin/media/simulation/Lehre/Vorlesungsskripte/Simulation/oosim_skript.pdf]. Accessed: 2017-04-08.
- [94] M. Hommel. Parallelisierte Simulationsprozesse für virtuelles Prototyping in der Automobilindustrie. Master's thesis, Braunschweig University of Technology, 2006.
- [95] E. Surewaard, M. Tiller, and D. Linzen. A Comparison of Different Methods for Battery and Supercapacitor Modelling. In *Hybrid Vehicle and Energy Storage Technologies*, June 23-25, 2003. SAE Technical Paper 2003-01-2290.
- [96] LMS Imagine.Lab AMESim. [https://www.plm.automation.siemens.com/de_de/products/lms/imagine-lab/amesim/]. Accessed: 2016-07-12.
- [97] LMS Imagine.Lab AMESim in-built user manual. Revision 14.2.
- [98] Matlab. [<http://de.mathworks.com/products/matlab/>]. Accessed: 2016-07-12.
- [99] Scilab. [<http://www.scilab.org/>]. Accessed: 2016-07-12.
- [100] I. K. Yoo, K. Simpson, M. Bell, and S. Majkowski. An Engine Coolant Temperature Model and Application for Cooling System Diagnosis. In *SAE 2000 World Congress*, March 6-9, 2000. SAE Technical Paper 2000-01-0939.

-
- [101] A. Haury and J. Volkering. Modelisation of the engine coolant warming-up behavior. Master's thesis, Chalmers University of Technology Göteborg, 2011.
- [102] R. G. Sargent. Verification and Validation of Simulation Models. In *2010 Winter Simulation Conference*, 2010.
- [103] M. Meywerk. *CAE-Methoden in der Fahrzeugtechnik*, pages 265–318. Springer Verlag, Berlin, Heidelberg, 2007.
- [104] A. Schumacher. *Optimierung mechanischer Strukturen - Grundlagen und industrielle Anwendungen*, pages 1–7, 94–104 and 135–160. Springer-Verlag Berlin Heidelberg, 2nd edition, 2013.
- [105] T. Krenek. Verbrauchsminimierung eines Hybridfahrzeuges im Neuen Europäischen Fahrzyklus. Master's thesis, Vienna University of Technology, 2011.
- [106] M. Montazeri-Gh, A. Poursamad, and B. Ghalichi. Application of genetic algorithm for optimization of control strategy on parallel hybrid electric vehicles. *Elsevier - Journal of The Franklin Institute*, 343:420–435, 2006.
- [107] L. Fang, S. Qin, G. Xu, T. Li, and K. Zhu. Simultaneous Optimization for Hybrid Electric Vehicle Parameters Based on Multi-Objective Genetic Algorithms. *Energies*, 4:532–544, 2011.
- [108] A. E. Baumal, J. J. McPhee, and P. H. Calamai. Application of genetic algorithms to the design optimization of an active vehicle suspension system. *Elsevier - Computer methods in applied mechanics and engineering*, 163:87–94, 1998.
- [109] K. Weicker. *Evolutionäre Algorithmen*. B. G. Teubner Verlag / GWV Fachverlage GmbH Wiesbaden, 2nd edition, 2007.
- [110] W. Domschke, A. Drexl, R. Klein, and A. Scholl. *Einführung in Operations Research*, pages 127–164. Springer-Verlag Berlin Heidelberg, 9th edition, 2015.
- [111] O. Kramer. *Computational Intelligence - Eine Einführung*, pages 13–58. Springer-Verlag Berlin Heidelberg, 2009.
- [112] IHS Inc. [<https://www.ihs.com/industry/automotive.html>]. Accessed: 2016-08-03.
- [113] European Commission Homepage - Reducing CO₂ emissions from passenger cars. [http://ec.europa.eu/clima/policies/transport/vehicles/cars/documentation_en.htm]. Accessed: 2016-05-25.
- [114] M. Scheidt, C. Brands, M. Kratzsch, and M. Günther. Kombinierte Miller-Atkinson-Strategie für Downsizing-Konzepte. *MTZ*, pages 14–21, 05 2014.
- [115] P. Kapus, M. Neubauer, and G. Fraidl. Die Zukunft des stöchiometrischen Ottomotors - minimaler Verbrauch und hohe Leistung. *MTZ*, pages 40–44, 11 2014.
- [116] R. Folkson. *Alternative Fuels and Advanced Vehicle Technologies for Improved Environmental Performance - Towards Zero Carbon Transportation*. Woodhead Publishing, 2014.
- [117] J.-C. Lin and S.-S. Hou. Influence of heat loss on the performance of an air-standard Atkinson cycle. *Elsevier - Applied Energy*, 84:904–920, 2007.
- [118] A. Al-Sarkhi, J. O. Jaber, and S. D. Probert. Efficiency of a Miller engine. *Elsevier - Applied Energy*, 83:343–351, 2006.
- [119] K. G. Dulepp. Automotive Technology for Better Fuel Efficiency. In *FIA-Foundation Symposium - Toward a Global Approach to Automotive Fuel Economy*, 2008.

- [120] H. Hoffmann, A. Loch, R. Widmann, G. Kreusen, D. Meehsen, and M. Rebbert. Zylinderabschaltung für Ventiltriebe mit Rollenschlepphebel. *MTZ*, pages 302–307, 04 2009.
- [121] C. Stan. *Alternative Antriebe für Automobile - Hybridsysteme, Brennstoffzellen, alternative Energieträger*, pages 47–53. Springer Verlag, Berlin, Heidelberg, 2005.
- [122] B. Helt, H. K. Weining, G. Karl, D. Panten, and K. Wunderlich. Verbrauch und Emissionen - Reduzierungskonzepte beim Ottomotor Teil 2. *MTZ*, pages 1022–1035, 12 2011.
- [123] Y. Duchaussoy, B. Covin, Y. Boccadoro, O. Meurisse, J. P. Mercier, and D. Levasseur. Renault Energy TCe 115 - The New Renault 1.2 GDI Turbocharged Enigne. In *Aachen Colloquium - Automobile and Engine Technology*, pages 91–110, 2011.
- [124] P. Setlur, J. R. Wagner, D. M. Dawson, and E. Marotta. An Advanced Engine Thermal Management System: Nonlinear Control and Test. *IEEE/ASME: Transactions on Mechatronics*, 10:210–220, 2005.
- [125] K. Reif. *Bosch Autoelektrik und Autoelektronik - Bordnetze, Sensoren und elektronische Systeme*, page 392 and 441. Vieweg+Teubner Verlag, Wiesbaden, 6th edition, 2011.
- [126] R. M. Fabis. *Beitrag zum Energiemanagement in Kfz-Bordnetzen*. PhD thesis, TU Berlin, 2006.
- [127] F. Wittmeier, N. Widdekce, J. Wiedemann, N. Lindener, and R. Armbruster. Reifenentwicklung unter Aerodynamischen Aspekten. *ATZ*, pages 144–150, 02 2013.
- [128] K. Reif. *Batterien, Bordnetze und Vernetzung*, page 23. Vieweg+Teubner Verlag, Wiesbaden, 2010.
- [129] M. Fleckner, M. Göhring, and L. Spiegel. Neue Strategien zur verbrauchsoptimalen Auslegung der Betriebsführung von Hybridfahrzeugen. In *Aachen Colloquium - Automobile and Engine Technology*, pages 681–708, 2009.
- [130] C. Hoff, C. Amsel, and A. Körner. The Dual Voltage Power System with 48V - Architecture, Potentials and Components. In *Aachen Colloquium - Automobile and Engine Technology*, pages 1537–1554, 2012.

A. Appendix: Legal fundamentals

A.1. Europe

A.1.1. Super-credits

Table A.1 shows the credit-factor crd by year y for vehicles which have less than 50 gCO₂/km. The sales volume of the vehicles are multiplied by the factor so that these vehicles count multiple times.

Table A.1.: Super-credit-factor by year for vehicles with less than 50 gCO₂/km [27] [28]

Year y	Factor crd
2012	3.5
2013	3.5
2014	2.5
2015	1.5
2016-2019	1
2020	2
2021	1.67
2022	1.33
from 2021	1

A.1.2. Phase-in period

Table A.2 shows how many of the newly registered vehicles have to be considered in the calculation of the average fleet CO₂ emissions per year. This phase-in period provides the advantage that vehicles with high CO₂ emissions can be removed for the first years.

Table A.2.: Phase-In: Percentage of registered vehicles considered by year [27] [28]

Year	% of fleet
2012	65%
2013	75%
2014	80%
2015 - 2019	100%
2020	95%
from 2021	100%

A.1.3. ECO innovations

The official homepage of the European Commission [113] provides a list of approved ECO innovations. ECO innovations are technologies that have no influence on the legal test cycle on the dyno test bench, but do affect real driving. They can be used for an additional reduction of the fleet-average CO₂ emissions up to 7 g/km. The following technologies are approved as ECO innovations:

- LED lamps for exterior lighting
- Solar panel on the roof
- High efficiency alternator (stator copper loss reduction, stator iron loss reduction, rectification loss reduction, use of MOSFET, reduced air gap, optimization of phase resistance)
- Coasting with ICE in idle running
- Enthalpy storage tank to reduce CO₂ emissions during cold-start and to improve warm-up
- Advanced MultiAir Technology to control the valve lift at medium and high engine load to reduce fuel consumption
- Navigation-based predictive hybrid vehicle operating strategy
- Engine compartment encapsulation to delay cool-down of the engine if the vehicle is parked

A.1.4. Definition of the test weight classes

Table A.3 shows the definition of the test weight class based on the curb weight. The test weight class represents the vehicle mass to be accelerated on the dyno test bench.

Table A.3.: Test weight classes for the NEDC [34]

Curb vehicle weight [kg]	Test weight class [kg]
$(CVW + 100) \leq 480$	455
$480 < (CVW + 100) \leq 540$	510
$540 < (CVW + 100) \leq 595$	570
$595 < (CVW + 100) \leq 650$	625
$650 < (CVW + 100) \leq 710$	680
$710 < (CVW + 100) \leq 765$	740
$765 < (CVW + 100) \leq 850$	800
$850 < (CVW + 100) \leq 965$	910
$965 < (CVW + 100) \leq 1080$	1020
$1080 < (CVW + 100) \leq 1190$	1130
$1190 < (CVW + 100) \leq 1305$	1250
$1305 < (CVW + 100) \leq 1420$	1360
$1420 < (CVW + 100) \leq 1530$	1470
$1530 < (CVW + 100) \leq 1640$	1590
$1640 < (CVW + 100) \leq 1760$	1700
$1760 < (CVW + 100) \leq 1870$	1810
$1870 < (CVW + 100) \leq 1980$	1930
$1980 < (CVW + 100) \leq 2100$	2040
$2100 < (CVW + 100) \leq 2210$	2150
$2210 < (CVW + 100) \leq 2380$	2270
$2380 < (CVW + 100) \leq 2610$	2270
$2610 < (CVW + 100)$	2270

A.1.5. ECE-R 101 test sequence for hybrid vehicles

The regulation ECE-R 101 [35] describes the test procedure for hybrid and electric vehicles. Hybrid-electric vehicles have two energy sources: fuel and electric energy from the traction battery. A traction battery is a battery which provides energy to propel a vehicle via an electric motor. In the standard regulation ECE-R 83 [34], only the fuel consumption / CO₂ emissions are taken into account. The second energy source is not considered and can influence the fuel consumption by charging / discharging the battery. The regulation ECE-R 101 is used if an electric motor / battery is able to drive the vehicle. In this doctoral thesis, this is needed to consider 48-V-hybrid technologies. In the case of hybrid vehicles, the difference in the traction battery capacity (Ah) before and after the driving cycle have to be measured to correct the CO₂ emissions. This difference Q_{Batt} is multiplied by a correction factor K_{fuel} . The official CO₂ emissions relate to an energy balance of the battery of 0 Ah. The correction factor is calculated from an NEDC testing set with n tests. In each NEDC i , the fuel consumption FC_i and the battery energy balance Q_i are measured. Here, at least one test from the test series should end in $Q_{\text{Batt}_i} < 0$ and at least one test should end in $Q_{\text{Batt}_i} > 0$. The correction factor is calculated with the following equation:

$$K_{\text{fuel}} = \frac{n \cdot \sum (Q_{\text{Batt}_i} \cdot FC_i) - \sum Q_i \cdot \sum FC_i}{n \cdot \sum (Q_{\text{Batt}_i}^2) - (\sum Q_{\text{Batt}_i})^2} \left[\frac{1}{100\text{km} \cdot \text{Ah}} \right]. \quad (\text{A.1})$$

The fuel consumption FC_0 of the official test is corrected as follows:

$$FC_0 = FC_i - K_{\text{fuel}} \cdot Q_{\text{Batt}_i} \quad (\text{A.2})$$

Before the official NEDC test, a precondition test is done a day before. For this reason, the SOC of HV battery in the official test is preconditioned. The test procedure in the automated simulation used in this thesis is shown in Figure A.1. The simulation has the advantage that the starting SOC can be freely defined. Five NEDC simulation runs are included. Four cycles are defined to have a fixed start with an initial SOC of 100%, 66%, 33% and 0%. The starting SOC of 100% and 0% are the prerequisite that at least one cycle has a positive and at least one cycle a negative energy balance. Out of these four cycles, the correction factor is calculated. The test using an initial SOC of 100% is also used as precondition for the official test. The final battery SOC of this test is used as the initial SOC for the fifth / official simulation run.

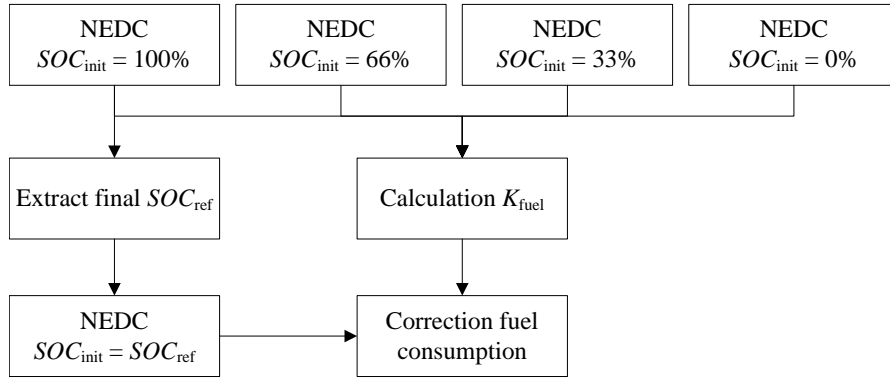


Figure A.1.: NEDC test sequence for hybrid vehicles

A.1.6. WLTP gear-shifting for manual transmission

In the WLTP, the gear-shifting profile is calculated for every vehicle individually. The detailed calculation is described in [38]. For the calculation, the following information is required:

- Maximum engine power P_{rated}
- The engine full load power as a function of the engine speed $P_{\text{wot}}(n)$
- Engine speed n_{rated} where the engine has its maximum power
- Engine speed $n_{\text{max}, 95}$ where 95% of the maximum power is reached
- Idle speed n_{idle}
- The minimum engine speed while driving $n_{\text{min}, \text{drive}}(\text{gear})$
- Number of forward gears ng and the ratio (engine speed to vehicle speed) ndv_i of each gear
- The gear ng_{vmax} in which the maximum vehicle speed is reached
- Road load / driving resistance F_0 , F_1 and F_2 of the vehicle
- Test mass TM .

Figure A.2 shows the principle calculation flow. Based on the speed profile $v(t)$, the required power $P_{\text{req}}(t)$ and the engine speed for every gear $n(t, \text{gear})$ are calculated. Depending on the engine speed, the available power $P_{\text{avail}}(t, \text{gear})$ is calculated. In the next step, the required power and the available power are compared in each time step. The minimum gear $\text{gear}_{\text{min}}(t)$ is selected where the available power is higher than the required power. In addition, some filter functions are included to prevent gear jumps as well as back-shift / up-shift iterations.

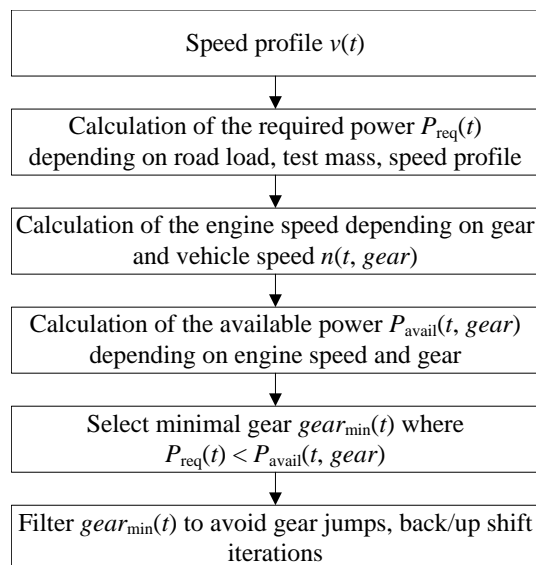


Figure A.2.: WLTP calculation process for the gear profile of a vehicle with manual transmission

A.1.7. WLTP monitoring electric power supply

The WLTP includes an energy balance ΔE_{reess} [Wh] of the electric power supply of the low-voltage power-net. The CO₂ emissions EM should be corrected by ΔEM with a balanced energy level ($\Delta E_{\text{reess}} = 0$) as follows:

$$\Delta EM = \frac{1}{0.0036} \cdot \Delta E_{\text{reess}} \cdot \frac{1}{\eta_{\text{Gen}}} \cdot \text{Willians}_{\text{factor}} \cdot \frac{1}{d}. \quad (\text{A.3})$$

where d is the distance driven, η_{Gen} is the efficiency factor of the alternator (defined as 67% in the regulation) and $\text{Willians}_{\text{factor}}$ is the combustion-process-specific Willians factor defined in the regulation (e.g. 174 gCO₂/MJ for petrol (E5) and naturally aspirated engines).

A.1.8. WLTP test sequence for hybrid vehicles

Similar to Appendices A.1.5 and A.1.7, hybrid vehicles also have a special test sequence and correction of the energy balance of the traction battery in the WLTP. The test sequence is defined as follows. First, a precondition test is performed. After a defined soak time, the official WLTC test is driven.

For the energy balance of the traction battery, the correction factor is defined as follows, by using n tests:

$$K_{\text{fuel}} = \frac{\sum_i ((EC_i - EC_{\text{avg}}) \cdot (FC_i - FC_{\text{avg}}))}{\sum_i (EC_i - EC_{\text{avg}})^2}. \quad (\text{A.4})$$

where EC_i is the electric energy consumption, and FC_i is the fuel consumption of a test cycle i . The values EC_{avg} and FC_{avg} are the average values of all tests. The test procedure used in the simulation environment is similar to the NEDC simulation sequences shown in Figure A.1.

A.2. China

A.2.1. Fuel consumption limits

Table A.4 provides an overview of the regulations for fuel consumption of vehicle-specific and on the fleet-average level.

Table A.4.: Overview of vehicle and fleet targets for China by year

Year	Vehicle limit	Fleet limit
2005 - 2007	Stage I - <i>GB 19578-2004</i> [39]	n/a
2008 - 2011	Stage II - <i>GB 19578-2004</i> [39]	n/a
2012 - 2015	Stage II - <i>GB 19578-2004</i> [39]	Stage III - <i>GB 27999-2011</i> [40]
from 2016	<i>GB 19578-2014</i> [41] (equal to Stage III limits)	Stage IV - <i>GB 27999-2014</i> [42]

Table A.5 summarizes the fuel consumption limitation for vehicles (VL) and fleet-average limit (CAFC) for the different kinds of vehicles: for MT¹, AT² and 3R³

A.2.2. Credits for new energy vehicles

Table A.6 shows the credit-factor crd for new energy vehicles and vehicles with ultra-low fuel consumption by year. New energy vehicles are BEV, FCV and PHEV. Vehicles with ultra-low fuel consumption are vehicles which are not new energy vehicles and have a fuel consumption less than or equal to 2.8 l/100km. Here, the sales volume of these vehicles will be multiplied by the relevant factor so that the vehicles count multiple times.

¹Passenger car with manual transmission

²Passenger car with automatic transmission

³Passenger car with three or more rows of seats

Table A.5.: Fuel consumption limitations in l/100km [39] [41] [40] [42]

Curb vehicle weight CVW [kg]	Stage I (VL)		Stage II		Stage III (CAFC)		Stage IV (CAFC)	
	Stage III (VL)		Stage IV (VL)		Stage III (CAFC)		Stage IV (CAFC)	
	MT	AT / 3R	MT	AT / 3R	MT	AT / 3R	MT / AT	3R
$CVW \leq 750$	7.2	7.6	6.2	6.6	5.2	5.6	4.3	4.5
$750 < CVW \leq 865$	7.2	7.6	6.5	6.9	5.5	5.9	4.3	4.5
$865 < CVW \leq 980$	7.7	8.2	7.0	7.4	5.8	6.2	4.3	4.5
$980 < CVW \leq 1090$	8.3	8.8	7.5	8.0	6.1	6.5	4.5	4.7
$1090 < CVW \leq 1205$	8.9	9.4	8.1	8.6	6.5	6.8	4.7	4.9
$1205 < CVW \leq 1320$	9.5	10.1	8.6	9.1	6.9	7.2	4.9	5.1
$1320 < CVW \leq 1430$	10.1	10.7	9.2	9.8	7.3	7.6	5.1	5.3
$1430 < CVW \leq 1540$	10.7	11.3	9.7	10.3	7.7	8.0	5.3	5.5
$1540 < CVW \leq 1660$	11.3	12.0	10.2	10.8	8.1	8.4	5.5	5.7
$1660 < CVW \leq 1770$	11.9	12.6	10.7	11.3	8.5	8.8	5.7	5.9
$1770 < CVW \leq 1880$	12.4	13.1	11.1	11.8	8.9	9.2	5.9	6.1
$1880 < CVW \leq 2000$	12.8	13.6	11.5	12.2	9.3	9.6	6.2	6.4
$2000 < CVW \leq 2110$	13.2	14.0	11.9	12.6	9.7	10.1	6.4	6.6
$2110 < CVW \leq 2280$	13.7	14.5	12.3	13.0	10.1	10.6	6.6	6.8
$2280 < CVW \leq 2510$	14.6	15.5	13.1	13.9	10.8	11.2	7.0	7.2
$2510 < CVW$	15.5	16.4	13.9	14.7	11.5	11.9	7.3	7.5

Table A.6.: Credits for vehicles [41] [42]

Year y	Credit-factor crd_y for new energy vehicles	Credit-factor crd_y for ultra-low fuel consumption vehicles
until 2015	no credit	no credit
2016-2017	5	3
2018-2019	3	2.5
from 2020	2	1.5

A.3. USA

A.3.1. Fuel economy and greenhouse gas limits for passenger cars

Table A.7 shows the characteristic parameters calculating the fuel economy target.

Table A.7.: Characteristic parameters for the fuel economy target

Year y	a	b	c	d
2012	35.95	27.95	0.0005308	0.0060507
2013	36.80	28.46	0.0005308	0.005410
2014	37.75	29.03	0.0005308	0.004725
2015	39.24	29.90	0.0005308	0.003719
2016	41.09	30.96	0.0005308	0.002573
2017	43.61	32.65	0.0005131	0.001896
2018	45.21	33.84	0.0004954	0.001811
2019	46.87	35.07	0.0004783	0.001729
2020	48.74	36.47	0.0004603	0.001643
2021	50.83	38.02	0.0004419	0.001555
2022	53.21	39.79	0.0004227	0.001463
2023	55.71	41.64	0.0004043	0.001375
2024	58.32	43.58	0.0003867	0.001290
2025	61.07	45.61	0.0003699	0.001210

The target $Tvfe$ in mpg for fuel economy for a year y depending on the vehicle footprint fp is defined as follows:

$$Tvfe \text{ [mpg]} = \frac{1}{\min\left(\max\left(c \cdot fp \text{ [ft}^2\text{]} + d, \frac{1}{a}\right), \frac{1}{b}\right)}. \quad (\text{A.5})$$

Table A.8 shows the characteristic parameters for calculating the greenhouse gas target.

Table A.8.: Characteristic parameters for the greenhouse gas target

Year y	A	B	C	D
2017	194.7	262.7	4.53	8.9
2018	184.9	250.1	4.35	6.5
2019	175.3	238.0	4.17	4.2
2020	166.1	226.2	4.01	1.9
2021	157.2	214.9	3.84	-0.4
2022	150.2	205.5	3.69	-1.1
2023	143.3	196.5	3.54	-1.8
2024	136.8	187.8	3.40	-2.5
2025	130.5	179.5	3.26	-3.2

The target $Tvghg$ in gCO₂/mile for greenhouse gas emission for a year y depending on the vehicle footprint fp is defined as follows:

$$T_{vghg} \left[\frac{\text{gCO}_2}{\text{mile}} \right] = \min (B, \max (A, C \cdot fp [ft^2] + D)) . \quad (\text{A.6})$$

A.3.2. Credits for alternative vehicles

Table A.9 shows the credit-factor *crd* for alternative vehicles (EV, FCV, PHEV) by year *y*. Here, the sales volume is multiplied by the factor so that the vehicles count multiple times.

Table A.9.: Credits for vehicles

Year <i>y</i>	Factor <i>crd</i> for EVs and FCVs	Factor <i>crd</i> for PHEVs
2017-2019	2.0	1.6
2020	1.75	1.45
2021	1.5	1.3

A.3.3. Off-cycle credits

The following tables show possible off-cycle technologies. The goal is comparable to that of the ECO innovations for the European regulation. Table A.10 shows credits which are related to the A/C system. Table A.11 shows other possible credits. Here, for some technologies a minimum percentage is given. This means in order to get the credit, the technologies have to be implemented in a defined minimum percentage of the vehicle fleet. The details for thermal control technologies are given in Table A.12.

Table A.10.: A/C efficiency credits [22]

Technology	Credit GHG [gCO ₂ /mi]	Credit FE [gpm]
Controlled variable-displacement compressor	1.5	0.000169
Controlled fixed-displacement or pneumatic variable-displacement compressor	1.0	0.000113
Recirculated air with closed-loop control on the air supply with sensor feedback	1.5	0.000169
Recirculated air with open-loop control on the air supply without sensor feedback	1.0	0.000113
Blower control	0.8	0.000090
Internal heat exchanger	1.0	0.000113
Improved evaporators and condensers	1.0	0.000113
Oil separator	0.8	0.000090

A.3.4. Definition of the test weight classes

Table A.13 shows an excerpt of the definition of the test weight class based on the curb weight.

Table A.11.: Off-cycle technologies [22]

Technology	Credit GHG [gCO ₂ /mi]	Credit FE [mpg]	minimum percentage of vehicles [%]
High-efficiency exterior lightning	1.1	0.000124	10
Engine heat recovery	0.7 per 100 W of capacity	0.0000778 per 100 W of capacity	n/a
Solar roof panels	3.0	0.000338	n/a
Active aerodynamic improvements	0.6	0.0000675	10
Engine start-stop	2.9	0.000326	10
Electric heater circulation pump	1.0	0.000123	n/a
Active transmission warm-up	1.8	0.000203	10
Active engine warm-up	1.8	0.000203	10
Thermal control (see Table A.12)	up to 3.0	up to 0.000338	n/a

Table A.12.: Thermal control technologies [22]

Technology	Credit GHG [gCO ₂ /mi]
Glass or plazing	≤ 2.9
Active seat ventilation	1.0
Solar reflective paint	0.4
Passive cabin ventilation	1.7
Active cabin ventilation	2.1

Table A.13.: Test weight classes for the FTP/HWFET

Curb vehicle weight [kg]	Test weight class [lbs] / [kg]
...	...
969 < (CVW) ≤ 1026	2500 / 1134
1026 < (CVW) ≤ 1083	2625 / 1191
1083 < (CVW) ≤ 1139	2750 / 1247
1139 < (CVW) ≤ 1196	2875 / 1304
1196 < (CVW) ≤ 1253	3000 / 1361
1253 < (CVW) ≤ 1310	3125 / 1417
1310 < (CVW) ≤ 1366	3250 / 1474
1366 < (CVW) ≤ 1423	3375 / 1531
1423 < (CVW) ≤ 1480	3500 / 1588
1480 < (CVW) ≤ 1536	3625 / 1644
1536 < (CVW) ≤ 1593	3750 / 1701
1593 < (CVW) ≤ 1650	3875 / 1758
1650 < (CVW) ≤ 1735	4000 / 1814
...	...

A.3.5. Test sequence for hybrid vehicles

For the US fuel consumption, the test is divided into two parts: FTP72⁴ and HWFET. Both tests are separate. In each test, the driving cycle is driven twice in sequence (cycle 1 and cycle 2) for hybrid-electric vehicles. The test procedure is described in [50].

The total fuel consumption FC_{test} of each test is calculated as follows:

$$\begin{aligned} FC_{\text{FTP72}} &= 0.43 \cdot \frac{FC_{c_1}}{d_{c_1}} + 0.57 \cdot \frac{FC_{c_2}}{d_{c_2}} \\ FC_{\text{HWFET}} &= 0 \cdot \frac{FC_{c_1}}{d_{c_1}} + 1 \cdot \frac{FC_{c_2}}{d_{c_2}} . \end{aligned} \quad (\text{A.7})$$

where FC_{c_i} is the absolute fuel consumption, and d_{c_i} is the distance driven in a cycle c_i .

In the SAE regulation, the SOC of the traction battery has to be measured. The prerequisite is that the SOC should be the same before and after the test, including a tolerance. No correction equation for the battery energy balance exists. The vehicle and traction battery should be preconditioned to achieve this requirement. Figure A.3 shows the simulation sequence for the automated simulation environment for example of the FTP72 test.

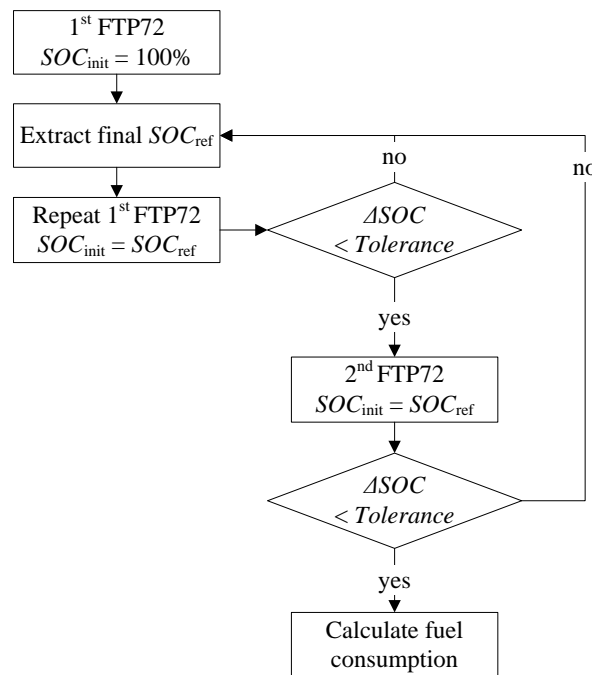


Figure A.3.: FTP72 test sequence for hybrid vehicles

⁴FTP72 represents the first two parts of the FTP75 and is used for vehicles with electrified power-train instead of the FTP75.

B. Appendix: Vehicle fundamentals

B.1. Internal combustion engine

B.1.1. Description of technologies

Miller and Atkinson cycle

The Miller and Atkinson cycles are a special modification of the valves. The focus of both strategies is the reduction of throttling losses of the gas exchange [114] and the delay of the compression towards the expansion [115]. The Atkinson cycle changes the exhaust valve opening time and intake valve closing time. The gas has the chance to expand closer to ambient pressure. A fuel consumption reduction can be achieved, but with a negative impact on the peak torque. The Miller cycle instead increases the compression ratio using an over-expanded cycle. A higher compression ratio leads to higher thermodynamic efficiency, but this also leads to a reduced compression stroke and available peak torque. [116] [117] [118]

Direct injection

When using a direct injection of the fuel into the cylinder, the throttle valve is no longer needed to regulate the fuel. Throttle losses can be reduced, particularly at partial load and lower speeds. In addition, the direct injection leads to vaporization of the fuel inside the combustion chamber, which has a cooling effect. It reduces the affection to self-ignition and improves the knock resistance. The lower temperature resulting from the cooling effect also improves the engine power. Direct injection has further advantages resulting from the higher valve overlapping times because no fuel is lost, and it allows for a higher compression ratio, which provides a higher thermodynamic efficiency. Two methods exist: homogeneous injection and stratified injection. The stratified injection is based on lean operation with excess oxygen. For this reason, a more complex exhaust after-treatment is needed to handle the nitrogen oxides resulting from the lean operation. [7] [22] [30] [53]

Variable valve train

A fixed valve train is always a compromise between all engine operating points, especially low vs. high engine speeds [47]. A variable valve train increases the degrees of freedom for valve opening and closing, which is called variable valve timing (VVT), and valve lift, which is called variable valve lift (VVL) [30] [52]. Throttle losses and pumping work can be reduced, and an optimum for each engine speed can be taken into account [7] [22] [47]. An 80% reduction of the throttle losses is possible at medium load and low speed. Setting the valve closing time can control the residual gas and leads to an internal exhaust gas recirculation. This reduces throttle losses

and improves the fuel-mixture [22] [30]. In addition, an improvement of the low-speed torque is possible [52]. The variable valve lift improves the fuel-mixture due to the sizing of the valve lap and the resulting fuel drift with higher speed [30]. Furthermore, with such systems the throttle valve can be completely removed, which leads to very low throttle and gas-exchange losses [7] [53]. Here, the valves can be controlled by hydraulic or electrical actuators. The system can be located on the inlet and outlet or only on the inlet side and can be controlled step-wise or continuously [53] [119].

Cylinder deactivation

If the engine is not operating at high load, cylinders can be deactivated. The missing torque has to be provided by the other activated cylinders. The cylinders will operate at a higher operation point [30]. Pump and throttle losses, as well as friction, will be reduced due to having fewer activated cylinders [7] [22] [51] [53]. Figure B.1 shows a typical efficiency map (black lines). The area of best efficiency (marked with $\eta \uparrow$) is at higher partial load. A cylinder deactivation leads to a switch of the operation point (point) of the remaining cylinders in direction to higher efficiency (gray lines). This leads to lower fuel consumption. The cylinder deactivation works as a dynamic downsizing [51] [53]. The burn mixture has to remain inside the deactivated cylinder to reduce the cool down [120].

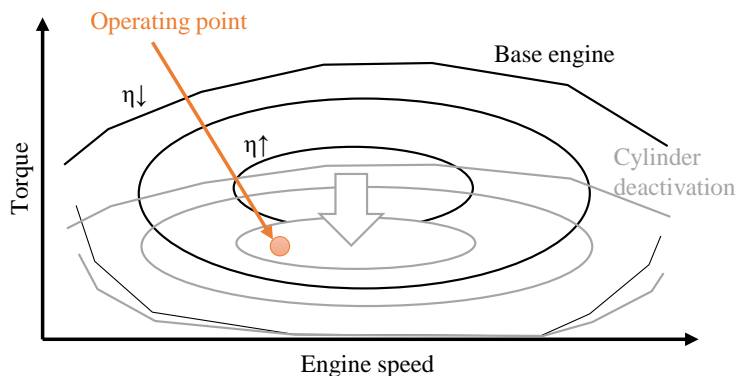


Figure B.1.: Principle of the down-scaled system efficiency map due to cylinder deactivation (based on [51])

Turbocharging and downsizing

Turbocharging increases the filling pressure in the combustion chamber, which leads to an increase in torque and power. This can be achieved via an exhaust turbocharger, a mechanical compressor or an electrical turbocharger. In the next step, the engine is downsized by reducing the number of cylinders or the swept volume. The downsized engine should have a comparable torque and power level towards the base engine. This leads to an improved engine operation area. The engine operating points move in regions with better efficiency [30]. Here, the improvement of efficiency due to downsizing is comparable with the effect on cylinder deactivation - scaling of the system efficiency map, but also of the available torque, as shown in Figure B.1. In addition, the smaller size of the engine leads to a reduction of pump, throttle and gas exchange losses and mechanical friction. The reduced sizes of the cylinder and cylinder wall reduce the thermal losses caused by the heat transfer to the engine block. Both effects lead to a further improvement

of the engine efficiency [7] [47] [51]. Here, the charging is limited by the knocking of gasoline engines, thermal and mechanical protection [51].

Variable compression

The thermodynamic efficiency depends on the compression ratio¹. The ratio stays in contrast between efficiency and maximum torque. In a normal engine, this ratio is fixed. Due to the knocking effect, the maximum possible compression ratio is currently around 12 for full load. In contrast, a compression ratio up to 15 is possible to improve the efficiency for partial load. Figure B.2 shows the principle relationship between the thermodynamic efficiency and the mean effective pressure (bmep). A variable mechanism to regulate the compression ratio depending on the operation point will reduce this conflict. [7] [30] [53]

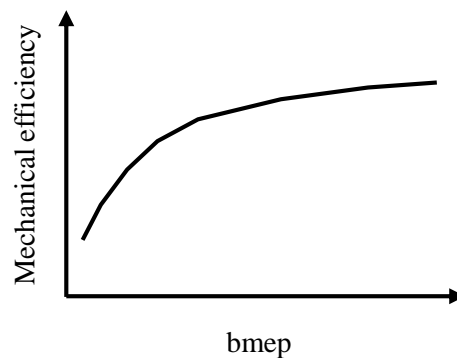


Figure B.2.: Mechanical efficiency depending on bmep (based on [51])

Exhaust gas recirculation

Remaining exhaust gas leads to less fresh mixture gas, reduces throttle losses and results in low pressure. The pressure and the compression inside the combustion chamber increase as well as the combustion temperature decreases. This results in a better thermodynamic efficiency. Exhaust gas recirculation can be implemented internally by using a VVT or externally. [7] [22][121]

¹ratio between the volume at the lower and upper dead centers [7]

B.1.2. Overview of technologies and their expected benefits

Table B.1 shows the overview of a literature research on measures to increase the efficiency of gasoline engines. Table B.2 shows the literature research on Diesel engines.

Table B.1.: Overview of measures to increase the efficiency of the gasoline engine

Measure	Benefit fuel consumption	Expected costs	Source
Direct injection (homogeneous)	1.5 to 1.6%	\$224 to 274 (for I4) \$338 to 413 (for V6)	[22]
Direct injection (homogeneous)	3%	€150	[7]
Direct injection (homogeneous)	3 to 4%	\$160 to 250	[119]
Direct injection (homogeneous)	3 to 4% (5% increase torque / power)	\$10 per injector \$50 high-pressure fuel pump \$10 for controller	[53]
Direct injection (lean burned)	8%	€500 to 600	[7]
Direct injection (lean burned)	8 to 13% (5% increase torque / power)	\$300 to 360 (\$40 per injector \$35 high-pressure fuel pump \$15 for controller \$180 to 240 for exhaust after-treatment)	[53]
Direct injection (lean burned)	15%		[30]
Direct injection (lean burned)	17 to 19%	\$1000 to 1500	[119]
Direct injection (lean burned)	15 to 20%	€700 to 1000	[5]
Direct injection (lean burned)	20%		[30]
VVL (intake)	1.1 to 1.7% (+3 to 4% torque)		[53]
Variable valve train	1.3 to 1.9% (intake) 2.1 to 2.7% (intake and exhaust) improve torque 1200 to 1500 rpm by 3 to 5%	\$33 to 37 per cam	[53]
Variable valve lift	1.8 to 2.6% (+4.5 to 5.5% torque)		[53]
Variable valve train	2%	€230	[83]

Dual cam phasing	2.0 to 2.7%	\$77 to 94 (for I4) \$165 to 201 (for V6)	[22]
Variable valve train (gasoline engine)	3% 8 to 10% (full variable)	€100 €300 to 360 (full variable)	[18]
Variable valve train	3 to 5%		[47]
Variable valve lift	3 to 4% (VVL alone)	\$15 per lifter and \$15 for oil supply	[53]
Discrete VVL	2.8 to 3.6%		[22]
VVL two-step	3 to 4%		[53]
Variable valve lift inlet 2-step	5% in NEDC		[18]
Variable valve train (lift, timing)	9%		[30]
Full variable valve lift and timing	11%	\$240 for I6 engine \$280 for V6 engine	[53]
VVL full variable	7 to 19% (+9.5 to 10.5% torque)		[53]
Half-camless valve	12% (15 to 20% higher low- end torque) 15% (full-camless)	\$400 \$800 (full-camless)	[53]
Variable valve lift	4 to 5% (2-Step) 7 to 8% (continuous) 15% (half-camless) 19 to 22% full cam-less	\$125 to 175 (2-Step) \$300 to 400 (continu- ous) \$400 to 600 (half- camless) \$1000 to 1500 (full- camless)	[119]
Half-camless valve and cylinder deactivation	17%		[53]
Full-camless	12.1 to 15.1% (+10 to 14% torque)		[53]
Valve control	10 to 15%	€250	[5]
Combination	2% (4 valves) 6% (+ 2 position VVLT) 8% (+ full VVLT) 10% (full VVLT + cylinder deactivation) 12% (VVLT + lean burn)		[52]
Cylinder deactivation	4.7 to 6.3%		[22]
Cylinder deactivation	5%	€100 to 120	[7]
Cylinder deactivation	5.6 to 7.6%		[53]
Cylinder deactivation	6 to 6.5% in FTP75 11.7% with VVT	\$15 per cylinder + \$15 control	[53]

Cylinder deactivation	6 to 8%		[122]
Cylinder deactivation	7%		[30]
Cylinder deactivation	around 7.5%		[47]
Cylinder deactivation and 2-step VVL	8.8 to 11.2%		[53]
Cylinder deactivation	up to 10%		[51]
Cylinder deactivation	16% in Japanese 10_15 mode cyle		[52]
Downsizing	5 to 10%		[61]
Downsize (24 bar from V6 to I4)	add 2.9 to 3.7%	\$382 to 509	[22]
Downsizing (gasoline engine)	4 to 6% (step 1: DI) 8 to 10% (step 2: DI + full variable VVT) 15 to 17% (step 3: new charging concepts)	step 1: €150 to 250 step 2: €400 to 500 step 3: €550 to 700 weight reduction 0.3 to 0.8%	[7]
Downsizing (super-charging)	4.7 to 5.3%	\$50 less to turbocharger	[53]
Downsizing (turbocharging only)	5.5 to 8.5% OR power increase 35 to 45%	\$170 to 190 (turbocharger) \$ 55 to 75 (intercooler) \$ 55 to 65 (engine upgrades) \$22 to 28 (control, sensors) \$ 25 to 35 (intake, exhaust modification) \$50 to 60 (turbocharger with variable geometry)	[53]
Turbocharging	+0.7 to 1.3% (+34 to 40% torque) = 5.7 to 8.3%		[53]
Downsize (18 bar from V6 to I4)	6.7 to 8.3%	\$170 to 248	[22]
Downsizing	8% (1.6 l to 1.2 l)		[123]
Downsizing	10 to 15%		[47]
Downsizing (turbocharging with GDI)	12 to 14% (DI homogeneous) up to 22% (DI lean burned)		[53]
Turbocharging and downsizing	13%		[30]

Downsizing (NEDC)	13% (3.0 l to 2.4 l) 18% (3.0 l to 1.8 l) 27% (3.0 l to 1.8 l with variable compression) 11.7% (3.0 l to 1.6 l with super charging) 15.3% (3.0 l to 1.6 l with variable compression and super charging) 7% (1.6 l to 1.0 l with turbo charging) 1% (1.6 l to 1.0 l with super charging) 11% (2.0 l to 1.4 l with DI and lean burned) 25% (2.0 l to 1.4 l with additional variable compression) 9.3% (2.0 l to 1.4 l)		[51]
Downsizing (turbo charging with GDI)	13 to 14% (DI homogenous) up to 25% (DI lean burned)	\$600 (homogenous) \$1500 (lean burned)	[119]
Strong downsizing	14%	€400	[83]
Downsizing	25%	+20% engine costs	[5]
Charging concepts	naturally aspired 100% (reference) turbo charging 97% high turbo charging 95% super charging 106% high engine speed concept 104%		[51]
Downsizing		\$500 to 600	[11]
Variable compression	4 to 6% 30 to 35% (with supercharged from 3.0l to 1.6l)	\$330 (V6) to 430 (V8)	[53]
Variable compression	7%	€500 to 600	[30]
Variable compression	up to 30%		[30]
New combustion process	20%		[30]
EGR (cooled)	4%	€200	[7]
Cooled EGR	3.5 to 3.6%	\$247 to 303	[22]
Exhaust gas recirculation	15%		[30]

Oil pump (variable)	1%		[61]
Variable oil pump	2%		[123]
Oil pump	2 to 3% friction reduction = 0.3 to 0.4% FE		[52]
Improved oil pump	2 to 3% friction reduction = 0.3 to 0.4% FE	€35	[83]
Reduce friction (variable oil pump)	4% (warm) 1.5% (warm-up)		[57]
Low-friction lubricants	0.5 to 0.8%		[22]
Lube oil (5W-20)	0.9 to 1.1%		[53]
Low-friction oil	1% (towards 5W-30)		[52]
Low-friction oil	1% (towards 5W-30)		[52]
Low-friction oil	1 to 2.2% in FTP (5W-30 to 5W-20)	\$0.25 per quart (5 quarts needed)	[53]
Friction improvements		roller earn follower \$0.5 each \$1 for lightweight valves \$1 for lightweight piston \$0.5 for improved piston coasting	[52]
Friction	1% (roller cams) 1.5% (opt. piston, rings, crankshaft)		[52]
Engine friction reduction	1.4 to 1.6%		[53]
Roller cam followers	1.8 to 2.2%		[53]
Low-friction materials	2%	€35	[83]
Engine friction reduction	2.0 to 2.7%		[22]
Friction reduction (overall: engine, transmission)	2 to 3%	€50 to 80	[7]
Friction reduction	2 to 4%	€50 to 80	[47]
Friction reduction	2 to 4%	\$30 to 70	[119] Friction Reduction
Advanced friction reduction	4 to 5%	\$100	[119] Friction Reduction
Friction reduction	10% reduction friction = 2% FE	€50 to 80	[53]
2-chamber oil sump	0.8%		[60]
2-chamber oil sump	0.5% NEDC and FTP75		[61]
Heat storage (5 kg with 80°C)	1% NEDC 0.7% FTP75		[61]
Split cooling (block and head)	1.5% NEDC 1.3% FTP75		[61]

Additional electric heating	0.5% NEDC 0.4% FTP75		[61]
Transmission oil warm-up	1% NEDC		[61]
All Thermal points combined	3%		[61]
Thermal-electric generator (200 W)	1 to 2% in NEDC		[63]
Thermal-electric generator	2%	€800	[7]
Idle speed reduction	1.5%		[57]
Fuel cut-off	10% NEDC	\$50 to 100 (sensors)	[11]
Multiple valves		\$110 to 120 (4 to 2)	[52]
Multiple valves	2 to 5% (4 to 2)		[47]

Table B.2.: Overview of measures to increase the efficiency of the Diesel engine

Measure	Benefit fuel consumption	Expected costs	Source
Common rail	1 to 2%		[61]
Variable valve train	1% weight increase 0.5%	€280	[18]
Variable valve train	1%	€250	[83]
Cylinder deactivation	3%	\$150 to 170	[7]
Downsizing	4% (step 2: high injection pressure, improved turbo charging) 7% (step 3: new charging concepts, optimized EGR)	step 2: €200 to 300 step 3: €400 to 500	[7]
Strong downsizing	10%	€600	[83]
Variable compression	4%	€500 to 600	[30]
EGR (cooled)	2% (improved EGR (cooling, flow) to base EGR)	€160 to 200 0.5% weight increase	[7]

B.2. Auxiliaries

Table B.3 provides an overview of results of literature research on measures to improve the energy demand for auxiliaries. Table B.4 provides an overview of the electrical power demand of consumers. Here, the focus is on the minimum auxiliaries required for driving.

Table B.3.: Overview of measures for improving energy demand of auxiliaries

Measure	Benefit fuel consumption	Expected costs	Source
Efficiency improved generator	efficiency 85% FE 0.4 to 0.8%	\$10 to 12	[53]
Generator with MOS-FET	3.5 gCO ₂ /km	€40	[2]
Improved air conditioning	0.16 l/100km 3.8 gCO ₂ /km (gasoline) 4.2 gCO ₂ /km (Diesel)	€60	[2]
Electric vacuum pump	around 100 W	€35	[2]
Electronic power management	1%		[61]
Auxiliary improvement	1 to 2%	€50	[5]
Energy Management	3% 5.4 gCO ₂ /km (gasoline) 4.3 gCO ₂ /km (Diesel)	€5	[2]
Electronic power management	3%		[123]
Auxiliary improvement	5%	€350	[83]
Improve control units	1.2 gCO ₂ /km NEDC		[2]
PWM control of lights	0.8 gCO ₂ /km NEDC		[2]
Halogen to LED light	2 to 3 gCO ₂ /km		[7]
Halogen to LED light	1.2 gCO ₂ /km NEDC		[2]
PWM fuel pump	1.9 gCO ₂ /km NEDC		[2]
Optimized cabin blower	1.9 gCO ₂ /km NEDC		[2]
Varioserv	around 230 W 0.2 l/100km 4.7 gCO ₂ /km (gasoline) 5.3 gCO ₂ /km (Diesel)	€100	[2]
HPS to Varioserv to EPS	Varioserv = 50% EPS = 10%		[2]
HPS to EPS	around 330 W		[67]
HPS to EPS	average power in standby EHPS: 20 W	€100 to 120 for EPS and EHPS €25 for EPS	[2]
EPS	0.8 to 1.5%		[22]
EPS	1.8 to 2.2 % FC	\$40 to 50 over HPS	[53]

EPS	3% FC		[61]
HPS to EPS	0.2 l/100km		[33]
EPS / EHPS instead of HPS	0.3 l/100km 7.1 gCO ₂ /km (gasoline) 8.0 gCO ₂ /km (Diesel) HPS = 0.35 l/100km EHPS = 0.07l/100km EPS = 0.02 l/100km	€120	[2]
Water pump with friction gear	1% NEDC	€20	[2]
Water pump with switchable MRF clutch	2 to 3% NEDC = 0.23 l/100km (gasoline) 0.16 l/100km (Diesel)	€35	[2]
Switchable mechanical cooling pump	3% 5.4 gCO ₂ /km (gasoline) 4.3 gCO ₂ /km (Diesel)	€35	[2]
Variable mechanical cooling pump	1% 1.8 gCO ₂ /km (gasoline) 1.4 gCO ₂ /km (Diesel)	€20	[2]
Variable mechanical water pump	1.3% NEDC 1.5% FTP75		[61]
Electric water pump	0.4 to 0.6%	\$ 30	[53]
Electric water pump	7.1 gCO ₂ /km NEDC	€45	[2]
Electric water pump and thermal management	3 to 5% max 0.39 l/100km = 9.1 gCO ₂ /km (gasoline) max 0.27 l/100km = 7.2 gCO ₂ /km (Diesel)	€50 to 80	[2]
Activate heating (e.g oil or coolant water) during recuperation	0.5 to 1% in NEDC		[70]
Thermal management	1%	€100	[123]
Thermal management	1 to 3%		[124]
Thermal management	2% (gasoline engine) 3% (Diesel engine)	€100	[83]
Demand-actuated (intelligent) thermal management	3 to 5% NEDC		[2]
Thermal management	3% NEDC		[61]

Table B.4.: Electrical power demand of consumers (for minimum auxiliaries)

Component	Power range	Source
Motor management and fuel pump	250 W	[125]
Ignition	20 W	[2]
Electric fuel pump	50 - 70 W	[2]
Injection	50 - 70 W	[2]
Motor management	175 - 200 W	[2]
Brake light	42 W	[2] [125]
Secondary air pump	500 W for 1 min	[126]

B.3. Transmission

Table B.5 shows an overview about of the results of literature research on measures to improve transmission efficiency.

Table B.5.: Overview of measures for reducing transmission losses

Measure	Benefit fuel consumption	Expected costs	Source
Change from front-longitudinal to front-traversal architecture	5%		[77]
Torque converter elimination	2 to 3%		[47]
Torque converter elimination	3 to 4%	\$100 to 150	[119]
Downspeeding	2 to 3%	€30	[7]
MT optimal gear ratio selection	2%		[61]
AT gear number		4 to 5 gears \$100 to 125	[52]
AT gear number		4 to 5 gears \$115 to 145 4 to 6 gears \$120 to 140 \$30 per gear above 6 gears	[53]
Friction reduction driveline		€50 per 1%	[83]
Highly efficient gearbox	2.2 to 3.7%	\$200 to 248	[22]
Improved 6AT	1.9 to 2.1%		[22]
Stiff brake pad calipers		\$60	[52]
Influence of transmission type (reference MT)	DCT = 95 to 96% AMT = 93% CVT = 101% AT = 102%		[51]
Influence of transmission type	from MT to AMT 2.5% from MT to DCT 4 to 5% from AT to DCT 8 to 9% from 6AT to 8AT 7% MT to CVT 3 to 4% 6AT to CVT 6 to 7%	from MT to AMT €250 from MT to DCT €500 from AT to DCT cost neutral from 6AT to 8AT €100 MT to CVT €600	[7]
Change MT to AMT	7-8%	€150 to 200	[119]
Change MT to 6AT	4 to 5%	\$100 to 150	[119]
Change MT to CVT		\$150 to \$240	[53]
Change MT to CVT	6 to 8%	\$150 to \$200	[119]

Change AMT to DCT		\$120 to 140	[53]
Change AT to 6DCT	3.4 to 4.1%		[22]
Change AT4 to DCT8		\$38 to 47	[22]
Change AT to DCT	6% for gasoline engine 5% for Diesel engine	€700	[83]
Change AT to CVT		4AT to CVT cost neutral	[52]

B.4. Vehicle

B.4.1. Vehicle weight

Table B.6 shows an overview of the results of literature research on measures to reduce vehicle weight.

Table B.6.: Overview of measures for weight reduction

Measure	Expected costs	Source
Parts not related to body	€120 to 180 per 1%	[7]
Parts related to body	€65 to 100 per 1%	[7]
	\$60 per 1% (5-10% possible with acceptable costs, 20% technically possible)	[119]
HSLA, SMC or RIM in BiW, closures and interior	\$0.4 to \$0.6 per lb. (2% possible)	[53]
Lightweight components not related to BiW	€25 per % (2% possible)	[83]
Additional aluminum castings in engine block, housings and wheels	\$0.60 to \$0.90 per lb. (5% possible)	[53]
Additional aluminum forging, load-bearing composites in suspension, driveshaft, seats and bumpers	\$0.9 to \$1.3 per lb. (5% possible)	[53]
Advanced steel in frame and BiW	\$0.25 to \$0.35 per lb. (8% possible)	[53]
High-strength steel	\$30 per % (up to 10% possible)	[83]

B.4.2. Aerodynamic drag

Table B.6 shows an overview of the results of literature research on measures to improve the aerodynamic drag coefficient c_d .

Table B.7.: Overview of measures for aerodynamic improvement

Measure	Benefit c_d	Expected costs	Source
General	1.5% for additional parts / 2% for design changes	€60 - 70	[7]
General	2.3 to 2.5%	\$173 to 210	[22]
Aerodynamics	4%	€1500	[5]
General		\$15-\$25 for 10% reduction \$30 for further 10% reduction	[53]
General		€50 for 2% reduction	[83]
Radiator shutter	0.008 - 0.02		[77]
Optimized radiator	0.02		[81]
Complete close of radiator	0.03 - 0.04		[77]
Complete underbody panel	0.005 - 0.015		[77]
Underbody panel	0.010 - 0.015 (engine compartment) 0.015 (rear) 0.005 - 0.011 (side) 0.01 (transmission tunnel)		[77]
Smooth underbody	0.015		[81]
Underbody cover (plastics)		\$25 - \$30	[52]
Vehicle speed depending on ground clearance	0.005 per 10 mm		[77]
Flush glass window		\$8 - \$10	[52]
Wheel skirts		\$5 - \$6	[52]
Wheel skirts	0.015 - 0.02		[53]
Wheel spoiler	0.008 front wheels 0.002 rear wheels		[77]
Wheel cover	0.003		[77]

Tire selection	0.003 (flat tire labeling) 0.01 (optimized (round) shoulder) 0.004 (rim cover) 0.005 per 10 mm (smaller tire)		[127]
Wheel selection and size	0.018		[77]
Optimized wheels	0.02		[81]
Remove side mirror	0.008		[77]
Adaptive spoiler	0.02		[77]
Optimized A pillar and side mirror	0.01		[81]
Rear diffuser	0.025		[81]
Optimized rear body	0.06		[81]

B.4.3. Rolling resistance and traction

Table B.8 shows an overview of the results of literature research on measures to improve the tire rolling resistance.

Table B.8.: Overview of measures to reduce the tire rolling resistance

Measure	Reduction f_r	Expected costs	Source
General	State-of-the-art: 0.6 - 0.9% (for PC) 0.9 - 1.2% (for luxury, sport and family vehicles) 0.7 - 0.9% (for compact van) 0.8 - 1.2% (for SUV) 0.5% (already commercially available)		[53]
General	State-of-the-art: 0.65 - 1.0% (for PC) 0.9 - 1.2% (for luxury, sport and family vehicles) 0.8 - 0.9% (for compact van) 1.2 - 1.4% (for SUV)	\$27 per tire for 0.2 to 0.3% reduction	[52]
General	1.9 to 2.0%		[22]
General	2% reduction	€25 - 40	[7]
General	2%	€100	[5]
General	3% reduction	€35	[83]
General	10% reduction	\$5 per tire for changed size and aspect ratio \$5 per tire for changed technologies	[53]
Increase diameter (from 16 to 20 inch)	16% reduction		[86]
Increase pressure by 1 bar	15 - 20% reduction		[77]
Increase pressure by 0.5 bar	25% reduction		[47]

B.5. Hybrid

B.5.1. Start-stop and generator control

Table B.9 shows an overview of the results of literature research on the potential of micro hybrids. A micro hybrid is characterized by the use of an engine start-stop system and / or a generator control.

Table B.9.: Overview of potential pf start-stop and generator control

Measure	Benefit	Expected costs	Source
Generator control	1.5 to 4%		[128]
Generator control	2 to 4% 0.23 l/100km gasoline engine 0.16 l/100km Diesel engine		[2]
Start-stop		\$200 to \$500 for stronger and deep cycle battery	[11]
Start-stop	1 to 2%		[61]
Start-stop	1.7 to 2.2%	\$343 to 446	[22]
Start-stop	3%		[123]
Start-stop	3.5 to 4.5%		[76]
Start-stop	3% (MT) / 4% (AT) in NEDC 6% (MT) / 8% (AT) in JC08		[33]
Start-stop	3.5 to 4%		[125]
Start-stop	3.9%		[129]
Start-stop	4.2 to 4.8%	around €100 for base start-stop and additional €200 for adaptation of automatic transmission and air-conditioning	[53]
Start-stop and sailing	0.5 l/100km (12 gCO ₂ /km) for start-stop 1 l/100km for extended start-stop		[130]

Start-stop and generator control	3.8% start-stop + 1% generator control (MT) 8% extended start-stop + 3% generator control and high-performance battery (MT) 5.5% start-stop + 1% generator control (AT) 10.5% extended start-stop + 3% generator control and high-performance battery (AT)		[64]
Start-stop and generator control	5 to 10%		[30]
Start-stop and generator control	6 to 7%	€350 to 425 due to stronger generator and deep cycle battery	[7]
Start-stop and generator control	7.8%		[129]

B.5.2. Mild-hybrid (48 V)

Table B.10 shows an overview of the results of literature research on the potential of mild-hybrids. Here mild-hybrid are defined as using a 48 V level.

Table B.10.: Overview of potential for mild-hybrid (48 V)

Measure	Potential	Expected costs	Source
Mild-hybrid		\$300 to \$1200 per kWh battery \$15 to \$20 per kW electric motor \$200 to \$400 for wiring and transmission adaptation	[11]
Mild-hybrid	9 to 13% for P1 topology	€1400 to 1500	[7]
Mild-hybrid (P1)	11 to 15% (FTP) 2.5 to 3.5% (HWFET) 8 to 9% (combined)	\$1200 for 10 kW motor and lead-acid battery \$1850 for 12 kW motor and NiMH battery	[53]
Mild-hybrid	14.7%		[129]
Mild-hybrid	up to 15%		[76]
Mild-hybrid	up to 15%		[125]
Mild-hybrid	15 to 20%		[30]

C. Appendix: Simulation

C.1. Control Logic

C.1.1. Engine start-stop

Figure C.1 shows the principle flow chart for an engine start-stop control logic. This logic is implemented in the simulation model. Here, the focus is on the usage in the legal fuel consumption test cycles and not on real road driving. The decision to stop the engine is based on a set of preconditions:

- The engine should be warm (temperature of the coolant above a defined level T_{ref}).
- The battery SOC should be above a defined level SOC_{ref} .
- The vehicle speed should be below a defined level v_{ref} .
- For manual transmissions, neutral gear should be engaged, and the clutch pedal should be released.
- For automatic transmissions, the brake pedal should be pressed.

If all conditions are fulfilled, a timer is started. If the timer achieves a defined time and all conditions are still fulfilled, the engine is stopped. If the clutch pedal is pressed (for manual transmission) or the brake pedal is released (for automatic transmission), the starter cranks the engine. After reaching a defined engine speed n_{ref} , the starter is deactivated, and the engine controls to idle speed.

In the measures considered, both the engine start-stop and sailing are simulated. For the normal engine start-stop, the reference vehicle speed v_{ref} is set to 0.1 km/h, which represents vehicle stand still. To analyze the potential of sailing, this reference vehicle speed is set to a higher value, so the engine can also stop while driving. An additional control signal is required to the transmission control unit. In the case of an engine stop request, the clutches should be open, or the neutral gear should be engaged. In the case of manual transmission, sailing is not possible because the gear profile is fixed. The neutral gear, which is a prerequisite for engine stop, is only engaged during vehicle stand still.

C.1.2. Generator control

Figure C.2 shows the principle flow chart for a generator control logic. This logic is implemented in the simulation model. Here, the focus is on usage in the legal fuel consumption test cycles and not on real road driving. The logic is divided into two states:

- Driving: The voltage level is set to a low level to force battery discharge.
- Recuperation: The voltage level is set to a high level to charge the battery. Here, the physical limits of the battery have to be considered.

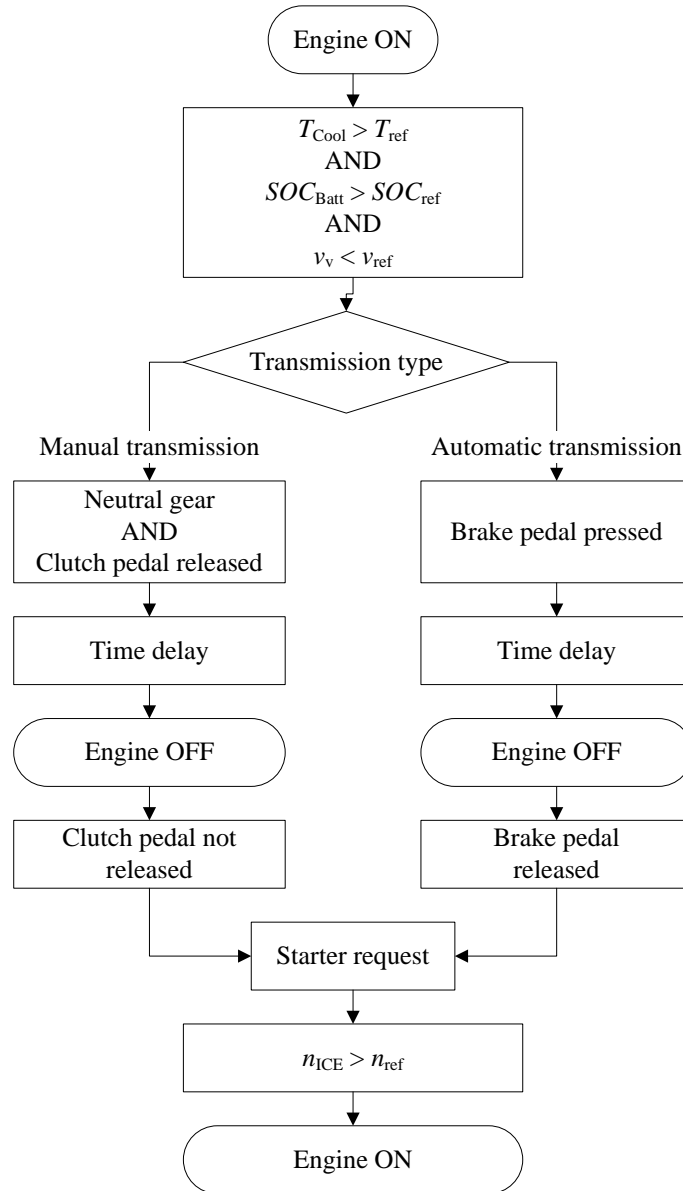


Figure C.1.: Principle flow chart for engine start and stop logic

The decision between the two states is based on prerequisites. The state *recuperation* is selected when the brake pedal is pressed and the engine is connected to the power-train (clutch is closed and gear is selected). Otherwise, the state *driving* is used.

C.1.3. Cylinder deactivation

Figure C.3 shows the principle flow chart for a cylinder deactivation control logic. This logic is implemented in the simulation model. Here, the focus is on usage in the legal fuel consumption test cycles and not on real road driving.

The engine model has to be parametrized with different combustion modes. For example, different fuel consumption maps may be required. In this example, combustion mode 1 is the normal operation, and mode 2 is the cylinder deactivation state.

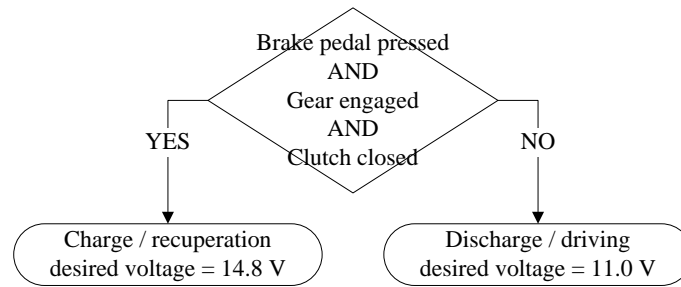


Figure C.2.: Principle flow chart for a generator control

Three prerequisites have to be met:

- The engine should be warm (temperature of the coolant above a defined level T_{ref}).
- The torque request should be lower than a reference torque curve M_{ref} (depending on speed).
- A time hysteresis must be implemented to prevent too frequent iterations.

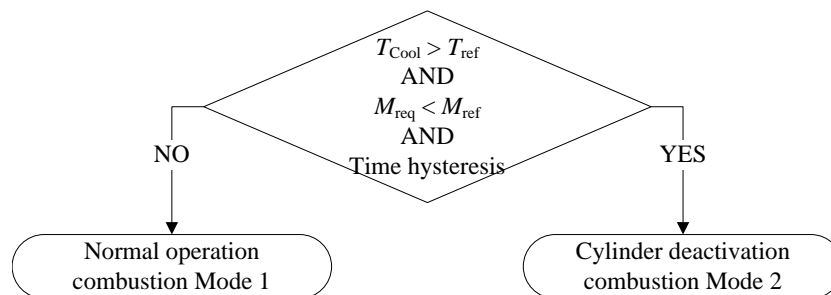


Figure C.3.: Principle flow chart for a cylinder deactivation control

C.2. Validation of the baseline simulation model

The measurement points of the vehicle used are illustrated in Figure C.4 and listed in Table C.1.

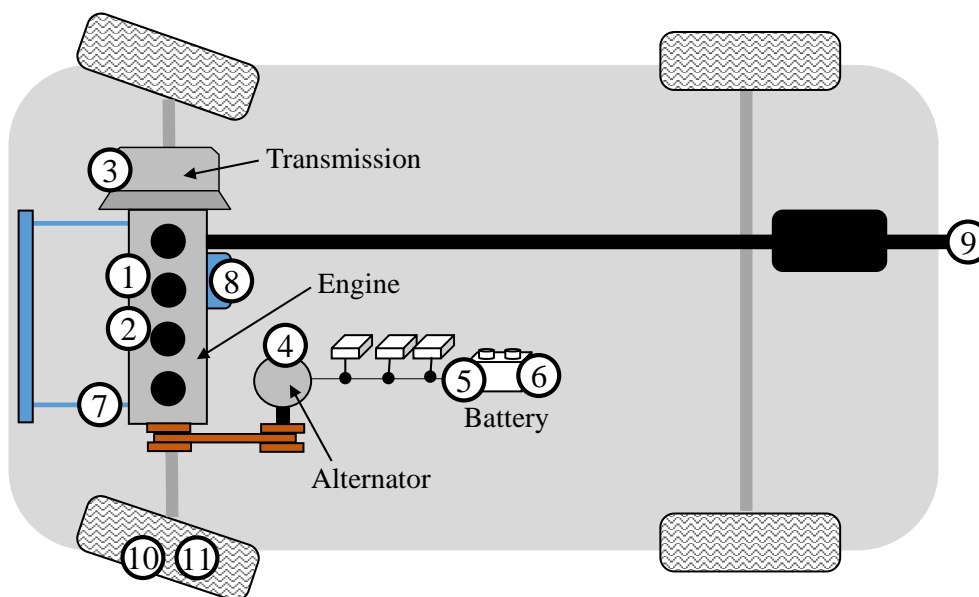


Figure C.4.: Measurement points

Table C.1.: Measurement points

Measurement point #	Description	Equipment	Tolerance
1	Engine speed	Vehicle CAN	n/a
2	Engine torque	Vehicle CAN	n/a
3	Actual gear	Vehicle CAN	n/a
4	Alternator current	Current clamp 50 A (LEM HTR 50)	2% of I_{nom}
5	Battery current	Current clamp 50 A (LEM HTR 50)	2% of I_{nom}
6	Battery voltage	AD module	0.05%
7	Coolant temperature	Vehicle CAN	n/a
8	Engine oil temperature	Vehicle CAN	n/a
9	CO ₂ emissions	Test bench	0.8%
10	Vehicle speed	Test bench	0.08 km/h
10	Vehicle speed	GPS (Racelogic VBOX 3i)	0.1 km/h
11	Distance	Test bench	0.08%

The measurements for driving performance were done on the Magna Steyr test track in Graz with a flat straightaway of 350 m. No detailed specifications for the test track (e.g. flatness)

were available. To compensate for the influence of the small slope on the test track, the driving performance measurements were done in both directions.

The measurements for fuel consumption / CO₂ emissions were done on the 4WD chassis dynamometer at Magna Steyr Engineering in Graz. An overview of the test bench is shown in Figure C.5. The vehicle is fixed on the test bench. The tires are located on controllable rollers, that simulate forces of a real road. Airstream is needed for the cooling of components (e.g. radiator). Also sun-light simulation is possible for thermal testing. The CO₂ emissions and exhaust emissions are measured with a measuring system. The specifications of the exhaust emission measuring system are shown in Figure C.6. The chassis dynamometer has the following specifications [Source: Magna Steyr test bench description]:

- Accredited according to ISO/ IEC 17025:2007
- Front axle drive power 2x150 kW
- Rear axle drive power 2x200 kW
- Wheelbase 1,800 mm to 4,200 mm
- Track width 900 mm to 2,300 mm
- Maximum speed 260 km/h
- Curb weight simulation 550 to 4,500 kg
- 200,000 m³/h air stream at 140 km/h and 200 km/h
- Test cell temperature from -35 to +55°C
- 1,200 W/m² sun lighting system
- Permission for H₂ and CNG vehicles
- High/low temperature pre-conditioning in separate container
- Sufficient standard (23°C) temperature soaking positions
- Exhaust emission measuring system

Figure C.7 shows the validation of the WLTC. Based on the validated NEDC simulation / measurement, the WLTC was analyzed with the same vehicle parameters. Only the vehicle inertia was adapted according to the WLTP. Figures C.8 and C.9 show the validation of driving performance in the case of a full-throttle 0 to 100 km/h acceleration and a full-throttle 60 to 100 km/h acceleration with back-shift. For the 60 to 100 km/h acceleration, the control time of the back-shift was adapted to the measurement. In the 0 to 100 km/h acceleration, the shifting procedure including torque limitation was also validated.

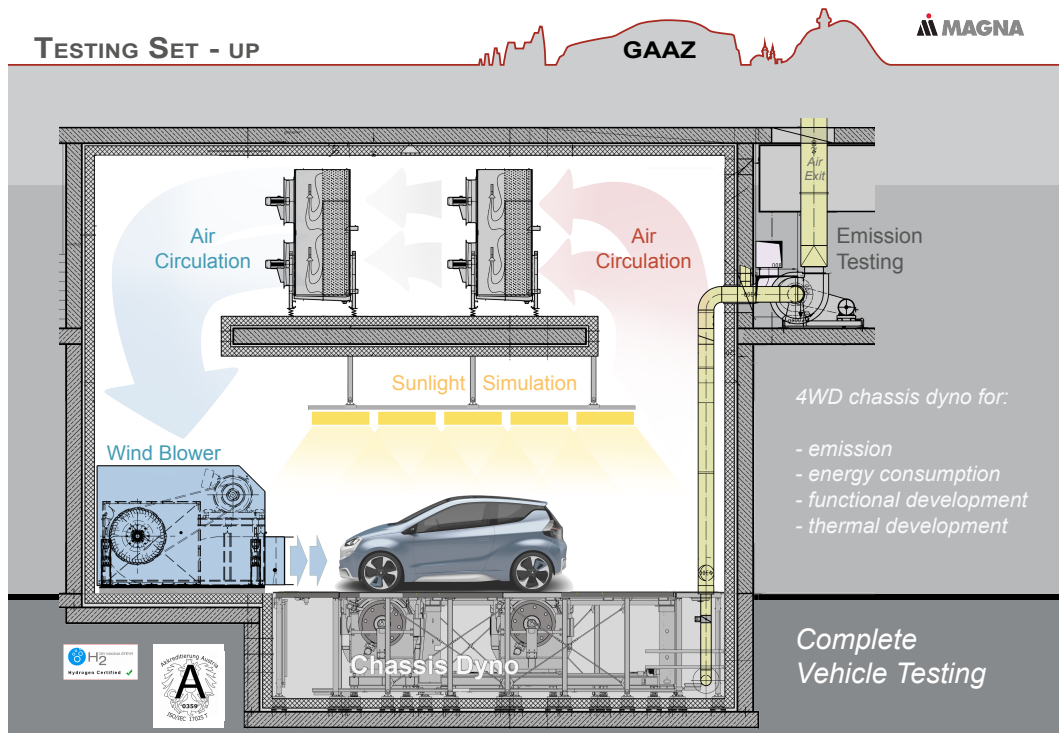



Figure C.5.: Layout of the 4WD chassis dyno used [Source: Magna Steyr test bench description]



Specifications	Description
<ul style="list-style-type: none"> • CVS AVL i60: 2,5 - 27 m³/min • heated sampling lines and bags • 12 bags, clean/dirty separated • CO: 50 ppm - 10 % • CO₂: 0,5 - 20 % • THC: 3 - 20.000 ppm C₃ • CH₄: 9 - 20.000 ppm C₁ • NO_X: 3 - 10.000 ppm • O₂: 25 % • Particulate mass • Particulate number (AVL APC 489) 	<ul style="list-style-type: none"> • SULEV CVS Exhaust emission measurement for development, homologation & CoP • 2-Line Modal Raw Emission Bench • Gasoline, Diesel & alternative Fuels • Passenger Cars & LDV

Figure C.6.: Specification exhaust measuring system [Source: Magna Steyr test bench description]

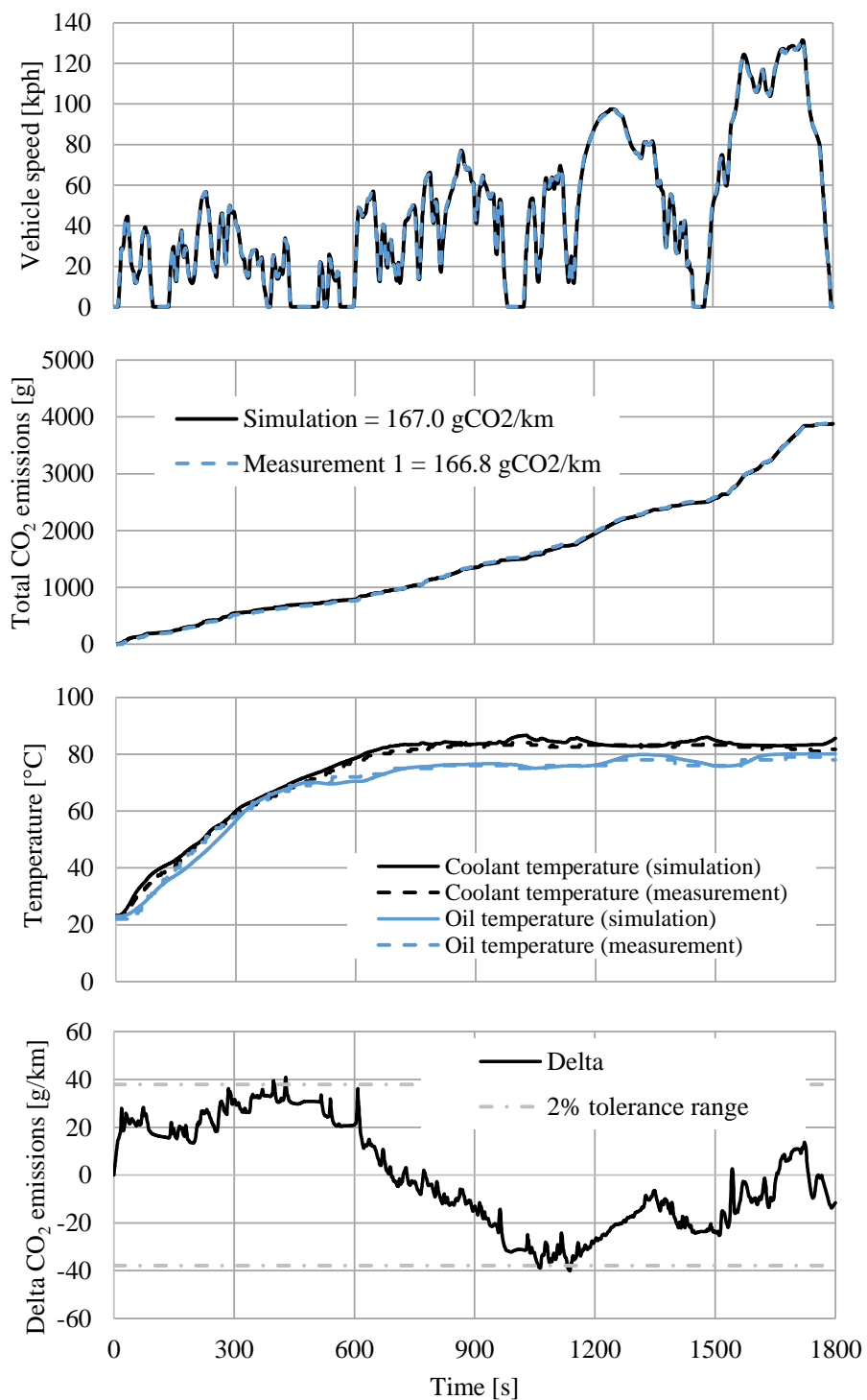


Figure C.7.: Comparison of simulation and measurement, maneuver: WLTC

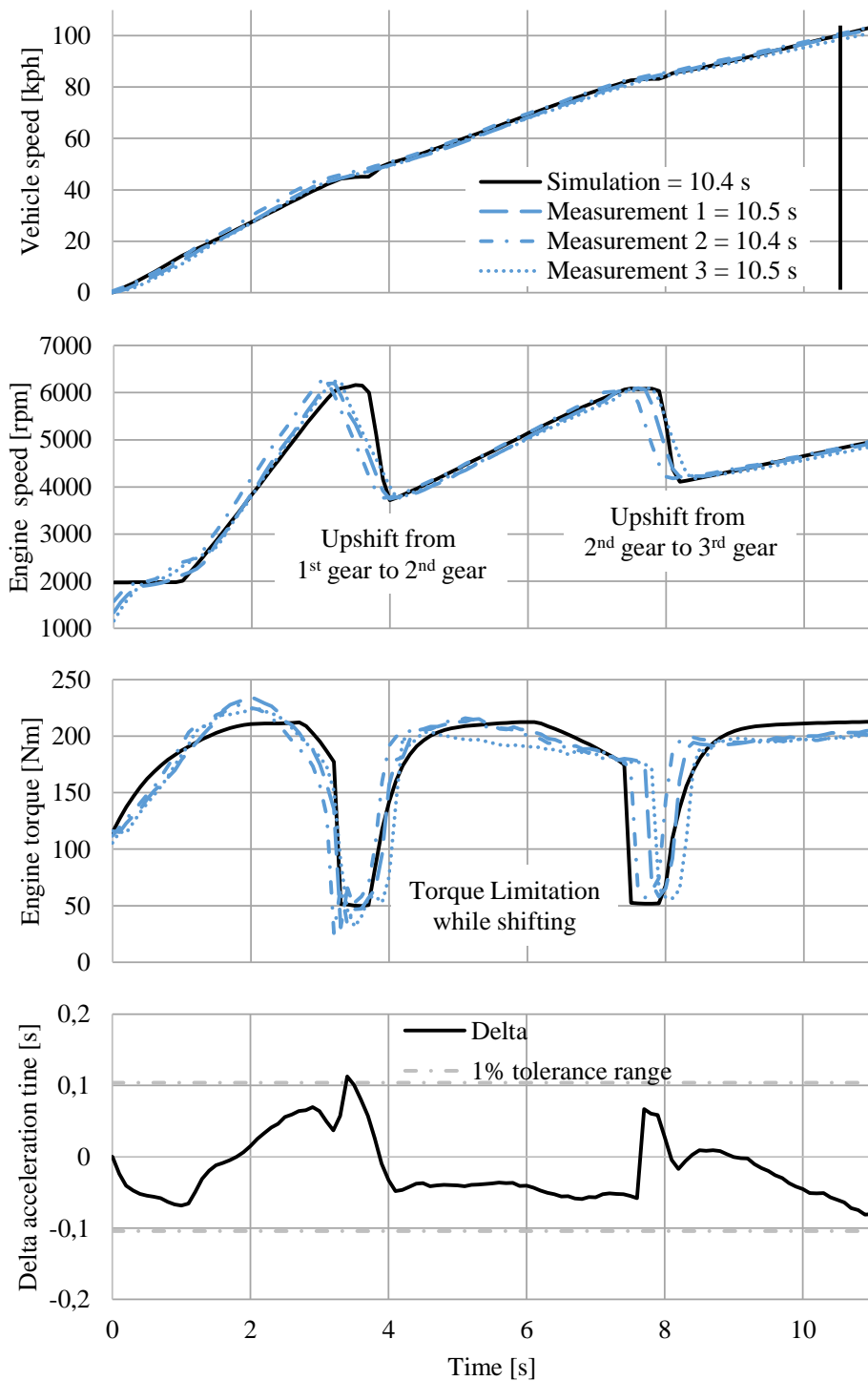


Figure C.8.: Comparison of simulation and measurement, maneuver: Full-throttle acceleration from 0 to 100 kph

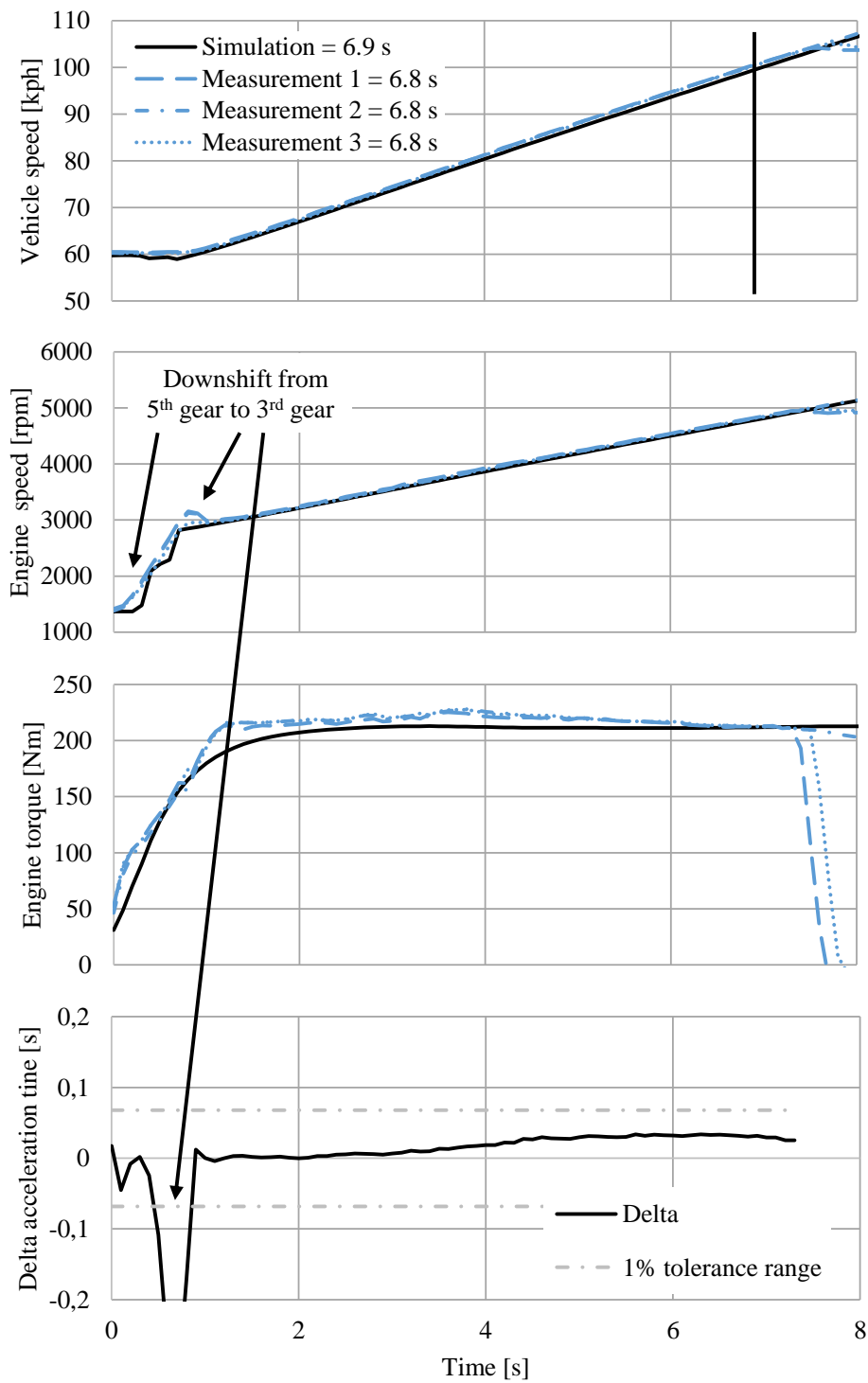


Figure C.9.: Comparison of simulation and measurement, maneuver: Full-throttle acceleration from 60 to 100 kph in D Mode

C.3. Automation

C.3.1. Definitions of components

The following listings show excerpts from the data-sheet definitions of the components and the definition of measures.

Listing C.1 shows a reduced example of the parameters to define the required engine parameters. The engine is defined by maximum power, torque and speed. In addition, the swept volume, number of cylinders and the engine dynamic have to be defined. The characteristic maps are stored in a folder. Characteristic maps are needed for the fuel consumption (BSFC) depending on engine speed and torque, the friction torque depending on engine speed and oil temperature, the fuel load torque curve depending on the engine speed and the reference torque for the control logic of cylinder deactivation. Furthermore, inputs for the control are given. For the control, the desired idle speed and fuel resume speed¹ are given. Both values can be defined in relation to the engine temperature. In addition, the control of the cylinder deactivation (see Appendix C.1.3) is defined here. The cylinder deactivation can be activated and deactivated. Furthermore, two values for a time hysteresis are given to prevent too frequent switching.

Listing C.1: Exemplary source code for engine data

```
// Motor: 1.6l Gasoline 130 kW

// characteristic maps
Eng_File = VehConfDirEng+'gasoline_130kW'; // storage folder of engine maps (full
    load torque = f(engine speed), fuel consumption = f(engine speed, engine
    torque), friction torque = f(engine speed, oil temperature), reference torque
    curve for cylinder deactivation)

// general data
Eng_MaxPwrVal = 130; // max power [kW]
Eng_MaxTrqVal = 300; // max engine speed [Nm]
Eng_MaxSpd = 6600; // max speed [rpm]
Eng_Dynamic = 2; // engine dynamic: 1 - naturally aspirated / 2 - turbo
Eng_Swept_V = 1.6; // swept value [liter]
Eng_NumCyl = 4; // number of cylinders
Eng_IdleSpd = 700; // idle speed for warm engine [1/min]

// fuel cut-off
Eng_FCO_ResumeSpd = '1100'; // fuel resume speed [1/min]

// cylinder deactivation
Eng_CylDeact_State = 0; // status of cylinder deactivation: 0 - disable / 1 -
    enable
Eng_CylDeact_TimeOnMax = 30; // max time deactivated of cylinders [sec]
Eng_CylDeact_TimeOffMin = 30; // min time between two cylinder deactivation phases
    [sec]
```

Listing C.2 shows a reduced example of the parameters to define a transmission. The transmission is defined by its type and number of gears. In addition, the inertias for both sides of the clutch are defined here. This means the crankshaft on the one side and the transmission input-shaft on the other side. Other important additional parameters are the gear ratios, the efficiency factors and torque losses. Here, the efficiency / torque loss can be defined in relation

¹The fuel resume speed defines the state of the fuel cut-off if the accelerator pedal is released. Above the resume speed, no fuel is injected (fuel cut-off). Below the speed threshold, fuel is injected due to driving comfort.

to the temperature. For the control of an automatic transmission, the shifting map is important. In [68], [69], [75] and [76], typical control logics for gear-shifting are explained in more detail.

Listing C.2: Exemplary source code for transmission data

```
// Transmission: Manual 6-speed Transmission

// general
T_Type = 1; // transmission type: 1=MT / 2=AMT / 3=AT / 4=DCT / 5=CVT
T_NumGear = 6; // number forward gears
T_ShiftMap = 'Shifting_6gear.data'; // shifting map
T_InertiaEng = 0.15; // inertia crankshaft, clutch [kg*m**2]
T_InertiaShaft = 0.01; // inertia transmission input shaft [kg*m**2]

// gear ratio
T_G1 = 3.818; // ratio gear 1
T_G2 = 2.158; // ratio gear 2
T_G3 = 1.475; // ratio gear 3
T_G4 = 1.067; // ratio gear 4
T_G5 = 0.875; // ratio gear 5
T_G6 = 0.744; // ratio gear 6
T_LossMap = 'TorqueLoss.data'; // torque loss map

// differential
T_GF = 3.941; // ratio final drive / differential
T_Eff_GF = 0.98; // efficiency of final drive
```

Listing C.3 shows a reduced example of the parameters to define a wheel. Three parameters are important: the dynamic radius², the inertia and the rolling resistance curve depending on vehicle speed. Different inertias can be defined for front and rear wheels due to the fact that side-shaft and differential are included in the values.

Listing C.3: Exemplary source code for wheel data

```
// Wheel: 205/60 R16
Wheel_Rdyn = 0.317; // dynamic rolling radius [m]
Wheel_Inertia_Frnt = 1.17; // inertia front tire (incl. side-shaft) [kg*m**2]
Wheel_Inertia_Rr = 1.1; // inertia rear tire [kg*m**2]
Wheel_fRollMap = 'RollingCoefficient.data'; // rolling resistance coefficient
// depending on vehicle speed
```

Listing C.4 shows a reduced example of the parameters to define control functions for the engine start-stop (see Appendix C.1.1) and the generator control (see Appendix C.1.2). For the engine start-stop function the coolant temperature and vehicle speed threshold have to be defined. The input of the two voltage level are required for the generator control. Both functions are configurable and can be activated or deactivated.

Listing C.4: Exemplary source code for control logic data

```
// Start-stop
Hyb_StSt_Active = 0; // start-stop: 0 = inactive / 1 = active
Hyb_StSt_Ton = 55; // coolant temperature above start-stop is active [degC]
Hyb_StSt_RefSpeed = 0.1; // reference speed to allow engine stop [kph]
```

²The dynamic radius is the distance between the center of the wheel and the road. It is caused by the deformation of the tire and defines the rolling circumference.

```

// Regulated voltage control
Hyb_RVC_Active = 0; // RVC: 0 = inactive / 1 = active
Hyb_RVC_Vref = 11.0; // reference voltage for no recuperation [V]
Hyb_RVC_VrefRecu = 14.8; // reference voltage for recuperation [V]

```

Listing C.5 shows a reduced example of the parameters to define the auxiliaries. First, the alternator has to be defined by the maximum current and the power loss map. The low-voltage battery is defined by the initial battery SOC, the capacity and the physical data for the open circuit voltage and the internal resistance. The belt drive is defined by its efficiency factor and the ratio to the various consumers. Due to the fact that electrification of auxiliaries is one measure to improve CO₂ emissions, switch-variables are implemented. Depending on the mode, an auxiliary is deactivated, simulated as mechanical drag torque or simulated as electrical load. For the electrical load, a power demand is defined. For the mechanical load, drag torque curves are defined.

Listing C.5: Exemplary source code for auxiliary data

```

// Auxiliaries: standard

// alternator
Aux_Alt_MaxCurr = 'Alternator_MaxCurrent.data'; // max current [A]
Aux_Alt_PowerLoss = 'Alternator_PowerLoss.data'; // power loss map [W]

// battery
Aux_Batt_SOCinit = 100; // initial SOC at simulation start [%]
Aux_Batt_Capa = 60; // nominal capacity [Ah]
Aux_Batt_Volt = 'Voltage-vs-SOC.data'; // open circuit voltage [V]
Aux_Batt_Ohm = 'ohmR-vs-SOC.data'; // internal resistance [ohm]

// belt drive
Aux_Belt_eta = 0.97; // efficiency factor of belt drive
Aux_Belt_Alt_Ratio = 2.4; // ratio alternator (engine->alternator)
Aux_Belt_WaPu_Ratio = 1; // ratio mechanical water pump (engine->pump)
Aux_Belt_Klima_Ratio = 1; // ratio AC compressor (engine->compressor)
Aux_Belt_Steer_Ratio = 1; // ratio power steering pump (engine->pump)
Aux_Belt_OilPu_Ratio = 1; // ratio oil pump (engine->pump)
Aux_Belt_VakuPu_Ratio = 1; // ratio vacuum pump (engine->pump)

// specification electrical auxiliaries
Aux_Elec_Base_P = 360; // power onboard electronic [W]

// specification mechanical auxiliaries
Aux_Mech_WaPu_Map = 'WaPu_Map_Trq.data'; // torque demand of water pump [Nm]
Aux_Mech_Klima_Map = 'KlimaKompr_Map_Trq.data'; // torque demand of AC compressor
[Nm]
Aux_Mech_VakuPu_Map = 'VakuPu_Curve_Trq.data'; // torque demand of vacuum pump [Nm]
]
Aux_Mech_OilPu_Map = 'OilPu_Curve_Trq.data'; // torque demand of oil pump [Nm]
Aux_Mech_Steer_Map = 'ServoPu_Curve_Trq.data'; // torque demand of power steering
pump [Nm]

// mode of auxiliaries
// 0 = off
// 1 = electrical
// 2 = mechanical
Aux_Mode_WaPu = 0; // mode water pump
Aux_Mode_Klima = 0; // mode AC compressor
Aux_Mode_VakuPu = 0; // mode vacuum pump
Aux_Mode_OilPu = 0; // mode oil pump

```

```
| Aux_Mode_Steer = 0; // mode power steering pump
```

C.3.2. Definitions of measures

Listing 4.4 shows further examples for the definition of measures.

Listing C.6: Exemplary source code to describe a measure

```
// — ID 1: 1.0 Gasoline VVT and VVL —
i=1;
M_Type(i) = 2; // type: 1 = simulation, 2 = relative, 3 = absolute
M_global(i) = 1; // type of measure: 0 = local, vehicle specific / 1 = global

// boundary constraints
M_Market(i,:) = [1 1 1]; // 1 = EU, 2=US, 3=CN considered: 1=EU, 2=US, 3=CN
M_ConsVeh(i,:) = [0]; // considered vehicles
M_ConsEng(i,:) = [1]; // considered engines, only 1.0 gasoline engine
M_ConsTrans(i,:) = [0]; // considered transmission
M_ConsCyc(i,:) = [1 1 1 1 0 0 0]; // considered cycles, only for fuel consumption
    cycles

// sub-variant 1: 'VVL 2-step'
M_Result(i,2) = -0.02; // in case of relative or absolute type
M_Model(i,2) = 0; // used simulation model, 0 = reference model from base vehicle
M_Cost(i,2) = 70; // additional cost of measure [\euro]

// sub-variant 2: 'VVL full variable'
M_Result(i,2) = -0.05;
M_Model(i,2) = 0;
M_Cost(i,2) = 240;

// sub-variant 3: 'VVL half-camless'
M_Result(i,2) = -0.11;
M_Model(i,2) = 0;
M_Cost(i,2) = 290;

// sub-variant 4: 'VVL full-camless'
M_Result(i,2) = -0.15;
M_Model(i,2) = 0;
M_Cost(i,2) = 640;

M_VarNum(i) = 4; // number of sub-variants for measure i

// ...

// — ID 21: Water pump —
i=21;
M_Type(i) = 1; // type: 1 = simulation, 2 = relative, 3 = absolute
M_global(i) = 1; // type of measure: 0 = local, vehicle specific / 1 = global

// boundary constraints
M_Market(i,:) = [1 1 1]; // 1 = EU, 2=US, 3=CN considered: 1=EU, 2=US, 3=CN
M_ConsVeh(i,:) = [0]; // considered vehicles
M_ConsEng(i,:) = [0]; // considered engines
M_ConsTrans(i,:) = [0]; // considered transmission
M_ConsCyc(i,:) = [1 1 1 1 1 1 1]; // considered cycles

// sub-variant 1: 'Switchable water pump'
M_Result(i,1) = 0; // in case of relative or absolute type
```

```

M_Model(i,1) = 0; // used simulation model, 0 = reference model from base vehicle
M_Cost(i,1) = 20; // additional cost of measure [\euro]
M_Value(i,15,1) = 10; // mode for water pump
M_Value(i,16,1) = 'WaPu_Map_Trq_Switchable.data'; // drag torque map of water pump

// sub-variant 2: 'Electric water pump'
M_Result(i,2) = 0;
M_Model(i,2) = 0;
M_Cost(i,2) = 45;
M_Value(i,15,1) = 2;

M_VarNum(i) = 2; // number of sub-variants for measure i

// ...

// --- ID 23: PWM fuel pump ---
i=23;
M_Type(i) = 3; // type: 1 = simulation, 2 = relative, 3 = absolute
M_global(i) = 1; // type of measure: 0 = local, vehicle specific / 1 = global

// boundary constraints
M_Market(i,:) = [1 1 1]; // 1 = EU, 2=US, 3=CN considered: 1=EU, 2=US, 3=CN
M_ConsVeh(i,:) = [0]; // considered vehicles
M_ConsEng(i,[1 2 3 4]) = [1 2 3 4]; // considered engines, only for gasoline
engines
M_ConsTrans(i,:) = [0]; // considered transmission
M_ConsCyc(i,:) = [1 1 1 1 0 0 0]; // considered cycles, only for fuel consumption
cycles

// sub-variant 1: 'PWM fuel pump'
M_Result(i,1) = -0.08; // in case of relative or absolute type
M_Model(i,1) = 0; // used simulation model, 0 = reference model from base vehicle
M_Cost(i,1) = 10; // additional cost of measure [\euro]

M_VarNum(i) = 1; // number of sub-variants for measure i

// ...

// --- ID 26: Rolling resistance ---
i=26;
M_Type(i) = 1; // type: 1 = simulation, 2 = relative, 3 = absolute
M_global(i) = 0; // type of measure: 0 = local, vehicle specific / 1 = global

// boundary constraints
M_Market(i,:) = [1 1 1]; // 1 = EU, 2=US, 3=CN considered: 1=EU, 2=US, 3=CN
M_ConsVeh(i,:) = [0]; // considered vehicles
M_ConsEng(i,:) = [0]; // considered engines
M_ConsTrans(i,:) = [0]; // considered transmission
M_ConsCyc(i,:) = [1 1 1 1 1 1 1]; // considered cycles

// sub-variant 1: 'Rolling resist 0.80'
M_Result(i,1) = 0; // in case of relative or absolute type
M_Model(i,1) = 0; // used simulation model, 0 = reference model from base vehicle
M_Cost(i,1) = 30; // additional cost of measure [\euro]
M_Value(i,11,1) = 0.008; // rolling resistance coefficient

// sub-variant 2: 'Rolling resist 0.75'
M_Result(i,1) = 0;
M_Model(i,1) = 0;
M_Cost(i,1) = 70;
M_Value(i,11,1) = 0.0075;

```

```

// sub-variant 3: 'Rolling resist 0.70'
M_Result(i,1) = 0;
M_Model(i,1) = 0;
M_Cost(i,1) = 120;
M_Value(i,11,1) = 0.007;

// sub-variant 4: 'Rolling resist 0.65'
M_Result(i,1) = 0;
M_Model(i,1) = 0;
M_Cost(i,1) = 180;
M_Value(i,11,1) = 0.0065;

M_VarNum(i) = 4; // number of sub-variants for measure i

// ...

// --- ID 31: Aero wheel skirts C-segment ---
i=1;
M_Type(i) = 1; // type: 1 = simulation, 2 = relative, 3 = absolute
M_global(i) = 1; // type of measure: 0 = local, vehicle specific / 1 = global

// boundary constraints
M_Market(i,:) = [1 1 1]; // 1 = EU, 2=US, 3=CN considered: 1=EU, 2=US, 3=CN
M_ConsVeh(i,[1 2 3 4 5 6 7 8 9 10 11 12]) = [4 5 6 7 8 9 21 22 23 24 25 26]; //
    considered vehicles, only for C-segment vehicles
M_ConsEng(i,:) = [0]; // considered engines
M_ConsTrans(i,:) = [0]; // considered transmission
M_ConsCyc(i,:) = [1 1 1 1 1 1 1]; // considered cycles

// sub-variant 1: 'Aero wheel skirts'
M_Result(i,1) = 0; // in case of relative or absolute type
M_Model(i,1) = 0; // used simulation model, 0 = reference model from base vehicle
M_Cost(i,1) = 20; // additional cost of measure [\euro]
M_Value(i,6,1) = -0.02; // Delta Cd

M_VarNum(i) = 1; // number of sub-variants for measure i

// ...

// --- ID 47: Electrification: start-stop / generator control / 48-V-hybrid ---
i=47;
M_Type(i) = 1; // type: 1 = simulation, 2 = relative, 3 = absolute
M_global(i) = 0; // type of measure: 0 = local, vehicle specific / 1 = global

// boundary constraints
M_Market(i,:) = [1 1 1]; // 1 = EU, 2=US, 3=CN considered: 1=EU, 2=US, 3=CN
M_ConsVeh(i,:) = [0]; // considered vehicles
M_ConsEng(i,:) = [0]; // considered engines, only for gasoline engines
M_ConsTrans(i,[1 2]) = [1 2]; // considered transmission, only for manual
    transmission
M_ConsCyc(i,:) = [1 1 1 1 1 1 1]; // considered cycle

// sub-variant 1: 'Engine start-stop'
M_Result(i,1) = 0; // in case of relative or absolute type
M_Model(i,1) = 0; // used simulation model, 0 = reference model from base vehicle
M_Cost(i,1) = 300; // additional cost of measure [\euro]
M_Value(i,23,1) = 'MicroHybrid_StSt'; // File Definition Operating Strategy

// sub-variant 2: 'Engine start-stop and sailing'
M_Result(i,1) = 0;

```

```

M_Model(i,1) = 0;
M_Cost(i,1) = 350;
M_Value(i,23,1) = 'MicroHybrid_Sail';

// sub-variant 3: 'Generator control'
M_Result(i,1) = 0;
M_Model(i,1) = 0;
M_Cost(i,1) = 250;
M_Value(i,23,1) = 'MicroHybrid_GC';

// sub-variant 4: 'Engine start-stop and generator control'
M_Result(i,1) = 0;
M_Model(i,1) = 0;
M_Cost(i,1) = 370;
M_Value(i,23,1) = 'MicroHybrid_StSt_GC';

// sub-variant 51: 'Engine start-stop and sailing and generator control'
M_Result(i,1) = 0;
M_Model(i,1) = 0;
M_Cost(i,1) = 420;
M_Value(i,23,1) = 'MicroHybrid_Sail_GC';

// sub-variant 6: '48 V P0 200 Wh 8 kW'
M_Result(i,1) = 0;
M_Model(i,1) = 3; // used simulation model, 0 = reference model from base vehicle
    > use simulation model 3 with 48-V-hybrid power-train
M_Cost(i,1) = 1000;
M_Value(i,23,1) = 'Hybrid_48V_P0';

// sub-variant 7: '48 V P1 200 Wh 12 kW'
M_Result(i,1) = 0;
M_Model(i,1) = 3; // used simulation model, 0 = reference model from base vehicle
    > use simulation model 3 with 48-V-hybrid power-train
M_Cost(i,1) = 1200;
M_Value(i,23,1) = 'Hybrid_48V_P1';

M_VarNum(i) = 7; // number of sub-variants for measure i

// ...

```


D. Appendix: Fleet definition

D.1. Vehicle definition

Table D.1 shows the vehicle configurations which were used for the analysis and application of the optimization algorithm in Chapter 6. The overview shows the numbering of the vehicles, the segment, the market and the assumed sales volume. In this example, no sales volume by year is considered. The vehicles are further defined by the engine type and power, transmission type, aerodynamics, tire and the curb weight. The curb weight and the footprint are required for the calculation of the fleet-average status and targets. The bottom part of the table shows the status of fuel consumption and driving performance from the simulation of the baseline vehicle. Depending on the market, different driving cycles for fuel consumption are evaluated: the NEDC and WLTC for Europe, the NEDC for China, and the EPA2 (FTP75 and HWFET) for the USA. The vehicle analysis in Chapter 6.2 is based on vehicle #5. The platform analysis in Chapter 6.3 is based on all C-segment vehicles for the EU market. Vehicles #1 to 20 are used for the fleet analysis in Chapter 6.4.

In addition, Table D.2 shows the sales volume by year.

Table D.1.: Definition of the vehicles

Vehicle #	1	2	3	4
Segment	A hatchback	B hatchback		C hatchback
Market	EU			
Sales volume per year	35T	24T	67T	24T
Engine	Gasoline 60 kW	Diesel 60 kW	Gasoline 60 kW	Diesel 80 kW
Transmission	6-speed MT			
CVW	1045 kg	1130 kg	1055 kg	1300 kg
c_d	0.32	0.32		0.31
A_x	2.05 m ²	2.10 m ²		2.20 m ²
Footprint				
Tire	185/65 R15	185/70 R14		205/60 R16
Baseline Simulation Result				
NEDC [l/100km]	5.9	5.2	6.0	5.7
WLTC [l/100km]	5.8	4.9	5.9	5.4
EPA 2-cycle [l/100km]				
Acceleration 0 ... 100 kph [s]	12.8	12.3	12.9	10.6
Passing time 80 ... 120 kph (5 th gear) [s]	12.9	9.2	12.9	7.5
Maximum speed [kph]	180	175	179	188

Vehicle #	5	6	7	8
Segment	C hatchback		C sedan	
Market	EU		CN	
Sales volume per year	45T	11T	125T	230T
Engine	Gasoline 100 kW	Gasoline 130 kW	Gasoline 100 kW	
Transmission	6-speed MT			6-speed DCT
CVW	1320 kg	1415 kg	1330 kg	1380 kg
c_d	0.31			
A_x	2.20 m ²			
Footprint				
Tire	205/60 R16			
Baseline Simulation Result				
NEDC [l/100km]	7.0	7.3	7.1	6.4
WLTC [l/100km]	6.8	6.8		
EPA 2-cycle [l/100km]				
Acceleration 0 ... 100 kph [s]	10.4	8.8	10.8	10.1
Passing time 80 ... 120 kph (5 th gear) [s]	11.6	8.2	12.3	13.1
Maximum speed [kph]	208	222	208	208

Vehicle #	9	10	11	12
Segment	C sedan	C SUV		
Market	US	EU		
Sales volume per year	118T	22T	9T	14T
Engine	Gasoline 130 kW	Diesel 120 kW		Gasoline 130 kW
Transmission	6-speed DCT	6-speed MT	6-speed DCT	6-speed MT
CVW	1550 kg	1880 kg	1900 kg	1695 kg
c_d	0.31	0.38		
A_x	2.20 m ²	2.65 m ²		
Footprint	2.685 m * 1.545 m = 44.7 sqft			
Tire	235/45 R18	235/60 R17		
Baseline Simulation Result				
NEDC [l/100km]		7.0	6.6	8.0
WLTC [l/100km]		6.9	6.7	7.9
EPA 2-cycle [l/100km]	6.1			
Acceleration 0 ... 100 kph [s]	8.2	11.7	9.9	10.0
Passing time 80 ... 120 kph (5 th gear) [s]	8.8	9.2	9.4	11.2
Maximum speed [kph]	224	191	196	199

Vehicle #	13	14	15	16
Segment	C SUV		D sedan	
Market	CN	US	CN	
Sales volume per year	130T	190T	41T	43T
Engine	Gasoline 220 kW		Gasoline 100 kW	Gasoline 130 kW
Transmission	6-speed DCT			
CVW	1790 kg	1790 kg	1460 kg	1535 kg
c_d	0.38		0.29	
A_x	2.65 m ²		2.25 m ²	
Footprint		2.685 m * 1.545 m = 44.7 sqft		
Tire	225/65 R17		215/60 R16	
Baseline Simulation Result				
NEDC [l/100km]	9.7		6.5	6.6
WLTC [l/100km]				
EPA 2-cycle [l/100km]		8.6		
Acceleration 0 ... 100 kph [s]	7.3	7.0	10.9	9.2
Passing time 80 ... 120 kph (5 th gear) [s]	9.7	8.9	14.1	9.4
Maximum speed [kph]	236	236	209	226

Vehicle #	17	18	19	20
Segment	D sedan		VAN	
Market	US		EU	
Sales volume per year	43T	105T	48T	22T
Engine	Gasoline 130 kW	Gasoline 220 kW	Diesel 80 kW	Gasoline 100 kW
Transmission	6-speed DCT		6-speed MT	
CVW	1635 kg	1665 kg	1625 kg	1500 kg
c_d	0.29		0.32	
A_x	2.25 m ²		2.45 m ²	
Footprint	2.740 m * 1.59 m= 46.8 sqft			
Tire	235/50 R17	245/40 R19	215/60 R16	
Baseline Simulation Result				
NEDC [l/100km]			6.2	7.4
WLTC [l/100km]			6.0	7.4
EPA 2-cycle [l/100km]	6.1	7.9		
Acceleration 0 ... 100 kph [s]	9.1	7.6	12.2	11.4
Passing time 80 ... 120 kph (5 th gear) [s]	9.1	7.2	9.4	13.8
Maximum speed [kph]	226	261	187	198

Vehicle #	21	22	23	24
Segment	C hatchback			
Market	EU			
Sales volume per year	5T	1T	5T	9T
Engine	Diesel 120 kW		Gasoline 60 kW	Gasoline 100 kW
Transmission	6-speed MT	6-speed DCT	6-speed MT	6-speed DCT
CVW	1430 kg	1465 kg	1300 kg	1370 kg
c_d	0.31			
A_x	2.20 m ²			
Footprint				
Tire	205/60 R16			
Baseline Simulation Result				
NEDC [l/100km]	5.9	5.2	6.2	6.4
WLTC [l/100km]	5.6	5.4	6.5	6.7
EPA 2-cycle [l/100km]				
Acceleration 0 ... 100 kph [s]	11.7	10.2	15.4	10.1
Passing time 80 ... 120 kph (5 th gear) [s]	8.6	8.7	17.8	13.1
Maximum speed [kph]	188	202	177	207

Vehicle #	25	26
Segment	C hatchback	
Market	EU	
Sales volume per year	3T	1T
Engine	Gasoline 130 kW	Gasoline 220 kW
Transmission	6-speed DCT	6-speed MT
CVW	1440 kg	1475 kg
c_d	0.31	
A_x	2.20 m ²	
Footprint		
Tire	205/60 R16	
Baseline Simulation Result		
NEDC [l/100km]	6.6	9.9
WLTC [l/100km]	6.6	8.7
EPA 2-cycle [l/100km]		
Acceleration 0 ... 100 kph [s]	8.3	7.6
Passing time 80 ... 120 kph (5 th gear) [s]	8.6	6.9
Maximum speed [kph]	223	252

Table D.2.: Sales volume by year, in thousands

Year Vehicle #	2020	2021	2022	2023	2024	2025
4	12	24	24	24	24	12
5	21.5	43	43	43	43	21.5
6	5.5	11	11	11	11	5.5
21	0	2.5	5	5	5	1.25
22	0	0.25	1	1	0.25	0
23	0	2.5	5	5	5	1.25
24	0	4.5	9	9	9	2.25
25	0	0.75	3	3	3	0.75
26	0	0.5	1	1	0.5	0

D.2. Measure definition

Table D.3 shows the measures / technologies to improve CO₂ emissions which were used for the analysis and application of the optimization algorithm in Chapter 6. The first column shows the number of the measure which was used in various walk down charts. The second column defines the sub-variants of each measure. The measures are defined by a description and a cost value. Both the cost value and the result of the influence in the driving cycles from of the simulation are the inputs for the optimization. The last column shows whether a measure is local or global. If a measure is global, it is specified for which vehicle this measure is used. The global measures can be restricted to an engine, a transmission, a segment, a market or all vehicles.

Table D.3.: Definition of the measures

#	Sub-variant	Description	Cost [€]	Global restrictions
1	1	VVLT 2-step	70	Gasoline 60 kW
	2	VVLT full variable	240	
	3	VVLT half-camless	290	
	4	VVLT full-camless	640	
2	1	VVLT 2-step	70	Gasoline 100 kW
	2	VVLT full variable	240	
	3	VVLT half-camless	290	
	4	VVLT full-camless	640	
3	1	VVLT half-camless	50	Gasoline 130 kW
	2	VVLT full-camless	400	
4	1	VVLT half-camless	120	Gasoline 220 kW
	2	VVLT full-camless	650	
5	1	Direct injection	200	Gasoline 60 kW
6	1	Direct injection	200	Gasoline 100 kW
7	1	Direct injection	300	Gasoline 220 kW
8	1	Turbocharge / downsize step 1	200	Gasoline 220 kW
	2	Turbocharge / Downsize step 2	400	
9	1	Cylinder deactivation	120	Gasoline 100 kW
10	1	Cylinder deactivation	120	Gasoline 130 kW
11	1	Cylinder deactivation	150	Gasoline 220 kW
12	1	Exhaust gas recirculation	200	Gasoline 60 kW
13	1	Exhaust gas recirculation	200	Gasoline 100 kW
14	1	Exhaust gas recirculation	200	Gasoline 130 kW
15	1	Exhaust gas recirculation	200	Gasoline 220 kW
16	1	Engine friction reduction step 1	35	Gasoline 60 kW
	2	Engine friction reduction step 2	70	
17	1	Engine friction reduction step 1	35	Gasoline 100 kW
	2	Engine friction reduction step 2	70	
18	1	Engine friction reduction step 1	35	Gasoline 130 kW
	2	Engine friction reduction step 2	70	
19	1	Engine Friction Reduction Step 1	35	Gasoline 220 kW
	2	Engine Friction Reduction Step 2	70	

20	1	Decouple AC compressor	60	local
21	1	Switchable water pump	20	all vehicles
	2	Electric water pump	45	
22	1	Intelligent thermal management (-2%)	100	all vehicles
23	1	PWM fuel pump	10	all vehicles
24	1	Improved alternator	40	local
25	1	Start-stop	300	local
	2	Start-stop with sailing	350	
	3	Intelligent generator control	250	
	4	Start-stop and intelligent generator control	370	
	5	Start-stop with sailing and intelligent generator control	420	
26	1	Reduce rolling resistance (0.8%)	30	local
	2	Reduce rolling resistance (0.75%)	70	
	3	Reduce rolling resistance (0.7%)	120	
	4	Reduce rolling resistance (0.65%)	180	
27	1	Underbody cover ($c_d - 0.03$)	25	local
28	1	Wheel spoiler ($c_d - 0.005$)	20	local
29	1	Wheel skirts ($c_d - 0.02$)	20	A-segment
30	1	Wheel skirts ($c_d - 0.02$)	20	B-segment
31	1	Wheel skirts ($c_d - 0.02$)	20	C-segment
32	1	Wheel skirts ($c_d - 0.02$)	20	SUV-segment
33	1	Wheel skirts ($c_d - 0.02$)	20	D-segment
34	1	Wheel skirts ($c_d - 0.02$)	20	VAN-segment
35	1	Active Grill Shutter ($c_d - 0.03$)	30	all vehicles
36	1	Weight reduction (-10 kg)	20	A-segment
	2	Weight reduction (-20 kg)	45	
	3	Weight reduction (-30 kg)	75	
	4	Weight reduction (-40 kg)	110	
	5	Weight reduction (-50 kg)	150	
	6	Weight reduction (-60 kg)	195	
	7	Weight reduction (-70 kg)	245	
	8	Weight reduction (-80 kg)	300	
	9	Weight reduction (-90 kg)	360	
	10	Weight reduction (-100 kg)	425	
	11	Weight reduction (-110 kg)	495	
	12	Weight reduction (-120 kg)	575	
37	1	Weight reduction (-10 kg)	20	B-segment
	2	Weight reduction (-20 kg)	45	
	3	Weight reduction (-30 kg)	75	
	4	Weight reduction (-40 kg)	110	
	5	Weight reduction (-50 kg)	150	
	6	Weight reduction (-60 kg)	195	
	7	Weight reduction (-70 kg)	245	
	8	Weight reduction (-80 kg)	300	
	9	Weight reduction (-90 kg)	360	

	10	Weight reduction (-100 kg)	425	
	11	Weight reduction (-110 kg)	495	
	12	Weight reduction (-120 kg)	575	
38	1	Weight reduction (-10 kg)	20	C-segment
	2	Weight reduction (-20 kg)	45	
	3	Weight reduction (-30 kg)	75	
	4	Weight reduction (-40 kg)	110	
	5	Weight reduction (-50 kg)	150	
	6	Weight reduction (-60 kg)	195	
	7	Weight reduction (-70 kg)	245	
	8	Weight reduction (-80 kg)	300	
	9	Weight reduction (-90 kg)	360	
	10	Weight reduction (-100 kg)	425	
	11	Weight reduction (-110 kg)	495	
	12	Weight reduction (-120 kg)	575	
39	1	Weight reduction (-10 kg)	20	SUV-segment
	2	Weight reduction (-20 kg)	45	
	3	Weight reduction (-30 kg)	75	
	4	Weight reduction (-40 kg)	110	
	5	Weight reduction (-50 kg)	150	
	6	Weight reduction (-60 kg)	195	
	7	Weight reduction (-70 kg)	245	
	8	Weight reduction (-80 kg)	300	
	9	Weight reduction (-90 kg)	360	
	10	Weight reduction (-100 kg)	425	
	11	Weight reduction (-110 kg)	495	
	12	Weight reduction (-120 kg)	575	
40	1	Weight reduction (-10 kg)	20	D-segment
	2	Weight reduction (-20 kg)	45	
	3	Weight reduction (-30 kg)	75	
	4	Weight reduction (-40 kg)	110	
	5	Weight reduction (-50 kg)	150	
	6	Weight reduction (-60 kg)	195	
	7	Weight reduction (-70 kg)	245	
	8	Weight reduction (-80 kg)	300	
	9	Weight reduction (-90 kg)	360	
	10	Weight reduction (-100 kg)	425	
	11	Weight reduction (-110 kg)	495	
	12	Weight reduction (-120 kg)	575	
41	1	Weight reduction (-10 kg)	30	VAN-segment
	2	Weight reduction (-20 kg)	45	
	3	Weight reduction (-30 kg)	75	
	4	Weight reduction (-40 kg)	110	
	5	Weight reduction (-50 kg)	150	
	6	Weight reduction (-60 kg)	195	
	7	Weight reduction (-70 kg)	245	
	8	Weight reduction (-80 kg)	300	
	9	Weight reduction (-90 kg)	360	
	10	Weight reduction (-100 kg)	425	

	11	Weight reduction (-110 kg)	495	
	12	Weight reduction (-120 kg)	575	
42	1	Change final drive (4.29)	0	local, but only MT
	2	Change final drive (3.73)	0	
	3	Change final drive (3.35)	0	
44	1	Change final drive (3.32)	0	local, but only DCT
	2	Change final drive (3.87)	0	
	3	Change final drive (3.53)	0	
	4	Change final drive (3.16)	0	
	5	Change final drive (2.89)	0	
	6	Change final drive (2.64)	0	
44	1	1 g CO ₂ penalty	5	local, but only EU
	2	2 g CO ₂ penalty	20	
	3	3 g CO ₂ penalty	45	
	4	4 g CO ₂ penalty	140	
	5	5 g CO ₂ penalty	235	
	6	6 g CO ₂ penalty	330	
47	1	Start-stop	300	local, but only MT
	2	Start-stop with sailing	350	
	3	Intelligent generator control	250	
	4	Start-stop and intelligent generator control	370	
	5	Start-stop with sailing and intelligent generator control	420	
	6	48-V-hybrid P0	1000	
	7	48-V-hybrid P1	1200	
48	1	Start-stop	300	local, but only DCT
	2	Start-stop with sailing	350	
	3	Intelligent generator control	250	
	4	Start-stop and intelligent generator control	370	
	5	Start-stop with sailing and intelligent generator control	420	
	6	48-V-hybrid P0	1000	
	7	48-V-hybrid P1	1200	
	8	48-V-hybrid P2	1500	
49	1	Seebeck heat recovery (100 W)	200	local

E. Appendix: Optimization

E.1. Utility analysis

The selection of the type of optimization algorithm is based on a utility analysis. The basis for the analysis is the overview of advantages and disadvantages of optimization algorithms, as shown in Table 5.1 in Chapter 5.4.1. For the utility analysis, the rating is converted to numbers of “0” to “2”, as shown in Table E.1. The analysis is done based on a weighting of the three characteristics. Due to the non-linear characteristic, as shown in Figure 5.2 in Chapter 5.4.1, the most important characteristic is the smoothness requirement of the objective function. Here, the weighting is set to 0.6. This characteristic is the most important for the success of the algorithm. The number of parameters is weighted with 0.3. This characteristic is important to handle a vehicle fleet because the number of parameters increases with the number of vehicles, cycles and measures up to several hundred. The less important characteristic is the convergence, weighted with 0.1. This characteristic defines the computation time. The rating multiplied by the weighting show that a *Genetic Algorithm* and *Simulated Annealing* have the best fit.

Table E.1.: Utility analysis of optimization algorithms

	Smoothness	Number n_P	Convergence	Result
SPX	1	1	1	1.0
JAC	0	0	1	0.1
GA	2	2	0	1.8
SA	2	2	0	1.8
GN	0	0	2	0.2
Weighting	0.6	0.3	0.1	

E.2. Vehicle-based optimization

The following example shows the principle workflow of the vehicle-based optimization and the relevance of the target and cost function. The first step is shown in Table E.2. For every cycle, the cycle-based optimization is executed. Every cycle i_c has a parameter vector \mathbf{m}_{i_c} to achieve the given target individually. The parameter vectors of the cycles can differ. Different measures are selected, as well as different sub-variants. The goal is to fix measures and sub-variants to adjust the different solutions. Therefore, the different parameter vectors are compared. The solution is described by two parameters: the equality ratio er and the total costs c . The total costs are the cumulated values of the costs of all selected measures of all solutions, which reads:

$$c = \sum_{i_m=1}^{n_m} \max_{1 \leq i_c \leq n_c} (M_c(i_m, \mathbf{m}_{i_c}(i_m))) . \quad (\text{E.1})$$

The equality ratio er is the sum of the weightings mw of all measures, which reads:

$$er = \sum_{i_m=1}^{n_m} mw(i_m) . \quad (\text{E.2})$$

Here, the weighting of a measure standardizes its influence on the driving cycles. If a measure is not selected in any solution, or if the same measure and sub-variant is the same in all solutions, the weighting factor is set to zero.

Table E.2.: Initial solution

Measure i_m	CBO NEDC m_{NEDC}	CBO 0...100 kph $m_{t,0,100}$	CBO 80...120 kph $m_{t,80,120}$	CBO max speed $m_{v_{\text{max}}}$	Weighting $mw /$ Equality rating er	Costs c [€]
#2	3	0	0	0	$mw = 1.2$	$M_c(2,3) = 290$
#17	2	0	0	0	$mw = 0.3$	$M_c(17,2) = 70$
#21	1	2	0	0	$mw = 331.8$	$M_c(21,2) = 45$
#23	1	0	0	0	$mw = 0.1$	$M_c(23,1) = 10$
#26	6	0	0	0	$mw = 377.1$	$M_c(26,1) = 30$
#27	1	1	1	1	-	$M_c(27,1) = 25$
#31	1	1	1	1	-	$M_c(31,1) = 20$
#35	1	0	0	0	$mw = 247.4$	$M_c(35,1) = 30$
#38	0	8	0	0	$mw = 3569.6$	$M_c(38,8) = 300$
#42	3	1	1	0	$mw = 6345.4$	$M_c(42,3) = 0$
Total					$er = 10872.9$	$c = 820$

An example of the calculation of the weighting factor mw of a measure is shown in Table E.3. Four inputs are required for the calculation: the baseline status s_{bl} , the target t and the potential s_p of each driving cycle, as well as the influence of the measures and sub-variants m_{Δ} . In the first step, the difference between the baseline status and the target, as well as the difference between the baseline status and the potential, are calculated. Dividing the two values gives a weighting of the cycle cw , see Equation (5.32). The next step is analyzed for each measure individually (in this example, for measures #17 and #42). The maximum and minimum influence of the sub-variant are extracted and weighted by the difference d_2 and the cycle-weighting factor cw , see Equations (5.33) and (5.34). These steps are performed for each driving cycle. The final weighting factor for a measure results from the maximum of the weighted maximum influences minus the minimum of the weighted minimum influences, see Equation (5.35). In addition, the number of cycles considered is included. A measure can have an influence on one cycle up to all cycles. In this example, measure #17 influences only the NEDC ($n_{c, m} = 1$), while measure #42 influences all cycles ($n_{c, m} = 4$). The importance of the measure is finally multiplied by the number of cycles considered $n_{c, m}$. Measures which influence many cycles are more important than measures that influence only one cycle.

The next step in the optimization is to select a measure which should be fixed. Here, n_{child} measures should be chosen. The basis is a random selection of the measures, but the statistical distribution of the probability is influenced by the weighting mw of the measures. Thus, measures with a high weighting are preferred. Table E.4 shows an example with the selection of five measures. Here, all possible sub-variants of the selected measures are considered, and they

Table E.3.: Calculation example for the weighting factor

Cycle i_c	NEDC [l/100km]	0...100 kph [s]	80...120 kph [s]	Max speed [kph]
Baseline s_{bl}	7.0	10.4	11.6	208
Target t	5.1	9.8	10.1	216
Potential s_p	3.8	9.4	8.8	225
Delta $d_1 = (s_{bl} - t)$	1.9	0.6	1.5	7.8
Delta $d_2 = (s_{bl} - s_p)$	3.2	1.0	2.8	16.8
$cw = \frac{d_1}{d_2}$	0.6	0.6	0.5	0.5
Sub-variant range of measure #17				
Max influence $d_{max}^* = \max_{i_{svar}} (17, i_{svar})$	0	0	0	0
Min influence $d_{min}^* = \min_{i_{svar}} (17, i_{svar})$	-0.16	0	0	0
Weighted max influence $d_{max} = d_{max}^* \cdot \frac{cw}{d_2}$	0	0	0	0
Weighted min influence $d_{min} = d_{min}^* \cdot \frac{cw}{d_2}$	-0.03	0	0	0
Number of cycles n_{c17}	1			
$mw(17) = (\max(d_{max}) - \min(d_{min})) \cdot 10^{n_{c17}} = 0.03 * 10^1 = 0.3$				
Sub-variant range of measure #42				
Max influence d_{max}^*	0.27	0.17	2.36	0
Min influence d_{min}^*	-0.4	-0.14	-0.96	-1.65
Weighted max influence d_{max}	0.05	0.11	0.45	0
Weighted min influence d_{min}	-0.07	-0.09	-0.18	-0.05
Number of cycles n_{c42}	4			
$mw(42) = (0.45 - (-0.18)) * 10^4 = 0.63 * 10^4 = 6345.4$				

define the complete children generation. Thus, in this case, instead of five, 27 children are now available. For each child, the first step (see Table E.2) is repeated. However, the selected measure is fixed as a prerequisite. For each child, the weighting factor and costs are calculated. Due to the afore mentioned prerequisite of fixing a measure, it may be the case that not all cycles will achieve their target. Thus, a solution is no longer possible. Such measures are marked with “n/a” and filtered out.

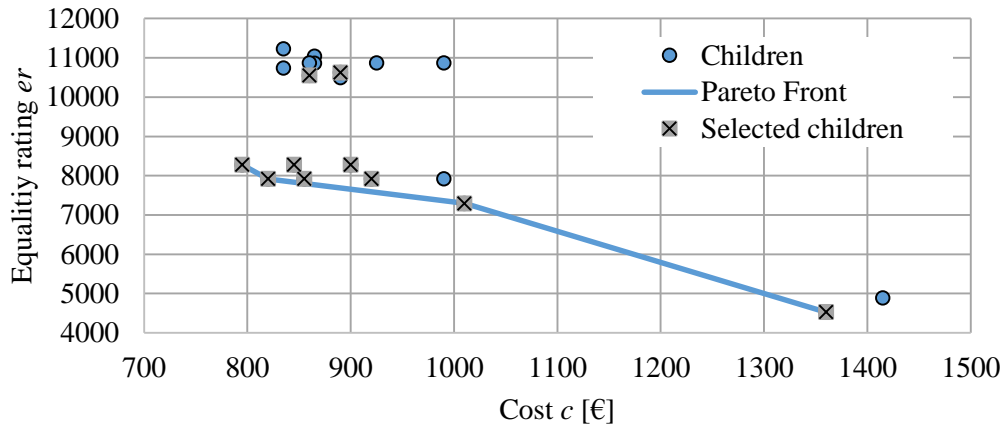
Out of the remaining solutions, a *Pareto Front* is generated, as shown in Figure E.1. The figure shows the possible children with dots, the *Pareto Front* with a line, and the selected children with a square. The selected children represent the new parent solutions.

In an iteration loop, measures are fixed steps by step, with the aim of harmonizing the cycle-optimized solutions. The solutions of one parent after six iteration steps is shown in Table E.5. It can be seen that six measures are fixed, but measures are still different. In further iteration steps, more measures will be fixed and aligned until a parameter vector is found where all cycles

Table E.4.: *Pareto Front*

Measure i_m	Sub-variant $m(i_m)$	Equality rating er	Total costs c [€]
42	0	4887.3	1415
	1	4528.3	1360
	2	n/a	
	3	n/a	
26	0	10495.9	890
	1	10550.8	860
	2	10743.2	835
	3	11040.0	865
	4	10864.3	865
38	0	n/a	
	1	n/a	
	2	n/a	
	3	n/a	
	4	n/a	
	5	8278.6	900
	6	8278.6	795
	7	8278.6	845
	8	7919.3	820
	9	7919.3	855
	10	7919.3	920
	11	7919.3	990
	12	7294.7	1010
17	0	10872.9	990
	1	10872.8	925
	2	10872.6	860
35	0	10625.7	890
	1	11232.2	835

are equal in their individual solutions (equality rating $er = 0$).

Figure E.1.: Example of a *Pareto Front* for the selection of childrenTable E.5.: Example of a parent after 6th iteration step

Measure i_m	CBO NEDC m_{NEDC}	CBO 0...100 kph $m_{t,0-100}$	CBO 80...120 kph $m_{t,80-120}$	CBO max speed $m_{v\text{max}}$	Equality rating er	Total costs c [€]
#2	3	0	0	0	1.2	$M_c(2, 3) = 290$
#6	1	0	0	0	0.3	$M_c(6, 1) = 200$
#17	2	0	0	0	0.3	$M_c(17, 2) = 70$
#20	1	0	1	0	0.3	$M_c(20, 1) = 60$
#21	2				fixed	$M_c(21, 2) = 45$
#23	1	0	0	0	0.1	$M_c(23, 1) = 10$
#25	0	0	3	0	501.2	$M_c(25, 3) = 250$
#26	3				fixed	$M_c(26, 3) = 120$
#27	1	1	1	1	-	$M_c(27, 1) = 25$
#28	1				fixed	$M_c(28, 1) = 20$
#31	1	1	1	1	-	$M_c(31, 1) = 20$
#35	-1				fixed	0
#38	10				fixed	$M_c(38, 10) = 425$
#42	-1				fixed	0
Total					800	1535

E.3. Optimization of a platform

The following appendix shows the detailed results of the platform optimization in Chapter 6.3.

Table E.6 shows the impact on the driving performance status if the vehicle optimization is only based on the NEDC target. If the driving performance becomes worse due to the NEDC-based optimization, the values are printed in italics.

Table E.6.: Results of the vehicle-specific NEDC-based optimization and impact on driving performance

Vehicle	NEDC [l/100km]	0...100 kph [s]	80...120 kph [s]	Max speed [kph]
#4	4.7	10.0	<i>8.4</i>	207
#5	5.1	<i>10.5</i>	<i>13.8</i>	220
#6	5.5	<i>8.9</i>	<i>9.6</i>	238
#21	4.9	11.0	<i>9.7</i>	206
#22	4.7	10.1	<i>9.9</i>	207
#23	4.6	15.2	<i>21.7</i>	191
#24	4.9	10.0	13.1	223
#25	5.1	8.1	<i>9.8</i>	239
#26	6.8	7.7	<i>8.0</i>	256

Table E.7 shows the selection of sub-variants of global measures when vehicles are optimized individually. The columns show the vehicles of the platform, and the rows show the global measures. Global measures are not available in each vehicle. If a measure is not available, the sub-variant is marked with “-”. Measures which are printed in bold are selected with the same sub-variant. Otherwise, if the selection of sub-variants is different, the measures are printed in italics.

Table E.8 shows the influence on the fleet optimization based on a fleet-average CO₂ emissions target.

Table E.7.: Comparison of global measures if vehicles are optimized individually

Vehicle / Measure	#4	#5	#6	#21	#22	#23	#24	#25	#26
#2	-	3	-	-	-	-	3	-	-
#3	-	-	1	-	-	-	-	1	-
#6	-	1	-	-	-	-	0	-	-
#9	-	0	-	-	-	-	0	-	-
#10	-	-	0	-	-	-	-	0	-
#13	-	0	-	-	-	-	0	-	-
#14	-	-	1	-	-	-	-	0	-
#17	-	2	-	-	-	-	2	-	-
#18	-	-	2	-	-	-	-	2	-
#21	1	1	0	2	0	2	1	1	1
#22	1	0	1	0	0	1	0	0	1
#23	-	1	1	-	-	1	1	1	1
#31	1	1	1	1	0	1	1	1	1
#35	1	1	1	1	0	1	1	1	1
#38	1	3	4	1	0	0	0	1	0

Table E.8.: Influence of the NEDC fleet-average target optimization on vehicle targets

Vehicle	Baseline [gCO ₂ /km]	Initial target [gCO ₂ /km]	Fleet- optimized target [gCO ₂ /km]
#4	151.2	124.2	134.2
#5	164.0	119.7	114.0
#6	170.2	129.1	123.1
#21	155.0	129.5	150.9
#22	140.0	124.2	136.6
#23	145.4	108.0	111.3
#24	150.0	115.0	96.6
#25	154.3	119.7	121.7
#26	231.9	159.6	199.8
Fleet-average	159.2	121.7	121.7